THE INFLUENCE OF ULTRAVIOLET B RADIATION ON HUMAN EPIDERMIS

MARY-JANE SPENCER

A thesis presented for the degree of doctor of philosophy

University of Edinburgh

1994

Acknowledgements.

I would like to thank my two supervisors, Dr. M.J. Tidman and Professor J.A.A. Hunter, for their support and encouragement during the course of this work. I would also like to thank Dr. J.P. Vestey, Dr. S.E. Kelly, Dr. N.C. Hepburn, Dr. G.C. Priestley, Dr. R.A. Aldridge, M. Gray and E. McVittie for their advice and donation of tissue.

I am extremely grateful for the use of the transmission electron microscope in the department of Anatomy, the confocal laser scanning microscope in the department of Pathology (with the guidance of D.S. Cunningham), and the fluorescence-activated cell analyser in the department of Haematology (with the assistance of Dr. J.A. Ross). I also thank Dr. J. Gilmour for the analysis of urocanic acid and tumour necrosis factor-α content of suction blister fluid, and analysis of epidermal urocanic acid.

I also wish to thank Dr. K. Guy for the generous donation of monoclonal antibodies, DA6.231, B7/21 and TU22.

Finally I thank my husband for his support and enthusiasm throughout the period of study and dedicate this thesis to him.

Declaration

I declare that the work described in this thesis is my own and that the thesis has been composed by myself

M.-J. Spencer

CONTENTS

ABBREVIATIONS

AFP	Alpha fetoprotein
ANOVAR	Analysis of variance
APC	Antigen-presenting cell
ATPase	Adenosine triphosphatase
BG	Birbeck granule
CH	Contact hypersensitivity
DC	Dendritic cell
DH	Delayed type hypersensitivity
DNCB	Dinitrochlorobenzene
DNFB	Dinitrofluorobenzene
EC	Epidermal cell
FCS	Foetal calf serum
FITC	Fluorescein isothiocyanate
GAM-G15 or GAM-G30	15 or 30nm gold particles conjugated to goat anti-mouse IgG
GM-CSF	Granulocyte macrophage colony-stimulating factor
HEV	High endothelial venule
HLA	Human leukocyte-associated
HSV	Herpes simplex virus
ICAM	Intercellular adhesion molecule
IFN	Interferon
IL	Interleukin
LC	Langerhans cell
LFA	Lymphocyte function-associated
Lps	Lipopolysaccharide
MECLR	Mixed epidermal cell leukocyte reaction
MED	Minimal erythemal dose
MHC	Major histocompatibility complex
MHC I	MHC class I
MHC II	MHC class II
NK	Natural killer
NRS	20% normal rabbit serum
PBS/BSA/Azide/NRS	Phosphate buffered saline/ 0.01% bovine serum albumin/ 0.02% sodium azide/ 20% normal rabbit serum
PUVA	Psoralen photochemotherapy
r	Correlation coefficient
SALT	Skin-associated lymphoid tissue
SIS	The "skin immune system"
TCR	T cell antigen receptor
TGF α,β	Transforming growth factor α and β
TNCB	Trinitrochlorobenzene
TNF	Tumour necrosis factor
TNP	Trinitrophenol
UCA	Urocanic acid
UVA	Ultraviolet A
UVB	Ultraviolet B
UVC	Ultraviolet C
UVR	Ultraviolet radiation
VLA	Very late antigen

ABSTRACT:

It has been well-documented that ultraviolet B (UVB) irradiation results in suppression of the delayed hypersensitivity response to various antigens encountered in the epidermis, although the mechanism for this is unknown. UVB also causes depletion of Langerhans cells (LCs) and alterations in their morphology, but the role of the LC, which is the principal epidermal antigen-presenting cell, in UVB-evoked immunosuppression is not clear. There is controversy as to whether the apparent depletion of LCs which follows UVB exposure reflects a genuine decrease in cell numbers or simply a reduced expression of the cell-surface antigens used to demonstrate them. Most previous studies were undertaken *in vitro*, used experimental animals or UVB doses which differ greatly from normal environmental or therapeutic levels. The aim of this work was to study the relationship between UVB and the LC by examining the influence of moderate, suberythemal doses of UVB, such as are used to treat psoriasis, on epidermal LC morphology, numbers and surface expression of CD1a and major histocompatibility class II (MHC II) antigens in human skin.

A six week course of UVB irradiation, using our standard therapeutic regimen for the treatment of psoriasis (total doses of UVB ranged from 2.58-5.58 J/cm$^{2)}$, was administered to nine healthy subjects. The morphology and number of LCs, and the distribution and expression of certain LC surface antigens were studied in control and in UVB-irradiated epidermis. The study of LC morphology prior to UVB irradiation, using the technique of confocal laser scanning microscopy, revealed that their dendrites extended mainly in the horizontal plane of the epidermis and dendrite numbers ranged between two and nine per cell. Adjacent LCs were in close apposition, but there was little contact between them. The majority of normal unirradiated epidermal LCs expressed HLA-DP, HLA-DQ and HLA-DR antigens, which were demonstrated by a quantitative ultrastructural immunogold method using image analysis, although a small proportion either did not express these antigens or expressed them at high surface densities. This indicates that phenotypic heterogeneity may exist with respect to the surface expression of MHC II antigens on LCs. There was a uniform distribution of these antigens on the surface of LCs derived from both control and UVB-irradiated epidermis.

LCs from UVB-irradiated epidermis, examined using confocal laser scanning microscopy, possessed fewer dendrites than non-irradiated cells. The mean dendrite length was unaltered, but the median dendrite length was reduced after UVB

exposure. This appeared to be due to the retention of fewer dendrites, most of which were short, but some of which were extremely long. UVB irradiation caused significant reduction in the number of epidermal LCs detected by surface expression of CD1a, pan MHC II, HLA-DP, HLA-DQ, HLA-DR antigens using light microscopical immunoperoxidase and immunofluorescence labelling techniques. However, the expression of CD1a and MHC II antigens, detected by immunogold labelling, was increased on the surface of residual LCs after UVB irradiation.

In conclusion, a true reduction in the number of LCs occurs after UVB exposure which cannot be explained simply by the loss of LC surface antigen expression. These studies have defined the UVB-induced changes in LC morphology, numbers and antigen expression in normal human skin.

Chapter 1 Introduction

1.1 General introduction

Human responses to sunlight are complex. Although sunlight is necessary for a wide range of metabolic and other physiological processes, it has harmful as well as beneficial effects. Sunlight can cause photodermatoses, cataracts, inflammation of the eyes, wrinkling and ageing of the skin, sunburn, suppression of cutaneous immune responses and skin malignancy.

The solar spectrum that reaches the Earth's surface includes ultraviolet (wavelength 290-400nm), visible (400-700nm), and infrared radiation (fig. 1.1). Ultraviolet radiation (UVR) is arbitrarily subdivided into 3 wavebands (Coblentz, 1932 cited by Parrish *et al.*, 1978).

Ultraviolet C (UVC) is radiation with wavelengths from 200-280nm which are the shortest to be transmitted through air. All radiation with a wavelength less than 290nm is absorbed by the ozone layer in the upper atmosphere. Therefore, UVC does not normally reach ground level. Radiation in the UVC range is, however, biologically active. UVC is lethal to micro-organisms, and has been shown to cause skin erythema (Hausser, 1928 cited by Rottier, 1953) and immunosuppression (Baadsgaard *et al.*, 1987a).

Mid-range UVR or ultraviolet B (UVB), with wavelengths from 280-320nm, reaches the Earth in relatively small quantities. These wavelengths are biologically very active and are the most effective for production of sunburn in man, as well as immunosuppression and the induction of skin cancers in laboratory animals (Blum, 1959; Baadsgaard, 1991). Moreover, there is strong epidemiological evidence to suggest that solar UVB causes skin cancer in man (Blum, 1959).

The UVR wavelengths from 320-400nm are termed ultraviolet A (UVA). Although UVA is not readily absorbed by protein or nucleic acids and is only mildly erythemogenic, much greater amounts reach the ground than either UVC or UVB. The oncogenicity of UVA has not yet been established, despite the suggestion that it can promote tumours at very high doses and be co-carcinogenic when administered in conjunction with UVB (Sterenborg *et al.*, 1990; Talve, Sterback and Jansen, 1990). The demonstration that UVA can eliminate Langerhans cells (LCs) from exposed skin without reducing the contact hypersensitivity (CH) response suggests that it might have immunosuppressive effects (Morison *et al.*, 1984).

Figure 1.1: The solar spectrum

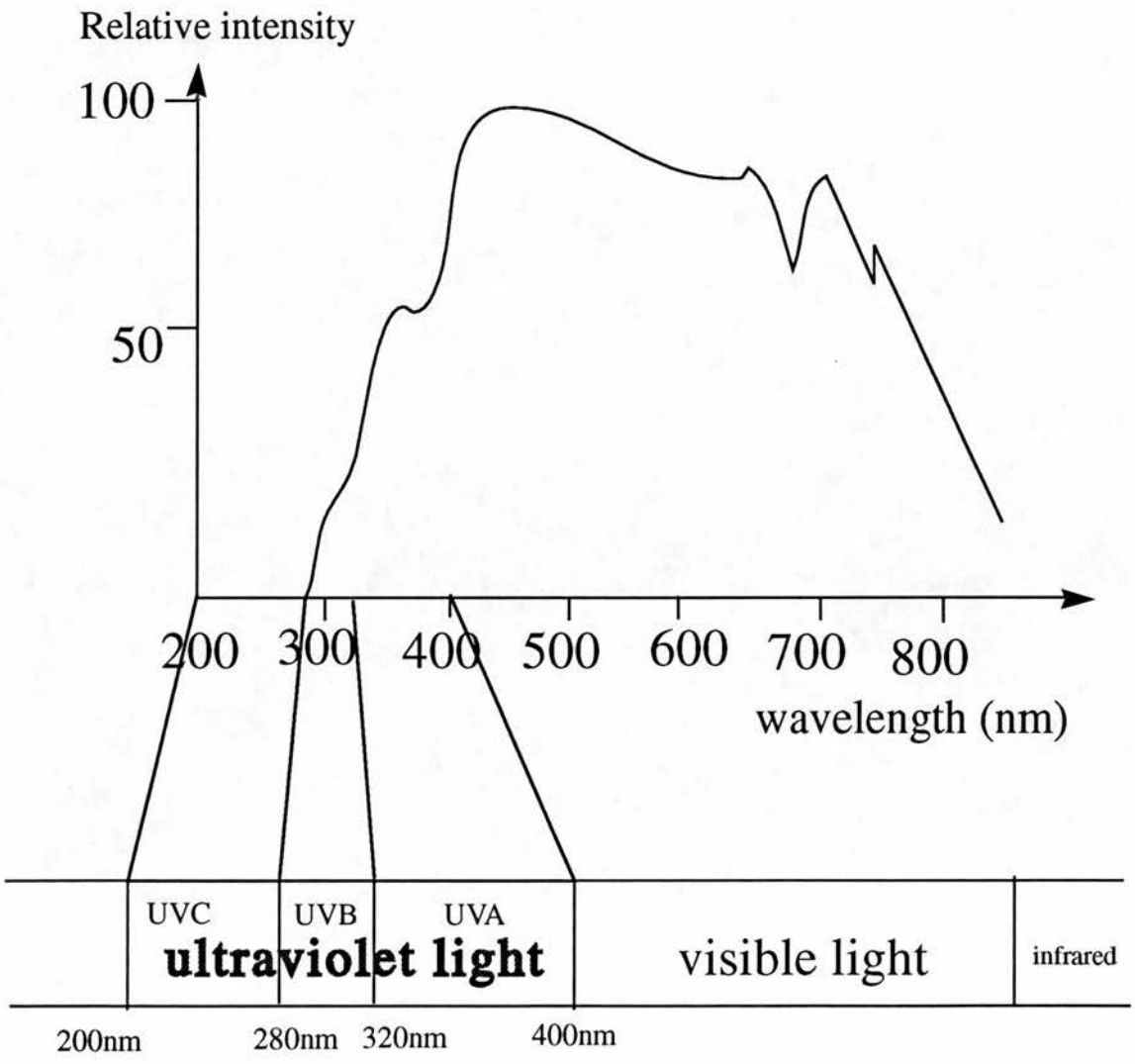

1.2 UV therapy for skin diseases

At the turn of the century, the Danish physician Niels Finsen won the third Nobel prize for his early work on phototherapy of cutaneous tuberculosis (Finsen, 1901). Today UV therapy is used to treat many different types of skin disease: the most common treatments being UVB phototherapy and psoralen photochemotherapy (PUVA)(Table 1).

UVB phototherapy is primarily used to treat inflammatory dermatoses such as psoriasis, acne, eczema and polymorphic light eruption. Phototherapy regimens are very variable with respect to the irradiation schedules and the equipment used. However, a typical conventional regimen might consist of 3 treatments per week for 4-6 weeks until the disease is cleared, which may then be reduced to 1 or 2 times per week for a short period of maintenance. The whole body may be exposed to irradiation within a cabinet lined with fluorescent bulbs. The beneficial effects of UVB in the treatment of such conditions may rely on the alteration or suppression of immune mechanisms which mediate the diseases.

The use of psoralens as photosensitizers is an ancient practice. Written documentation of the use of chemical substances in the environment combined with sun exposure to treat vitiligo dates to 1400BC (Fitzpatrick and Pathak, 1959). In the past 50 years, there has been much progress in the scientific study of psoralens and photochemotherapy. PUVA was introduced in 1974 as an alternative treatment for psoriasis and other dermatological diseases (Parrish *et al.*, 1974). During photochemotherapy, the patient ingests a psoralen photosensitizer such as 5- or 8-methoxypsoralen and then receives UVA radiation two hours later. An alternative to ingesting the psoralen is to bathe in a dilute solution of psoralen immediately (usually 15-30 mins.) prior to irradiation. UVA is administered to the whole body in a cabinet lined with UVA tubes. Clearance of psoriasis usually requires approximately 20 sessions over 4-10 weeks. Maintainance treatment following clearance can be given, although most dermatologists prefer to give short courses of PUVA without maintenance therapy to reduce the cumulative dose of radiation. In controlled studies PUVA has also been an effective treatment for several other skin diseases (Green *et al.*, 1992).

Table 1.1. Efficacy of phototherapy and photochemotherapy in the treatment of skin diseases.

SKIN DISEASE	UVB	PUVA
psoriasis	√	√
atopic eczema	√	√
polymorphic light eruption	√	√
mycosis fungoides	+/-	√
lichen planus		√
vitiligo		√
solar urticaria	+/-	√
photosensitive eczema		√
actinic reticuloid		√
pityriasis lichenoides chronica	√	√

Despite enormous research efforts to examine the animal response to UVR, there is still relatively little work concerning the human response. The few investigations into the effects of UVR on humans have generally employed unusually low or high doses *in vivo* or have used *in vitro* techniques which may have little relevance to solar UVR doses commonly encountered or those used therapeutically.

Decreases in stratospheric ozone over the Northern Hemisphere reached a record low in January and February 1992, and ozone depletion at 40^{o}N was estimated to be approximately 6% per decade (Stolarski *et al.*, 1992). The ozone layer shields the surface of the earth against all UVC and some UVB radiation. Therefore an increasing proportion of sunlight which reaches the earth will consist of UVB radiation. Thus, it will become increasingly important to investigate the influence of UVB on human health in doses relevant to solar UVB exposure.

The following sections review work concerning the skin immune system, antigen processing and presentation, and the effects of both chronic and acute UVR exposure on the skin.

1.3 The skin immune system

In 1978 Streilein proposed a novel theory in which the skin encompassed a separate branch of the immune system, the skin-associated lymphoid tissue (SALT), specialized to cope with the antigenic demands imposed upon it by the external environment. SALT was reported to be similar to other putative specialized branches of the immune system, such as the gut-associated lymphoid tissue. He postulated that the surveillance of skin for alterations or abnormalities is a continuous process performed by a pool of recirculating epidermotropic T lymphocytes. Evidence in favour of this hypothesis was drawn from the fact that large numbers of Cluster of Differentiation (CD) 4+ve T cells may migrate into the epidermis in lesions of cutaneous T cell lymphoma (Streilein, 1978; Haynes *et al.*, 1982). According to this theory, LCs would process antigens which penetrate the skin and present the antigens to recirculating T cells, either in the epidermis, dermis or within draining lymph nodes. Keratinocytes and endothelial cells were also considered to be integral parts of SALT (Streilein, 1978).

It is now clear that the skin is an active immunological organ and that many other cell types are participants in SALT (examples are given in table 1.2). This larger and more complex system is now more commonly known as the "skin immune system" (SIS) (Bos and Kapsenberg, 1986). Some of the principal cells of the SIS are discussed below and shown in fig. 1.2.

Figure 1.2: Cells of the skin immune system.

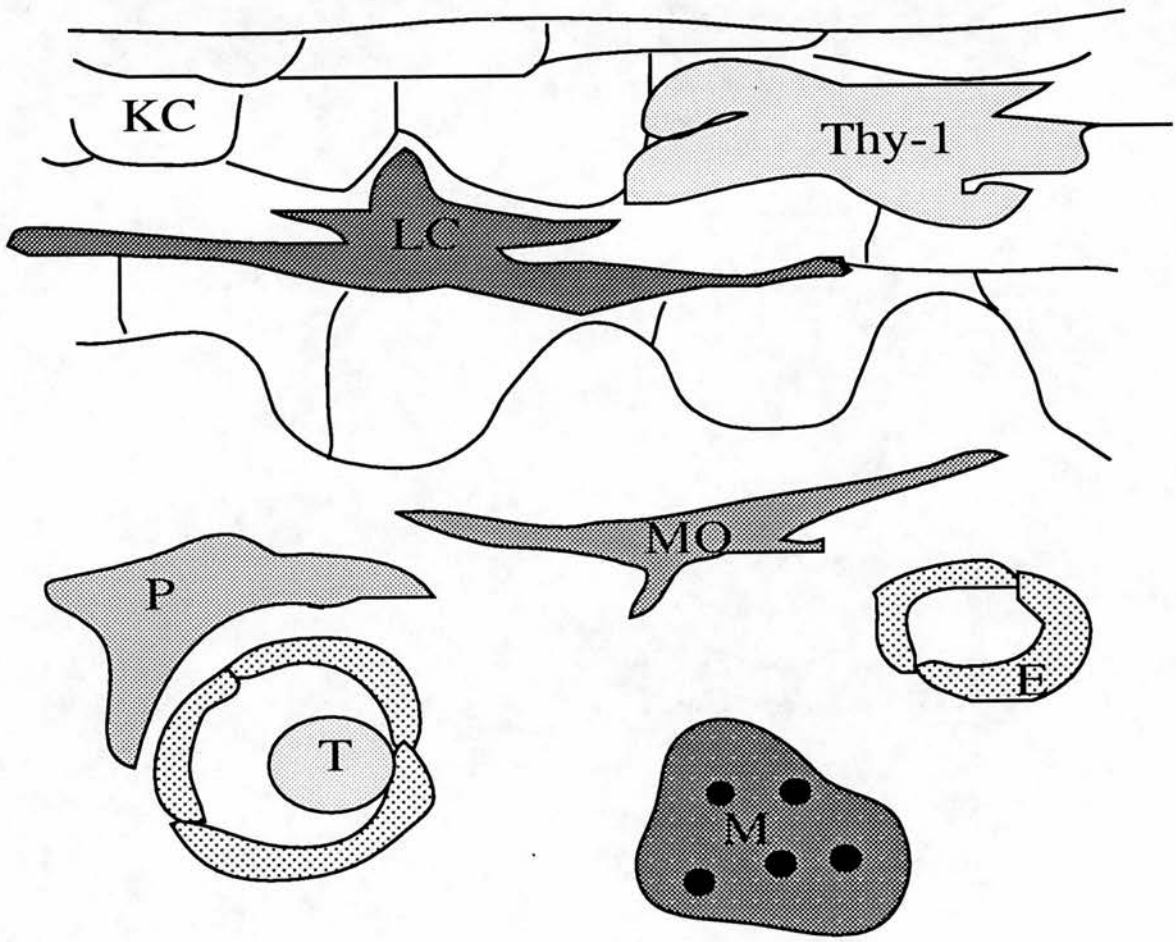

KC: keratinocyte
LC: Langerhans cell
Thy-1: Thy-1+ve cell
T: T cell
E: endothelium
P: perivascular MHCII+ve cell
M: mast cell
MO: macrophage

Table 1.2 Cellular constituents of the SIS

CELLULAR CONSTITUENTS OF THE SIS
Langerhans cells (Indeterminate cells)
keratinocytes
T lymphocytes
Thy-1 positive dendritic cells (present in murine epidermis only)
perivascular dermal MHC II+ve cells
veiled cells
macrophages
endothelial cells
ultraviolet resistant dendritic epidermal cells (mice only)
natural killer cells
B cells
mast cells
neutrophils

LANGERHANS CELLS were originally identified by Paul Langerhans in 1868, using a gold stain thought to be specific for neural tissue. They were initially believed to be of neural origin, but are now considered to be bone marrow-derived, dendritic antigen-presenting cells (APCs) that express many surface-bound molecules including surface adenosine triphosphatase (ATPase) activity, CD1a,c, and CD4 (Katz et al., 1979; De Panfilis *et al.*, 1988). Surface major histocompatibility class II (MHC II) molecules (Human leukocyte-associated, HLA-DP,-DQ,-DR) are constitutively expressed by LCs in approximately equal amounts (Sontheimer *et al.*, 1986). Receptors for the Fc portion of IgG, receptors for the Fc portion of IgE (Torresani *et al.*, 1991), the type 3 complement receptor (De Panfilis *et al.*, 1990a), and certain integrin molecules are also expressed on LC surfaces. The main type of cell necessary for presentation of antigen encountered in the epidermis for cell-mediated immune responses belongs to the family of bone marrow-derived dendritic cells which may be ontogenically related. They are all cells with a dendritic morphology and include LCs, indeterminate cells, veiled cells, dendritic cells (DCs) of peripheral blood, perivascular dermal MHC II+ve cells and interdigitating cells of the lymph node paracortex (Knight *et al.*, 1992). DCs are bone marrow-derived cells which are present in peripheral blood, become distributed in small numbers throughout all tissues

(e.g. LCs in epidermis) and move via afferent lymphatics to the paracortex of lymph nodes (MacPherson, 1989).

LCs make up approximately 2-8% of the total epidermal cell (EC) population (Hunter, 1983; Bjercke *et al.*, 1987; Hanau *et al.*, 1988). They mainly occupy a suprabasal epidermal position, with their dendrites lying in close proximity to those of neighbouring LCs (fig. 1.3), to give rise to a discontinuous network (Shelley and Juhlin, 1976). Their position within the epidermis suggests that they are one of the first lines of immunological defence against pathological organisms penetrating the skin.

Precursors of LCs have been identified in peripheral blood and appear to be increased in the peripheral blood of subjects who have lost skin through burns (Gothelf *et al.*, 1988). LCs appear to reside within murine epidermis for around 3 weeks (Katz *et al.*, 1979; Toews *et al.*, 1980a). Phototherapy, photochemotherapy and natural sunlight deplete the skin of LCs (Zelickson and Mottaz, 1970; Aberer *et al.*, 1986) and after PUVA, the time required for repopulation of human epidermis by LCs is also approximately 3 weeks (Friedmann *et al.*, 1983). Further discussion of UV-induced depletion of LCs is given in section 1.9. Intra-epidermal LCs occasionally undergo mitosis *in situ* (de Fraissinette *et al.*, 1988; Miyauchi and Hashimoto, 1989) and may be lost by exfoliation (Davis, Mackenzie and Hart, 1988). LC proliferation may occur during the recovery of LC numbers after UV irradiation (Miyauchi and Hashimoto, 1987; Bos, Teunissen and Kapsenberg, 1988).

Distinguishing ultrastructural features of LCs (figs. 1.4 and 1.5), include an indented nucleus, prominent Golgi apparatus and the unique cytoplasmic organelle, the Birbeck granule (BG; Birbeck *et al.*, 1961). The BG is the most reliable means of identifying LC. It is a rod-shaped organelle that is sometimes associated with a vacuole, giving it an appearance similar to a tennis racket (fig. 1.5). Usually BGs are situated close to the Golgi apparatus, but they are sometimes continuous with the cell membrane. Recently a BG-specific monoclonal antibody has been raised, called LAG (Kashihara *et al.*, 1986). BGs associated with cell surfaces have been shown to take up lanthanum and peroxidase from the extracellular space (Hunter, 1983; Gawkrodger *et al.*, 1989; Bartosik, 1992). The function of these granules may be secretory or endocytic (Wolff and Schreiner, 1970; Takigawa *et al.*, 1985; Takahashi and Hashimoto, 1985). Lending support to the latter view, the receptor-mediated endocytosis of both CD1a and HLA-DR antigens has been shown to involve BGs. Therefore, the granules are a possible means for intracellular transport of both CD1a and HLA-DR molecules (Hanau *et al.*, 1987,1989). Furthermore, the uptake of peroxidase by LCs involves the

formation of BGs at the cytomembrane which are able to transport the substance to the endosomal compartment (Bartosik, 1992).

An immunological role for LCs was first suggested in 1973 when Silberberg noted direct contact between LCs and lymphocytes at sites of CH reactions (Silberberg, 1973). The CH response is a form of delayed type hypersensitivity (DH) reaction in which the antigen penetrates into skin and is first encountered there. Presentation of antigen by LCs to naive T cells is believed to occur within the epidermis or draining lymph node and results in the clonal proliferation of an antigen-specific T cell subpopulation in the draining lymph node (Turk, 1971; Shelley and Juhlin, 1977; Jones *et al.*, 1989). These T cells form a long-lived clone of circulating memory and effector T cells which can recognize and rapidly respond to a second exposure to the antigen (Turk and Oort, 1963). The typical inflammatory reaction (associated with a dermal T cell and macrophage infiltrate) becomes apparent in skin a number of hours after the second contact has occurred, and is maximal at 24-48 hours.

LCs have been identified in dermal lymphatics draining the site of CH reactions (Silberberg *et al.*, 1976; Macatonia *et al.*, 1987). Furthermore, DCs isolated from draining lymph nodes may be derived from epidermal LCs. The observation that both LCs and DCs express the cell surface antigen recognised by the antibody, NLDC-145, supports this hypothesis (Kraal *et al.*, 1986). Moreover, the short-term culture of murine LCs alters their function, phenotype and morphology such that they resemble lymphoid DCs, a process which may be similar to *in vivo* maturation of LCs after they migrate to dermal lymphatics. These alterations may be mediated by the cytokines, granulocyte macrophage colony-stimulating factor (GM-CSF) and interleukin (IL)-1 (Schuler and Steinman, 1985; Heufler, Koch and Schuler, 1988; Koch *et al.*, 1990). Whether the alterations to murine LCs induced *in vitro* bear any resemblance to events *in vivo* is currently being investigated. It has been argued that the phenotypic and functional changes induced in human LCs *in vitro* might be simply attributed to recovery from the trypsinization process used to isolate the cells (Teunissen *et al.*, 1991a). Others have shown a sharp rise in the number of antigen-bearing DCs in draining lymph nodes following the skin painting of mice with contact sensitizers, and a proportion of DCs bear high levels of antigen. Such antigen-bearing DCs are MHC II +ve, intercellular adhesion molecule (ICAM)-1+ve, readily form clusters with T cells both *in situ* and *in vitro*, and are potent stimulators of *in vitro* primary and secondary T cell proliferative responses (Knight *et al.*, 1985; Macatonia *et al.*, 1987; Cumberbatch

Figure 1.3: Langerhans cells in a sheet of human epidermis, viewed 'en face' and labelled using anti-CD1a primary antibody and an immunoperoxidase technique. Magnification 125 x

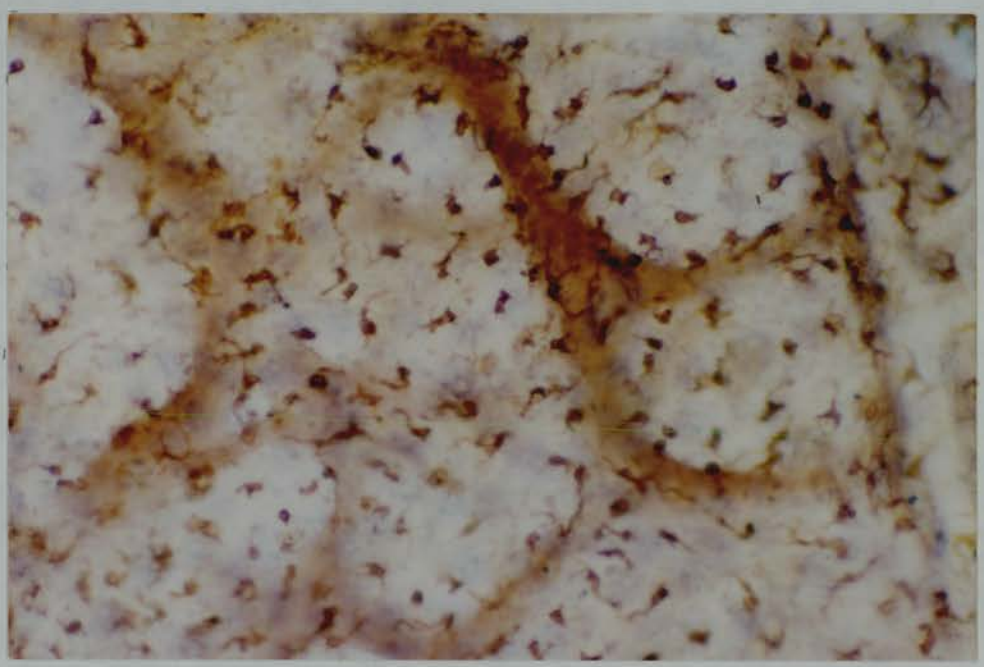

Figure 1.4: Human Langerhans cell within the epidermis, showing indented nucleus (asterisk), centriole (arrow) and cytoplasmic Birbeck granules (arrowheads).
Magnification 9,300 x

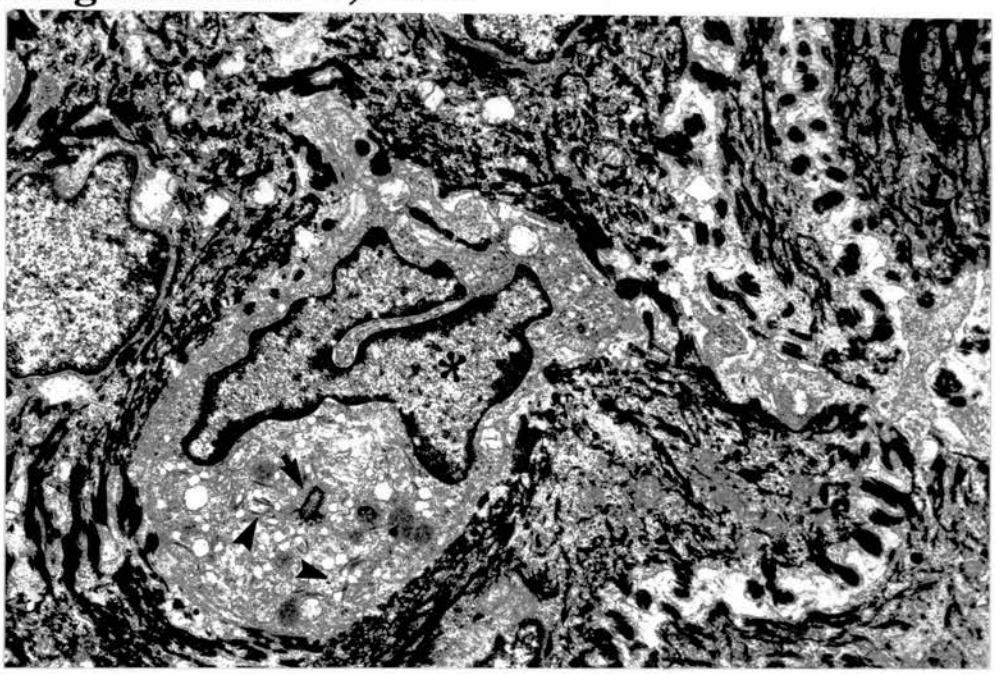

Figure 1.5: Birbeck granules (arrowheads) within the cytoplasm of a human epidermal Langerhans cell.
Magnification 72,000 x

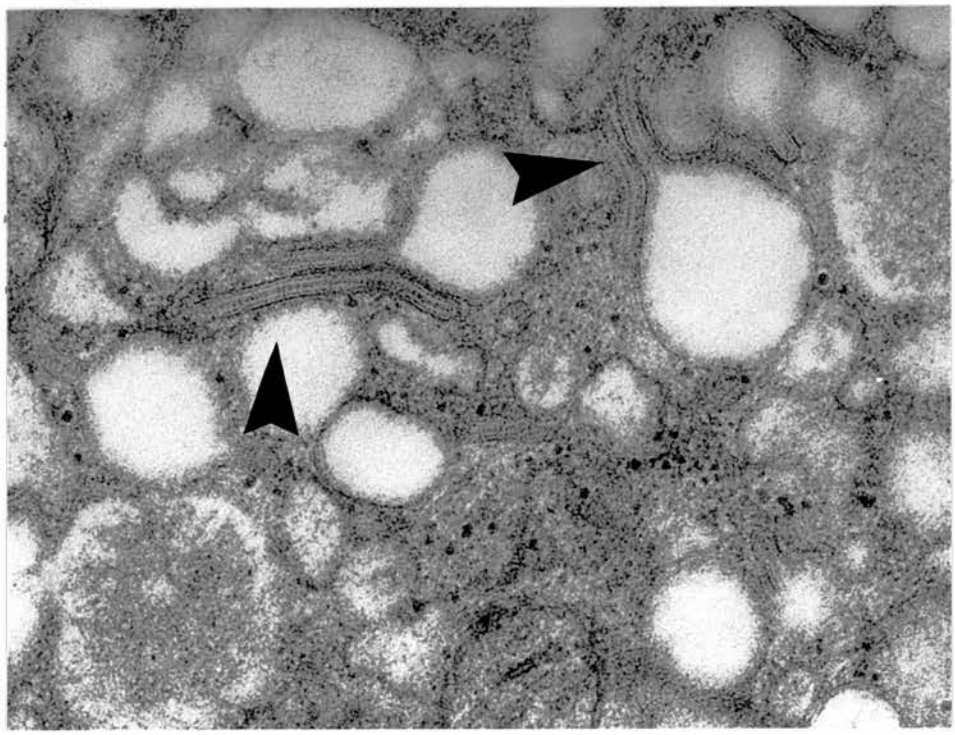

and Kimber, 1990; Kimber *et al.*, 1990; Cumberbatch, Illingworth and Kimber, 1991). The number of antigen-bearing cells in lymph nodes is maximal at 48 hours and returns to normal by 4 days, a time course that is similar to that of the loss of LCs from the skin after antigen sensitization. Therefore, the application of antigen on mouse skin appears to stimulate LC migration to draining lymph nodes where these antigen-bearing cells are detected as DCs. The migration of LCs to draining lymph nodes in mice may be induced by the cytokines, tumour necrosis factor (TNF)-α and IL-1 (Cumberbatch and Kimber, 1992a).

Much information, albeit circumstantial, has accumulated to support the hypothesis that LCs can present antigen to T lymphocytes (Stingl *et al.*, 1978; Ptak *et al.*, 1980; Wolff and Stingl, 1983). LCs are the only cell type in normal human skin, with the exception of acrosyringeal keratinocytes, to express membrane-associated MHC II molecules (Carr *et al.*, 1986; McGregor *et al.*, 1991). This implies that they can process and present antigen. LCs are able to present a wide variety of antigens including alloantigens, tumour antigens, soluble antigens such as nickel, some viral antigens and particulate antigens such as tuberculin purified protein derivative to T cells *in vitro* (Bjercke *et al.*, 1984; Sontheimer, 1985; Rasanen *et al.*, 1986; Res *et al.*, 1987; Everness *et al.*, 1988; Grabbe *et al.*, 1991). They can present antigen to both Th1 and Th2 lymphocytes (see section on lymphocytes, p11; Tiegs *et al.*, 1990). They also appear to be the primary stimulators of both allogeneic and syngeneic mixed lymphocyte reactions (Braathen and Thorsby, 1980; Stingl *et al.*, 1981). In addition, LCs can prime effector cells such as cytotoxic T cells (McKinney and Streilein, 1989), and play a pivotal role in many DH reactions such as induction of CH and the rejection of skin grafts (Streilein and Bergstresser, 1983). Murine skin that is depleted of LCs by UV irradiation, or that is naturally deficient in LCs, does not support the induction of CH to dinitrofluorobenzene (DNFB; Toews *et al.*, 1980b). The depletion of LCs in human skin by topical steroid or by PUVA therapy also reduces antigen presentation *in vitro* (Ashworth, Kahan, and Breathnach, 1989a,b). Furthermore, LC depletion in murine epidermis by UVR *in vivo* leads to prolonged skin graft survival in allogeneic recipients (Odling, Halliday and Muller, 1987). Finally LCs may even be responsible for presentation of viral and tumour-associated antigens (Wolf and Stingl, 1983). The enrichment of LCs in EC suspensions *in vitro* has been shown to enhance the presentation of candida and herpes simplex virus (HSV) antigens (Bjercke *et al.*, 1984).

LCs express certain integrins on their surfaces. Integrin molecules consist of an α subunit bound non-covalently to a β subunit. There are 3 distinct subfamilies of integrins expressing different although homologous β subunits, β1, β2 and β3. The β1

subfamily consists of the very late antigen (VLA) proteins and are involved in cell-matrix as well as cell-cell interactions. The β2 subfamily of leukocyte integrins consist of Lymphocyte function-associated (LFA)-1, Mac-1, and p150-95 molecules. The β3 subfamily of cytadhesion molecules consists of gpIIa/IIIa and the vitronectin receptor. LCs and basal keratinocytes express the integrin β1 subunit (Staquet *et al.*, 1989; Le Varlet *et al.*, 1991) and LCs express the β2 subunit of leukocyte integrins CD11b/CD18 and CD11c/CD18 in addition to ICAM-1 which might facilitate their adhesion to T cells (De Panfilis *et al.*, 1989). The expression of LFA-3 has been demonstrated on LCs and may be important for LFA-3/CD2 antigen-specific recognition by T cells (De Panfilis *et al.*, 1991). The interaction of LC integrin molecules with ligands on T cells is required for optimal stimulation of the mixed epidermal cell leukocyte reaction (MECLR) and the pre-incubation of LCs with anti-CD11a/CD18 and anti-ICAM-1 antibodies inhibits the reaction to a similar extent to anti-HLA-DR antibody (Simon *et al.*, 1991a).

When APCs present antigen to T lymphocytes, the APCs produce IL-1 which, in subnanogram quantities, activates T cells in the presence of antigen and causes them to secrete IL-2. Isolated human LCs produce the cytokines IL-1β and IL-6 (Schreiber *et al.*, 1992).

"INDETERMINATE CELLS" are resident within the normal epidermis and are HLA-DR +ve, CD1a +ve APCs with a dendritic morphology that is similar to that of LCs. Their lack of cell-specific intracellular organelles such as pre-melanosomes (seen in melanocytes), the granules that characterize Merkel cells or BGs has lead to the definition of "indeterminate cells" (Breathnach, 1975). For many years indeterminate cells were considered to differ from LCs by their absence of BGs on ultrathin sectioning. However a recent detailed ultrastructural study demonstrated that "indeterminate cells" may simply represent a sampling phenomenon in which ultrathin sections of LCs which contained no BGs were mistaken as a separate cell type (Silberberg-Sinakin *et al.*, 1980; Bartosik *et al.*, 1991). Cells that are morphologically similar to "indeterminate cells" and that are CD1a and CD1c +ve have been detected in the papillary dermis (Murphy *et al.*, 1983; Van de Rijn *et al.*, 1984). Moreover, dermal cells have been described which are transitional between dermal "indeterminate cells" and epidermal LCs (Breathnach, 1980). The relationship between these cells is unclear, but there is speculation that they represent LC precursors or LCs migrating from the skin to the draining lymph nodes (Bos and Kapsenberg, 1986).

KERATINOCYTES make up approximately 96% of the total EC pool and form a multi-layered sheet of cells. Their most important function is to produce an impermeable horny layer at the surface of the epidermis, which prevents the absorption and penetration of various pathogens and harmful agents (such as bacteria, viruses, chemicals and UVR). Murine keratinocytes produce macrophage colony stimulating factor, GM-CSF, IL-1β, contra IL-1, IL-3, IL-7 and IL-10, whereas human keratinocytes produce IL-1α and β, IL-3-like factor, IL-6, IL-8, IFN–α, epidermal-cell derived lymphocyte differentiation factor, transforming growth factor α and β (TGF α,β), GM-CSF and TNF α,β. This suggests that keratinocytes probably play an active role in the SIS (Matsue *et al.*, 1992; Schreiber *et al.*, 1992).

Usually, keratinocytes do not express MHC II, except for a small subpopulation of cells in the acrosyringium of sweat glands (Carr *et al.,* 1986; McGregor *et al.*, 1991). Under the influence of T cell-derived γ-interferon (IFN) in inflammatory dermatoses, however, or after *in vitro* stimulation with γ-IFN, the majority of keratinocytes can be induced to synthesize MHC II (Volc-Platzer *et al.*, 1985; Nickoloff *et al.,* 1985; Aubock *et al.*, 1986; Barker *et al.*, 1988). They then express more HLA-DR than -DP or -DQ (Gawkrodger *et al.*, 1987; Volc-Platzer *et al.*, 1988). Keratinocytes that are HLA-DR+ve can cause lymphoproliferation *in vitro* but will not do so unless exogenous IL-2 is present (Nickoloff *et al.*, 1986; Morhenn and Nickoloff, 1987). HLA-DR+ve keratinocytes may augment the presentation of purified protein derivative of tuberculin antigen *in vitro* by ECs (Tjernlund and Scheynius, 1987). However, if LCs are removed from the EC suspensions, antigen presentation is abolished (Scheynius *et al.*, 1988). Incubation of murine trinitrophenol (TNP)-modified MHC II+ve keratinocytes with TNP-specific T cell clones results in unresponsiveness of the T cells to subsequent stimulation with TNP-modified LCs. In this case MHC II+ve keratinocytes seem to have been providing downregulatory signals to T cells (Gaspari,Jenkins and Katz, 1988).

LYMPHOCYTES consist of two major functionally distinct subsets: B-lymphocytes which produce antibodies in humoral immune responses, and T-lymphocytes which interact with cell-associated antigens in cell-mediated immune responses (Miller, 1966).

Human T cells express the CD3 T cell antigen receptor (TCR) and the receptor for sheep red blood cells (CD11). A subdivision of T cells separates helper and delayed hypersensitivity T cells (that express the CD4 antigen and generally upregulate immune responses), from suppressor and cytotoxic T cells (that express the CD8 antigen and

generally suppress immune responses). CD4 positive T cells are further subdivided into two groups: helper and suppressor-inducer lymphocytes (Morimoto *et al.*, 1985a, b). Both mouse and human T helper cells can be divided into Th1 and Th2 subsets that are distinguished by functional criteria and by their cytokine profile. Th1 cells produce IL-2 and γ-IFN and are primarily involved in providing help for DH reactions, whereas Th2 cells are more efficient at mediating help for antibody production and secrete IL-4, IL-5, and IL-10 (Noelle and Snow, 1992).

The lymphocytes located in skin are mainly T cells, and most are found in the dermis around vascular channels and appendages. Dermal perivascular/appendageal lymphocytes are a mixture of both CD4 and CD8+ve T cells. Epidermal lymphocytes are sparsely distributed and predominantly of the CD2+ve/CD3+ve/CD8+ve phenotype. However, more sensitive staining techniques have revealed greater numbers of epidermal CD4+ve suppressor-inducer T cells than originally suspected (Rowden *et al.*, 1988).

T cells often return to and accumulate in sites at which they first became activated to an antigen (Scheper *et al.*, 1985; Drijvestijn and Hamann, 1989). The mechanism by which they migrate to a specific site may involve expression of cell surface integrin molecules, 'addressins', on cells within those tissues. Such 'addressins' may interact with lymphocyte-specific integrin molecules on the surface of T cells. For example, migrating T cells interact with endothelium via the T cell integrin LFA-1 and the 'addressin' ICAM-1 which is present primarily on endothelia of draining lymph nodes and to a lesser degree on vascular channels (Hogg, 1989). Epidermotropic migration of a T cell clone can be inhibited *in vivo* and *in vitro* by monoclonal antibodies against LFA-1 (Shiohara *et al.*, 1988). Increased expression of 'addressins' occurs after exposure to cytokines including γ–IFN, IL-1 and TNF secreted by activated helper T cells and macrophages.

THY-1 +VE CELLS are MHC class II -ve, bone marrow-derived dendritic T cells which are only present in murine epidermis and that express abundant surface-bound Thy-1 antigens (Tschachler *et al.*, 1983; Bergstresser *et al.*, 1983; Breathnach and Katz, 1984). The CD3 antigen is expressed by these cells in association with the TCR γ/δ heterodimer, in contrast to the majority of peripheral T lymphocytes which express the TCR α/β heterodimer (Krueger and Stingl, 1989). Evidence suggests that Thy-1 +ve cells have cytotoxic capabilities similar to natural killer (NK) cells and that they may activate suppressor T cell circuits (Sullivan *et al.*, 1986; Okamoto and Kripke, 1987). The ratio of LCs to Thy-1 +ve cells correlates well with the intensity of a DH response

oxazolone and trinitrochlorobenzene (TNCB; Bigby *et al.*, 1987). However, there is no evidence that Thy-1+ve cells can transport antigen to draining lymph nodes (Cumberbatch and Kimber, 1990).
There is no Thy-1 positivity or reactivity in human epidermis. However, a possible human equivalent of the Thy-1+ve cell has been described (Bos *et al.*, 1988) which is sparsely distributed through the epidermis and is distinguishable by its expression of the γ/δ TCR.

PERIVASCULAR DERMAL MHC II+VE CELLS express high density of MHC II, Factor XIIIa, HLA-DR, HLA-DQ, OKM5 and mono1 (Cooper *et al.*, 1986; Cerio *et al.*, 1989) but not CD1, Factor VIII or Thy-1.2 (Sontheimer *et al.*, 1989). Murine dermal MHC II+ve cells can present antigen in DH responses, and may present antigen to T cells migrating through the dermis (Tse and Cooper, 1990).

VEILED CELLS are DCs found in afferent lymphatics (Drexhage *et al.*, 1979). They express HLA-DR, CD1a, receptors for Fc and C3, but not surface immunoglobulins (Balfour *et al.*, 1981). Occasional veiled cells contain BGs and might represent LCs migrating from epidermis to lymphatics (Silberberg-Sinakin *et al.*, 1980; Macatonia *et al.*, 1987). On arrival in the paracortex of lymph nodes, veiled cells may become RFD1 +ve interdigitating cells which present antigen to T cells (Bos and Kapsenberg, 1986). Veiled cells, DCs from draining lymph nodes and LCs all react with the antibody NLDC-145 indicating that these cells may be related in origin (Kraal *et al.*, 1986).

MACROPHAGES are MHC II+ve antigen presenting cells which in skin are present mainly in papillary dermis and also scattered through the reticular dermis (Bos and Kapsenberg, 1986). The presentation of antigen by macrophages in most *in vitro* models, however, is much less efficient than by dendritic APCs (Van Voorhis *et al.*, 1983).

ENDOTHELIAL CELLS are normally MHC II-ve, but like fibroblasts and keratinocytes described above, can be induced to become MHC II+ve under the influence of γ-IFN (Pober *et al.*, 1983). Whether these cells are able to initiate primary T cell responses is unknown.

Specialized endothelial cells which constitute high endothelial venules (HEV) are found in lymph nodes and may facilitate the migration of lymphocytes across the vessel wall. However, HEV are not present in normal skin and have only been described in some

inflammatory skin conditions (Drijvestijn and Hamann, 1989). Therefore, HEV are unlikely to play a major role in skin T cell infiltration.

1.4 The major histocompatibility complex.

The human MHC is located on the short arm of chromosome six, and comprises three classes of proteins (fig. 1.6). Almost all nucleated cells express MHC class I (MHC I) antigens. Human cell surface MHC I antigens consist of two polypeptide chains, composed of a highly polymorphic heavy chain (~45 kDa) that spans the cell membrane, and a non-polymorphic non-covalently attached light chain (~12 kDa) that is extracellular. The light chain, β2-microglobulin, is encoded by chromosome 15, whereas the heavy chain is encoded by the HLA-A,-B, and -C loci of chromosome six. The heavy chain consists of five domains, one cytoplasmic, one transmembrane, and three extracellular. The antigen-binding groove has been detected by X-ray crystallography on the upper surface of the MHC I molecule (Bjorkman *et al.*, 1987).

The CD1 family comprise at least three different cell surface glycoproteins, CD1a, CD1b and CD1c, which are encoded within chromosome six and have molecular masses of 49, 45, and 43 kDa respectively. They are considered to be non-classical MHC I molecules and are expressed on cortical thymocytes, leukemic T cells, dendritic cells and LCs. Although they are similar in gene structure to MHC I molecules, possessing a highly conserved domain which is homologous with the domain that binds β2-microglobulin, they differ from MHC I in that they lack significant polymorphism. The function of these molecules has not yet been established. Recently, CD1 molecules have been reported to act as ligands recognized by certain T cell lines (Porcelli *et al.*, 1989; Faure *et al.*, 1990; Balk *et al.*, 1991). This raises the speculation that they may be involved in the activation of T cells by accessory cells. Indeed, a recent report has shown that CD1a molecules may play a role in the activation of allogeneic T cells (Moulon *et al.*, 1991).

The expression of MHC II antigens is limited to a group of cells collectively known as accessory cells, which include APCs which constitutively express MHC II, and certain other cell types which can be induced to express MHC II. Many types of accessory cell have been identified, such as B cells, macrophages, spleen DCs, lymph node follicular DCs, blood DCs, veiled cells, LCs, activated T cells, vascular endothelial cells, and keratinocytes.

Cell surface MHC II glycoproteins are heterodimers, consisting of non-covalently linked α chains (~34 kDa) and β chains (~29kDa; fig. 1.7). The human HLA-D region encodes the MHC II glycoproteins, and is divided into three main subregions: HLA-DP, HLA-DQ and HLA-DR, but also includes genes called DNα and DOβ, the products of which have not yet been detected (see fig. 1.6). These molecules are highly polymorphic, the greatest polymorphisms occurring in the HLA-DQ α chain and the β chains of all three loci (reviewed by Trowsdale *et al.*, 1985). A further increase in the repertoire of MHC II antigen expression exists if hybrid molecules form, such as the α chain from one HLA-DQ allele associating with the β chain of a different HLA-DQ allele (Giles *et al.*, 1985). In mice, the MHC region is found on chromosome 17. The I region of the murine MHC corresponds to the human HLA-D region and includes genes for MHC II molecules. Products of the I region are termed Ia antigens, which is also the generic name for human HLA-D products. The exact molecular structure of MHC II molecules by X-ray crystallography has not yet been achieved. By analogy with MHC I structure, it is assumed that the peptide binding site consists of a platform of eight strands of β-pleated sheet with two α-helices on the boundaries (Brown *et al.*, 1988; Gerlier and Rabourdin-Combe, 1989).

Expression of MHC II molecules on APCs can be modulated by soluble mediators. IL-4, γ-IFN, and GM-CSF induce, whereas prostaglandins E1 and E2, α-fetoprotein, and colony stimulating factor-1 inhibit MHC II synthesis and expression (Snyder *et al.*, 1982; Willman *et al.*, 1989). Qualitative or quantitative variation of MHC II expression may influence cellular function (Janeway *et al.*, 1984). For example, pre-incubation of monocytes *in vitro* with γ-IFN augmented the expression of HLA-DP and HLA-DQ as well as the antigen presenting function of these cells (Gonwa, Frost and Karr, 1986).

The functions of the HLA-D region products may be similar or overlapping. All three types of MHC II antigen can induce suppressor T cells (Sasportes *et al.*, 1978; Pawelec *et al.*, 1984; Odum *et al.*, 1986; Hirayama *et al.*, 1987) and act as restriction elements for T cell proliferation (Qvigstad *et al.*, 1984). Furthermore, HLA-DR, HLA-DP and possibly HLA-DQ (although this is difficult to establish due to tight linkage disequilibrium between HLA-DQ and HLA-DR) can act as transplantation antigens (Olerup *et al.*, 1990). All three MHC II loci appear to be involved in the presentation of HSV by ECs, and the presentation of nickel and chlamydial antigens by peripheral blood adherent cells to T cells (Qvigstad *et al.*, 1984; Emtestam *et al.*, 1988; Everness *et al.*, 1988; Vestey, 1990a).

Figure 1.6: The human MHC

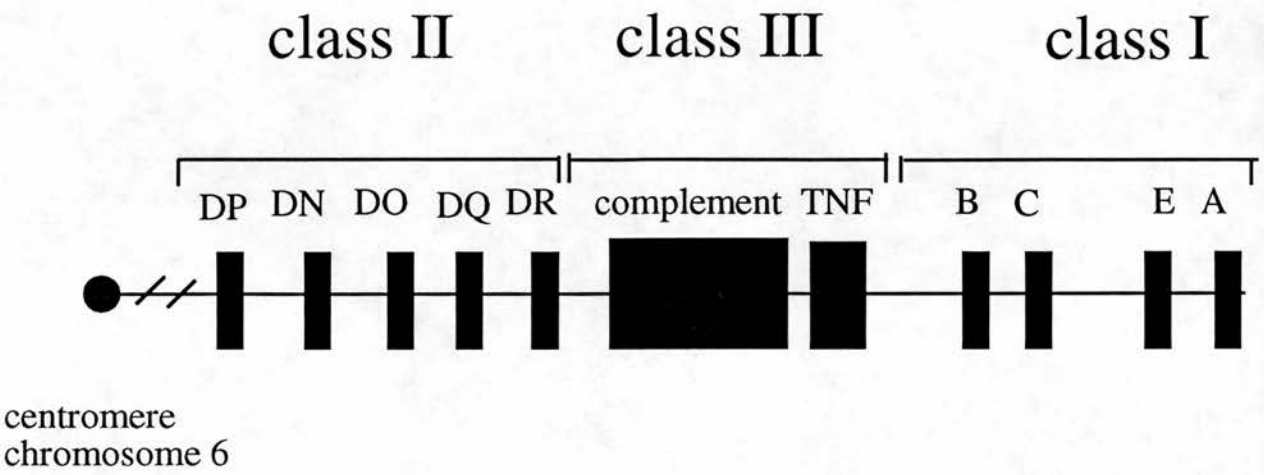

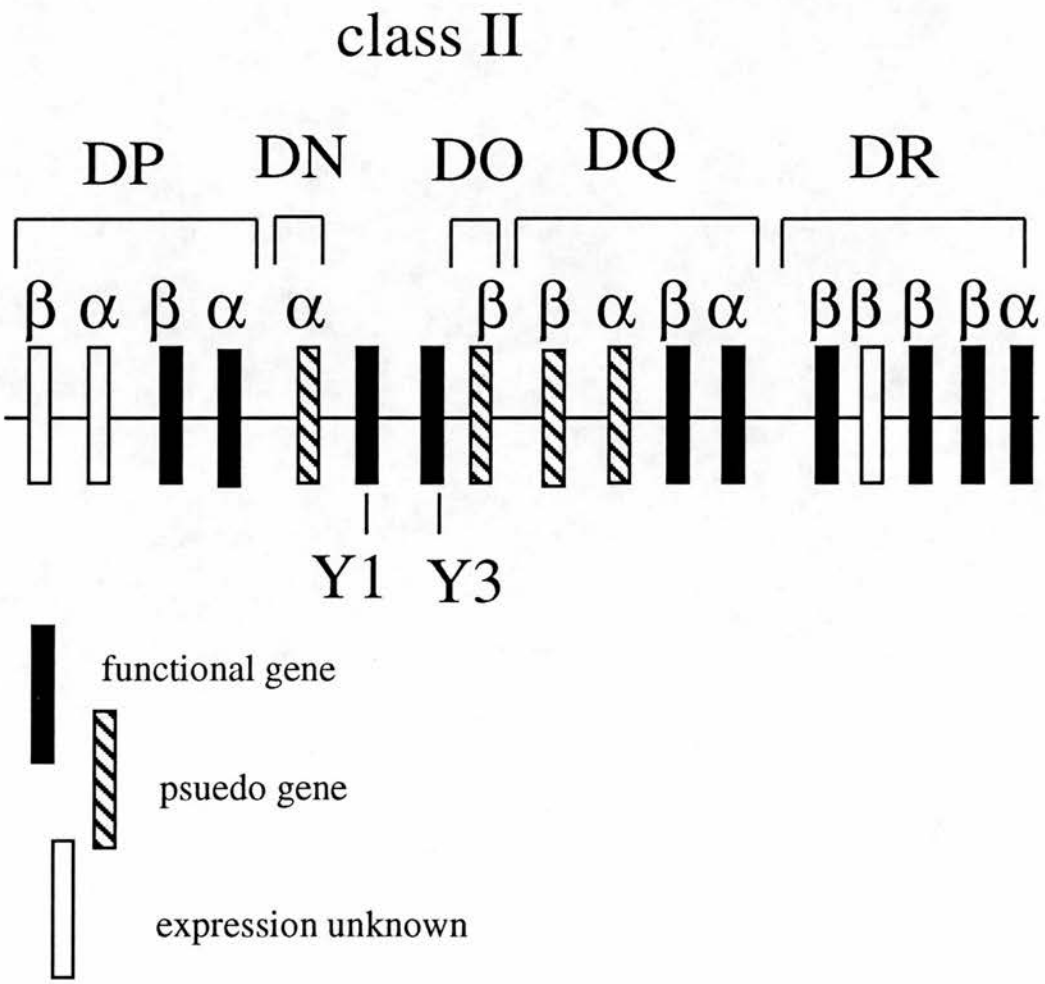

Figure 1.7

MHC CLASS II ANTIGEN

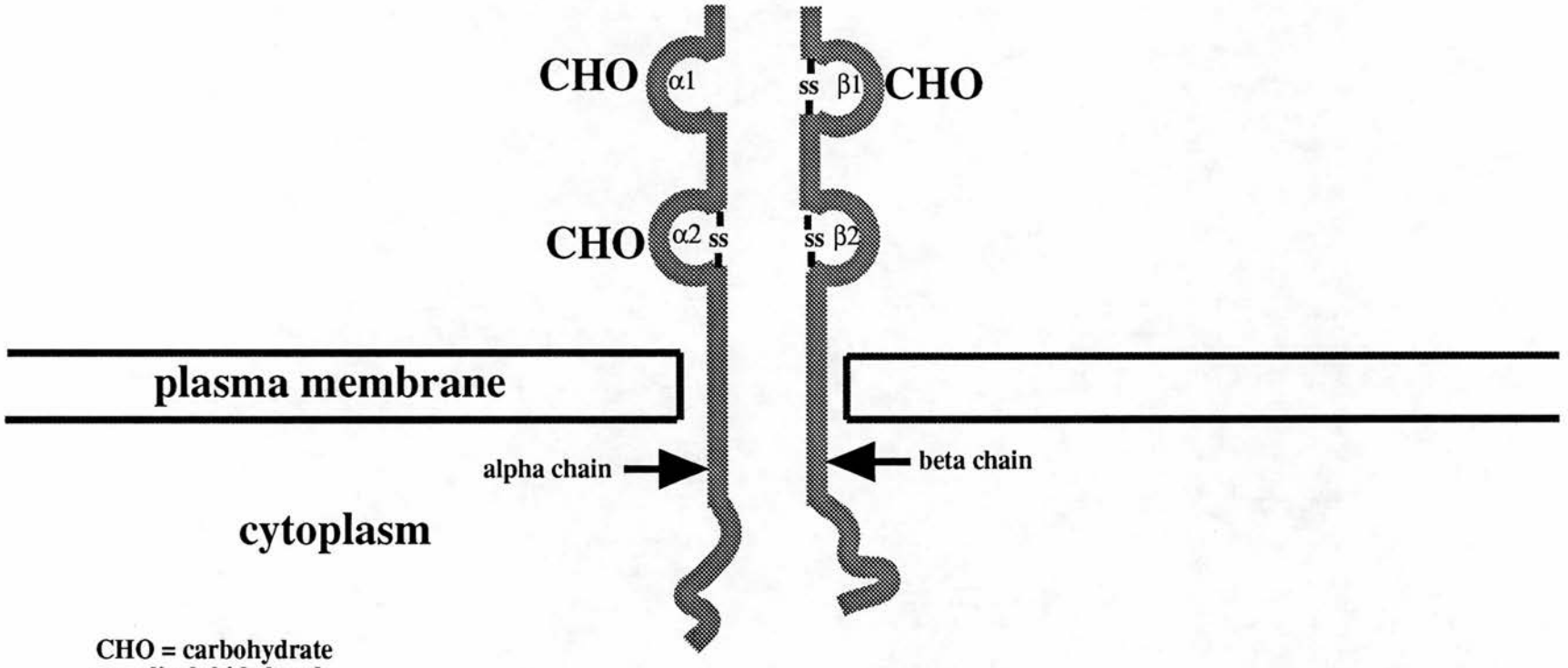

Conversely, it has been suggested that HLA-DP, HLA-DQ and HLA-DR have different functions. Evidence from *in vitro* studies suggest that HLA-DQ molecules may be involved in the activation of HLA-DR +ve cytotoxic and suppressor subpopulations of T cells whereas HLA-DR molecules may be directly involved in T helper cell proliferation (Navarette *et al.*,1985; Nieda *et al.*,1988). Most plastic-adherent cells (monocytes) of peripheral blood express HLA-DP and HLA-DR in varying amounts (Nunez *et al.*, 1984). However, less than half of them express detectable levels of HLA-DQ (Chen *et al.*, 1984). The HLA-DQ +ve adherent cell subset is responsible for presentation of *C. albicans* to T cells and is more effective than the HLA-DQ -ve subset in stimulation of autologous mixed lymphocyte reactions (Gonwa *et al.*, 1983). Both the HLA-DQ+ve dendritic cells and monocytes are more efficient stimulators of allogeneic T cells than the HLA-DQ-ve component of adherent cells (Nunez *et al.*, 1985). Nunez *et al.* have shown that concomitant expression of HLA-DQ and high levels of HLA-DR are phenotypic markers of the main stimulatory adherent cell subset. It is not clear whether these molecules are directly involved in antigen presentation or whether they are simply markers for the ability to present antigen (Brooks and Moore, 1988). There is also evidence that particular HLA-DQ molecules (HLA-DQw1 expressed on T cells) are involved in the induction of suppressor T cells (Festenstein and Ollier, 1987), and the activation of suppressor T cells by APCs during the presentation of *Schistosoma japonicum* antigen and Streptococcal cell wall antigen to CD4+ve T cells (Hirayama *et al.*, 1987). Activated T cells which are HLA-DP+ve are capable of suppressor T cell induction and may provide a negative feedback mechanism for the cellular immune response (Pawalec *et al.*, 1984).

The class II region of the MHC also contains genes whose products may be proteases for degradation of peptides, and others which may mediate transport of these peptides from the cytosol to the endoplasmic reticulum for the association with MHC I molecules. These particular genes have been named Ham-1, Ham-2, Lmp-2 and Lmp-7 in the mouse or Ring12, Ring 4, Ring 10 and Ring11 in the human (Monaco, 1992).

The products of MHC class III loci include proteins of diverse function such as TNFα and β, in addition to components of the complement system (C2, C4A, C4B, Factor B).

Presentation of antigen by macrophages to T cells can only occur if the cells are histocompatible (Rosenthal and Shevach, 1973). The expression of MHC antigens is a pre-requisite for the presentation of antigen by any cell, because T cells can only recognize a complex consisting of the antigen and either an MHC class I or a class II molecule. The requirement for an association between MHC I or II molecules and

antigen, to enable that antigen to be presented to a lymphocyte, is called MHC restriction. In general, CD4+ve T cells are restricted by MHC II molecules (Thomas *et al.*, 1977) and CD8+ve T cells are restricted by MHC I molecules (Zinkernagel and Doherty, 1975) but there may be some overlap between the two groups (Braciale, 1987).

1.5 Antigen processing and presentation.

The processing of antigen for MHC I and II restricted presentation is fundamentally different (Germain, 1986; Bevan, 1987). In general, antigens that are synthesized within the cell or targeted to the cytosol, such as intracellular pathogenic bacteria and peptides derived from viruses, endogenous antigens, are presented in the context of MHC I molecules. Conversely, antigens internalized from the extracellular space, exogenous antigens, are presented in the context of MHC II molecules, but there are exceptions to this rule (Unanue, 1992). The site of antigen processing appears to be cytoplasmic and the interaction of antigen with MHC I molecules appears to occur within the endoplasmic reticulum (Braciale, 1992). Binding of MHC I to peptide stabilizes MHC I in its association with β2-microglobulin and is followed by assembly and transport to the cell surface. Virally infected cells which synthesize viral proteins, present these proteins to CD8+ve T cells in the context of MHC I molecules (Townsend and Bodmer, 1989; Long and Jackobson, 1989). Viral peptides of 8-9 amino acid residues in length have recently been shown to bind directly to MHC I molecules (Chen and Parham, 1989; Bouillot *et al.*, 1989; Rotzschke *et al.*, 1990). However, some viral proteins produced in the cytosol are presented by MHC II at a lower efficiency than those presented by MHC I (Hackett *et al.*, 1991).

APCs internalize most exogenous proteins into endosomes and break them down into peptide fragments either in acidic endosomes or in lysosomes. Then the antigen fragments are linked to MHC II molecules most probably in endosomes, and presented to CD4+ve T cells (Jenssen, 1990; Unanue, 1992). MHC II molecules become more stable upon binding with peptide (Germain and Hendrix, 1991). Before MHC II molecules are expressed on a cell surface, they are associated with an invariant chain (reviewed by Cresswell, 1992). The invariant chain may protect the antigen-binding site of MHC II molecules from being saturated with self-derived peptides, before reaching the cell surface (Teyton *et al.*, 1990). In addition, the invariant chain may facilitate transport of the MHC/antigen complex out of the endoplasmic reticulum via endosomes to the cell surface (Lotteau *et al.*, 1991). Antigen processing by LCs correlated with MHC II biosynthesis and expression of the invariant chain (Pure *et al.*, 1990). Furthermore, MHC II+ve fibroblasts which were unable to process or present antigen to

some T cell hybridomas, gained the ability to do so after experimentally increasing levels of invariant chains (Stockinger *et al.*, 1989). The precise function(s) of the invariant chain, however, awaits clarification.

1.6 The T cell response to antigen.

The TCR is a molecular complex on the surface of T lymphocytes that is responsible for recognition of processed antigen associated with MHC on APCs (Marrack and Kappler, 1986; Davis and Bjorkman, 1988). The Ti portion of the TCR is the antigen-specific binding component and is a disulphide linked a/b heterodimer on the majority of T cells. Non-covalently associated with the Ti heterodimer are the CD3 subunits (CD3γ, CD3δ, CD3ε, CD3ζ, CD3η). Since CD3 subunits have extensive cytoplasmic tails compared with the Ti heterodimer subunits, they are almost certainly involved in transducing signals from the cell surface across the cell membrane into the intracellular compartment (Frank *et al.*, 1990). In addition to the TCR complex, CD4 or CD8 molecules on the T cell surface may be involved in the interaction with MHC and antigen on APCs (Emmrich, 1988).

The binding of the TCR complex with MHC and antigenic peptide is, in most model systems, insufficient to activate T cells. A further group of T cell surface molecules appear to co-stimulate T cells that are bound via TCR/MHC-antigenic peptide, enabling the T cells to become fully activated (fig. 1.8). Some T cell accessory receptor molecules and their ligands have recently been defined. For example, three receptor-ligand couplets have been characterized for T cell APC interaction: CD2 and LFA-3; LFA-1 and ICAM-1; CD28 and B7. It is now clear that T cell activation is a complex process involving both adhesion and signal transduction. Co-stimulation of T cells can also be achieved by ligands that are extracellular matrix proteins. Examples of T cell adhesion receptors for such ligands are members of the VLA or β1 (CD29) subfamily of integrins.

The binding of T cells to APCs is followed by production of IL-1 by the APC. IL-1 in association with antigenic stimulation causes signal transduction through the TCR complex. This is initiated by calcium ion mobilization and activation of protein kinase C. IL-2 is then secreted by T cells, which induces the further expression of IL-2 receptors on activated T cells (Koyasu *et al.*, 1991). Binding of IL-2 to receptors on the surface of activated T cells also stimulates them to proliferate.

Figure 1.8 The interaction between T cell and APC

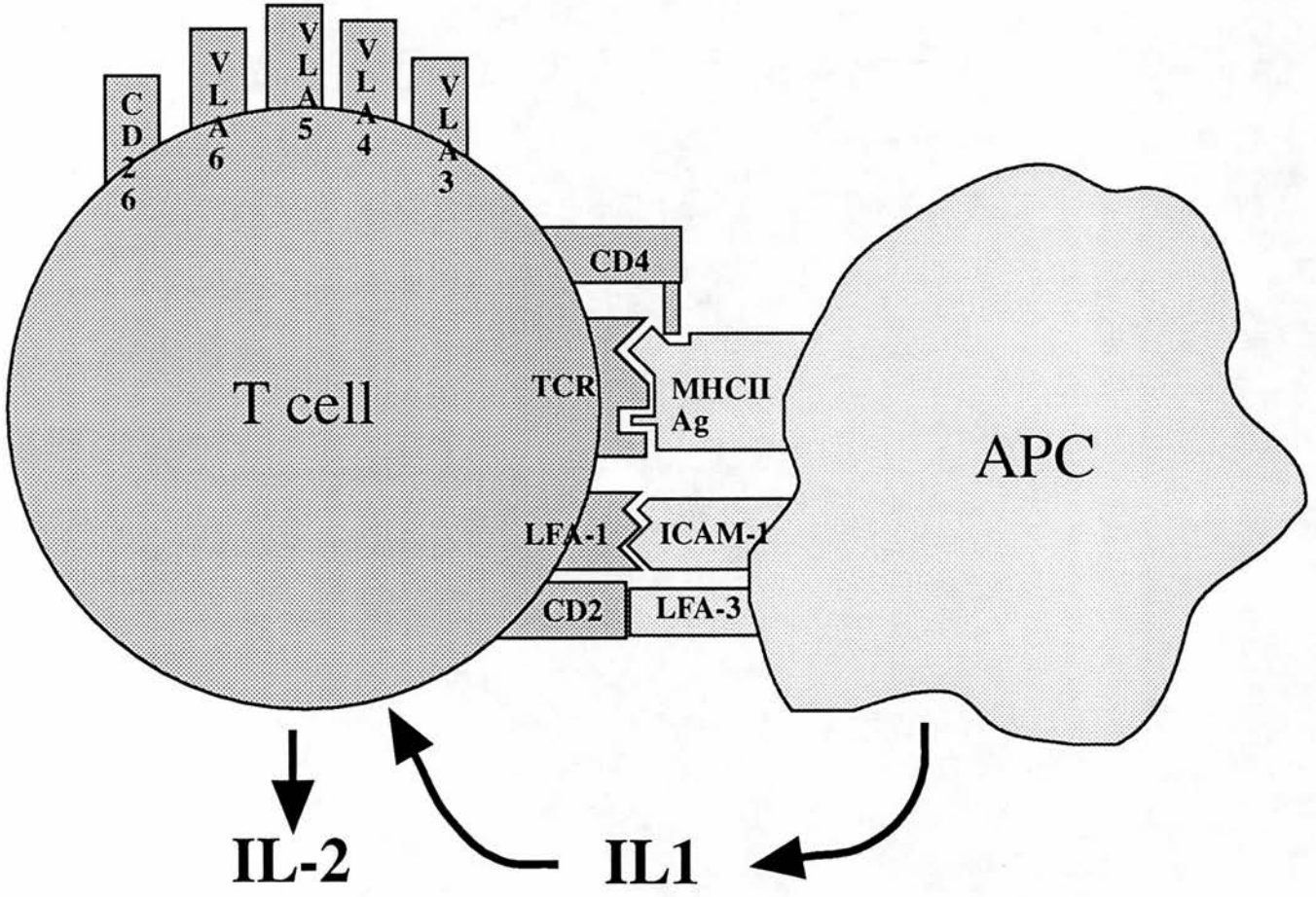

1.7 The penetration of skin by UVR

The penetration of UV radiation into skin depends upon its scattering and absorption (Anderson and Parrish, 1981; Wan, Anderson and Parrish, 1981). The depth of this penetration is wavelength dependant. Radiation of short wavelength tends to penetrate tissues less well than that of longer wavelength. This is partly due to the greater scattering of short wavelength radiation, mainly by non-absorptive particles or molecules with a size of less than 1/100 of the wavelength. In addition, nucleic acids and proteins absorb mainly in the UVC and shorter UVB wavelengths so there are many chromophores available in skin for these wavebands. Very little radiation with wavelength shorter than 290nm penetrates the epidermis (Bickers, 1989).

Absorption of radiation is more important than scattering in determining the depth of penetration of UV and visible radiation through the epidermis. Absorption depends on epidermal thickness and the effectiveness of epidermal chromophores. Radiation which is absorbed by chromophores, causes excitation of electrons leading to a biological response. In the epidermis, the major chromophores are proteins containing aromatic amino acids, nucleic acids, melanin and urocanic acid (UCA; Tabachnick, 1957; Parrish *et al.*, 1982). Each chromophore has a unique absorption spectrum and tissue distribution. Since proteins and nucleic acids are present in all cells, their distribution and concentration is relatively constant throughout the epidermis. However, UCA is concentrated mainly in stratum corneum. Early studies indicated that human skin has an absorption maximum at 270-280nm and minimum at 250-260nm, an absorption spectrum similar to that of proteins (Bachem and Reed, 1930).

Melanocytes are dendritic cells that rest on the basal lamina. They account for approximately 2% of the total EC population. Melanin is produced in melanocytes by the conversion of tyrosine by the enzyme tyrosinase to L-DOPA which is further polymerized and then packaged into melanosomes (organelles of ~1μm diameter). Melanosomes are transferred into neighbouring keratinocytes where their distribution largely accounts for skin colour. The total amount of melanin, its stability within keratinocytes and the relative increase in melanin production after UVR are mainly under genetic control.

Melanin absorbs wavelengths between 250 and 700nm, having the greatest effect on shorter wavelengths. The total amount of epidermal melanin, therefore, dictates the degree to which UV radiation can penetrate skin (Everett *et al.*, 1966; Kligman, 1969;

UROCANIC ACID is derived from the breakdown products of keratohyalin granules, components of keratinocytes within the stratum granulosum and stratum corneum Scott, 1981; Scott *et al.*, 1982). Keratohyalin granules contain large amounts of the amino acid histidine. The deamination of histidine by the enzyme histidase (histidine-ammonia-lyase) occurs particularly in the stratum corneum and the liver, producing UCA (Baden and Pathak, 1967). In the liver, UCA is further metabolized by the enzyme urocanase to form glutamic acid which is then excreted in the urine. The absence of urocanase in stratum corneum results in accumulation of UCA. After absorption of UV either *in vitro* or in mammalian skin, UCA undergoes isomerization from the naturally occurring *trans*-isomer to the *cis*-isomer (Morrison *et al.*, 1980; Norval *et al.*, 1989a; Pasanen *et al.*, 1990).

UCA in normal guinea-pig skin, extracted by acid treatment of the skin, is reported to be responsible for 80% of UV absorption. The absorption maximum for UCA in vitro is 264nm, whilst isomerization efficiency is greatest at 313nm (Morrison *et al.*, 1984). Furthermore, an increase in the total concentration of UCA in skin after irradiation of up to 2 minimal erythemal doses (MEDs) of UVR has been reported and is associated with increased keratinization. Analysis of UCA in successive Sellotape strips of the epidermis show that the majority is located in the 7 uppermost layers and that 40% of UCA in the first Sellotape strip of sun-protected skin is in the *cis*-isomer. After UVB irradiation of human skin at a dose of 4 mJ/cm^2, the isomerization of UCA from the *trans* - to the *cis* - form is detected only in the outermost stratum corneum. After a higher dose of UVR (32 mJ/cm^2) the isomerization of UCA to the *cis*- form has reached a 60% level which is detectable throughout the stratum corneum (Norval *et al.*, 1989a).

Postulated roles for UCA in skin include those of a natural "sun-screening" agent i.e. a photoprotective substance against actinic DNA damage and, in contrast, a photoreceptor mediating UV-induced immunosuppression (Zenisek *et al.*, 1955; De Fabo and Noonan, 1983a,b; Morrison, 1985). The latter role is now supported by a great deal of experimental evidence (Morrison *et al.*, 1985; Norval *et al.*, 1989b,c). In animal models *cis*-UCA mimics many of the effects of UVB irradiation. For example, painting *cis* -UCA onto mouse skin *in vivo* induces antigen-specific suppressor T cells and prevents the induction of DH responses (Ross *et al.*, 1986, 1987). Injection of *cis* - but not *trans* - UCA *in vivo* into mice, suppresses antigen presentation by splenic DCs (Noonan *et al.*, 1988). The molecular target for *cis* -UCA may be histamine receptors (Norval *et al.*, 1990; Palazynski *et al.*, 1992) or DNA, since UCA *in vitro* can form photoadducts with DNA (Farrow *et al.*, 1990).

1.8 Acute effects of UVR on skin

Many mediators are released by ECs following exposure to erythemal doses of UVR, including histamine (Hawk *et al.*, 1983), prostaglandin E2 (Mathur and Gandhi, 1972; Black *et al.*, 1980), prostaglandin F2, D2, prostacyclin and 12-hydroxyeicosatetraenoic acid (Black, Hensby and Greaves, 1982). Indomethacin, an inhibitor of prostaglandin synthesis, inhibits the initial stage of UVB-induced erythema (Snyder and Eaglstein, 1974). After 24 hours, prostaglandin levels return to normal and indomethacin has no inhibitory effects on erythema. Eicosanoids have been implicated as mediators in UVB-induced inflammation (Punnonen *et al.*, 1987). The secretion of eicosanoid precursors by cultured keratinocytes, and their incorporation into neutral lipids on epidermal cell membranes, has been demonstrated after UVB irradiation. UV irradiation has also been shown to effect the production of a variety of cytokines from both human and murine epidermal cells (fig. 1.9). The secretion of IL-1, causing the expression of high affinity IL-1 receptors by keratinocytes (see section 1.9,p33), IL-3, IL-6, TNF α and β, TGF-α and β, and GM-CSF are induced by UVR (Schwarz and Luger, 1989). UVR also induces the production of an inhibitor of IL-1 and a serum suppressor factor with a molecular mass of 15-50 kDa (Schwarz *et al.*, 1986; Schwarz *et al.*, 1988).

The skin undergoes a number of important changes in response to UVR, that minimize the damage done by exposure to radiation, protect the organism from future exposures and repair the damage that has already occurred. The initial response to UVR is damage resulting in sunburn with the classical signs of erythema, swelling and pain. This is followed by protective changes including thickening of the epidermis and stratum corneum, and increased epidermal pigmentation.

The erythemal response to UVR is an indication of increased blood flow caused by dermal blood vessel dilatation, which becomes visible after a mean increase in cutaneous blood volume of 38% over normal values in caucasian skin (Wan, Parrish and Jaenicke, 1983). In human skin erythema begins several hours after UVB exposure, and is maximal 12-24 hours later.

The erythemal action spectrum can be obtained by plotting the reciprocal of the lowest dose of UVR required to induce a defined grade of erythema against the wavelength of incident radiation. For minimal erythema the most active wavelengths are 250-290nm, with rapidly decreasing activity above 290nm. Therefore, a thousand times more energy is required to produce minimal erythema at 320nm as at 290nm. The proportion of UVA in natural sunlight is much greater than UVB, therefore its contribution to

erythema is significant. Approximately 15% of the noon-time radiation responsible for erythema is within the UVA range, and the percentage increases during the later hours of the day (Frain-Bell, 1985). Resistance to UV-induced erythema is conferred by pigmentation due to both racial skin colour and, to a lesser degree, tanning (Cripps, 1981).

The first step in the inflammatory process may involve epidermal modification or damage followed by the release of mediators which diffuse into the dermis, causing dilatation of blood vessels. Lysosomal damage with the associated release of hydrolytic enzymes in UV-exposed ECs may play a role in the development of erythema. However, severely UV damaged cells may sometimes contain intact lysosomes (Honigsmann, Wolff and Konrad, 1974).

Histological changes are apparent in human skin within 30 mins of UV irradiation (Gilchrest *et al.*, 1981). Damage to keratinocytes results in their transformation to "sunburn cells", with brightly eosinophilic cytoplasm and pyknotic nuclei. Intercellular oedema develops in epidermis, and epidermal cell nucleoli become prominent in cells which otherwise appear normal. The epidermis thickens in response to UVR due to an increased mitotic rate. The cytokine TGF-α has been implicated in UV-induced epidermal hyperplasia (Murphy *et al.*, 1991).

LCs are also susceptible to UVR. The alterations to LCs as a result of UVB exposure are given in section 1.9.

Melanocytes become vacuolated and swollen in response to UVR, but return to normal within 24 hours. Immediate pigmentation is induced by UVA during UV exposure and reaches a maximum immediately after irradiation. This response is caused by transferral of pre-existing melanosomes from melanocytes into keratinocytes and oxidation of melanin (Pathak and Stratton, 1968). Delayed pigmentation (tanning), due mainly to UVB, occurs within 72 hours of UVR exposure and is caused by increased numbers of melanocytes and increased melanogenesis.

Dermal endothelial cells enlarge within 30 minutes of UV exposure, causing the occlusion of blood vessels. Perivenular oedema is also noted in early erythemal responses. Perivascular infiltrates accumulate, consisting mainly of mononuclear cells. The number of mast cells decreases shortly (1-4 hours) after irradiation and within 24 hours returns to normal.

Figure 1.9: The influence of UVB irradiation on the epidermis.

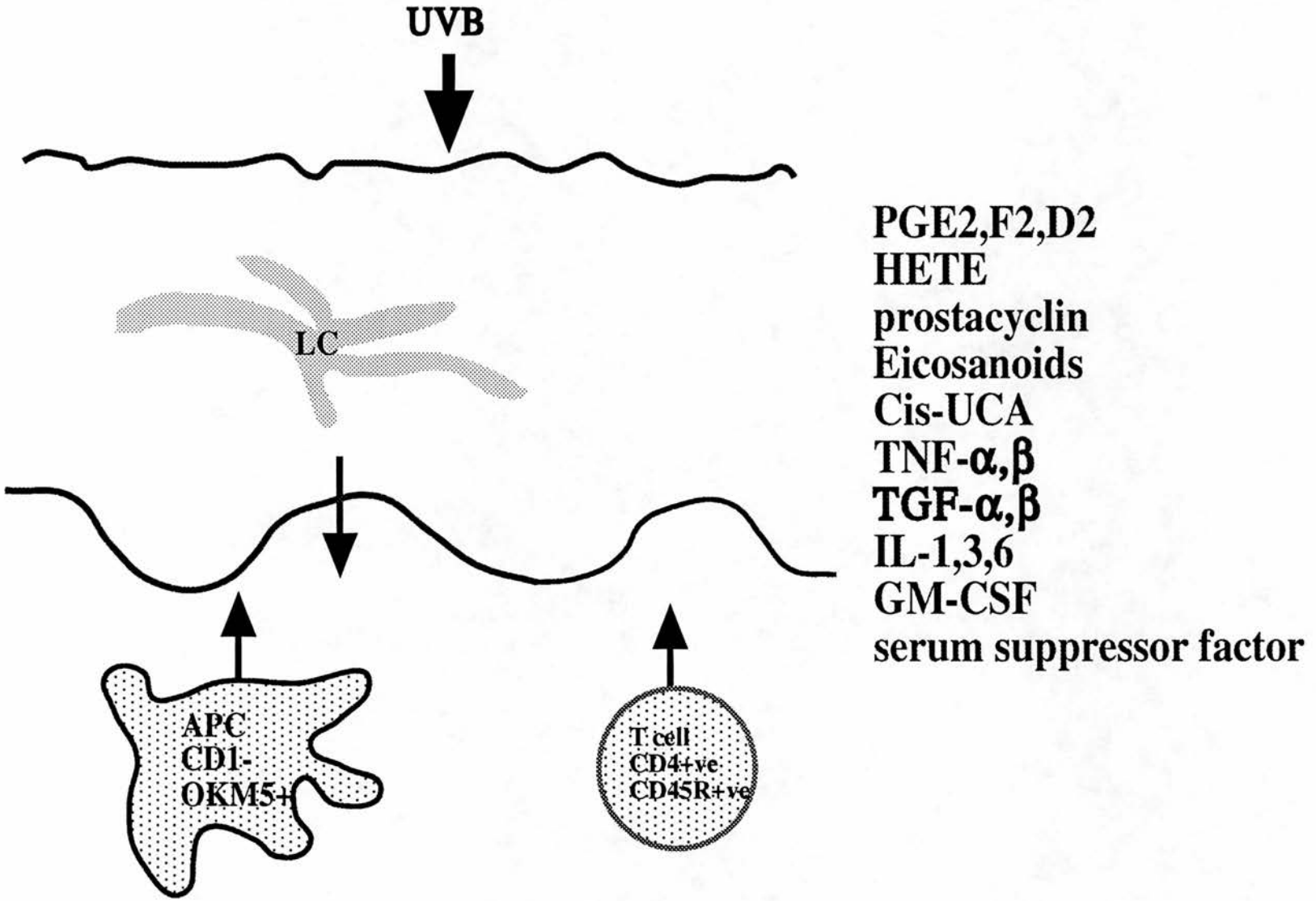

1.9 Chronic effects of UVR on skin

Solar radiation is an important contributing factor to ageing of the skin (photo-ageing), giving chronically sun-exposed skin a wrinkled appearance that is similar to that of skin with naturally occurring age-induced changes. Most of the histological alterations associated with photo-ageing take place within the dermis. Regular use of sunscreens containing molecules that absorb UVB may inhibit photo-ageing (Plastow, Harrison and Young, 1988). Further protection against photo-ageing may be conferred by adding a UVA filter in sunscreen preparations (Young, 1990). Therefore both UVA and UVB appear to contribute to the photo-ageing process.

Epidemiological studies have revealed a relationship between long-term cumulative sun exposure and increased risk of developing squamous cell and basal cell carcinomata. Malignant changes leading to these two types of skin cancer occur most frequently on sun-exposed skin and a correlation exists between geographic latitude and the incidence of skin malignancy (Scotto and Fears, 1987). The correlation between sun exposure and risk of developing malignant melanoma is less clear. Most types of malignant melanoma, with the exception of lentigo maligna melanoma, may occur on covered body sites. However, UV irradiation is also a significant risk factor for the development of malignant melanoma (Lee, 1982). The prevalence of skin cancer is inversely related to the degree of melanogenic pigmentation in skin (Doll *et al.*, 1970) and the incidence of malignant transformation increases with age, which might be due to both the cumulative dose of UVR and by implication cumulative damage to the skin and decreased immunological surveillance.

The risk of an individual developing sunlight-associated cancer is probably dependent in part upon their genetic make-up. Some people are more likely to develop skin malignancy than others, particularly those with celtic ancestry, light hair and eyes, and those who freckle rather than tan in response to UVR. The greatest risk factor for malignant melanoma is a history of melanoma in a first degree relative together with a family history of the dysplastic naevus syndrome (Greene *et al.*, 1987). The dysplastic naevus is a naevus which contains atypical and hyperplastic melanocytes, and when many of these naevi occur on an individual, that person is said to have the dysplastic naevus syndrome. However, the occurrence of such factors is rare, and other factors may also predispose to melanoma. The most common risk factors associated with sporadic melanoma appear to be the total number of naevi, presence of freckles and atypical naevi, and episodes of severe sunburn (Mackie, Freudenberger and Aitchison, 1989).

The UVB component of sunlight is thought to be mainly responsible for photocarcinogenesis (Green *et al.*, 1978; Vitiliano and Urbach, 1980). Multiple smaller doses of UVR may be less carcinogenic than single, large doses. This implies that some steps of the carcinogenic process can be reversible or repairable (Blum, 1959; Forbes *et al.*, 1978).

Induction of UV-induced skin neoplasms is probably the result of direct DNA damage or alteration of DNA in ECs followed by inaccurate or faulty repair and the release of free radicals, causing the cells to divide and become unresponsive to normal growth-regulating factors (Harber and Bickers, 1981; Cerutti, 1985). It appears that DNA becomes extensively demethylated after UV exposure possibly allowing the expression of genes which were repressed prior to irradiation (Lieberman *et al.*, 1983). Two-dimensional electrophoresis of UV-exposed keratinocytes reveal expression of proteins which are not expressed in normal unirradiated skin. However, these proteins have not yet been characterized (Kartasova *et al.*, 1988).

One of the effects of UVR may be the induction of lesions in DNA, one example of which is the cyclobutyl pyrimidine dimer formed by covalent bonding between adjacent pyrimidine residues on the same strand of DNA (Patrick *et al.*, 1976) These lesions may be repaired by a process known as photoreactivation (Setlow and Setlow, 1963). In this process, pyrimidine dimers are split and the integrity of the DNA is restored by the action of the photoreactivating enzyme which is activated by visible light (Cook, 1970). The skin condition xeroderma pigmentosum is a rare autosomal recessive disorder which is characterized by sun sensitivity, cutaneous and ocular abnormalities, and an associated risk of multiple skin neoplasms which may result at least in part from faulty DNA repair mechanisms. Cells from patients with xeroderma pigmentosum are defective in the repair pathways which excise pyrimidine dimers from UV-exposed DNA. This observation may implicate DNA damage with pyrimidine dimer formation and faulty or inadequate repair for the induction of UV-induced human neoplasia (Kraemer, Lee and Scotto, 1984).

Work with animal models suggests that, under normal circumstances, developing neoplasms may be detected and eliminated by the immune system. This may perhaps explain the observation that individuals with suppressed immune responses, such as organ transplant recipients, who receive immunosuppressive drugs, suffer from increased incidence of skin tumours (Boyle *et al.*, 1984). However, only chronically immunosuppressed patients lacking a specific HLA allele appear to exhibit an increased risk of developing skin cancer (Bouwes Bavinck *et al.*, 1989).

Neoplasia in human skin appears to be associated with alterations in LCs (Sontheimer *et al.*, 1984; Odling, Halliday and Muller, 1987;Yoshikawa *et al.*, 1990a; Brash *et al.*, 1991).

Hence UVR may be considered a "complete" carcinogen, since it can be a tumour initiator, by damaging EC DNA and causing free radical release, and may also be a tumour promoter, by altering the immune response to tumour antigens. This may lead to failure of the immune system to recognize tumour antigens and/or to destroy malignant cells (Kripke, 1983).

1.10 UVB-Induced immunosuppression.

Immunomodulation resulting from cutaneous UVB exposure in both man and laboratory animals has been intensively studied in recent years. Irradiation of mice with either high or low doses of UVB results in systemic or local immunosuppression respectively. These types of UVB-induced immunosuppression are discussed in the following sections.

<u>The high dose model of UVB-induced immunosuppression.</u>

Studies relating to the immunological effects of UVR on the skin, and the immunology of UV-induced tumourogenesis started with the observation in mice that UV-induced tumours are strongly antigenic. If such tumours are transplanted into mice of the same strain (syngeneic), the recipients reject them efficiently (Kripke, 1974). However, in syngeneic mice immunosuppressed by UVR, such tumours are not rejected but continue to grow (Kripke, 1977).

UV-induced susceptibility to tumour growth in mice has been intensively investigated. The wavelengths responsible for tumour susceptibility in albino mice are between 250 and 320nm (DeFabo and Kripke, 1980; Noonan *et al.*, 1981). The susceptibility of mice to the growth of UV-induced tumours is independant of whether it is administered in multiple small doses or as a single large dose (DeFabo and Kripke, 1980).

Treating mice with high dose UVR not only interferes with tumour rejection but also suppresses CH responses, a phenomenon that is independant of the site of irradiation (Kripke and Fisher, 1976; Jessup *et al.*, 1978). Thus the exposure of mice to high doses of UVR appears to suppress systemic as well as local cutaneous immune responses (De Gruijl and Van der Leun, 1982). It has been demonstrated that transfer

of splenic lymphoid cells from UV-irradiated mice to normal recipients confers susceptibility to tumour growth. When T cells are removed from the lymphoid cells, susceptibility to tumour growth is eliminated (Spellman and Daynes, 1977). The immunosuppressive effects of lymphoid cells from UV-irradiated mice may therefore be due to the presence of T cells with suppressor function.

In mice, tumour transplant rejection is associated with the production of tumour-specific cytotoxic T cells *in vitro*. Addition of UVR-induced T cells with suppressor function to the *in vitro* cytotoxic reaction, had no suppressive effect (Thorn *et al.*, 1981). Therefore, the T cells with suppressor function induced by UVR do not appear to act on the cytotoxic T cells directly. On the other hand, lymphocytes from immunized UV-irradiated mice reduced the cytotoxic response when restimulated *in vitro*. It is possible that these UV-induced T cells with suppressor function might prevent the generation of secondary cytotoxic memory cells after repeated antigenic stimulation (Thorn, 1978).

The mechanism responsible for UV-induced systemic immunosuppression is poorly understood, although it has been associated with morphologic and functional changes in splenic macrophages and the presence of hapten-specific T cells with suppressor function (Jessup *et al.*, 1978; Noonan *et al.*, 1981). UV-induced alterations in DNA appear to be an initiating or essential step in producing this type of immunosuppression (Morison, 1990). In addition, mediators produced by UV-irradiated ECs may also be involved (see section 1.8).

The evidence just described has been derived from high dose UVB regimens, with repeated doses of 540 mJ/cm^2, which is much higher than doses normally tolerated by humans. Information concerning the human situation and utilizing lower doses of UVB is still relatively scarce.

The low-dose model of UVB-induced immunosuppression

Using a guinea-pig model, it was observed that a 14 day course of relatively low dose UVB suppresses the induction of CH to the antigen dinitrochlorobenzene (DNCB) when it was painted onto UV-irradiated skin (Haniszko and Suskind, 1963). These doses of UVB did not suppress CH at sites which were not irradiated and were thus believed to cause local immunosuppression. Since then, both UVB and PUVA have been shown to partially inhibit the induction of CH to DNCB in the albino guinea-pig (Morison *et al.*, 1981). UVB-irradiated mice were unable to initiate DH responses to HSV and certain microorganisms (Howie *et al.*, 1986; Giannini, 1986), whilst induction

of DH responses to other microorganisms, BCG and *Candida albicans* , remained unchanged, although the number of BCG mycobacteria recovered from the lymphatics of UVB exposed mice was significantly increased (Jeevan *et al.*, 1992).

In animals UVB suppresses the induction of CH, but enhances the elicitation of CH responses (Polla *et al.*, 1986). Since the induction of CH would appear to involve antigen presentation to naive T cells, whereas the elicitation of CH would appear to involve antigen presentation to antigen-specific memory T cells, UVB may prevent LC interaction with naive T cells (Streilein *et al.*, 1990; Simon *et al.*, 1992).

The influence of low dose UVB on LCs

Since evidence suggests that LC are crucial APC for the induction of CH, the effect of low dose UVB on CH may be attributable to loss of LC function. Low dose UV-induced immunosuppression has been attributed to alterations in LC numbers, morphology, surface molecule expression and function (Aberer *et al.*, 1981; Lynch *et al.*, 1981; Iacobelli *et al.*, 1985; Hanau *et al.*, 1985; Simon *et al.*, 1992), and the appearance of hapten-specific suppressor-inducer CD4+ve CD45RA+ve T cells (Baadsgaard *et al.*, 1988, 1990). Inflammatory mediators (see section 1.8, p23) and *cis*-UCA may play an active role in low dose UVB-induced immunosuppression. However, both high and low dose models of UVB-immunomodulation were found to have the same wavelength dependencies (Noonan and DeFabo, 1990).

The mechanisms by which UV alters the appearance and function of LCs are largely unknown. LC surface antigen expression may be altered, and LC DNA and/or membrane damage may be involved (Iacobelli *et al.*, 1985; Koulu *et al.*, 1985; Aberer *et al.*, 1986).

The effect of low dose UVB on LC function

The administration of very low doses of UVB ($100J/m^2 = 10mJ/cm^2$ once a day for 4 days) prevented the induction of DNCB sensitization and reduced the number of ATPase +ve LCs in murine skin from 800 cells/mm^2 to <50 cells/mm^2 (Toews *et al.*, 1980b). The LCs displayed altered morphology after UVB irradiation: they were contracted, darkly stained and lacked dendrites. On recovery from UVB, the number of ATPase +ve LCs returned to normal levels. The number of ATPase +ve LCs in skin during recovery from UVB was proportional to the capacity of the skin to become

sensitized to DNFB and UVB irradiated skin became specifically unresponsive or tolerant to a normally immunizing dose of DNFB.

An *in vitro* murine model of CH has been developed by culturing antigen-specific T cells with antigen-pulsed ECs, and measuring the T cell proliferative response (Stingl *et al.*, 1981). The T cell response was abolished by adding anti-MHC II antibody and complement to the ECs, which depletes a small fraction, which are probably LCs. When the ECs were pretreated with UVB at doses of 25-600J/m^2 before culture with T cells, the T cell response to various antigens was diminished in a UV dose-dependent manner. They concluded that UVB may directly prevent antigen presentation by LCs. Similar experiments have shown that low dose UVB irradiation of antigen (TNCB)-pulsed murine ECs *in vitro* which are then introduced subcutaneously back into mice could prevent their immunization and cause suppression of the expected CH response (Sauder *et al.*, 1981).

Intravenous infusion of trinitrophenol (TNP)-pulsed LCs into mice resulted in normal CH responses, similar to those induced by skin painting with hapten. However, TNP-LCs that were irradiated with 200J/m^2 UVB *in vitro* prior to infusion, caused diminished CH responses. When these mice were challenged with the hapten at a later date, their CH responses were still diminished (Cruz *et al.*, 1989). This low dose UVB was not cytotoxic to LCs but induced long-term downregulation of CH responses mediated by LCs the function of which had changed from one that induces an immune response to one that induces tolerance.

Subsequent work revealed that murine LCs incubated with antigen normally induced the proliferation of antigen-specific murine CD4+ve T cells, consisting of Th1 and to a lesser extent Th2 (Tiegs *et al.*, 1990; Simon *et al.*, 1990). LCs which had been incubated with antigen and then UVB irradiated (200J/m^2), lost the ability to stimulate the Th1 subset of murine CD4+ve T cells which appear to be responsible for mediating DH responses, but retained the ability to stimulate Th2 cells (Simon *et al.*, 1990). This process appears to be due to functional inactivation of Th1 cells rather than their physical deletion, since the Th1 cells retained the ability to proliferate in response to exogenous IL-2 (Simon *et al.*, 1991b).

Thus, low dose UVB appears to deplete the epidermis of LCs *in vivo* and inhibit the antigen-presenting function of murine LCs *in vitro*.

The mechanism by which low dose UVB alters LCs

Although low dose UVB exposure depletes epidermal LCs in all strains of mice and in all humans tested so far, UVB-induced impairment of the induction of CH to DNCB in untanned caucasian skin has been shown in one study to occur only in approximately 40% of normal humans who are termed "UVB susceptible", whilst 60% display normal induction of CH to DNCB after UVB exposure and have been termed "UVB resistant" (Yoshikawa *et al.*, 1990). The incidence of UVB susceptibility in healthy volunteers in that study was around 30-40%, in contrast to 92% in patients with a past history of basal or squamous cell carcinoma. Susceptibility to UVB, therefore, might be a risk factor for skin cancer. However, recent results indicate that UVB resistance may not exist in humans (Cooper *et al.*,1992).

Inbred strains of mice show distinctions between "UVB resistant" and "UVB susceptible" strains which are genetically determined under polymorphic gene control, despite the fact that T cells with suppressor function are generated universally in mice after UVB irradiation (Streilein and Bergstresser, 1988; Glass *et al.*, 1990). In mice, at least two genetic loci govern this trait: Tnf-α and lipopolysaccharide (Lps; Yoshikawa and Streilein, 1990). Since normal induction of CH could be restored in "UVB susceptible" strains of mice by treatment with anti-TNF–α antibodies prior to application of hapten, it is possible that susceptibility to UVB may be mediated by excessive production or release of TNF-α (Yoshikawa, Kurimoto and Streilein, 1992).

UVB exposure may give rise to local TNF-α secretion by keratinocytes (Kock *et al.*, 1990). Intradermal injection of TNF-α or *cis*-UCA at the site of application of a contact allergen in mice, prevents the induction of CH, enhances the elicitation of CH and alters LC number and morphology in a manner similar to that achieved by low dose UVB (Yoshikawa and Streilein, 1990; Streilein *et al.*, 1990). These effects of TNF-α and *cis*-UCA may be specific since they can be abolished with neutralizing anti-TNF-α antibodies which implies that the effects of *cis*-UCA may be mediated via TNF-α. Furthermore, intradermal injection of TNF-α in mice can induce the accumulation of DCs into draining lymph nodes, and may provide a signal for LC migration from the epidermis (Cumberbatch and Kimber, 1992a).

However, anti-TNF-α antibodies did not prevent the loss of LC function *in vitro* induced by UVB irradiation (Simon *et al.*, 1991c). Thus both TNF-α and UVB can act as suppressors of LC function but appear to do so via separate mechanisms. Interpretation of these results requires caution, since the doses of TNF-α and anti-

TNF-α injected into mice in such experimental protocols may bear little resemblance to those produced *in vivo* as a result of UVB exposure. Indeed, the amount of TNF-α produced in human suction blister fluid after a six week phototherapy course was measured in picogram quantities per ml as compared with the microgram quantities per ml injected experimentally into mice in the experiments described above (Gilmour *et al.*, 1993). Furthermore, it is probable that UVB-induced production of TNF-α *in vivo* occurs within the epidermis. Thus intradermal injection of TNF-α may not be an appropriate model for UVB-induced immunomodulation.

There is also evidence to suggest that altered production of IL-1 might contribute to the effects of UVB on LC function. Both increased and decreased IL-1 production have been reported after exposure of ECs to UVB (Ansel *et al.*, 1983; Sauder *et al.*, 1983; Gahring *et al.*, 1984; Luger, 1986; Kupper *et al.*, 1987). However, the addition of exogenous IL-1 only partially reconstituted the lymphoproliferative response when added to cultures of UVB-irradiated APCs *in vitro* (Sauder *et al.*, 1983). A specific inhibitor of IL-1 has also been detected in sera of mice exposed to UVB (Schwarz *et al.*, 1988).

Some studies have suggested that UV-induced alterations in LC morphology, number and/or phenotype may occur independantly of measurable immunological effects or at different wavelengths (Morison *et al.*, 1984; Noonan *et al.*, 1984). Nevertheless, LC are probably central to the development of cutaneous immune responses to antigens encountered in the epidermis and UV-induced alterations to LC appear to be important in the low-dose model of immunosuppression. Thus the examination of LC alterations may be relevant to the understanding of the low dose model of UVB-induced immunosuppression, and the possible consequences of therapeutic or environmental UV exposure of human skin.

The effect of low dose UVB on LC surface markers

Many membrane bound or soluble ligands are produced by LCs which appear to be involved in their optimal binding to and interaction with T cells (see section on lymphocytes, p11). UVB-induced alterations in the expression of LC surface molecules such as MHC II and adhesion molecules, including LFA-1, LFA-3 and ICAM-1, might play an important role in their functional capacity to activate helper T cells. Therefore much work has focussed on the modulation of LC surface expression of various molecules after UVB exposure.

Studies of UV irradiated animals and humans have generated conflicting results regarding LC surface MHC II, CD1a and ATPase expression. One study demonstrated an increase in murine MHC II +ve LCs (Nordlund *et al.*, 1981) while most others have reported decreases in guinea pig, murine and human ATPase +ve, MHC II +ve or CD1a +ve LCs after UV exposure (Zelickson and Mottaz, 1970; Toews *et al.*, 1980b; Lynch *et al.*, 1981; Hanau *et al.*, 1985; Humm and Cole, 1986; Koulu and Jansen, 1988). The UV-induced decrease in LC numbers in humans appear to be dose-dependent and vary according to time after UV exposure (Liu *et al.*, 1987; Koulu and Jansen, 1988). Racial variation is another factor to be considered, since greater UV-induced LC depletion occurs in the skin of celtic subjects than in darkly pigmented skin of aboriginal subjects (Scheibner *et al.*, 1987).

Human LC surface antigens appear to vary in their sensitivity to the effects of UVB, such that surface ATPase activity is more susceptible to UVB radiation than either MHC II or CD1a (Koulu *et al.*, 1985). It has been suggested that surface ATPase activity on LCs might be reduced after exposure to low dose UVB (Aberer *et al.*, 1981), and may be altered from a linear to an uneven pattern of staining (Iacobelli *et al.*, 1985). The significance of this finding is difficult to interpret since the function of LC surface ATPase activity remains obscure. However, exogenous ATP has been shown to increase plasma membrane permeability for certain cell types which leads to cell death (Gordon, 1986). Extracellular ATP may also be a mediator of T cell mediated cytotoxicity (Zanovello *et al.*, 1990). LC surface ATPase activity, therefore, may protect LCs against the potentially damaging effects of extracellular ATP. Indeed, the susceptibility of keratinocytes and macrophages to exogenous ATP appears to be far greater than that of LCs (Girolomoni *et al.*, 1992). The UVB-induced loss of LC surface ATPase might increase their susceptibility to ATP released from other cells which have been damaged as a result of UVB exposure.

It is possible that the decrease in LC numbers observed following UV irradiation using light microscopy may not reflect a genuine decrease in LC numbers but simply diminished expression of the particular surface antigen being utilized to demonstrate them. Thus the exposure of murine or human skin to moderately high doses of UVB administered over 4 consecutive days caused almost complete disappearance of MHCII +ve LCs and Thy-1 +ve dendritic ECs. However, ultrastructural examination revealed that many LCs were still present and were morphologically unaltered, whereas Thy-1 +ve cells were genuinely depleted (Aberer *et al.*, 1981, 1986). Similar results were also obtained after low dose UVB irradiation of guinea pig or murine skin using ATPase and MHC II markers (Hanau *et al.*, 1985; Humm and Cole, 1986). This implies that UVR

may modulate ATPase activity or CD1a or MHC II expression on the surface of LCs which remain in the epidermis, giving the spurious impression of a depletion in LC number.

A more direct and sensitive method for measuring cell surface molecule expression than light microscopy is fluorescent flow cytometry, which can be used to measure the intensity of fluorescent label on the surface of individual cells. Once again, disparate results have been obtained by different research groups. Fluorescent flow cytometric studies have demonstrated that exposure of human LCs or peripheral blood monocytes to UVB or PUVA therapy *in vitro* may be associated with retention of MHC II on LCs, but either depletion or retention of HLA-DR,-DP, and DQ on peripheral blood monocytes (Czernielewski *et al.*, 1984; Ashworth *et al.*, 1989b; Pamphilon *et al.*, 1989; Deeg and Sigarondinia, 1990). In contrast, canine DCs expressed between 30% and 40% less intense MHC II labelling 48 hours post UV irradiation (Aprile *et al.*, 1987), and the expression of LFA-1 on canine lymph node cells dropped from 95% to 5% as a result of UVB and UVC irradiation (Deeg *et al.*, 1987). Other work has revealed that the increased expression of ICAM-1 by murine LCs *in vitro* is abrogated by low dose UV exposure (Tang and Udey, 1991). The depletion of surface ICAM-1 from human LCs and peripheral blood monocytes by low dose UVB exposure has also been documented using flow cytometry (Krutmann *et al.*, 1990; Tang and Udey, 1992). However, the doses of UVB used in the former study, appear to have been cytotoxic to LCs when administered *in vitro* (Tang and Udey, 1992).

Although controversy exists with respect to the exact nature of LC alterations as a result of UVB irradiation, LC appear to be a target for cutaneous immunomodulation. In the murine model, it has been suggested that reduced ICAM-1 expression by irradiated LCs might prevent their co-stimulatory activity for Th1 cells (Simon *et al.*, 1992). Naive T cells, responding to antigen for the first time, include cells with TCRs of much lower affinity for antigen than the TCR of memory T cells. Thus, accessory signals by cell adhesion molecules and cytokines may be far more important for the activation of naive T cells than for the activation of memory T cells (Byrne *et al.*, 1989). Therefore, the decreased expression of ICAM-1 on UVB-irradiated LCs may specifically damage the immune response by naive T cells to cutaneous neoantigens.

Clearly further work is required to establish whether UVB modulates the expression of LC surface molecules in humans after *in vivo* irradiation. Little is known about the differential effects of UVB on the cell surface expression of human MHC II subregion products, HLA-DP-,DQ and -DR. Discrepancies in results from different research

groups may be a consequence of doses of UVR, the timing of examination after irradiation, or differential modulation of HLA-DP,-DQ or -DR by UVR. It is also possible that UV alters LC surface molecules qualitatively rather than quantitiatively.

Alternative APCs which may be involved in low-dose UVB induced immunosuppression

The evidence given above suggests that LC may be the epidermal targets principally responsible for the immunological consequences of low dose UVB. However, other ECs may also contribute to immunomodulation evoked by low dose UVB irradiation, such as keratinocytes, human HLA-DR+ve/CD1a-ve macrophages, murine Thy-1+ve dendritic ECs, and murine Ia+ve/Thy-1-ve ECs.

In humans, exposure to moderately high (erythemogenic) doses of UVB induces the appearance of a population of ECs which are HLA-DR+ve, OKM5+ve and CD1a-ve and which may preferentially activate T cells with suppressor-inducer and suppressor/cytotoxic function (Cooper *et al.*, 1985; Baadsgaard *et al.*, 1987a,b; Baadsgaard, Fox and Cooper, 1988; Baadsgaard *et al.*, 1990). This raises the possibility that heterogeneity among MHC II+ve ECs may exist, both in terms of their expression of CD1a and in their ability to induce or suppress immune responses.

In mice, antigen-bearing Thy-1+ve dendritic ECs suppress CH when introduced into syngeneic mice intravenously (Sullivan *et al.*, 1986). The immunosuppressive effect of Thy-1+ve dendritic ECs appears to be unaltered by *in vitro* low-dose UVB irradiation (Cruz *et al.*, 1989). After *in vivo* low dose UVB exposure, antigen-bearing Thy-1+ve dendritic ECs have been identified in draining lymph nodes, which may inhibit CH when injected into normal mice (Okamoto and Kripke, 1987). A further population of murine ECs which are UV-resistant and can activate suppressor T cells are identified by their expression of MHC II and their lack of Thy-1 expression (Granstein *et al.*, 1987).

In summary, low doses of UVB irradiation may cause an alteration in LC number, morphology and/or surface characteristics, so that the presentation of antigen is altered, resulting in immunosuppression. This immunosuppression prevents the induction of DH responses to antigens (to contact, tumour or microbial antigens) encountered in the epidermis. Whether such immunosuppression is the result of an active process (through the presentation of antigen in a different way, either by LCs or other APCs) or due to a passive process (through simply bypassing epidermal LC because of their decrease in number and/or impaired ability to present antigen) is unknown. There are

several possible explanations of low dose UVB-induced immunosuppression which are not necessarily mutually exclusive (fig. 1.9):

(1) the initiation of a chain of reactions starting with absorption of UV irradiation by UCA.

(2) the loss of epidermal LCs because of their damage or emigration from the epidermis, or defective LC function in irradiated skin, possibly due to disruption of their DNA or the structure or function of surface MHC II or adhesion molecules.

(3) the induction of APCs other than LCs, such as human CD1a-ve/DR+ve macrophages, human dermal dendrocytes, murine Thy-1+ve dendritic ECs, or murine Ia+ve/Thy-1-ve ECs, which may induce suppressor T cells.

(4) the production of immunosuppressive mediators by irradiated ECs.

(5) the UV-induced functional modification or damage to circulating immune cells in the dermal capillaries directly.

It is possible that UVB-induced immunosuppression may play a physiological role in preventing immunological reactivity to new (but not necessarily harmful) antigens produced in the skin as a result of cellular damage by UVB irradiation. This may prevent the induction of autoimmunity against UVB-induced neoantigens. However, such immunosuppression might have negative repercussions due to the loss of immune reactivity to UVB-induced tumour antigens or infectious agents.

1.11 Aims of the study

The aims of this study were to irradiate human subjects with moderate doses of UVB radiation, in similar fluences to those used therapeutically in our department and to those normally experienced in the environment, in order to document UVB-induced changes to epidermal LCs. As outlined in section 1.10, p35, the effects of UVB on the expression of LC surface antigens are unclear. Previous studies have not quantified the expression of surface MHC II or CD1a on normal and UVB-exposed LCs, nor have they documented the variation in expression of these molecules, or examined the influence of UVB irradiation on LC surface expression of MHC II subregion products (HLA-DP,HLA-DQ and HLA-DR). In addition, the observed changes in LC morphology after UVB exposure have not been well characterized. Therefore, various methods were used in this study to clarify the UVB-evoked alterations in:

1) LC number

2) LC morphology

3) LC expression of surface MHC II (pan-MHC II, HLA-DR, HLA-DQ and HLA-DP) and CD1a antigens.

Chapter 2 Materials and Methods

2.1 Subjects and irradiation schedules.

Nine volunteers were recruited from the Department of Dermatology, University of Edinburgh. The volunteer group consisted of four women and five men, with skin types I, II and III (mean age of 42 years, age range 29-59 years). All volunteers were healthy, but one volunteer had a history of atopic eczema. Subjects received the standard UVB regimen for treatment of psoriasis in our phototherapy unit. They were irradiated with incremental UV doses thrice weekly over a period of six weeks (between August and December) in a Waldmann 1000 UVB cabinet, lined with 26 Sylvania UV6 tubes (fig. 2.1). The main UV peak of these tubes occurs at a wavelength of 312nm (fig. 2.2). The UVB output measured in the centre of each of six banks of tubes (a-f, see below) is recorded in table 2.1.

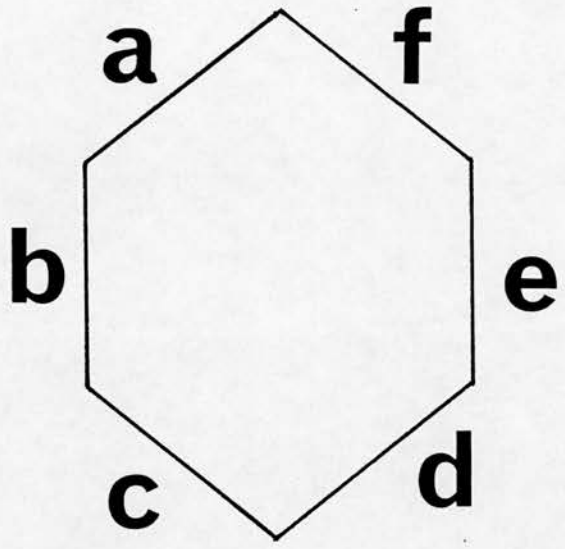

Table 2.1 The UVB output of the Waldmann 1000 cabinet.

Position within the UVB cabinet	UVB reading using a Waldmann meter on the UV6 scale (mW/cm^2)
a	0.90
b	1.02
c	0.96
d	0.82
e	0.94
f	0.93
mean	0.93

The initial UVB dose was 37mJ/cm^2 which was then increased by 50% and subsequently by smaller increments to a minimum of 15%. This regime was intended to be sub-erythemal. If a subject experienced erythema during treatment, the UVB dose was not increased until the inflammation subsided. The subjects received a total mean dose of 4.2J/cm^2 (range 2.58-5.58 J/cm^2), equivalent to a mean of 26 MEDs. This is a dose normally sufficient to clear stable plaque psoriasis.

During UVB irradiation, subjects wore clothing that exposed only the arms and positioned their inner arm (a site that is not normally exposed to UV) toward the UV6 tubes (figs. 2.3, 2.4). Between UVB treatments subjects refrained from exposing themselves to sunlight. The MED was calculated for each subject using a template consisting of 4 squares, each measuring 2cm^2, and irradiating the template positioned on the inner arm with incremental doses of UVB. The lowest dose of UVB to produce visible erythema at 48 hours was taken as the MED.

Figure 2.1: The Waldmann 1000 ultraviolet B cabinet.

Figure 2.2: Spectral emission of UV6 tubes in the Waldmann UVB cabinet.

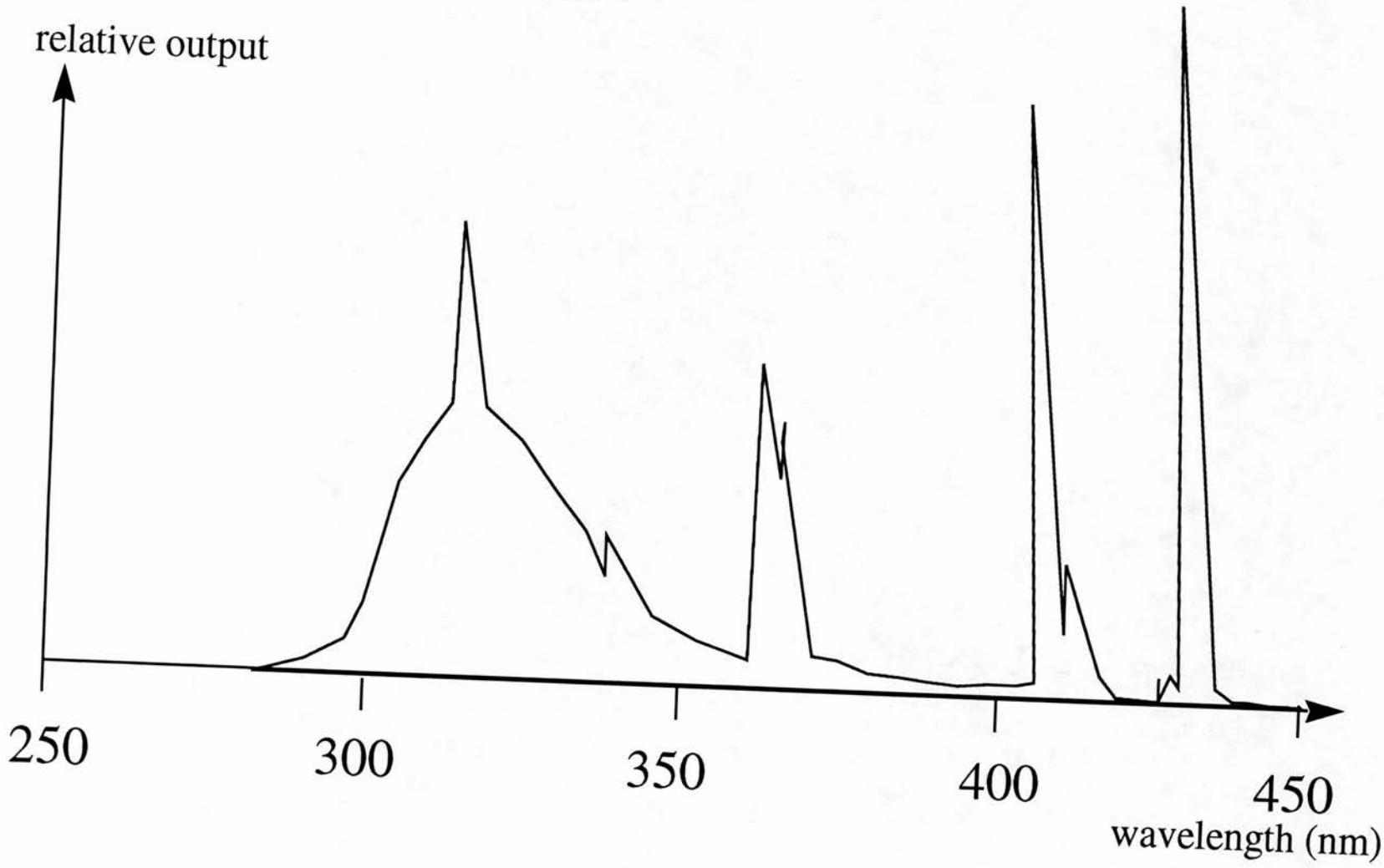

2.2 Preparation of epidermal samples.

Epidermal sheets were obtained with a suction blister device prior to UVB therapy and 48 hours after completion of UVB therapy (Kiistala and Mustakallio, 1967; Vestey *et al.*, 1990b). Four sterile cups, each producing five blisters of 5mm diameter, were attached to a vacuum pump and applied to the flexor aspects of the upper and lower arms at a suction pressure of 150mm Hg below atmospheric (fig. 2.5). After approximately two hours dermoepidermal separation had occurred (fig. 2.6). Confirmation that separation occurred within the lamina lucida of the epidermal basement membrane was gained by electron microscopy (figs. 2.7 - 2.10). The blister roofs were removed and divided for immunohistochemical labelling, confocal laser scanning microscopy and pre-embedding immunogold labelling. One blister roof from the forearm of each subject was snap frozen in liquid nitrogen, using a cryoprotectant (OCT), for immunohistochemical staining. In four subjects, a blister roof was prepared for confocal laser scanning microscopy. The remaining epidermal samples were incubated in 0.25% trypsin in Hanks buffered salt solution (Ca^{2+}, Mg^{2+}, and phenol red free; Flow laboratories, Irvine, Scotland) at 37°C for 1 hour for the purpose of immunogold transmission electron microscopy (TEM). The roofs were agitated and pipetted gently to form an EC suspension (fig. 2.11). ECs were washed twice in RPMI 1640 (Flow laboratories), containing 15% heat-inactivated foetal calf serum (FCS), and twice in RPMI 1640 alone, counted and then, using a haemocytometer, their viability determined by trypan blue exclusion (always > 80%).

2.3 Measurement of UCA and TNF-α .

In four subjects, suction blister fluid was collected before and after UVB irradiation and stored at -70°C for UCA and TNF-α analysis. UCA analysis was also performed on epidermal samples obtained using filter paper discs soaked in 0.1M KOH and applied to inner forearm, 30 mins, under Finn Chambers (Jansen *et al.*, 1991). Quantification of total epidermal UCA and the relative concentrations of the isomers was carried out by reverse phase high pressure liquid chromotography (HPLC; Norval *et al.*, 1988). HPLC was performed using a Waters 6000A solvent delivery system, a Rheodyne 7125 sample injection valve with a 20µl loop, a Waters M440 UV detector fixed at 254nm, a plotting integrator (Spectra-Physics autolab Minigrator), and a 15x4.6mm cartridge column (Capital HPLC, Scotland) packed with 5µm APS hypersil. The mobile phase was 10mM acetic acid, pH 5, and the flow rate 1.0 ml/min. TNF-α was measured using an ELISA kit with a quantitative 'sandwich' enzyme immunoassay technique (Research and Diagnostic Systems, Minneapolis, USA).

Figure 2.3: **The positioning of the inner arm and the clothing worn during irradiation are demonstrated by Professor Hunter outside the Waldmann 1000 UVB cabinet.**

Figure 2.4: **The arm of a subject who had finished the six week course of UVB phototherapy, showing tanning of the inner arm.**

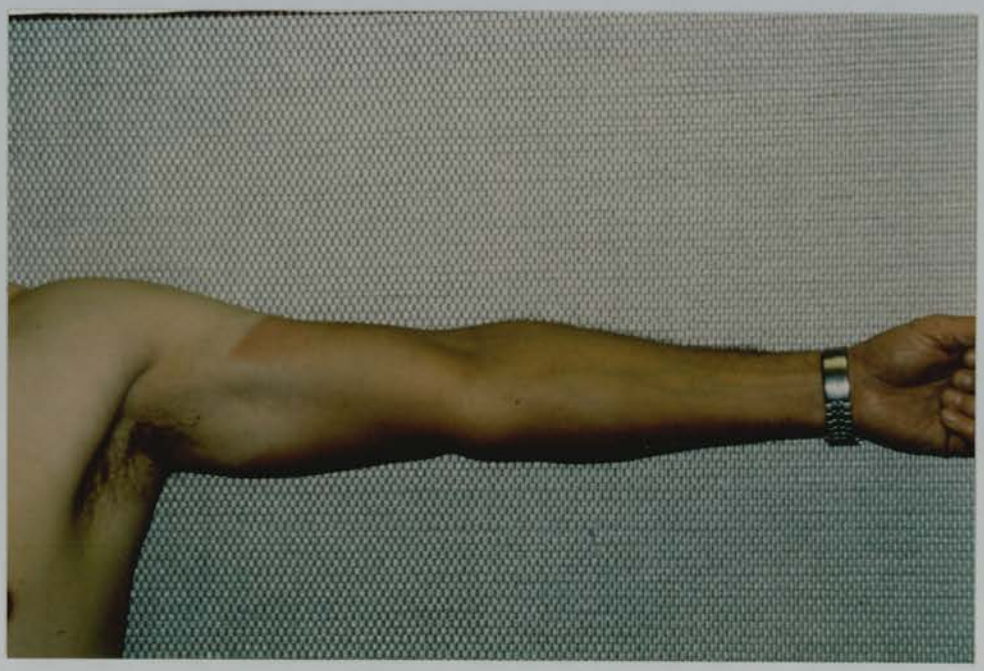

Figure 2.5: The suction blister device with two sterile cups attached.

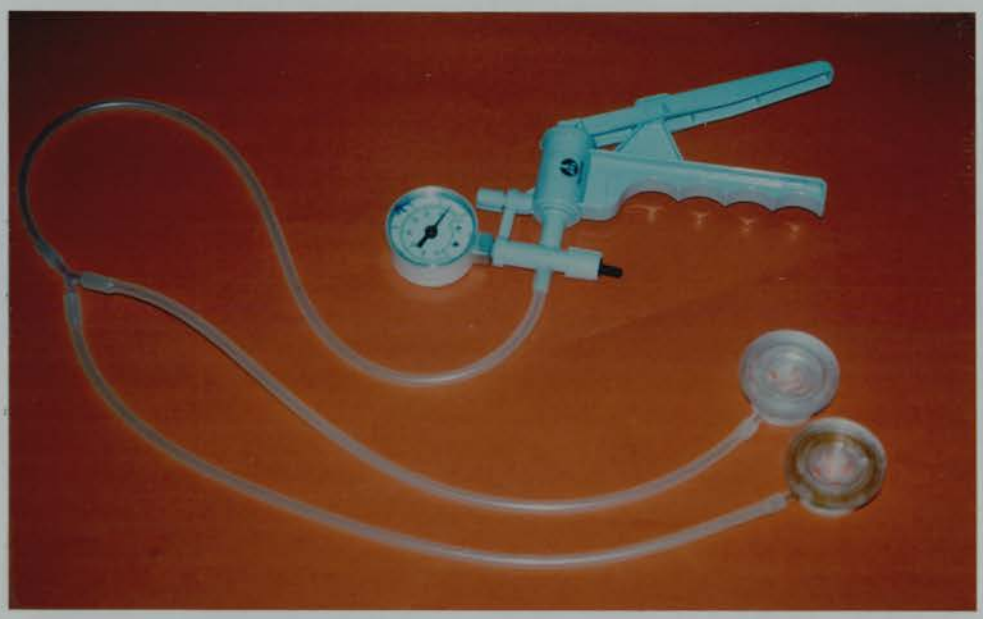

Figure 2.6: Blisters produced by the suction blister device.

Figure 2.7: **Diagram to show the suction blister technique for obtaining epidermal samples. The suction blister roof is excised by cutting through the epidermis, as indicated by the zig-zag lines.**

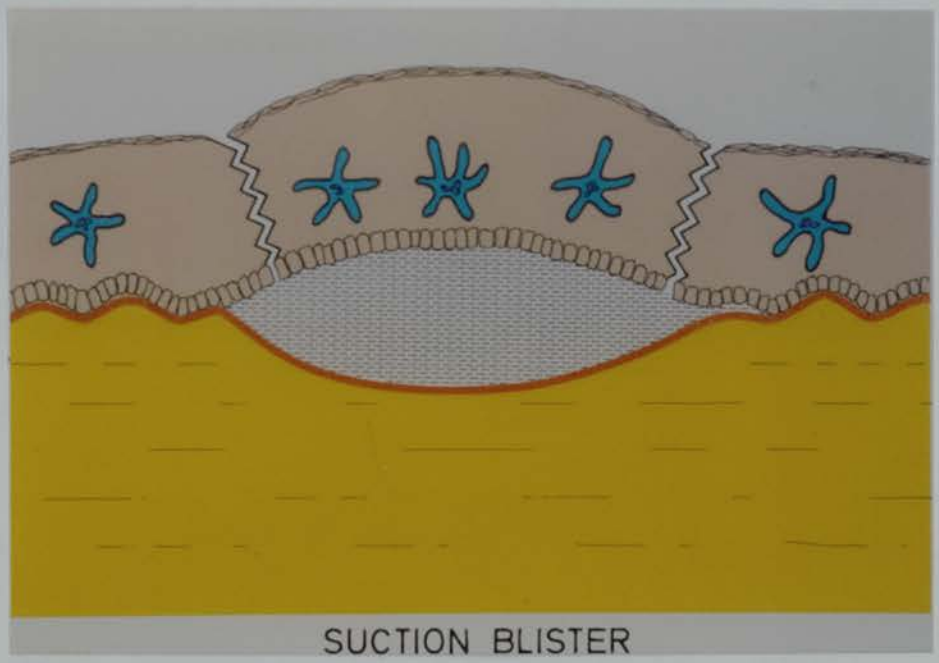

Figure 2.8: **Electron micrograph to show the lower portion of a suction blister roof. Note that some keratinocytes have become highly vacuolated (arrows), whereas the Langerhans cell (arrowhead) and melanocyte (asterisk) appear normal. Magnification 1,400 x**

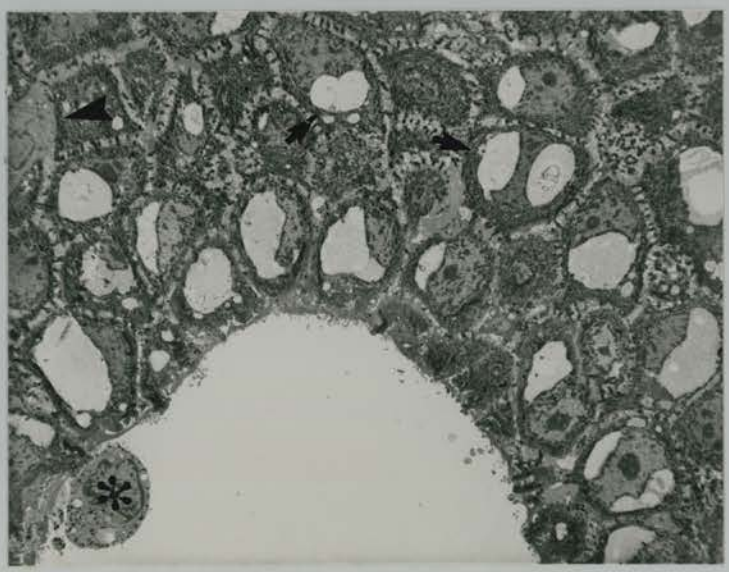

**Figure 2.9: Keratinocytes at the base of the suction blister roof show clean dermo-epidermal separation above the basement membrane.
Magnification 4,000 x**

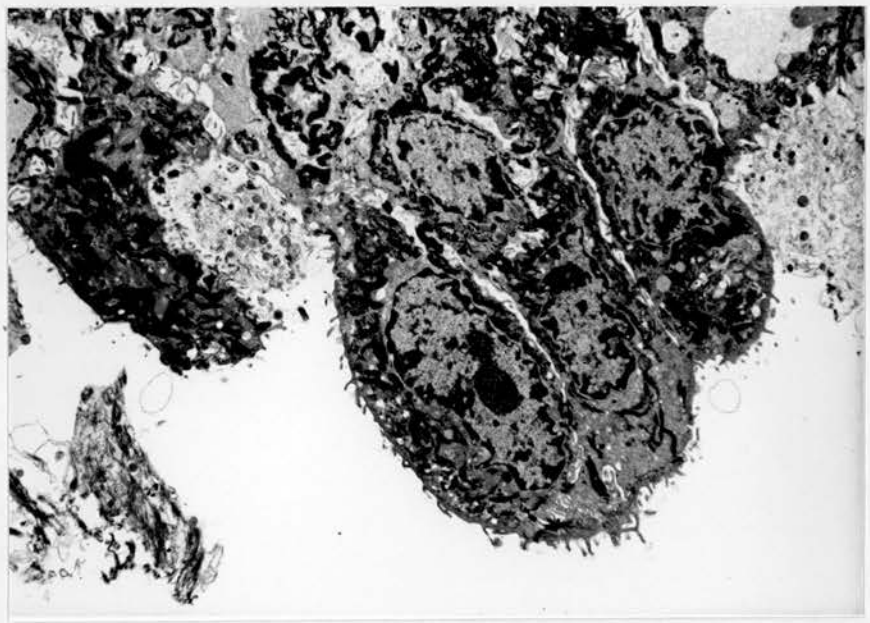

**Figure 2.10: Blister floor with melanocyte (asterisk). The basal lamina (arrowheads) of the basement membrane is attached to the blister floor.
Magnification 7,600 x**

Figure 2.11: Keratinocytes in epidermal cell suspension after trypsinization. Magnification 4,500x

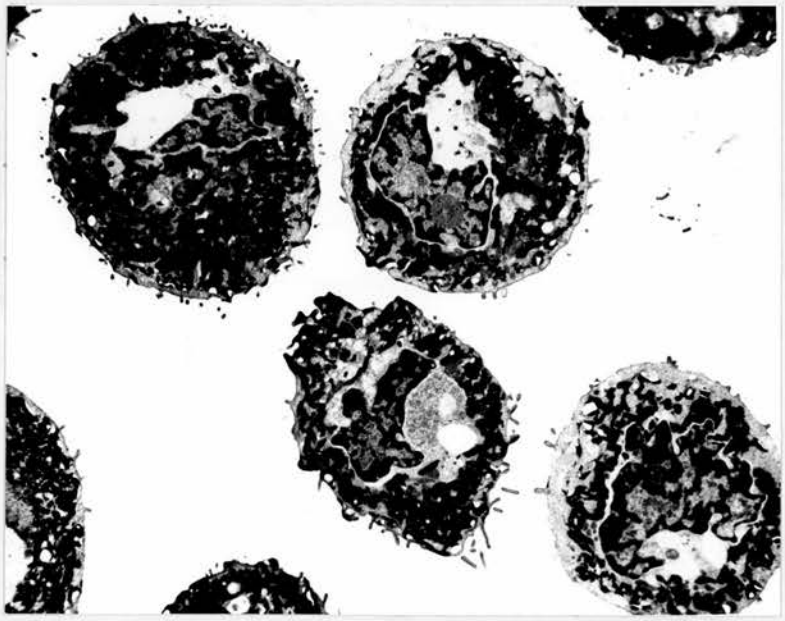

Briefly, 100µl of the samples and standards (serial dilutions of recombinant TNF-α) were incubated with buffer in a 96 well microtitre plate coated with murine monoclonal anti-TNF-α antibody, 2 hours at room temperature. The solutions were aspirated and the wells washed in buffer three times. Then a polyclonal antibody against TNF-α conjugated to horseradish peroxidase was added for 2 hours at room temperature, and the wells were washed three times in buffer. The amount of TNF-α was measured by a colorimetric reaction. After stopping colour development, TNF-α was detected by spectrophotometry at 450nm wavelength and the amount calculated from a standard curve. These measurements were made by Ms. Jill Gilmour, Department of Medical Microbiology, University of Edinburgh.

2.4 Monoclonal antibodies.

The monoclonal antibodies used in the following experiments are listed in table 2.2. The monoclonal antibody DA6.231 was used to label HLA-DP, -DQ, and -DR (Guy *et al.*, 1982), L243 was used to label HLA-DR, B7/21 to label HLA-DP (Watson *et al.*, 1983), and TU22 to label HLA-DQ (Pawelec *et al.*, 1982). OKT6 monoclonal antibody was used to label CD1a (Murphy *et al.*, 1983). The monoclonal antibodies against alpha fetoprotein were included in the study as irrelevant control antibodies for LCs, and have the same isotypes as the LC-specific antibodies.

Table 2.2 Monoclonal antibodies.

Antibody	sub-class	optimal dilutions*	source	specificity
DA6.231	IgG1	1/10	K.Guy	HLA-DP,DQ,DR
L243	IgG2a	1/10	B.Dickinson	HLA-DR
TU22	IgG2a	1/10,000	K.Guy	HLA-DQ
B7/21	IgG1	neat	K.Guy	HLA-DP
OKT6	IgG2a	1/100	B.Dickinson	CD1a
Anti-AFP	IgG1	1/10	Serotec	α-fetoprotein
Anti-AFP	IgG2a	1/10	Serotec	α-fetoprotein

*=optimal dilutions for both immunocytochemistry and for immunogold labelling.

2.5 Determination of optimal dilutions of monoclonal antibodies.

Optimal dilutions of the antibodies were determined by analysing antibody labelled ECs in suspension (10^6 cells per ml in RPMI 1640 medium) with a fluorescence

activated flow cytometer and FACScan software (Becton Dickinson, California, U.S.A.). Tubes containing 0.1 ml of the EC suspension were incubated for 20 mins with an equal volume of phosphate buffered saline/ 0.01% bovine serum albumin/ 0.02% sodium azide/ 20% normal rabbit serum (PBS/BSA/Azide/NRS) at 20°C. Varying dilutions of primary antibody (0.1ml) in PBS/BSA/Azide/NRS were added for 30 mins at 20°C, followed by 1ml of PBS/BSA/Azide/NRS. The cells were spun, the supernatant decanted, and 0.01 ml rabbit anti-mouse IgG, $F(ab')_2$ fraction, conjugated to fluorescein isothiocyanate (FITC; DAKO,UK) 1:80 added for 30 mins at 20°C. Then 1ml of PBS/BSA/Azide/NRS was added, the cells spun, the supernatant decanted and the cells were fixed in 1% formaldehyde. The flow cytometer calculated the mean intensity of fluorescent marker per cell. This value was plotted against antibody dilution to give the optimal dilutions for the antibodies listed in table 2.2. The analysis was repeated on four occasions using skin obtained from four patients who were undergoing breast reduction surgery. These dilutions were used to label ECs in suspension for immunogold labelling.

2.6 Labelling and enumeration of LC visualized by an immunohistochemical technique.

Cryostat sections (6μm) were cut perpendicular to the surface of the blister roofs from the forearm, air-dried, and fixed in acetone for 10 mins. The epidermal sections were stained by an indirect immunoperoxidase technique with the primary antibodies listed in table 2.2, at optimal dilutions determined by testing antibody titres on sections (which were identical to those used for EC suspensions), followed by peroxidase-conjugated rabbit anti-mouse IgG, diluted 1:20 in 20% normal rabbit serum (NRS) as the secondary antibody. Sections were incubated in NRS alone as a negative control. The range of antibodies against CD1a and MHC II molecules served as positive controls for each other. The reaction product was visualized with diaminobenzidine. Sections were counterstained with Mayer's haemalum. The number of positively-stained ECs were manually counted within two randomly-selected fields (objective lens magnification 10x) in each of five sections from all subjects both before and after UVB irradiation and expressed per millimetre of basal cell plasma membrane, measured by image analysis (Seescan, Cambridge, England). This metric measurement system was used because epidermal thickness was increased after UVB irradiation, and would give a spurious impression of LC depletion per unit area even if no absolute change in LC number had occurred. All positively-labelled ECs with a cell body in the section were counted.

2.7 Confocal laser scanning microscopy.

One blister roof was taken from the forearm of each of four subjects before and after UV irradiation. One subject donated tissue which was removed by scalpel without local anaesthetic. The blister roof was incubated in anti-CD1a antibody directly conjugated with FITC, diluted 1:100 in PBS/3% BSA, overnight at 4°C. No fixative was used in order to prevent any chemically-induced tissue shrinkage. The epidermal sheet was then washed 3 times, 10 mins each wash, in PBS/BSA and then mounted in Citifluor antifadent mountant (Citifluor Ltd., London, U.K.). The 488nm line from an argon ion laser was used to excite FITC. In each sample the total fluorescent area and the number of LCs were measured in five low power fields by image analysis (using a Kontron Ibas 20 analyser) before and after exposure to UVB using a Zeiss LSM 10 confocal microscope at an objective lens magnification of 40x and a zoom of 20x (800x magnification) with sections in the z plane separated by 1 μm. The morphology of ten CD1a+ LCs was examined in each sample. Every cell was optically sectioned throughout the entire z plane which involved taking a maximum of forty sections at a magnification of 3200x (40x objective lens with an 80x zoom), sections being separated by 0.5μm. The sections were superimposed to reconstruct two-dimensional images which represented the three-dimensional shape of the cells. The first section in a series of z sections through a cell was always positioned immediately above the cell, and the sections continued until no more fluorescent marker could be detected. Cell reconstructions in two dimensions were produced with the confocal laser scanning microscope and these images were saved onto 20 megabyte cartridge and analysed on an image analyser (Kontron IBAS 20) for dendrite numbers, lengths, perimeter of the entire cell, perimeter of the putative cell body, area of the entire cell and area of the putative cell body. Ten cells from one subject before and after UVB exposure were reconstructed to make three-dimensional cell images using an image analysis software package (Software provided by Vital Images Inc., Fairfield, U.S.A., and hardware by Silicon Graphics, U.S.A.).

2.8 Labelling of EC surface markers for immunogold TEM.

The ECs were prepared from blister roofs, as described above, and resuspended at a concentration of 10^6 ECs/ml prior to a light prefixation with periodate-lysine-paraformaldehyde. The ECs were then washed in cacodylate buffer (pH 7.4), blocked with PBS containing 1% BSA, 0.2% azide and 10% decomplemented human AB serum for 30 mins, and washed in PBS containing 0.1% BSA (PBS-0.1% BSA). The ECs were then labelled with the primary antibody, diluted in PBS-0.01% BSA, at

37°C for 30 mins, washed, and incubated with 15 or 30nm gold particles conjugated to goat anti-mouse IgG (GAM-G15 or GAM-G30, Janssen Pharmaceutica, Beerse, Belgium), diluted 1:2 in PBS-0.01% BSA, as described previously (De Panfilis *et al.*, 1990a). After washing in cacodylate buffer, the ECs were fixed and processed for TEM. Controls consisted of omission of the primary antibody or its substitution with another antibody of the same isotype (alpha-fetoprotein, IgG1 and IgG2a isotypes).

2.9 Processing of ECs for immunogold TEM.

The ECs were fixed in 2% formaldehyde and 2.5% glutaraldehyde in 0.04M cacodylate buffer, containing 0.05% calcium chloride and 5% sucrose (pH 7.4) and post-fixed in 2% aqueous osmium tetroxide (Karnovsky, 1965). The ECs were then dehydrated in a graded series of ethanol and embedded in Araldite CY212 (Agar Scientific Ltd., Essex, England). Ultrathin sections with a pale gold interference colour were cut on a LKB Ultratome III, post-stained with methanolic uranyl acetate and lead nitrate, mounted on 400 mesh copper grids, then viewed with a Philips EM301 electron microscope at an accelerating voltage of 60kV (fig. 2.12). A calibration grid with 2160 lines per mm (Agar Scientific, England) was photographed during each session on the electron microscope.

2.10 Measurement of section thickness.

The precise thickness of 22 ultrathin sections of pale gold interference colour was determined. The sections were collected on 400 mesh copper grids and re-embedded at 90° to the original plane of section. They were resectioned and measured directly from electron micrographs.

The next two sections describe methods for the examination of the distribution of CD1a and MHC II antigens over the surface of individual LCs.

2.11 Quantification of gold label on single ultrathin sections.

Electron micrographs of ten single LC sections for each antibody used in this study were divided into halves and into quarters. The gold particles on these portions of LC sections were manually counted and LC plasma membrane length was measured directly from electron micrograghs using planimetry. The results were expressed as gold particles per µm LC plasma membrane.

Figure 2.12: The Philips 301 transmission electron microscope.

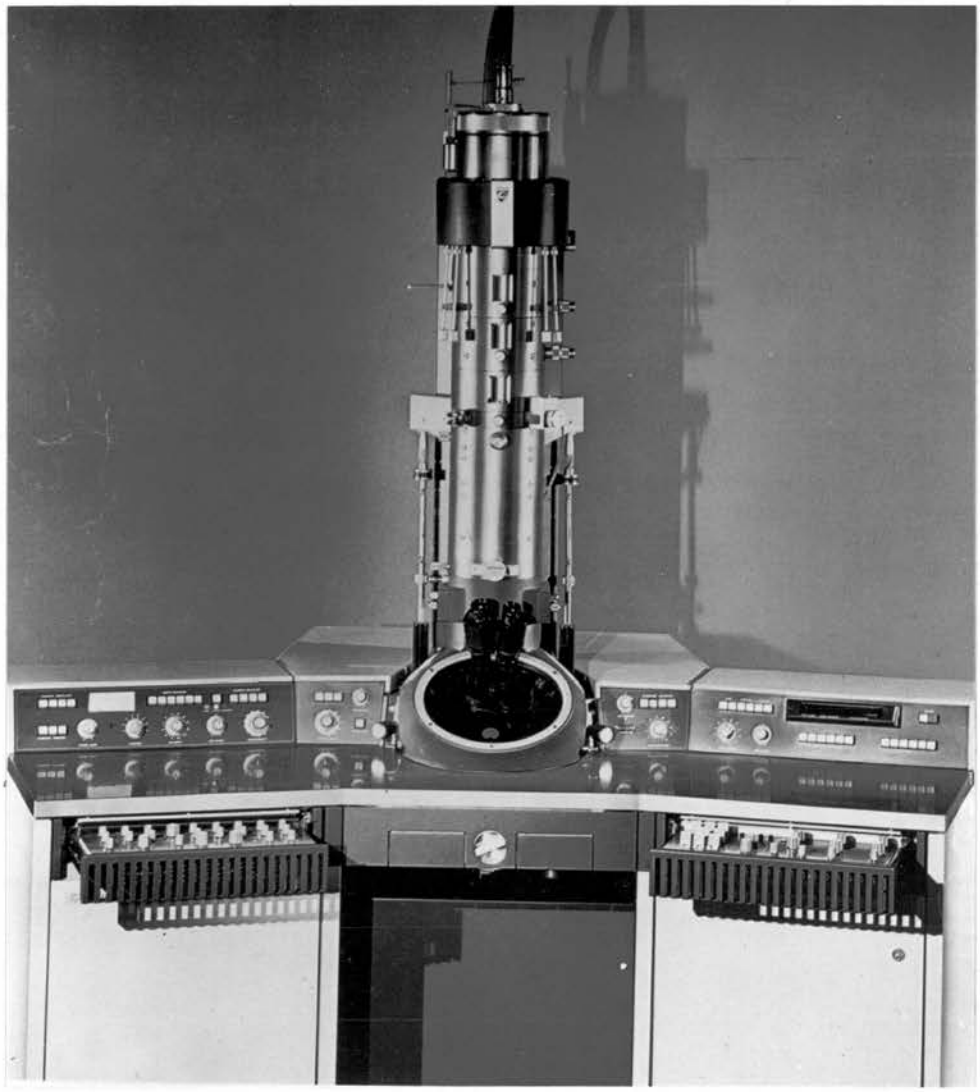

2.12 Quantification of gold label on a series of sections (step-sections) through single cells.

ECs were prepared before and after UVB irradiation and labelled with anti-CD1a and MHC II antibodies (DA6.231, L243, B7/21, Tu22), followed by GAM-G30. The distribution of the surface MHC II molecules on individual labelled cells was then calculated. The number of gold particles per μm plasma membrane was counted in two to five step-sections through each of fifteen DA6.231+ve, five B/721+ve, five TU22+ve and five L243+ve LCs and indeterminate cells before UVB and LCs after UVB irradiation (a total of 60 cells), derived equally from five subjects before and after UVB irradiation. Step-sections were separated by approximately 1 μm (every 20th section was examined) and all labelled ECs in that section were photographed at 2,800x and 5,900x magnifications. Recognition of individual LCs or indeterminate cells in adjacent step-sections was achieved by comparing neighbouring ECs. The number of gold particles was counted either manually or with the aid of image analysis and expressed per μm of plasma membrane. The plasma membrane length was measured either by planimetry of the cell perimeter on electron micrographs or by image analysis.

2.13 Determination of intra-subject variation of surface MHC II expression.

EC suspensions were prepared prior to UVB irradiation and labelled with anti-CD1a and MHC II antibodies (DA6.231, L243, B7/21, Tu22) followed by either GAM-G15 or GAM-G30. During an early stage of the study, GAM-G15 was used as a secondary antibody after labelling with anti-pan MHC II, DA6.231, solely for analysis of intra-subject variation of pan-MHC II expression by LCs. It was discovered that the image analysis system used here could neither accurately count nor separate closely adjacent 15nm gold particles, but it could do so for 30nm gold particles. Therefore all measurements of such 15nm gold particle densities were done manually and all subsequent labelling of EC suspensions was carried out using 30nm gold particles (the cell surface densities of which could be measured using image analysis). Steric hinderance may be caused by the use of large (30nm) gold particles conjugated to secondary antibody and prevent its penetration to the site of primary antibody attachment on the cell surface. Steric hinderance would thus lead to reduced densities of large gold particles on cell surfaces compared with densities of smaller gold particles. Steric hinderance in this study caused by use of 30nm gold particles may prevent the detection of absolute numbers of cell surface antigens, but would presumably be a constant factor for a given size of gold particle, and therefore allow a comparative quantitative measure of gold particle densities on cell surfaces.

Single sections through approximately 100 LCs and indeterminate cells from individual subjects were examined for each antibody (separate subjects for each antibody), to examine intra-individual variation in expression of these molecules. The same methods as above were used to determine the surface density of these antigens.

2.14 The effect of UVB on LC or indeterminate cell surface molecule expression.

The influence of a six week course of suberythemal UVB phototherapy on surface CD1a and MHC II expression by ECs from nine subjects was studied. EC suspensions were prepared from each volunteer before and after UVB irradiation and labelled with the primary antibodies listed in table 2.2, followed by GAM-G30 secondary antibody. The cell suspensions were processed and sectioned for TEM, and the number of gold particles per micron plasma membrane determined on five different LCs or indeterminate cells for each subject before UVB irradiation and five different LCs per subject after UVB irradiation. All positively labelled cells on a particular grid were photographed irrespective of whether the cells were partially obscured by grid bars, with the exception of very small cell portions with less than a quarter of the cell perimeter visible. Five cells per sample were then picked randomly for analysis.

2.15 A semi-automatic technique for measuring the density of gold label on ECs.

The gold label density on the surface of ECs was measured from the negatives of electron micrographs mounted on a light box, using an image analyser with an interactive (semi-automatic) software programme specifically developed by Seescan plc, Cambridge, Great Britain. This technique involved the automatic counting of gold particles by the computer, the results of which could be examined and edited manually. This allowed the operator of the image analyser to override the decision of the analyser, if, for example, the computer had counted two overlapping gold particles as one, or if gold particles had been either incorrectly omitted or incorrectly counted. Then the image analyser automatically measured the cell perimeter in μm, and calculated the density of gold particles per μm cell membrane.

2.16 Assessment of image analysis: correlation, repeatability and agreement with a manual technique.

Correlation: The density of gold label on a series of LCs was measured in two ways, 1) manually and 2) using the semi-automatic image analysis technique described

above. The two types of measurements were directly plotted to make an initial assessment of the correlation between them.

Repeatability: A series of fifteen cells were measured on two occasions both manually and by image analysis. The differences between the two measurements, the mean difference and the standard deviation of the differences were calculated. We expect 95% of the differences to vary by less than two standard deviations from the mean difference. This is the definition of a repeatability coefficient adopted by the British Standards Institution (British Standards Institution, 1979). The coefficient of repeatability was calculated for both methods.

Agreement: A statistical comparison was made between the manual and image analysis methods in order to establish whether the image analysis results were sufficiently similar to the manual results to be confident of their accuracy (Bland and Altman, 1986). A correlation coefficient was calculated. A high correlation coefficient (one that approaches a value of 1) indicates that the results obtained by the two methods are linearly related. However, this does not necessarily indicate that the methods agree. Agreement was assessed by examining the differences between the results and calculating the mean difference (d) and the standard deviation of the differences (s). The differences were plotted against the mean of the two results in order to highlight any discrepancies. The values falling between d + 2s and d - 2s were taken as the limits of agreement (95% of the differences will lie between these two limits). If the differences vary in a systematic way over the range of measurement i.e. the scatter of the differences increases as the measurement increases, then the limits of agreement would be wider than necessary for small measurements and narrower than necessary for large measurements. A log transformation of the data was performed where the differences between the measurements were proportional to the mean of the two measurements.

2.17 Statistics

The two sample t test was used to analyse data derived from the measurements of gold label density on single LC sections. The analysis of variance (ANOVAR) was used for statistical analysis of the data regarding UVB-induced alterations in cell morphology derived from confocal laser scanning microscopy, and LC surface MHC II expression derived from immunoperoxidase and immunogold labelling. A p value of < 0.05 was considered significant.

Results

Flow chart to show numbers of subjects and methodologies used:

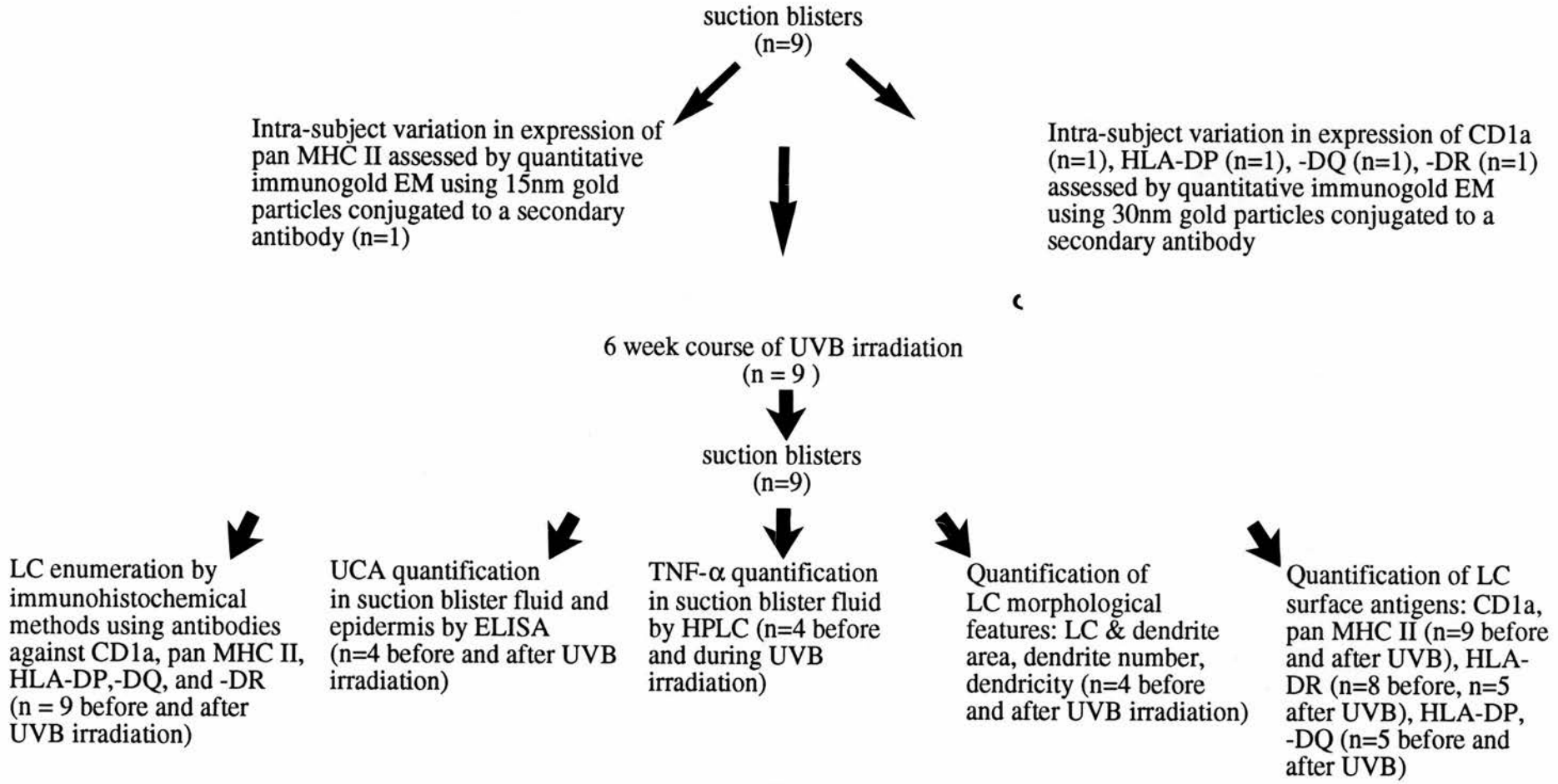

Chapter 3. Development of Techniques

3.1 Subjects, MED values and UVB doses received

The subject details are recorded in table 3.1. The subjects decided which skin type category they belonged to according to the system devised by Dr. Fitzpatrick and his colleagues in Boston, on the basis of their skin reactivity to the sun. In this system, people with:

skin type I - always burn and never tan;
skin type II - sometimes burn and never tan;
skin type III - never burn and sometimes tan;
skin type IV - never burn, always tan;
skin type V - Asian subjects;
skin type VI - Black African subjects.

Although this system is useful in predicting a person's sun sensitivity, it may not be as accurate as testing small areas of skin with increasing doses of UVR in order to determine the MED. This is demonstrated in table 3.1, in which subjects 2, 3, 4, 7 and 9 reported skin types which did not correspond well to the determined MED values.

Table 3.1

subject	initials	skin type	MED (mJ/cm^2)	total UVB (J/cm^2)	total UVB (MEDs)
1	MJT	II	148	4.1	27.6
2	JPV	III	148	3.6	24.5
3	EM	II	290	5.6	19.2
4	MJS	II	205	5.6	27.2
5	JAAH	II	148	5.6	37.7
6	SK	I	106	2.6	24.3
7	GCP	III	148	2.9	19.6
8	MG	III	290	5.6	19.2
9	NH	III	106	3.7	35.3

3.2 Optimal dilutions of monoclonal antibodies

The optimal antibody concentrations were determined using fluorescent flow cytometric analysis of labelling on ECs in suspension (described in section 2.5). The flow cytometer produces a stream of single cells and passes the cells through a laser

Figure 3.1: Histogram produced by fluorescent flow cytometric analysis of approximately 10^5 epidermal cells in suspension. The electronic "gates" are depicted as a box, which excluded the cluster of small particles of low granularity shown in the bottom left hand corner of the histogram.

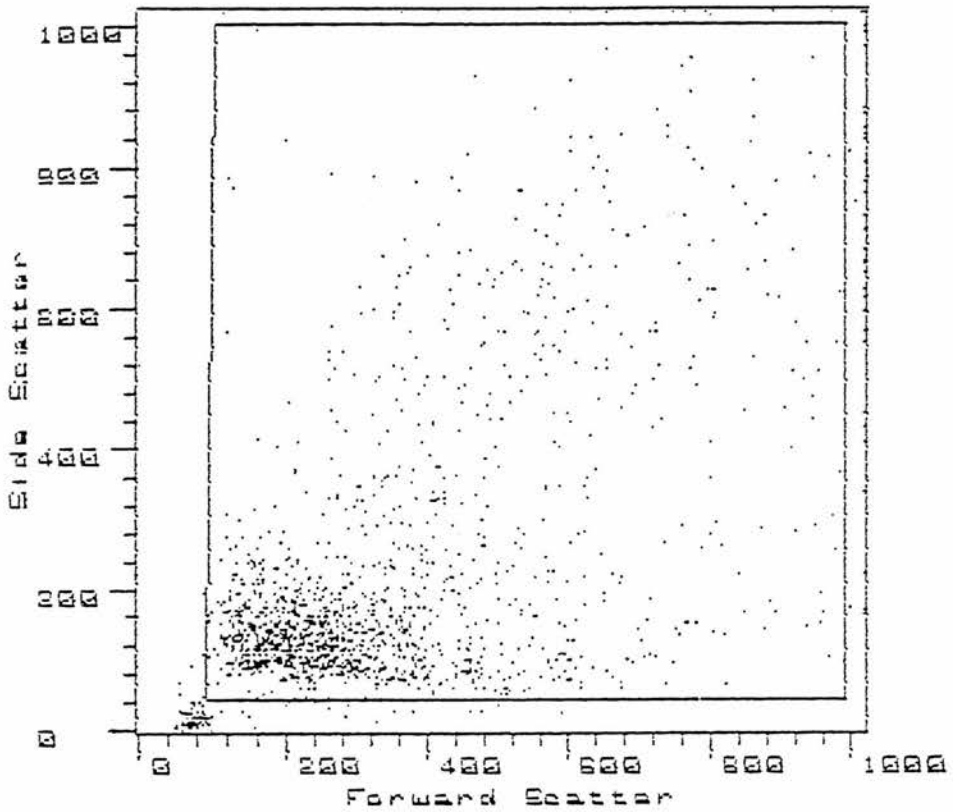

beam. The laser is deflected at a forward angle as a result of the cells passing through the beam, which is proportional to the cell size, and is deflected at a 90^{o} angle, which is proportional to cell granularity. This information can be used to construct a histogram and a typical example derived from this work is shown in figure 3.1. The cluster of material depicted in the bottom left hand corner of this histogram probably represents small particles, possibly ruptured cells, and was electronically "gated" out. The mean intensity of fluorescent labelling on positively labelled cells was plotted against the antibody dilution to give the optimal dilutions. Figure 3.2 shows the results from one experiment and table 3.2 shows the optimal dilutions. Note from figure 3.2d that although the optimal dilution of HLA-DP was apparently 1:100, the avidity of this antibody is very low, and therefore was used neat.

Table 3.2 The optimal dilutions of monoclonal antibodies against LC surface molecules.

Monoclonal antibody	optimal dilution
CD1a	1:100
DA6.231	1:10
L243	1:10
B7/21	neat
TU22	1:10,000

3.3 Development of the immunogold labelling technique

Variations in section thickness could influence the gold density measurements, with labelled cells on thick sections appearing to be more densely labelled than those on thin sections. Therefore uniformity of section thickness is desirable. Thus the thickness of sections selected for TEM was initially examined, as described in section 2.10. The mean thickness of 22 ultrathin sections of pale gold interference colour was found to be 68.15nm +/- 0.73 (standard error), data given in table 3.3. These results indicate that section thickness has a normal distribution with low standard error. Initially corrections were made for section thickness for gold label density measurements, but since the corrections made no significant difference to the result, these were considered unnecessary in further measurements (see appendix 6, abstract 1).

Figure 3.2a: Experiment to determine the limiting dilution of OKT6 (anti CD1a) monoclonal antibody.

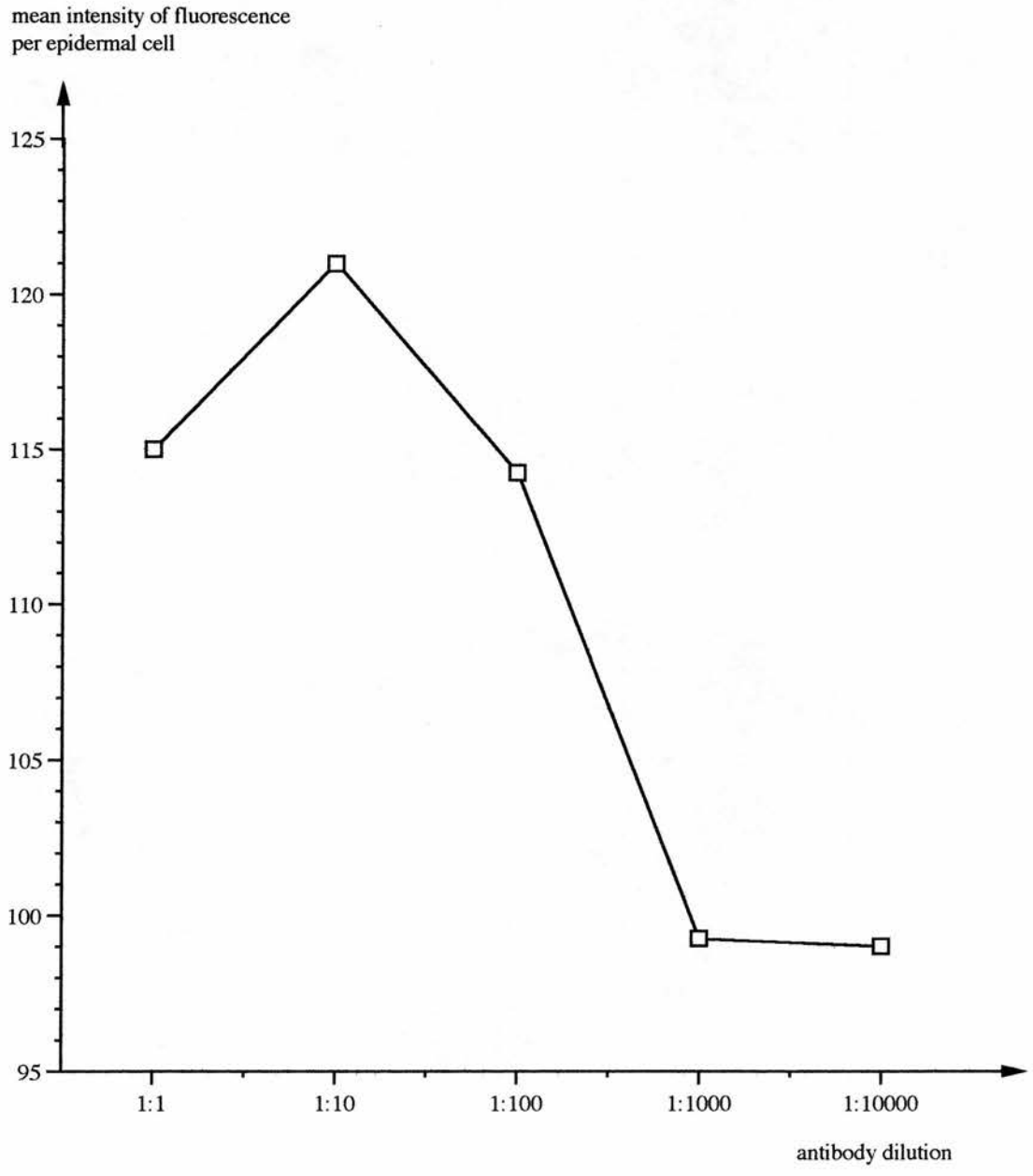

Figure 3.2b: Experiment to determine the limiting dilution of DA6.231 (anti pan MHC II) monoclonal antibody.

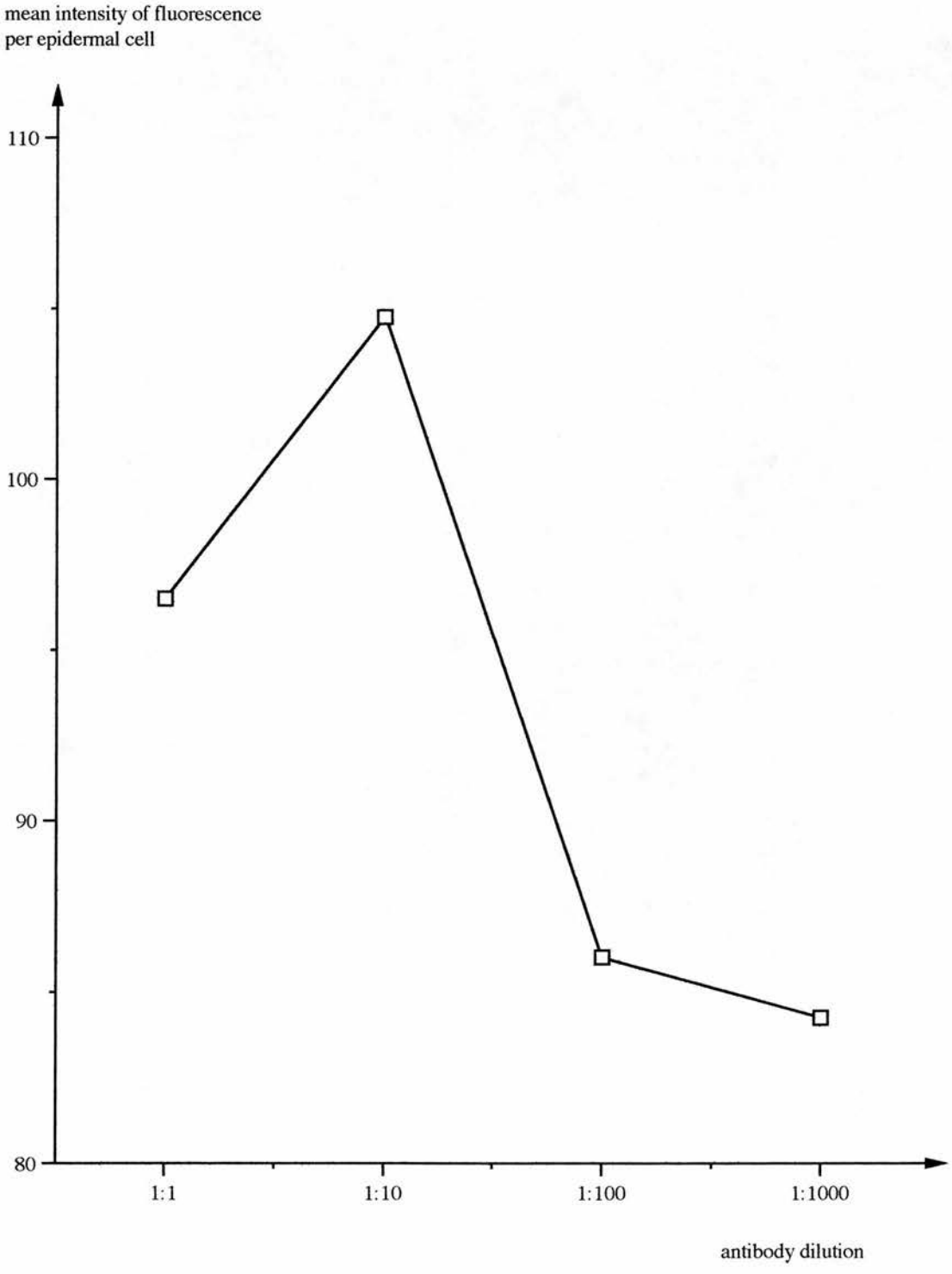

Figure 3.2c: Experiment to determine the limiting dilution of L243 (anti-HLA-DR) monoclonal antibody

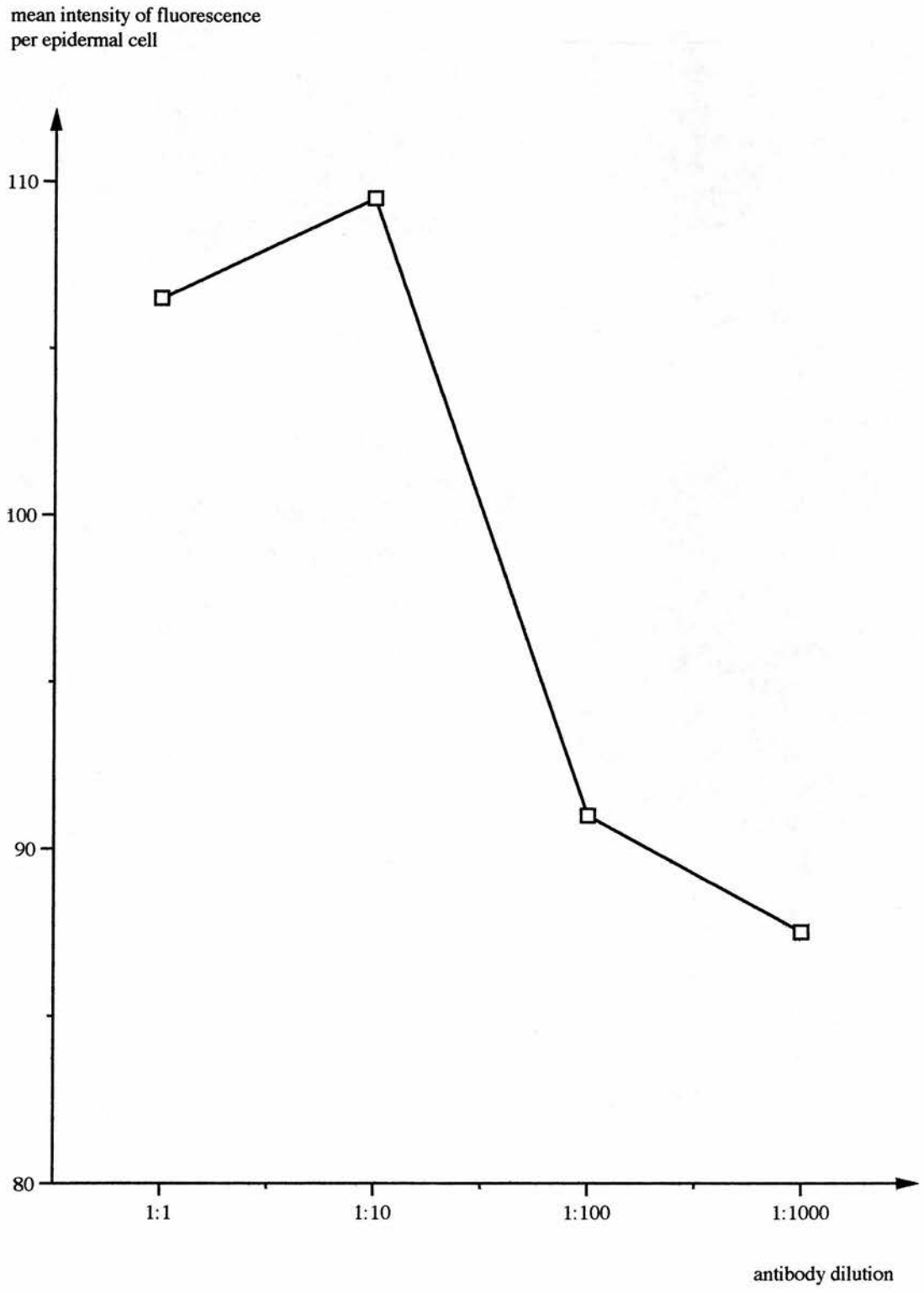

Figure 3.2d: Experiment to determine the limiting dilution of B7/21 (anti HLA-DP) monoclonal antibody.

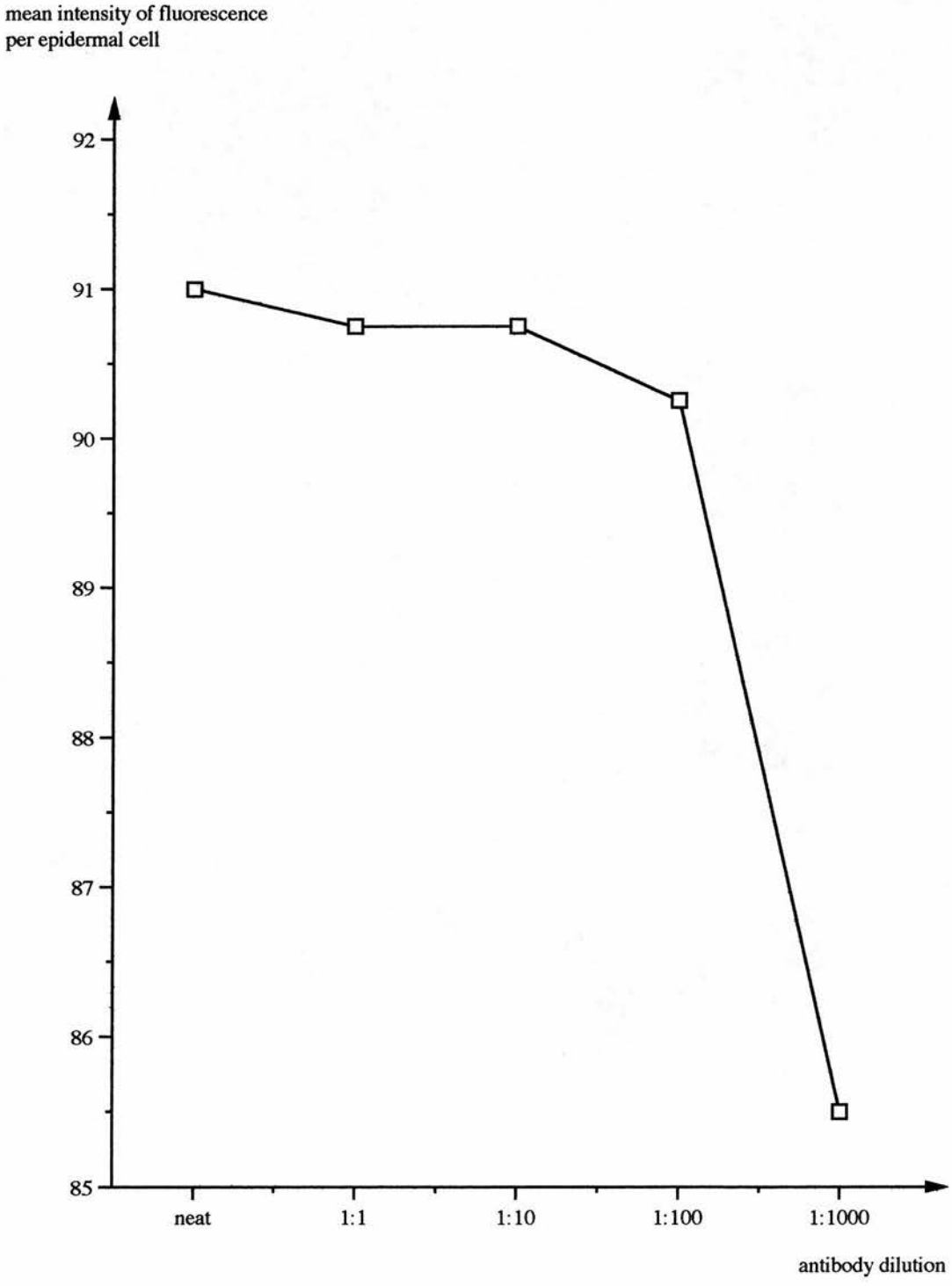

Figue 3.2e: Experiment to determine the limiting dilution of TU22 (anti HLA-DQ) monoclonal antibody.

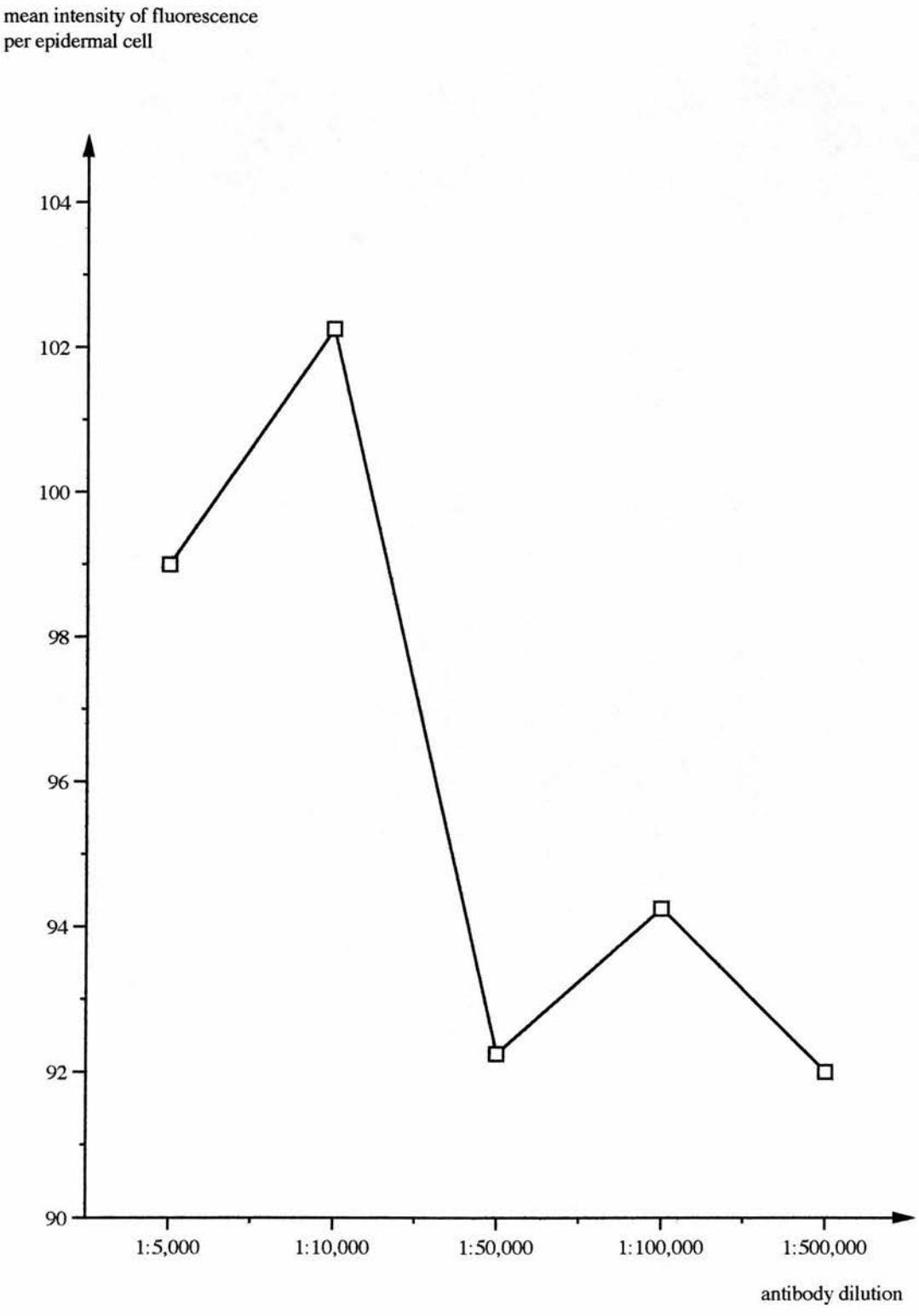

Table 3.3 Measurement of the thickness of ultrathin sections.

ultrathin section	section thickness (nm)	ultrathin section	section thickness (nm)
1	64.93	12	66.66
2	60.12	13	75.30
3	69.14	14	70.06
4	68.53	15	67.90
5	69.44	16	72.84
6	68.84	17	68.84
7	62.53	18	69.14
8	70.95	19	71.60
9	69.14	20	67.90
10	62.96	21	68.49
11	65.43	22	68.49

The distribution of gold label on ultrathin sections through LCs or indeterminate cells.

Quantification of gold label on the plasma membrane of one section through each of ten separate LCs, electron micrographs of which had been divided into halves and quarters, was performed for each monoclonal antibody. The results are given in appendix 1. The data were analysed by means of two sample t tests. No significant differences were detected between the measurements on quarter and half cell portions for any of the antibodies. This result indicates that the gold particle density is uniform over the surface of a single LC section.

The distribution of gold label on a series of sections (step-sections) through single cells (LCs and indeterminate cells).

Multiple sections were taken at equal intervals through single LCs and indeterminate cells (approximately 1 micron separated these step-sections) in order to examine the surface distribution of CD1a and MHC II molecules (fig. 3.3-3.10, table 3.5, appendix 2). The assessment of step-sections through 15 DA6.231+ve, 5 L243+ve, 5 TU22+ve

Figure 3.3:

a-c) Three step-sections through a single DA6.231+ve (pan MHC II+ve) Langerhans cell from unirradiated skin showing the uniformity of surface MHC II expression. The MHC II is labelled with DA6.231 primary antibody and secondary antibody conjugated to 30nm gold particles (arrows). Note the absence of labelling on neighbouring keratinocytes. d) Birbeck granules (arrowheads) within the Langerhans cell cytoplasm (inset from figure 3.3c).
Magnification a-c) 8,850 x
Magnification d) 37,800 x

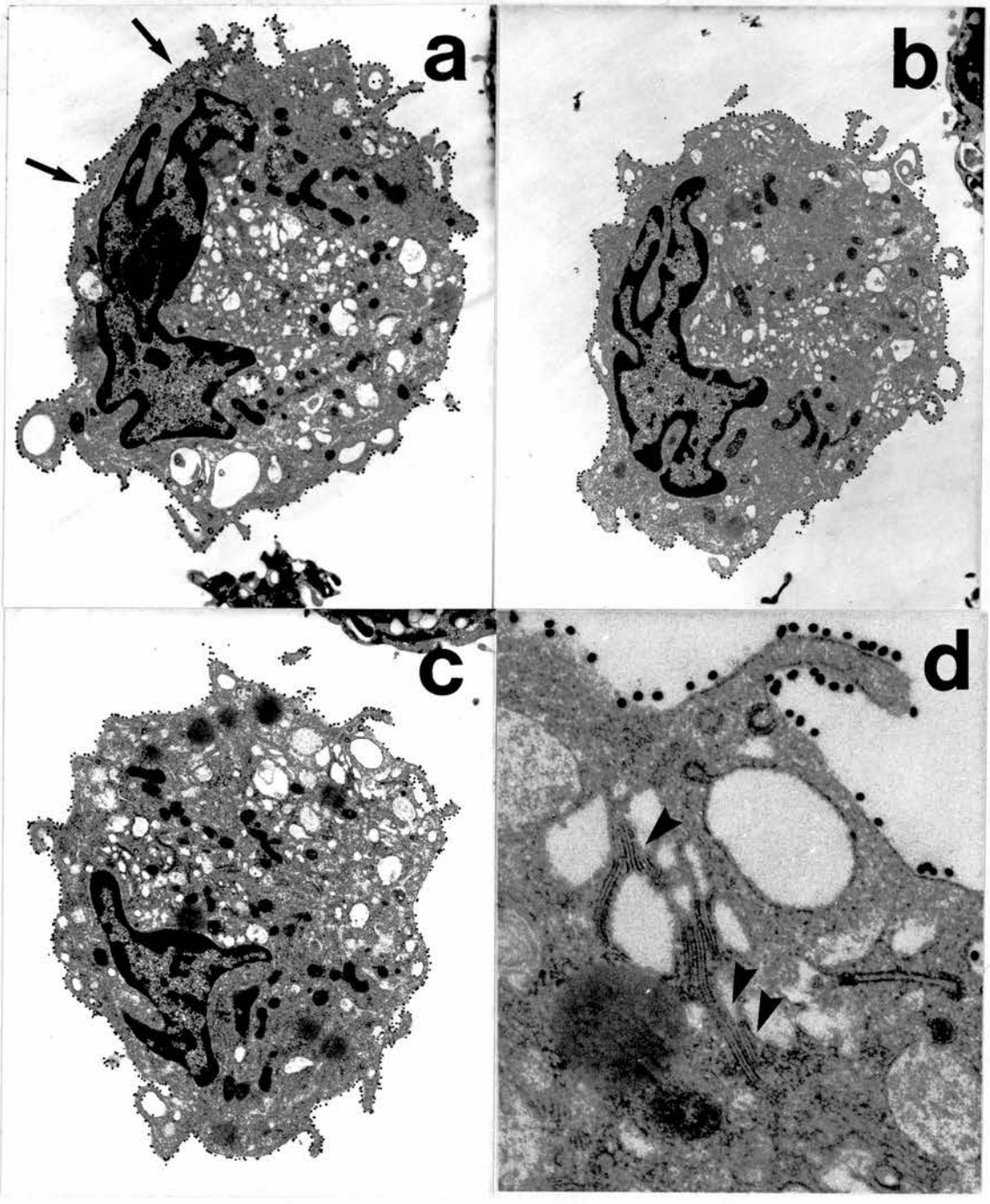

Figure 3.4:

a-c) Three step-sections through a single DA6.231+ve (pan MHC II+ve) Langerhans cell from UVB-irradiated skin showing the expression of a similar density of surface MHC II as that demonstrated on the surface of the control unirradiated Langerhans cell (see figure 3.3). The MHC II is labelled with DA6.231 primary antibody and secondary antibody conjugated to 30nm gold particles (arrows). Note that the Langerhans cell has a normal ultrastructural morphology. d) Birbeck granule (arrowhead) within the Langerhans cell cytoplasm (inset from figure 3.4b).
Magnification a-c) 9,100 x
Magnification d) 38,700 x

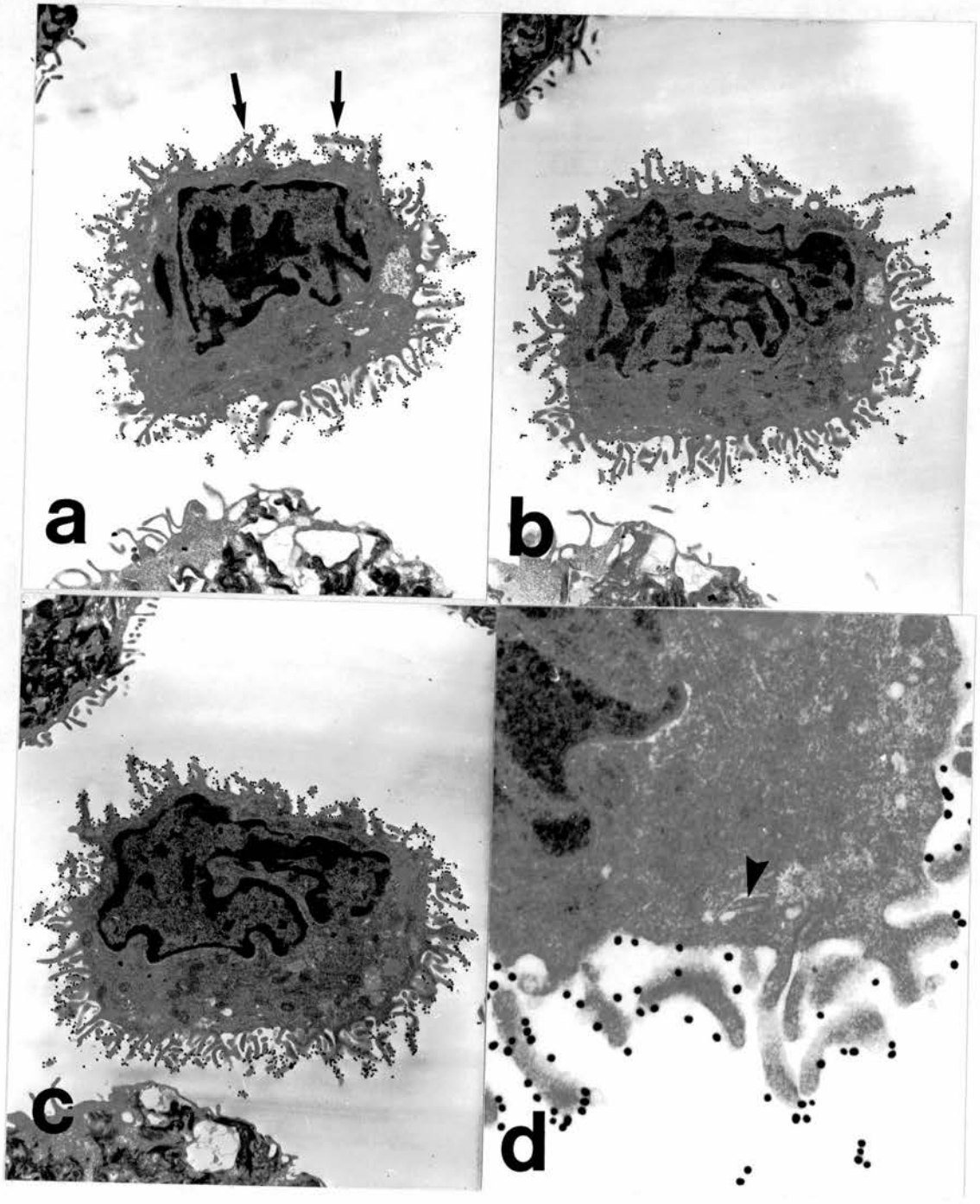

Figure 3.5:

a-c) Three step-sections through a single L243+ve (HLA-DR+ve) Langerhans cell from unirradiated skin. The cells are labelled with L243 primary antibody followed by a secondary antibody conjugated to 30nm gold particles. Note the uniform distribution of gold label over the cell surface. d) A Birbeck granule (arrowhead) is present within the Langerhans cell cytoplasm (inset from figure 3.5b).
Magnification a-c) 7,800 x
Magnification d) 36,400x

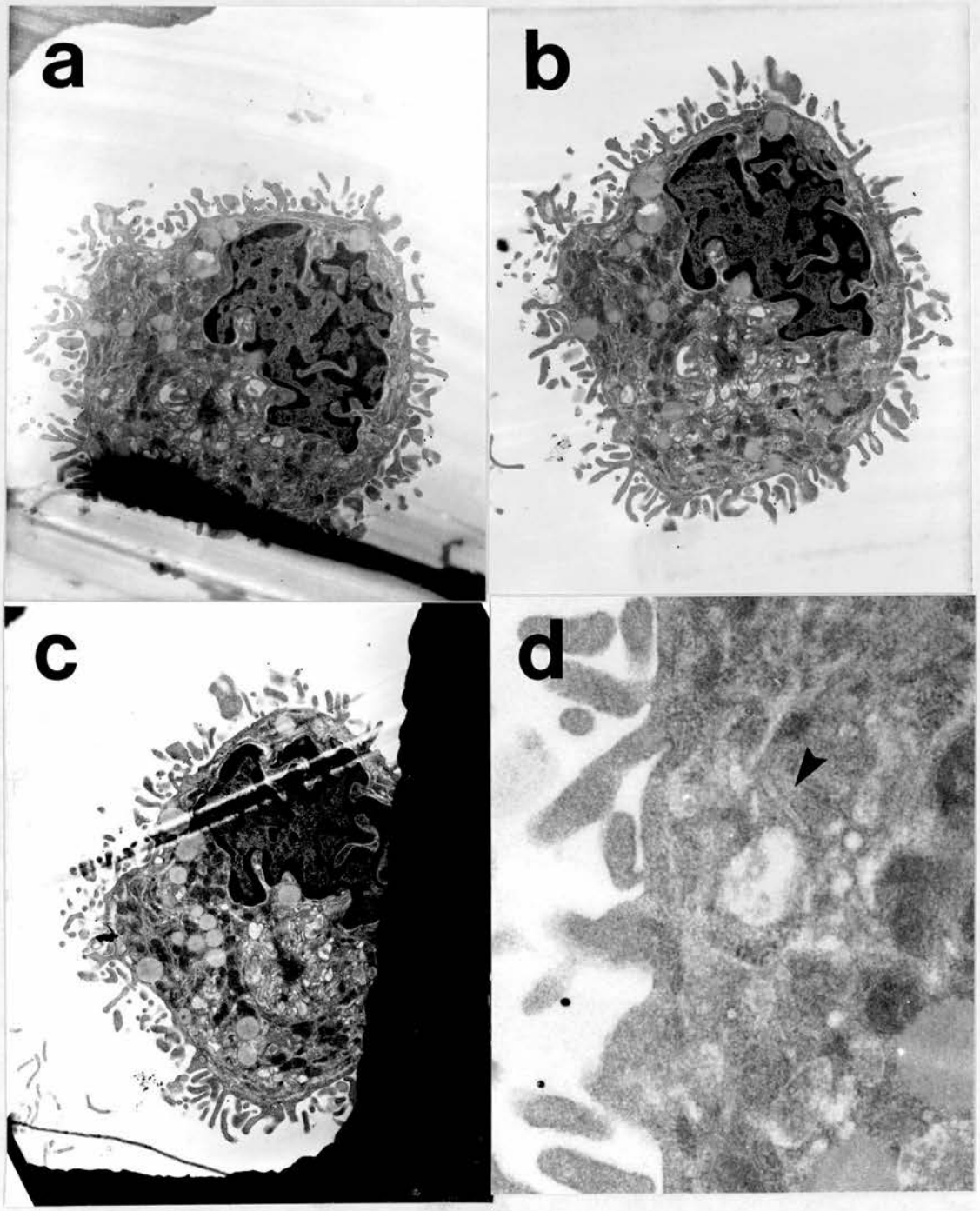

Figure 3.6:

a-c) Three step-sections through a single L243+ve (HLA-DR+ve) Langerhans cell from UVB-irradiated skin , labelled with L243 primary antibody and secondary antibody conjugated to 30nm gold particles. d) A Birbeck granule (arrowhead) is present within the Langerhans cell cytoplasm (inset from figure 3.6c).
Magnification a-c) 10,700 x
Magnification d) 36,500 x

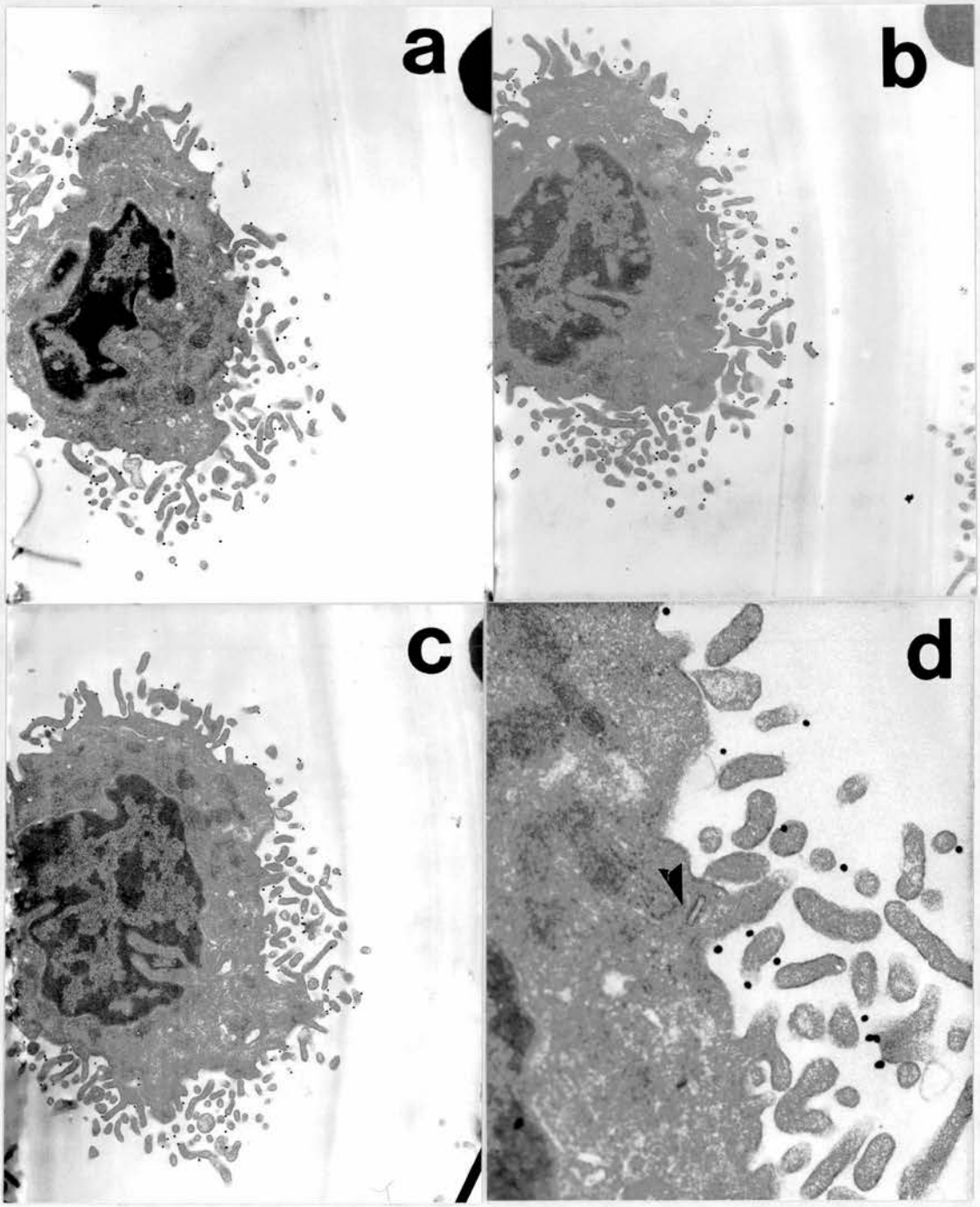

Figure 3.7:

a-c) Three step-sections through a single TU22+ve (HLA-DQ+ve) Langerhans cell from unirradiated skin. Surface HLA-DQ is labelled with TU22 primary antibody and a secondary antibody conjugated to 30nm gold particles. Note the sparse but uniform distribution of gold particles over the cell surface. d) Birbeck granules (arrowheads) are present within the cytoplasm of the section shown in figure 3.7c.
Magnification a-c) 8,400 x
Magnification d) 28,000 x

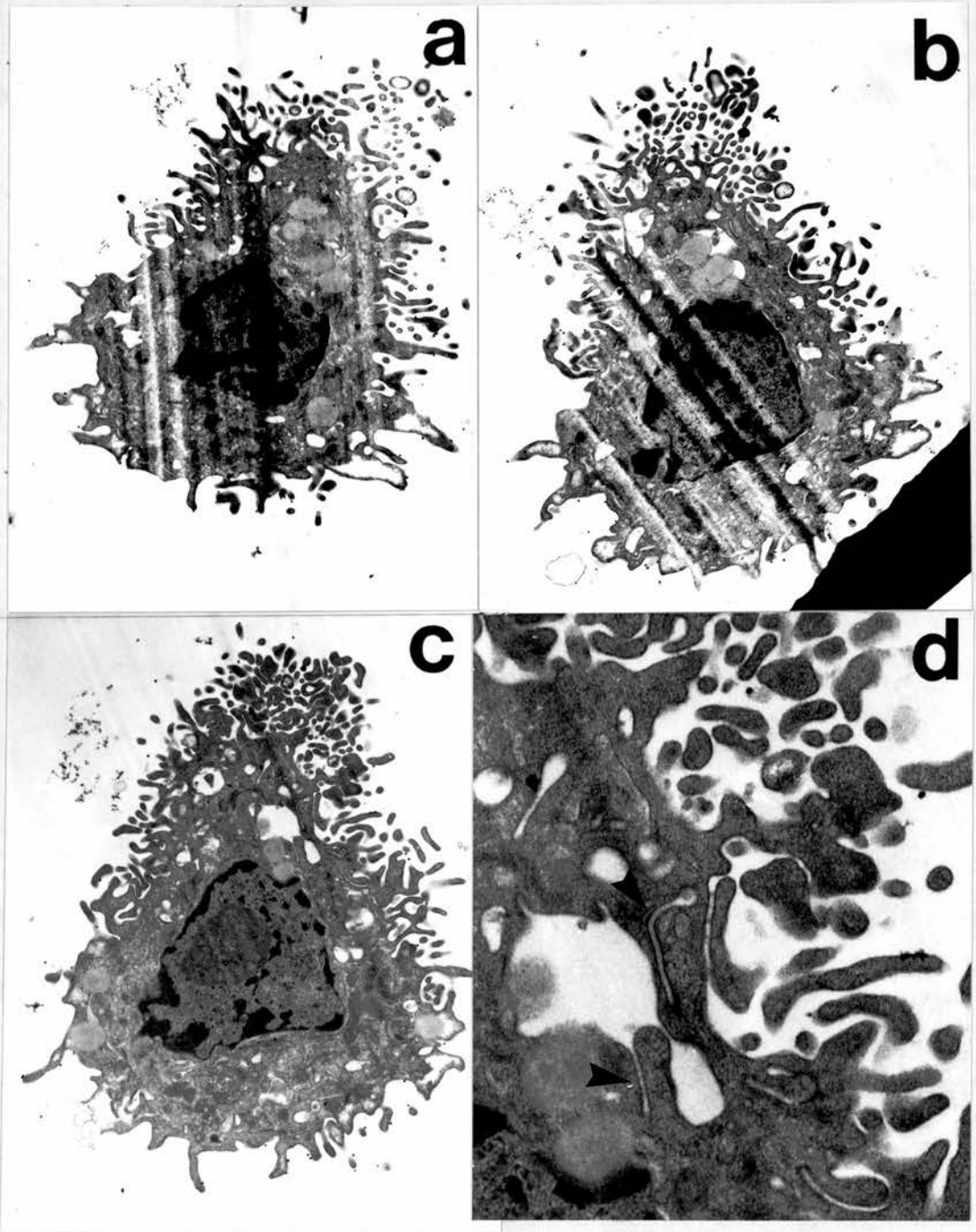

Figure 3.8:

a-c) Three step-sections through a single TU22+ve (HLA-DQ+ve) Langerhans cell from UVB-irradiated skin. The HLA-DQ is labelled on the cell surface by TU22 primary antibody and a secondary antibody conjugated to 30nm gold particles. d) Birbeck granules (arrowheads) within the Langerhans cell cytoplasm (inset from figure 3.8c).
Magnification a-c) 8,200 x
Magnification d) 26,650 x

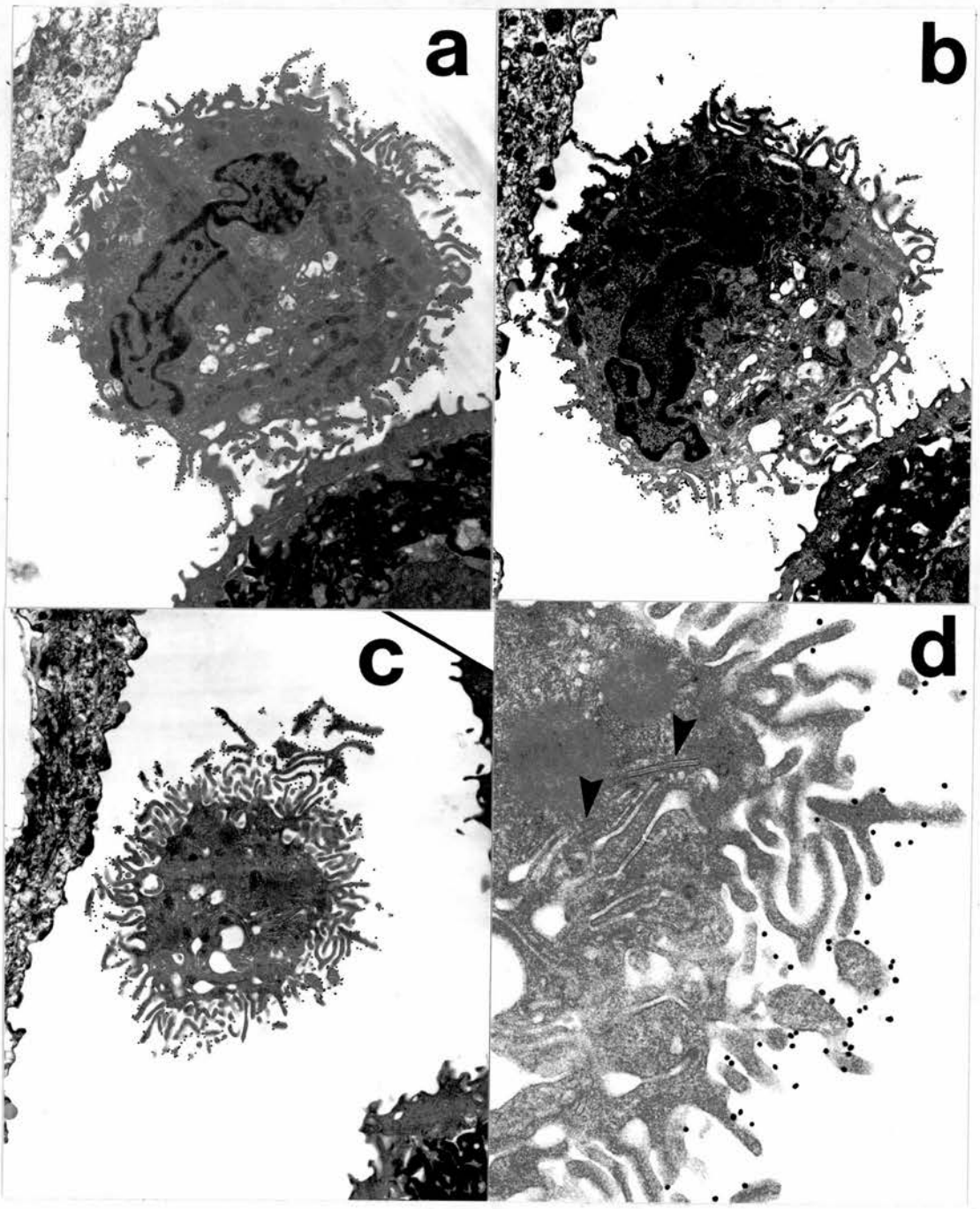

Figure 3.9:

a-c) Three step-sections through a single B721+ve (HLA-DP+ve) Langerhans cell from unirradiated skin showing the surface distribution of HLA-DP labelled with B721 primary antibody and secondary antibody conjugated to 30nm gold particles. d) Birbeck granules (arrowheads) near the surface of the Langerhans cell (inset from figure 3.9c).
Magnification a-c) 9,200 x
Magnification d) 36,800 x

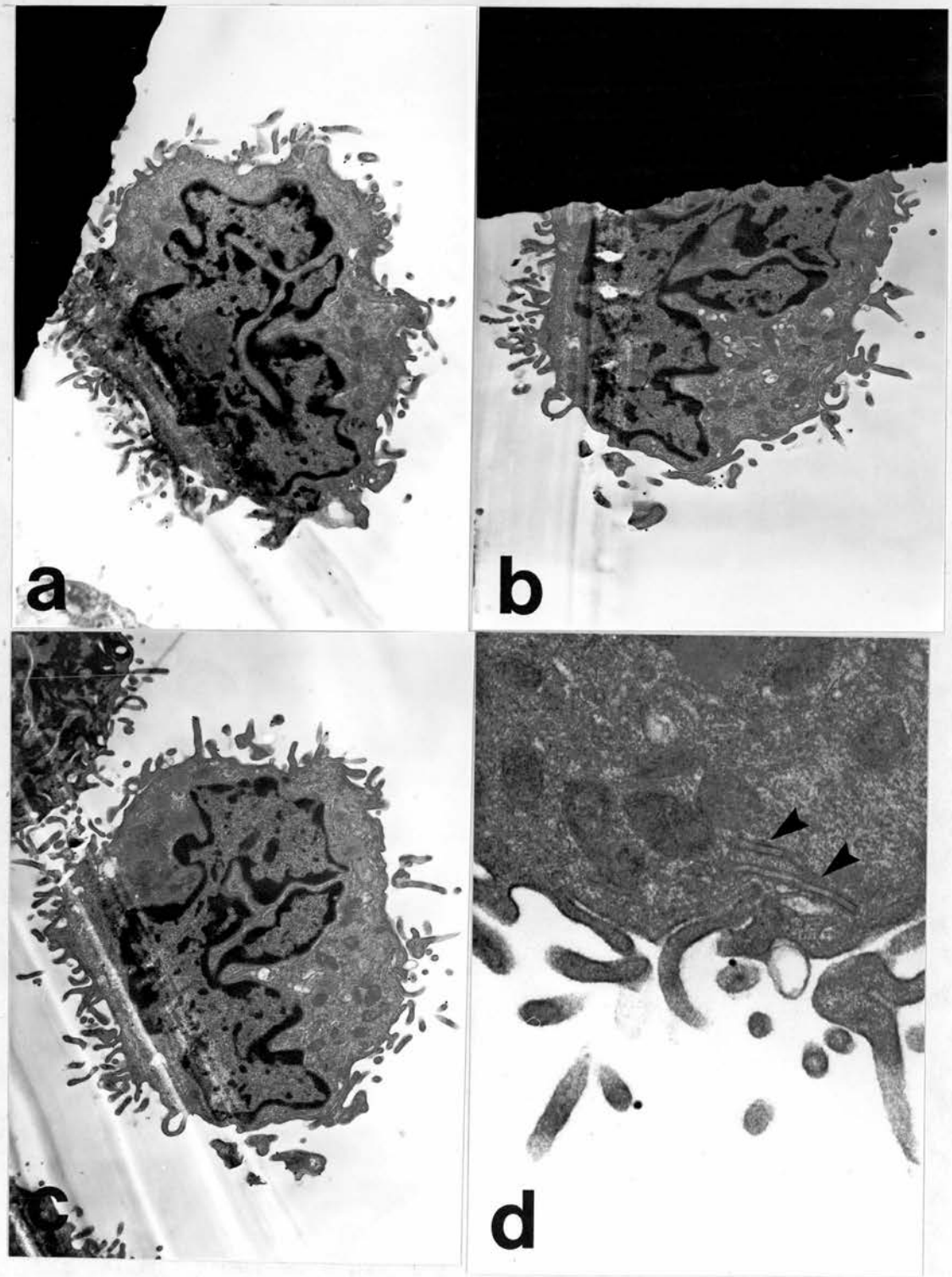

Figure 3.10:

a-c) Three step-sections through a single B721+ve (HLA-DP+ve) Langerhans cell from UVB-irradiated skin showing the surface distribution of HLA-DP labelled with B721 primary antibody and secondary antibody conjugated to 30nm gold particles. d) Birbeck granule (arrowhead) within the cell cytoplasm (inset from figure 3.10c).
Magnification a-c) 8,700 x
Magnification d) 34,800 x

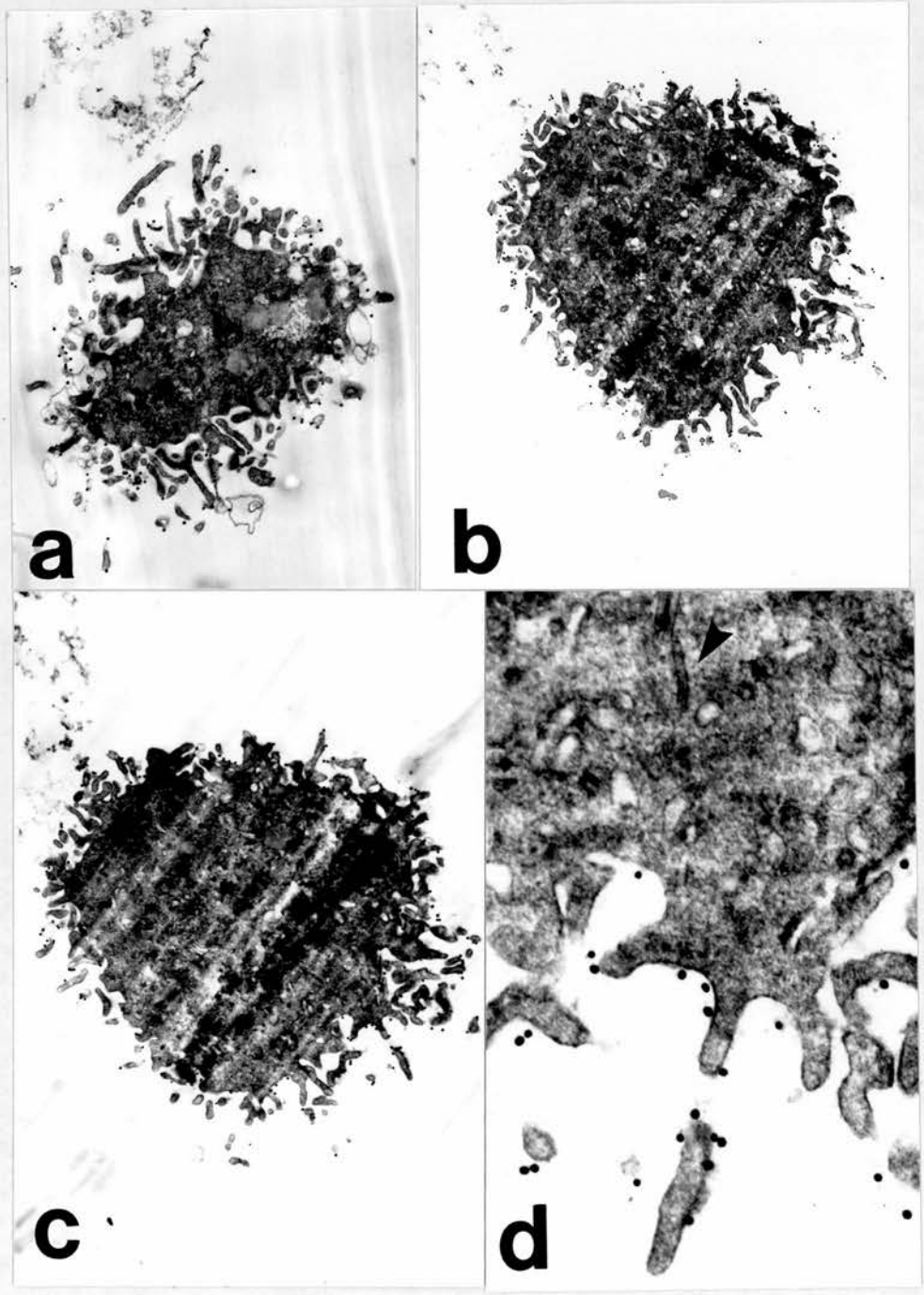

and 5 B721+ve LCs before and after UVB irradiation, showed that the density of gold label varied little between sections through a single cell. Gold particles appeared to be evenly distributed over the LC surface, with small standard errors. There was no evidence for clustering or capping of these surface molecules on either unirradiated LCs or indeterminate cells or UVB-exposed LCs.

Table 3.5 The mean density of surface MHC II on step-sections through 15 separate DA6.231 +ve LCs or indeterminate cells before and after a standard 6 week course of UVB radiation.

	pre UVB			post UVB		
LC	gp/μm	SEM	n*	gp/μm	SEM	n*
1	3.52	0.48	3	5.14	0.32	3
2	4.35	0.36	3	5.74	0.29	3
3	4.69	0.21	3	6.22	0.42	4
4	4.82	0.27	4	6.48	0.40	3
5	5.47	0.24	3	7.03	0.37	3
6	6.21	0.44	3	7.44	0.61	3
7	6.83	0.31	3	7.63	0.18	3
8	6.95	0.61	3	8.17	0.15	3
9	8.16	0.17	3	8.47	0.20	3
10	8.16	0.44	5	11.45	0.83	3
11	8.69	0.26	3	12.49	0.36	3
12	9.36	0.53	3	13.14	0.45	3
13	11.26	0.36	3	13.97	0.63	3
14	13.94	0.75	3	14.16	0.45	3
15	15.56	0.69	4	23.40	1.80	3

*n = number of sections per LC/ indeterminate cell

3.4 Assessment of the semi-automatic method for counting gold particles on the plasma membrane using image analysis.

The measurements of gold particle densities on ECs using a semi-automatic image analysis method were compared with manual measurements. The correlation between the semi-automatic and the manual measurements was initially assessed visually by

plotting them against each other and including the line of equality in the graph (fig. 3.11). The correlation coefficient (r) was calculated to be 0.91 and demonstrates that there is a high correlation between the two methods. However, it would be unusual if two methods designed to measure the same quantity were not related. The two sets of data were compared using a two sample t test, and the p value was $0.05>p>0.02$, indicating no significant difference. This result does not necessarily imply that the measurements derived from the two methods agree. Perfect correlation occurs if the points in our graph lie along any straight line, but perfect agreement only occurs if the points lie on the line of equality.

The agreement between the two methods was determined by analysing the differences between the measurements. The differences between the methods were then plotted against the mean measurement (fig. 3.12). The mean difference between measurements (manual - image analysis) was 0.3 gold particles/μm and the standard deviation was 1.4 gold particles/μm. Since the mean values obtained manually and by image analysis were found to be 4.4 and 4.1 respectively, the mean difference of 0.3 gold particles/μm represents a value of less than 10% of the mean measurement. Confidence intervals (95%) were derived from these data by calculating the mean difference plus or minus two times the standard deviation. The 95% confidence interval was between the values of 3.1 and -2.5, indicating that approximately 95% of the image analysis-derived measurements will have a value of between 3.1 gold particles/μm above and 2.5 gold particles/μm below that derived manually. The values plotted in figure 3.12 demonstrate that the scatter of differences increases with increased density of gold particles. The differences in measurements therefore appear to be greater than the actual ones for small values and less than the actual ones for large values. Analysis of log-transformed data may remove these systematic variations in the data. The log-transformed data reveal that 95% of the image analysis measurements will have values between 24% below and 41% above the manual ones.

Repeatability was examined by taking paired measurements by both methods on a series of fifteen cell sections (method outlined in section 2.15). The mean and standard deviations of the differences were calculated for each method and used to determine the repeatability coefficient. If we assume that the mean difference is zero, then the differences squared and summed, divided by n gives the square of the standard deviation. Table 3.6 gives the repeated measurements and table 3.7 gives the means and standard deviations of the differences and thus the repeatability coefficients for data obtained by the two methods. The repeatability coefficients are similar, with a lower

repeatability coefficient for the image analysis measurement system than for the manual one.

In conclusion, although the agreement between the two methods was not excellent, the repeatabilities were similar which is important if the systems are to be comparable. In addition, the image analysis method was much quicker than the manual one and was therefore adopted for most gold particle density measurements.

Fig. 3.11: Graph to compare the manual and semi-automatic techniques for quantifying gold label density on epidermal cells.

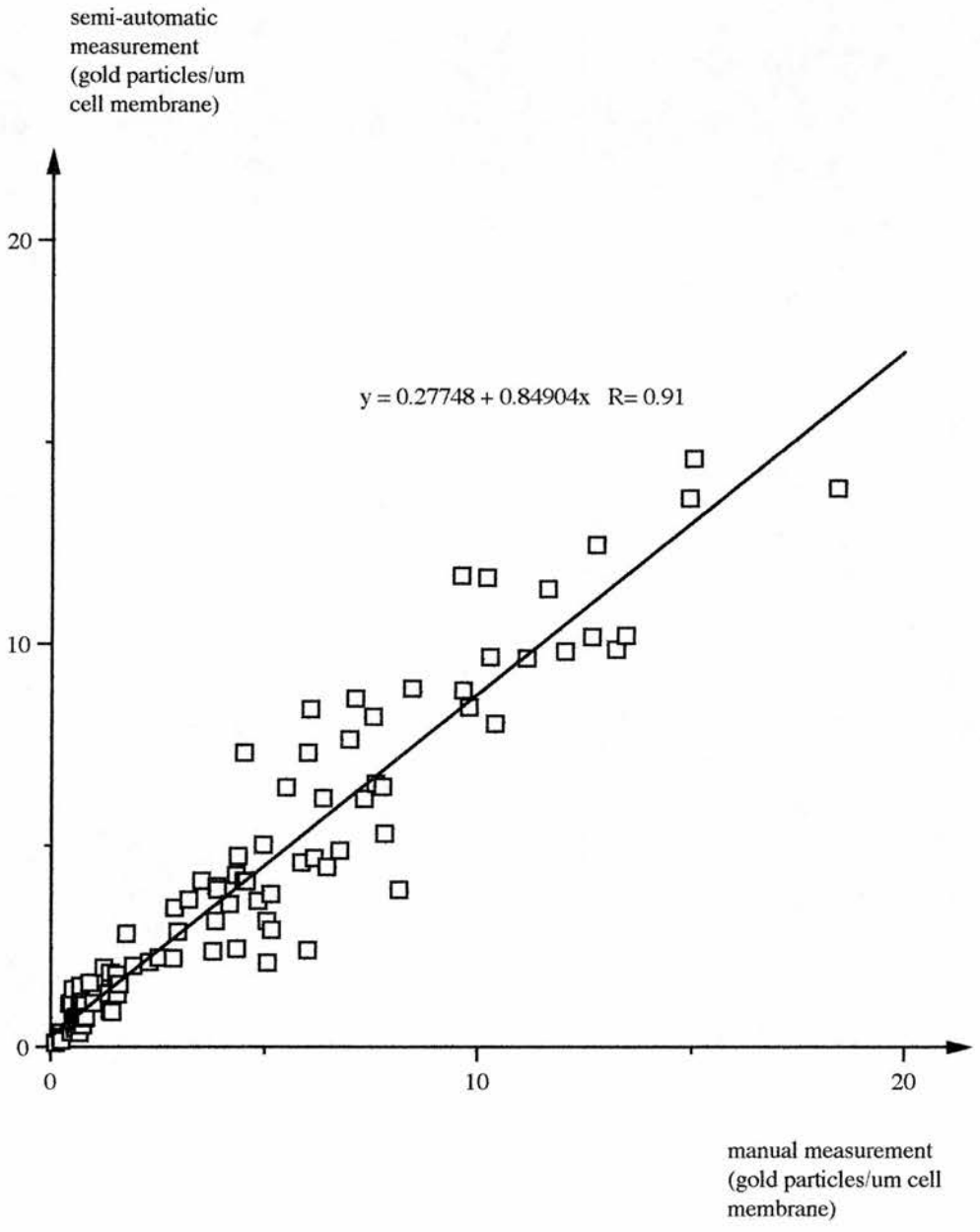

Figure 3.12: The mean of the two gold particle density measurements plotted against the difference between them.

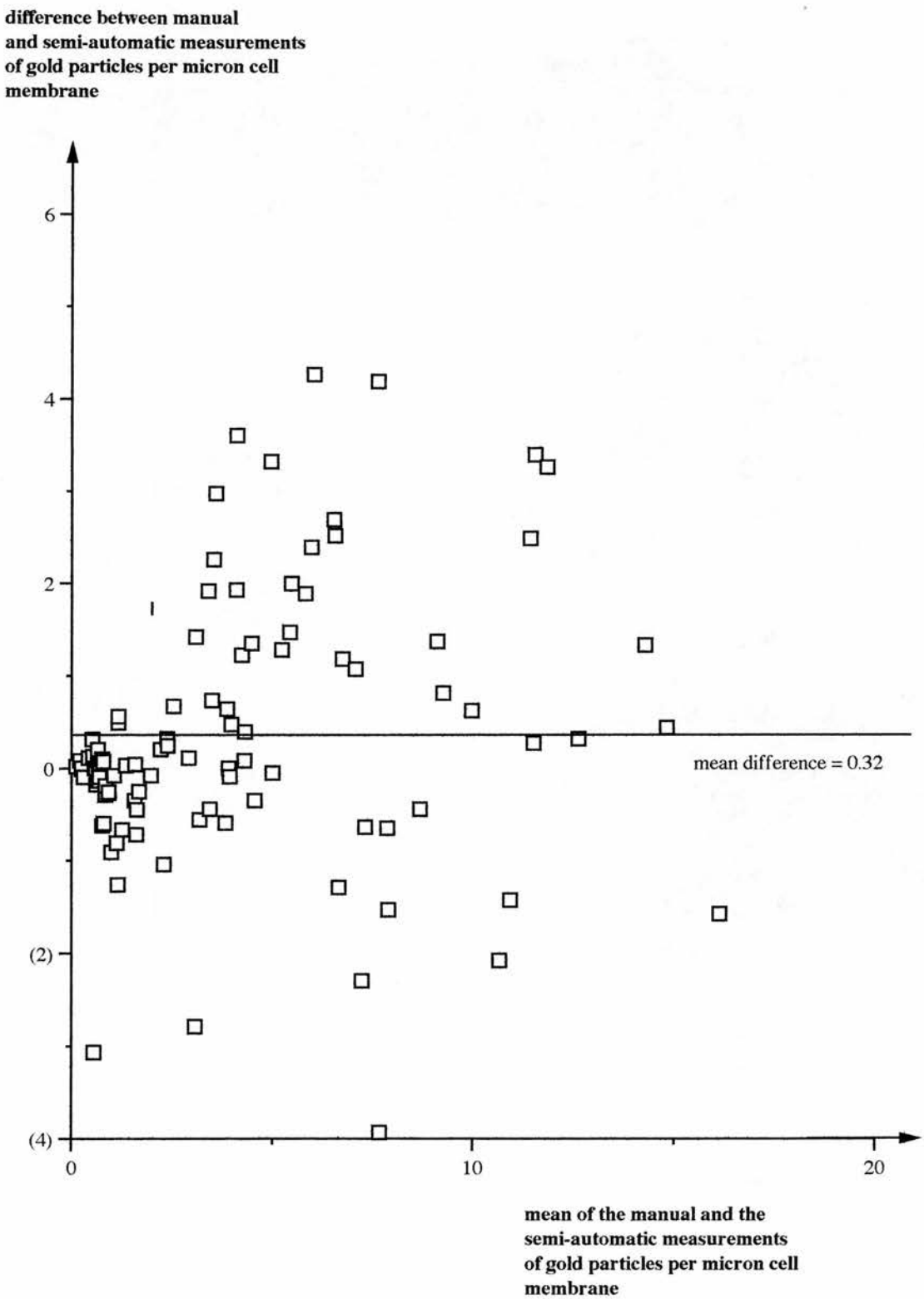

Table 3.6 Repeated gold label density measurements on 15 LC or indeterminate cell sections using manual and image analysis methods .

LC	1st manual count	2nd manual count	1st image analysis count	2nd image analysis count
1	17.57*	17.76	14.40	14.11
2	6.31	6.43	5.73	6.51
3	8.28	7.22	6.13	6.16
4	11.76	10.62	9.67	9.14
5	0.56	0.58	0.69	0.58
6	9.87	11.17	7.28	7.91
7	11.41	12.77	9.55	10.51
8	5.66	5.43	6.02	6.60
9	5.31	5.06	3.67	3.74
10	0.82	0.82	0.81	0.86
11	0.51	0.53	0.35	0.42
12	0.61	0.66	0.43	0.50
13	0.49	0.48	0.41	0.46
14	4.04	4.16	3.13	2.98
15	2.61	2.60	2.12	2.12

* measurements are expressed as gold particles/micron plasma membrane.

Table 3.7 The means and standard differences of repeated measurements given in table 3.6.

	manual	image analysis
mean difference	-0.03	-0.1
sd of differences	0.64	0.49
repeatability coefficient	1.28	0.98

Chapter 4 The Number, Morphology and Surface Antigen Expression of Human Epidermal LCs and Indeterminate Cells.

4.1 The number of CD1a+ve, pan MHC II+ve, HLA-DP+ve,-DQ+ve, and -DR +ve cells in human epidermis.

The number of CD1a+ve ECs and the percentage area of CD1a label in epidermal sheets from four subjects were determined using confocal laser scanning microscopy (see section 2.7, table 4.1, fig. 4.1).

Table 4.1 The mean number of CD1a+ve ECs and the mean percentage labelled area in 5 low power fields of epidermis.

subject	mean no. LCs /mm^2	sem*	mean % labelled area	sem*
SK	1030	54.6	5.6	0.6
GP	858	44.8	6.8	0.5
MG	302	18.0	2.0	0.3
NH	324	29.1	3.0	1.2

* standard error of the mean.

The numbers of CD1a+ve, DA6.231+ve, L243+ve, B7/21+ve and TU22+ve ECs were counted in vertical sections through epidermis (see sections 2.6, table 4.2, appendix 3 and figs 4.2-4.9). There was a small number of MHC II+ve non-dendritic ECs which were readily identified as cells of the acrosyringium and were not counted.

In general the CD1a+ve cell counts were greater than the DA6.231+ve cell counts, although statistical analysis revealed no significant differences between these values. However, HLA-DR labelling usually revealed fewer positive cells than those detected by either CD1a or pan MHC II labelling, but greater than those detected by HLA-DQ or HLA-DP labelling (although HLA-DQ positivity was not detected in two of nine subjects which were labelled using the immunoperoxidase technique). Statistical analysis showed significant differences between the numbers of antibody labelled ECs, such that the number of pan MHC II+ve and CD1a+ve ECs > HLA-DR+ve ECs > HLA-DQ+ve ECs > HLA-DP+ve ECs.

Figure 4.1: **Langerhans cells within an epidermal sheet labelled with OKT6 (anti-CD1a) antibody directly conjugated to fluorescein isothiocyanate.**
Magnification 2,700x

Figure 4.2: **Vertical section through a suction blister-derived epidermal sheet labelled without a primary antibody (control) using the immunoperoxidase method. The sections shown in figures 4.2-4.7 are all from subject 3.**
Magnification 80x

Figure 4.3: **Vertical section through a suction blister-derived epidermal sheet labelled with OKT6 (anti-CD1a) antibody using the immunoperoxidase method.**
Magnification 80x

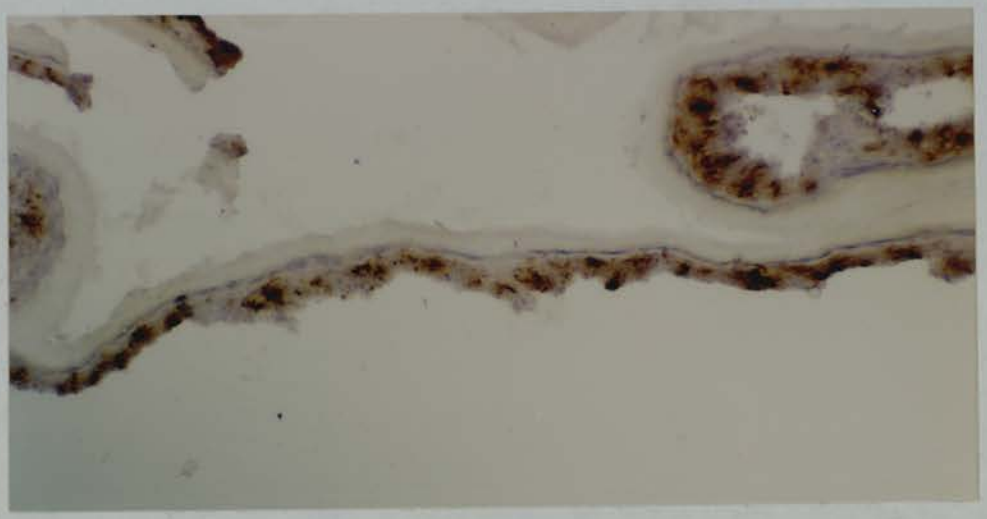

Figure 4.4: **Vertical section through a suction blister-derived epidermal sheet labelled with DA6.231 (anti-pan MHC II) antibody using the immunoperoxidase method. Note that figures 4.3 and 4.4 are serial sections.**
Magnification 80x

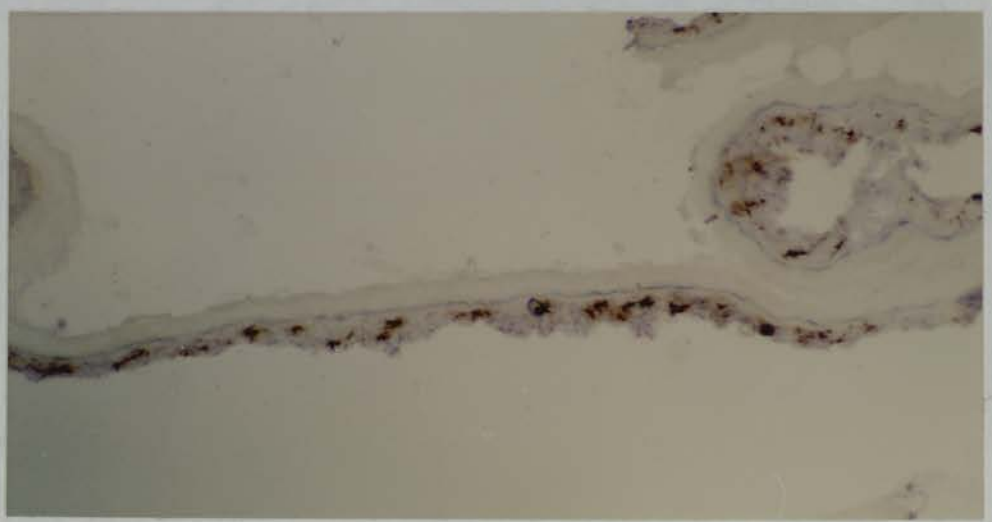

Figure 4.5: **Vertical section through a suction blister-derived epidermal sheet labelled with L243 (anti-HLA-DR) antibody using the immunoperoxidase method. Note that figures 4.2 and 4.5 are serial sections.**
Magnification 80x

Figure 4.6: **Vertical section through a suction blister-derived epidermal sheet labelled with TU22 (anti- HLA-DQ) antibody using the immunoperoxidase method. Note an absence of HLA-DQ+ve Langerhans cells in this section.**
Magnification 80x

Figure 4.7: **Vertical section through a suction blister-derived epidermal sheet labelled with B721 (anti-HLA-DP) antibody using the immunoperoxidase method.**
Magnification 80x

Figure 4.8: **Vertical section through a suction blister-derived epidermal sheet labelled with L243 (anti-HLA-DR) antibody using the immunoperoxidase method. Note that figures 4.8 and 4.9 are serial sections from subject 8.**
Magnification 80x

Figure 4.9: **Vertical section through a suction blister-derived epidermal sheet labelled with B721 (anti-HLA-DP) antibody using the immunoperoxidase method.**
Magnification 80x

Table 4.2 The mean number of CD1a+ve, pan MHC II+ve, HLA-DP+ve, HLA-DQ+ve, and HLA-DR+ve ECs per mm basal cell membrane meaured from five vertical sections through blister roofs of nine subjects.

subj	Monoclonal antibody				
	CD1a	**pan MHC II**	**HLA-DR**	**HLA-DQ**	**HLA-DP**
1	**37.38 (1.95)***	**29.26 (1.75)**	**21.09 (1.24)**	**13.18 (1.77)**	**8.73 (1.01)**
2	**23.20 (2.77)**	**19.91 (2.67)**	**15.50 (1.18)**	**13.02 (0.34)**	**10.05 (1.68)**
3	**21.07 (1.12)**	**23.25 (3.20)**	**16.31 (0.68)**	**0**	**6.83 (0.72)**
4	**24.75 (2.77)**	**22.89 (1.46)**	**16.65 (0.99)**	**5.72 (0.60)**	**6.14 (0.70)**
5	**35.76 (1.68)**	**33.09 (1.24)**	**19.10 (2.10)**	**14.03 (0.90)**	**6.99 (0.69)**
6	**20.62 (0.96)**	**18.51 (1.57)**	**17.13 (0.84)**	**11.39 (1.68)**	**6.14 (0.70)**
7	**20.28 (2.34)**	**19.11 (2.04)**	**20.21 (0.85)**	**0**	**11.87 (1.19)**
8	**21.13 (2.39)**	**21.82 (0.98)**	**20.26 (1.50)**	**16.44 (1.68)**	**12.93 (0.95)**
9	**14.10 (1.25)**	**15.91 (2.08)**	**12.57 (1.03)**	**4.43 (0.13)**	**5.90 (0.50)**

*numbers in parentheses represent the standard errors of the means.

4.2 The morphology of LCs.

Certain aspects of LC morphology *in situ* were examined with the aid of an image analyser using images obtained by confocal laser scanning microscopy of CD1a+ve ECs (see section 2.7). The data which relate to LC or indeterminate cell morphology and which were obtained from two-dimensional reconstructions are given in appendix 5. The graph in fig 4.10 demonstrates a correlation between the total cell area and the dendrite area, implying that only a certain proportion of a cell can be extended as dendrites.

Figure 4.10: Graph to show the LC dendrite area plotted against the total LC area.

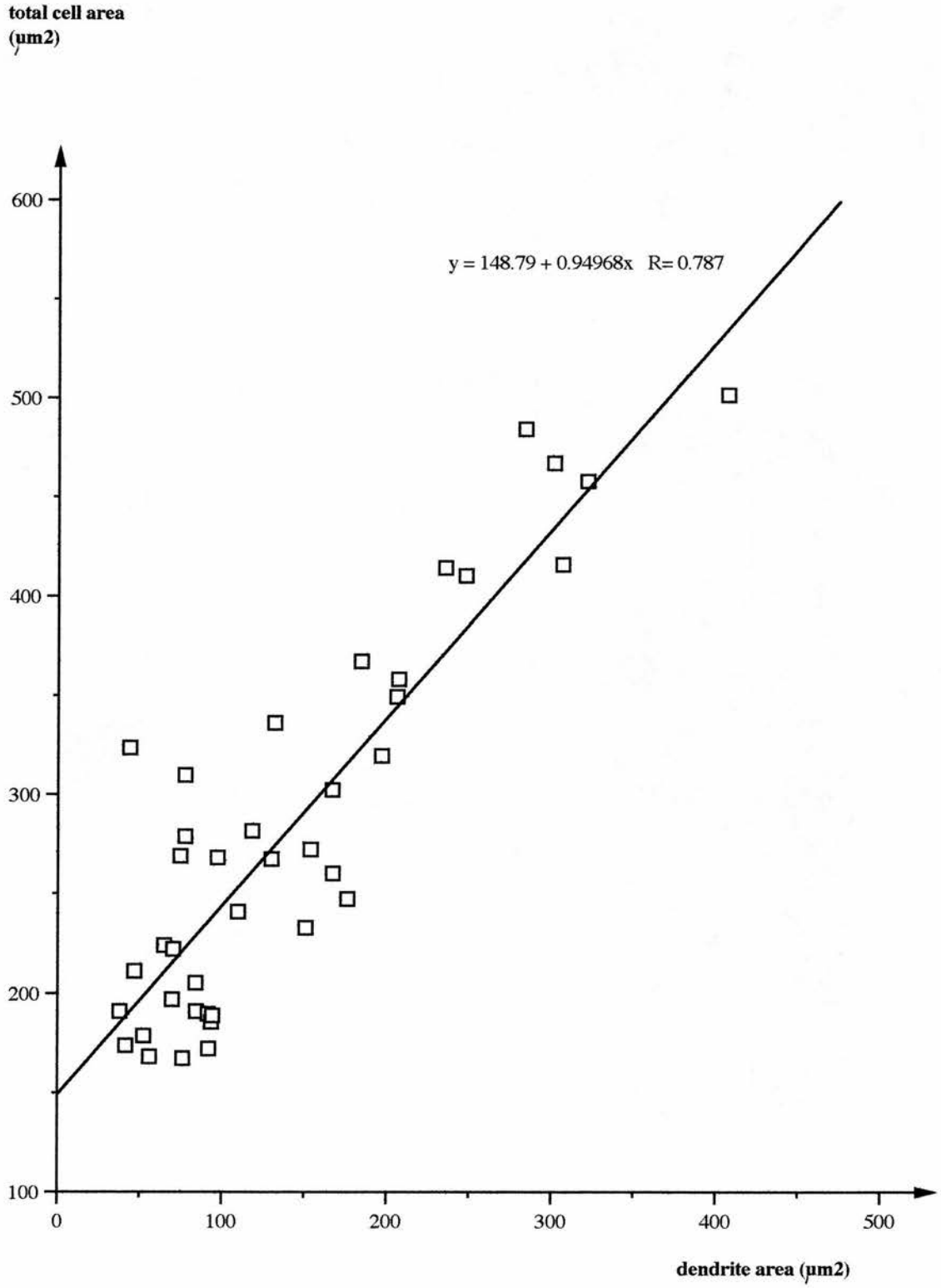

The mean cell area, dendrite area, dendrite number, dendrite length, and cell dendricity (defined as the cell perimeter divided by the putative cell body perimeter) are given in table 4.3. Examples of cell reconstructions in three-dimensions are given in figs. 4.11 to 4.16. These images show that LCs or indeterminate cells possess dendrites which appear to extend mainly in the horizontal plane within the epidermal sheet.

Table 4.3 Quantitative analysis of the morphology of CD1a+ve ECs reconstructed in two dimensions.

cell parameter n=40	mean	sem*	range
cell area (μm^2)	285	15.5	167-501
dendrite area (μm^2)	144	14.5	38-407
dendrite length (μm)	12.7	1.7	1.2-49.1
number of dendrites/cell	5.0	1.9	2-9
dendricity (arbitrary units)	3.4	0.2	1.7-7.4

* standard error of the mean

The ultrastructural morphology of control LCs in suspension was examined. The morphology of LCs in EC suspension was highly variable with respect to dendricity, electron density of cytoplasm, presence or absence of long cell surface projections or 'veils' and the shape of the cell section profile. The morphologies of these cells fell within five main categories:

I Cell round in profile, with microvillous surface.

II Cell round in profile with fewer surface microvilli than type I.

III Cell round in profile with fewer surface microvilli which are long (veils).

IV Cell round in profile with no surface microvilli and some damage to cytoplasm and/or membranes.

V Cell round in profile with no surface microvilli, an unusually high number of intracellular vacuoles and BGs, but intact plasma membrane.

Examples of cells with these morphological features are given in figures 5.11-21 (see pages 124-134).

Figure 4.11: **Three-dimensional reconstruction of a Langerhans cell *in situ* viewed from above.**

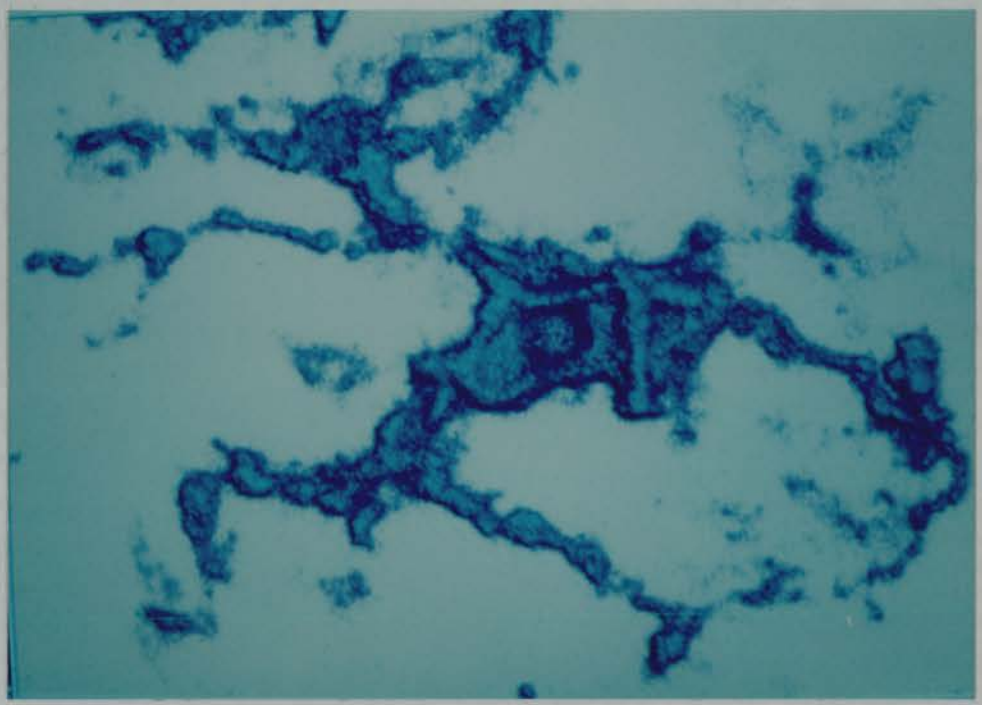

Figure 4.12: **The central image is the same as that in figure 4.11, whilst the surrounding images represent different views of the same cell which would be seen if the cell was rotated by steps of 30^{o} around its central axis. The images on the bottom left hand corner and that immediately below the top left hand corner represent side views of the cell. Note that dendrites do not appear to extend vertically in the epidermal sheet.**

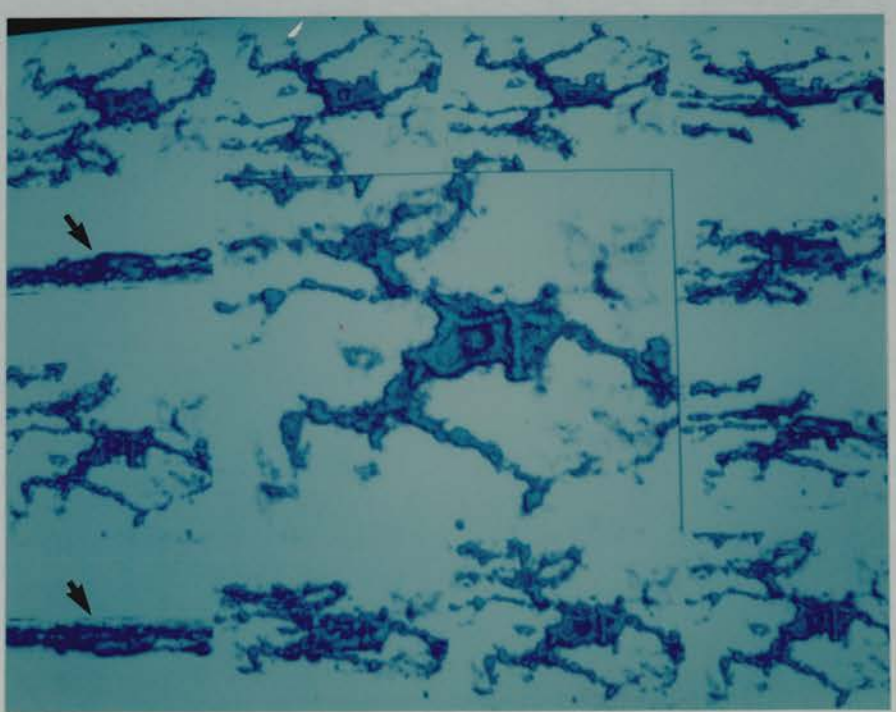

Figure 4.13: **Three-dimensional reconstruction of a Langerhans cell *in situ* viewed from above.**

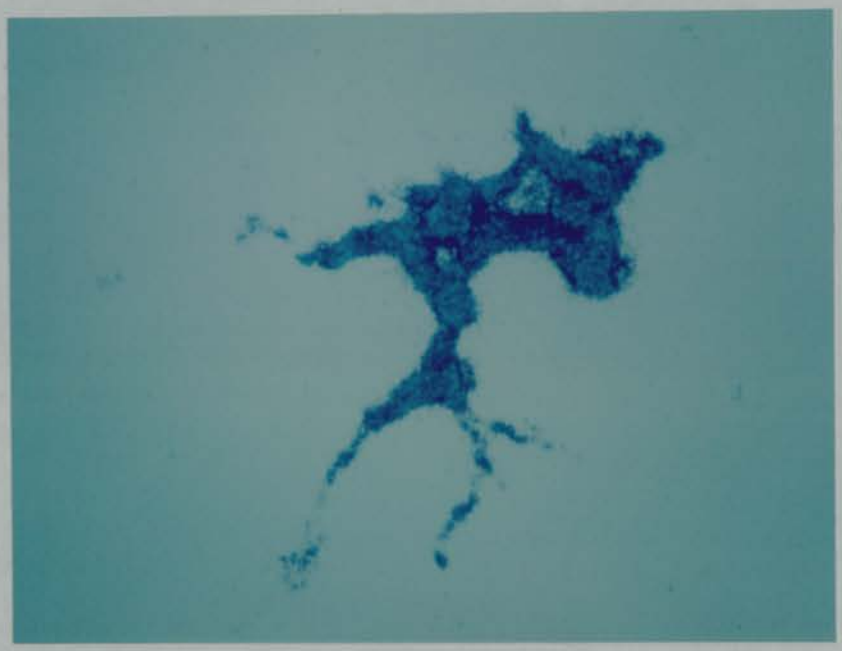

Figure 4.14: **The central image is the same as that in figure 4.13, whilst the surrounding images represent different views of the same cell which would be seen if the cell was rotated by steps of 30^{o} around its central axis. The images on the bottom left hand corner and that immediately below the top left hand corner represent side views of the cell. Note that dendrites appear to extend laterally and not vertically through the epidermis.**

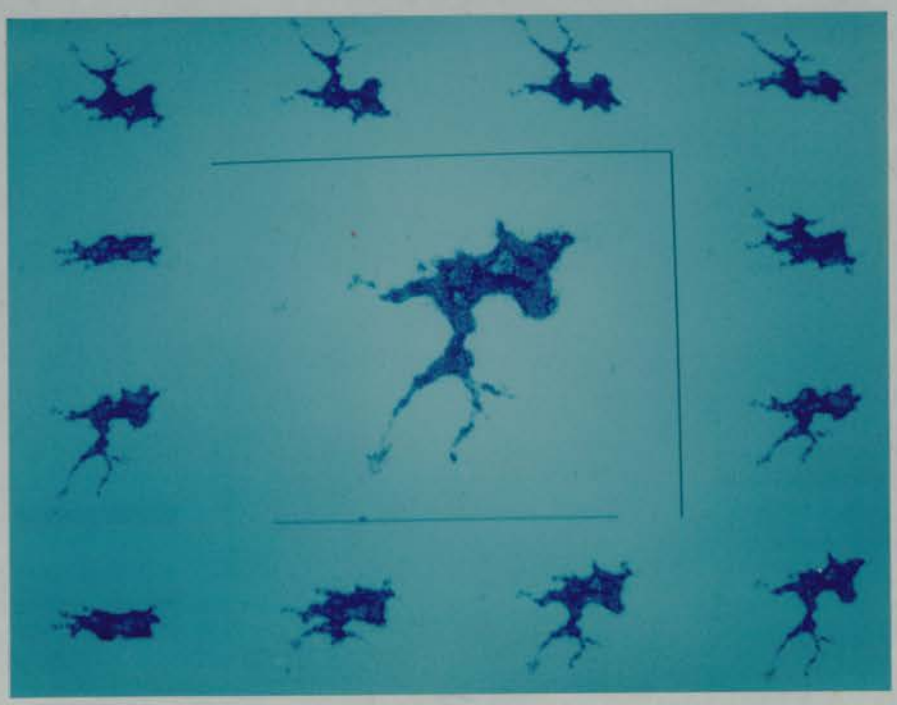

Figure 4.15: **Three-dimensional reconstruction of a Langerhans cell *in situ* viewed from above.**

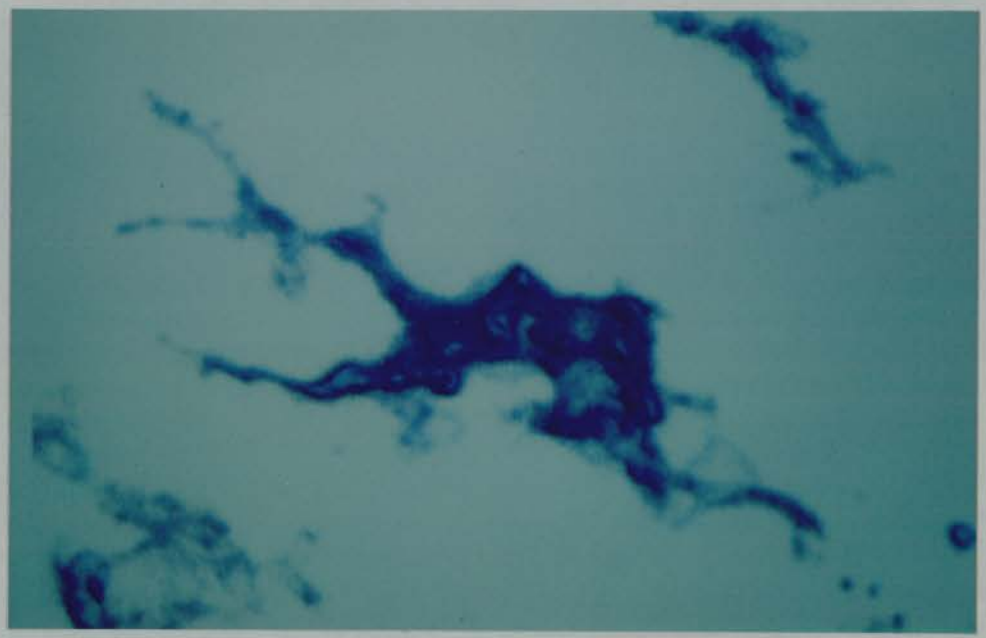

Figure 4.16: **Three-dimensional reconstruction of two neighbouring Langerhans cells *in situ* connected by a long, straight dendritic process.**

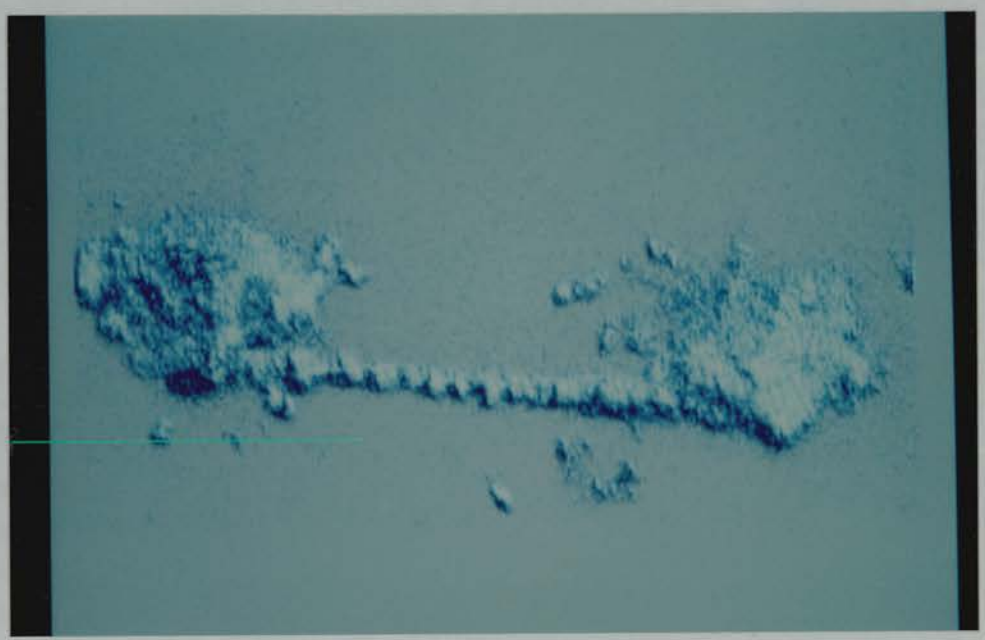

4.3 The expression of LC and indeterminate cell surface antigens.

Examination of sections through many normal LCs and indeterminate cells from one subject labelled with anti-pan MHC II monoclonal antibody (DA6.231) and another subject labelled with anti-CD1a monoclonal antibody (OKT6), revealed considerable variation in surface MHC II and CD1a densities between different cells which was normally distributed. There was no evidence for separate subpopulations of pan MHC II+ve or CD1a +ve cells expressing a higher or lower level of antigen. No pan MHC II-ve or CD1a-ve LCs or indeterminate cells were detected (fig. 4.17).

The label density on many sections through HLA-DR+ve LCs and indeterminate cells from an individual was variable, with differences approaching 45 fold. The frequency distribution approximated a normal curve but was skewed to the right (fig. 4.18). There were no HLA-DR-ve cells, but there was one particularly densely labelled cell (HLA-DR++ve) out of 71 cells examined.

The frequency distribution of label density on HLA-DQ+ve LCs and indeterminate cells was similar to that of HLA-DR+ve cells (fig. 4.19). The main difference, however, was the existence of one HLA-DQ-ve cell and three particularly densely labelled cells (HLA-DQ++ve). The label density on sections through a large number of different HLA-DQ+ve cells varied up to approximately 80 fold.

In contrast, the variation in label density on sections through HLA-DP+ve LCs and indeterminate cells was not normally distributed (fig. 4.20). Approximately 5% of these cells were particularly densely labelled (5 out of 97 cells) with anti-HLA-DP antibody and approximately 3% were HLA-DP-ve (3 out of 97). There was a variation in HLA-DP label density on sections through different cells which approached 400 fold.

LCs and indeterminate cells expressed similar densities of all three MHC II surface antigens, HLA-DP, -DQ and -DR. There was no evidence to support the claim that indeterminate cells express greater cell surface MHC II antigen densities than LCs (Dezutter-Dambuyant *et al.*, 1984).

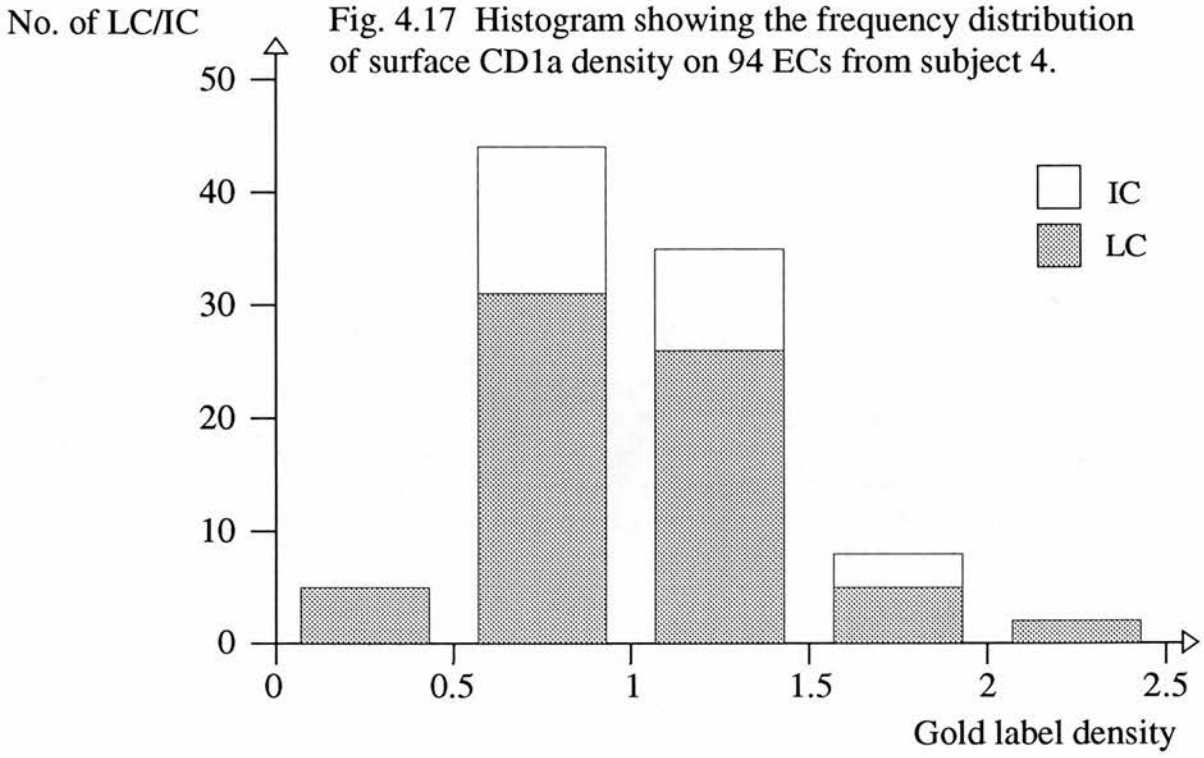

Fig. 4.17 Histogram showing the frequency distribution of surface CD1a density on 94 ECs from subject 4.

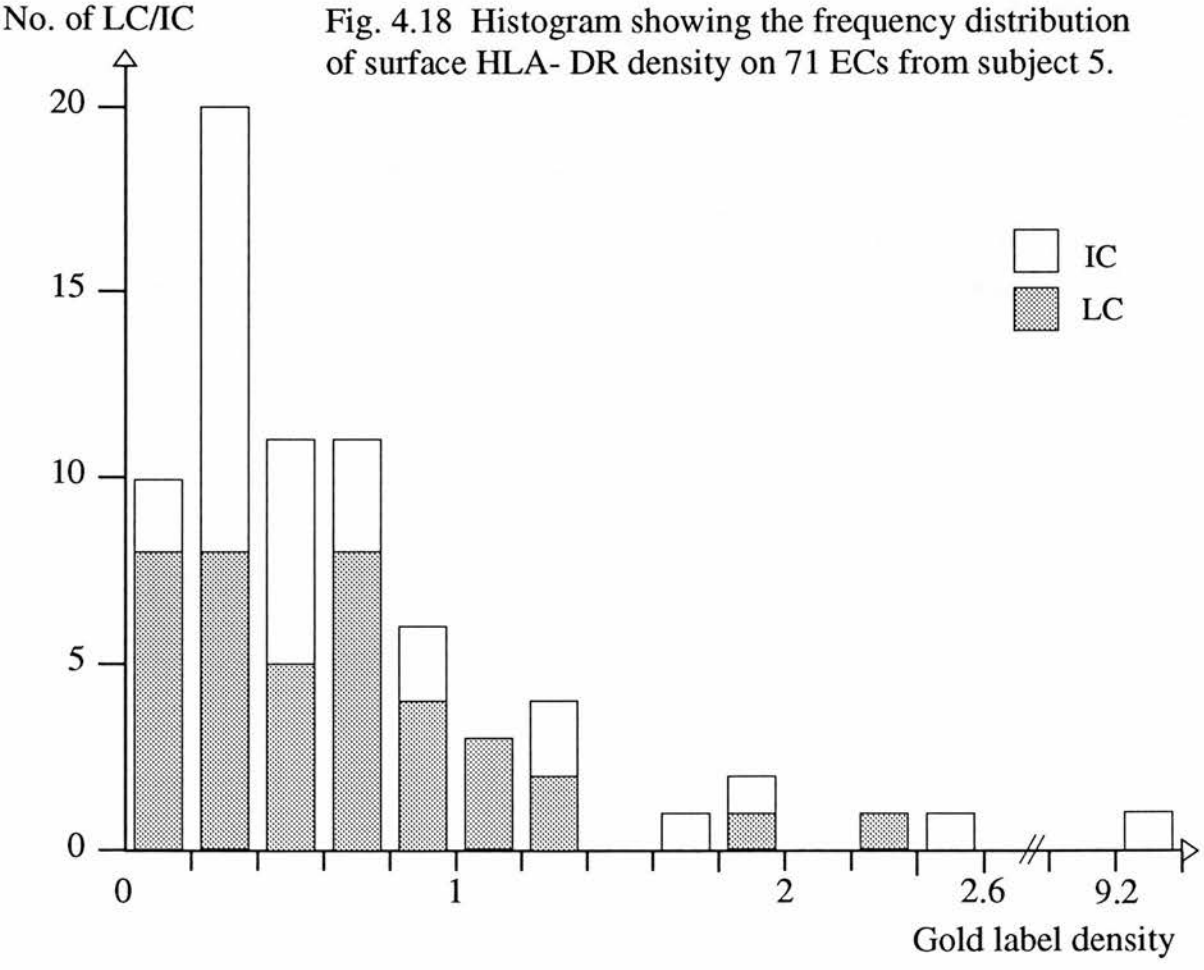

Fig. 4.18 Histogram showing the frequency distribution of surface HLA- DR density on 71 ECs from subject 5.

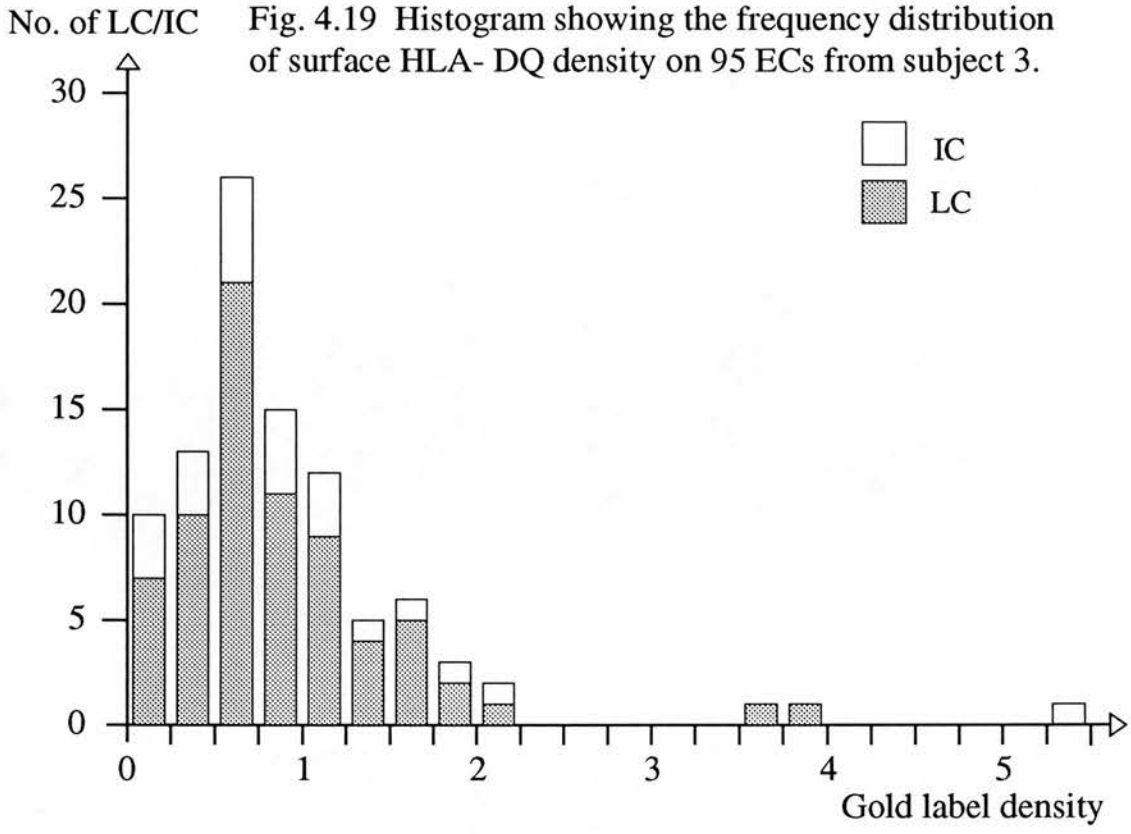

Fig. 4.19 Histogram showing the frequency distribution of surface HLA- DQ density on 95 ECs from subject 3.

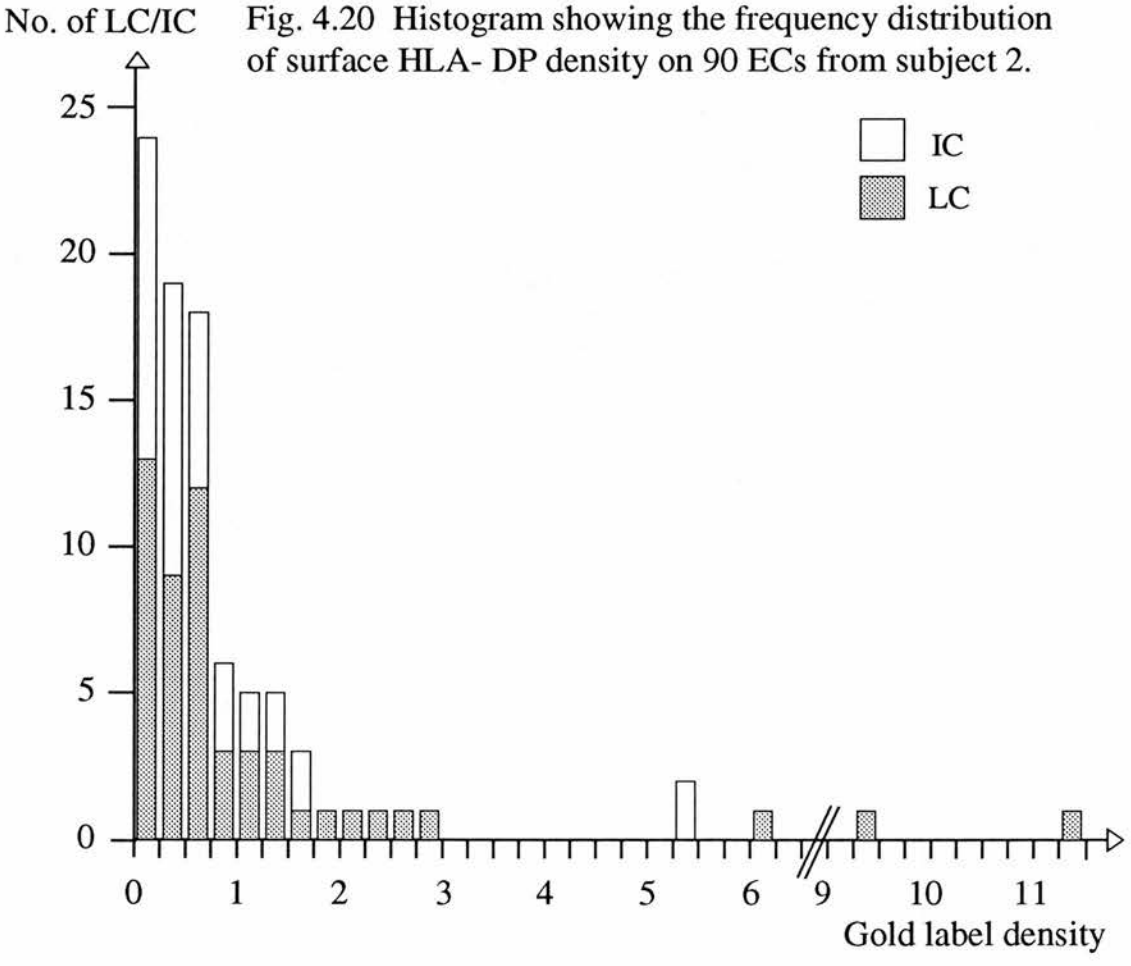

Fig. 4.20 Histogram showing the frequency distribution of surface HLA- DP density on 90 ECs from subject 2.

The density of surface CD1a, Pan-MHC II, HLA-DP, HLA-DQ and HLA-DR was quantified semi-automatically on five different positively labelled LC or indeterminate cell sections from each subject per antibody (for results see table 4.4 and appendix 4).

Table 4.4 The mean number of gold particles per micron plasma membrane on five CD1a+ve, pan MHC II+ve, HLA-DP+ve, HLA-DQ+ve, and HLA-DR+ve LCs or indeterminate cells per subject.

subj	Monoclonal antibody				
	CD1a	**pan MHC II**	**HLA-DR**	**HLA-DQ**	**HLA-DP**
1	**0.90 (0.45)***	**3.49 (0.33)**	**2.13 (1.24)**	**0.40 (0.08)**	**0.29 (0.08)**
2	**0.25 (0.05)**	**4.06 (1.13)**	**0.09 (0.05)**	**0.54 (0.20)**	**0.45 (0.13)**
3	**0.78 (0.11)**	**6.60 (1.29)**	**0.23 (0.03)**	**0.16 (0.04)**	**0.71 (0.14)**
4	**0.82 (0.22)**	**5.03 (1.24)**	**0.12 (0.03)**	**0.32 (0.10)**	**0.33 (0.13)**
5	**1.03 (0.23)**	**5.09 (0.94)**	**0.39 (0.13)**	**0.58 (0.13)**	**1.05 (0.16)**
6	**0.55 (0.09)**	**6.13 (0.47)**	**1.13 (0.74)**	**ND**	**ND**
7	**0.99 (0.06)**	**5.85 (0.74)**	**0.10 (0.06)**	**0**	**ND**
8	**0.24 (0.05)**	**5.33 (0.77)**	**0.35 (0.11)**	**ND**	**ND**
9	**1.51 (0.24)**	**4.77 (0.91)**	**ND**	**ND**	**ND**

*numbers in parentheses represent the standard errors of the means.

Chapter 5 The Influence of UVB Irradiation on LCs and on Epidermal Urocanic Acid and TNF-α Production.

page number

5.1 The number of CD1a+ve, pan MHC II+ve, HLA-DP+ve,-DQ+ve,-DR+ve ECs in UVB-irradiated epidermis.

The number of CD1a+ve ECs and the percentage area of CD1a label were determined in UVB exposed epidermal sheets using confocal laser scanning microscopy. The results are given in table 5.1 in which the results of table 4.1 are repeated for ease of reference.

Table 5.1 The number of CD1a+ve ECs and the percentage area of CD1a label a) before and b) after a standard 6 week course of UVB phototherapy.

a)

subject	mean no. LCs /mm^2	sem*	% labelled area	sem*
6 - SK	1030	54.6	5.6	0.6
7 - GP	858	44.8	6.88	0.5
8 - MG	302	18.0	2.0	0.3
9 - NH	324	29.1	3.0	1.2

b)

subject	mean no. LCs /mm^2	sem*	% labelled area	sem*
6 - SK	454	37.4	2.4	0.2
7 - GP	226	23.4	4.5	0.6
8 - MG	208	25.6	1.2	0.2
9 - NH	188	21.5	2.3	0.4

* standard error of the mean

Table 5.1 and fig. 5.1 shows that decreased numbers of CD1a+ve ECs and decreased areas of CD1a label were detected within epidermal sheets of four subjects. These differences proved to be statistically significant ($p<0.05$).

Figure 5.1: Langerhans cells within a UVB-irradiated epidermal sheet labelled with OKT6 (anti-CD1a) antibody directly conjugated to fluorescein isothiocyanate. Note the depletion of Langerhans cells after UV exposure by comparing figure 5.1 with figure 4.1.
Magnification 2,700 x

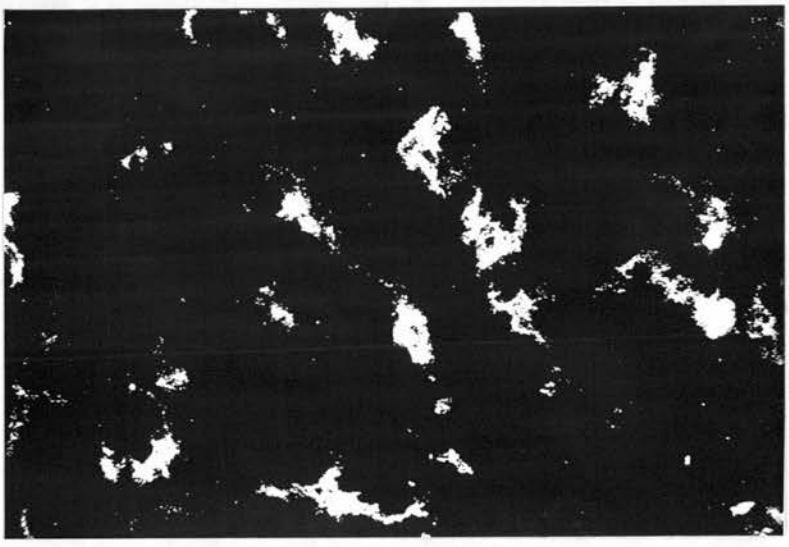

The numbers of CD1a+ve, DA6.231+ve, L243+ve, B7/21+ve and TU22+ve ECs in vertical sections through UVB-irradiated epidermis were counted (see appendix 3 for raw data and figs 5.2-5.6). There was a marked reduction of labelled cells in epidermal sections after the six week UVB phototherapy course, irrespective of the antibody used to visualize them. The only exception to this observation was found to be a rise in number of HLA-DQ labelled ECs in one subject (see appendix 3 and table 5.2). The data in table 5.2 a) has been copied from chapter 4 for ease of reference.

The intra-individual percentage decrease of labelled EC number measured with all of the LC specific antibodies were approximately equal, although inter-subject differences in LC number per mm basement membrane were great. Graphical representations of the decreases in cell number (labelled with all five LC-specific antibodies) for each subject demonstrates that the slopes of the lines are similar within each subject (fig. 5.7 a)-i)). The percentage decrease in LC (pan-MHC II+ve EC) number was weakly correlated (r=0.46) to the total number of MEDs of UVB that a subject had received, but was unrelated to the total number of Joules of UVB that a subject had received (fig. 5.7 j).

Analysis of variance was used to test the statistical significance of the decrease in LC or indeterminate cell number. The decrease in number of CD1a+ve, DA6.231+ve, L243+ve, TU22+ve and B7/21+ve ECs was shown to be highly significant ($p < 0.005$ for all antibodies).

Figure 5.2: **Vertical section through a suction blister-derived UVB-irradiated epidermal sheet labelled with OKT6 (anti-CD1a) antibody using the immunoperoxidase method. The sections shown in figures 5.2 - 5.6 are all from subject 3.**
Magnification 80 x

Figure 5.3: **Vertical section through a suction blister-derived UVB-irradiated epidermal sheet labelled with DA6.231 (anti-pan MHC II) antibody using the immunoperoxidase method. Note that figures 5.2 and 5.3 show serial sections.**
Magnification 80 x

Figure 5.4: **Vertical section through a suction blister-derived UVB-irradiated epidermal sheet labelled with L243 (anti-HLA-DR) antibody using the immunoperoxidase method.**
Magnification 80 x

Figure 5.5: **Vertical section through a suction blister-derived UVB-irradiated epidermal sheet labelled with TU22 (anti-HLA-DQ) antibody using the immunoperoxidase method.**
Magnification 80 x

Figure 5.6: Vertical section through a suction blister-derived UVB-irradiated epidermal sheet labelled with B721 (anti-HLA-DP) antibody using the immunoperoxidase method.
Magnification 80 x

Figure 5.7: Graphs showing the drop in numbers of CD1a+ve, panMHC II+ve, HLA-DP+ve, HLA-DQ+ve, HLA-DR+ve epidermal cells after a six week course of UVB irradiation.

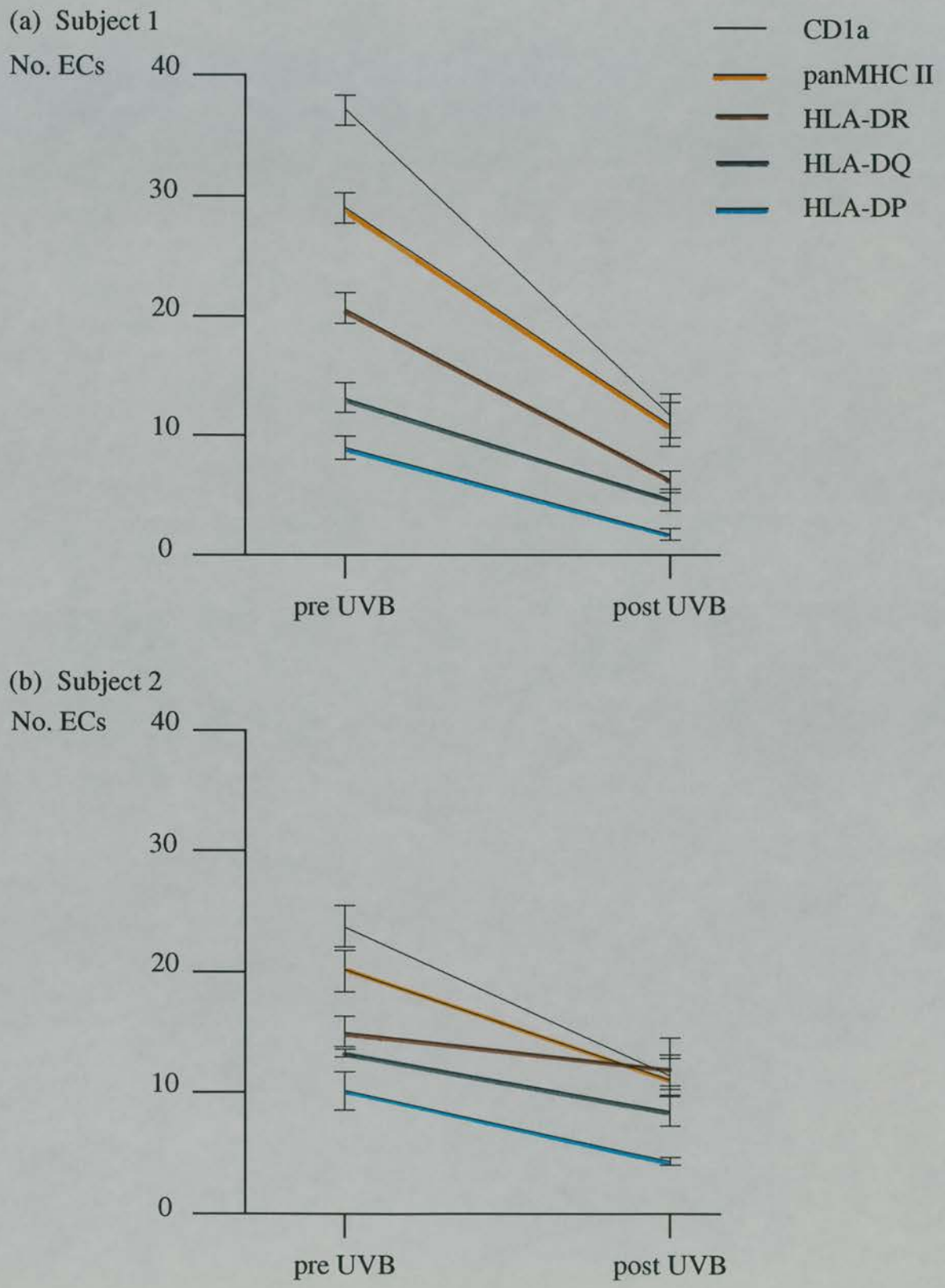

Figure 5.7: Graphs showing the drop in numbers of CD1a+ve, panMHC II+ve, HLA-DP+ve, HLA-DQ+ve, HLA-DR+ve epidermal cells after a six week course of UVB irradiation.

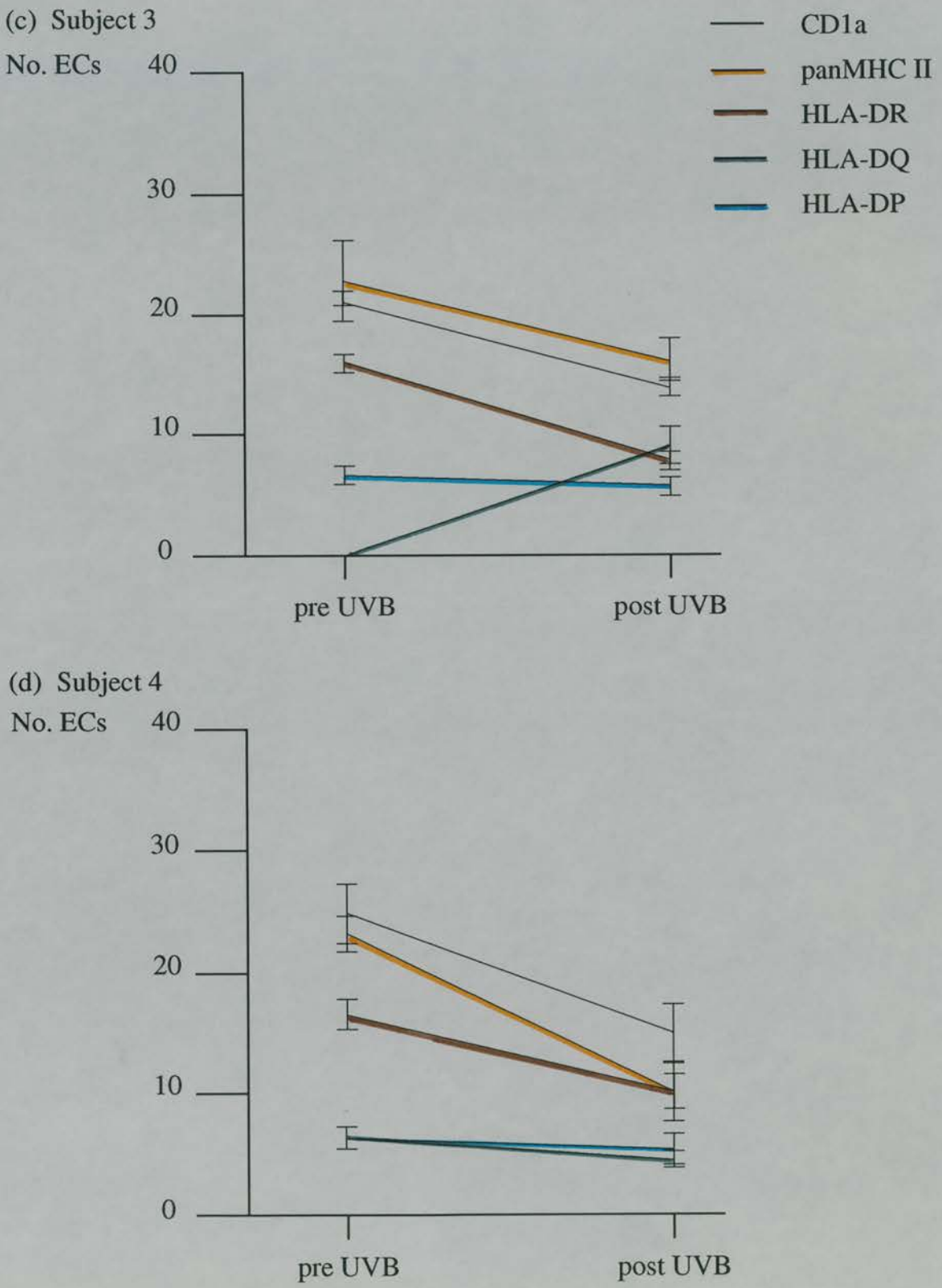

Figure 5.7: Graphs showing the drop in numbers of CD1a+ve, panMHC II+ve, HLA-DP+ve, HLA-DQ+ve, HLA-DR+ve epidermal cells after a six week course of UVB irradiation.

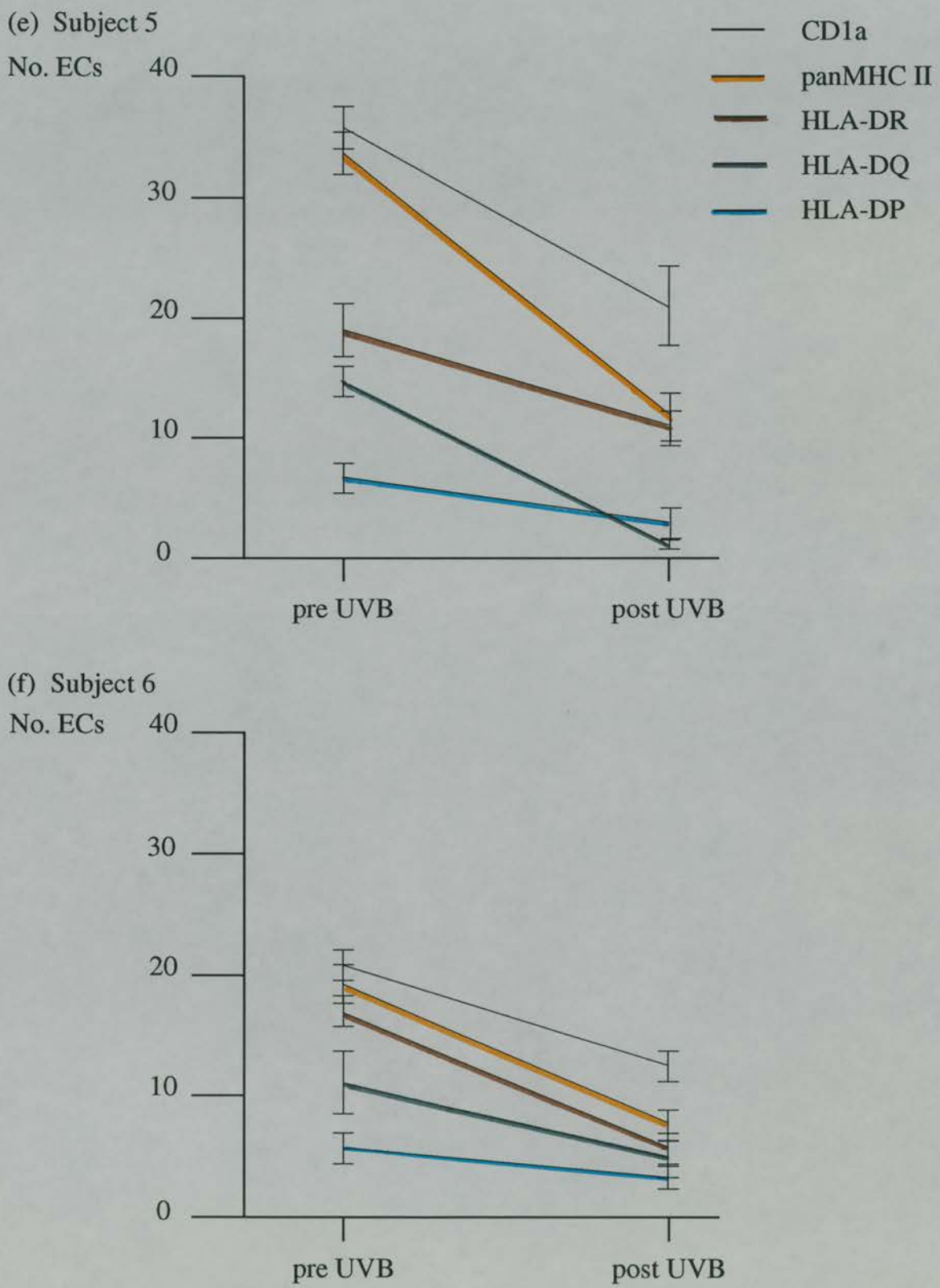

Figure 5.7: Graphs showing the drop in numbers of CD1a+ve, panMHC II+ve, HLA-DP+ve, HLA-DQ+ve, HLA-DR+ve epidermal cells after a six week course of UVB irradiation.

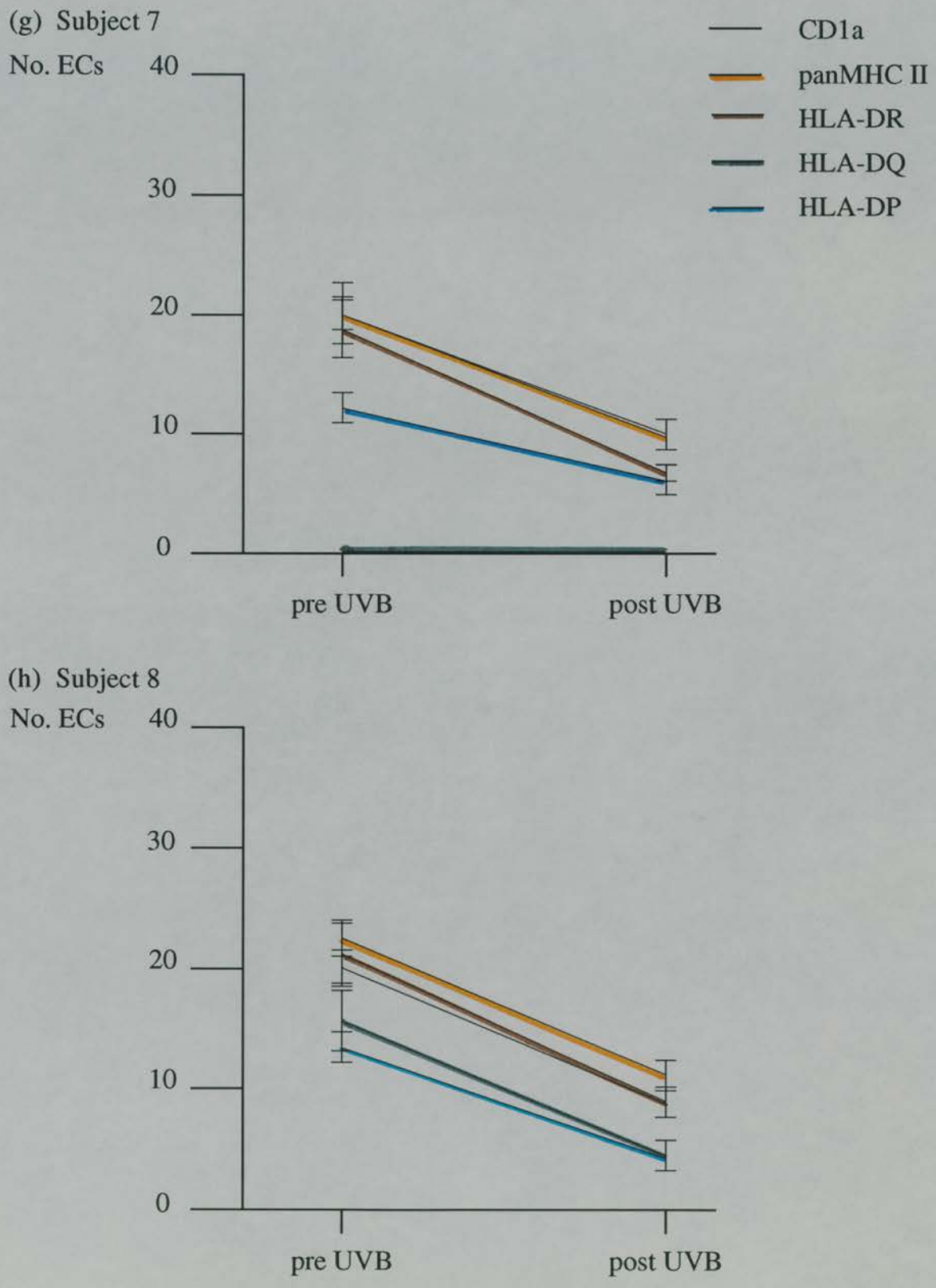

Figure 5.7: Graphs showing the drop in numbers of CD1a+ve, panMHC II+ve, HLA-DP+ve, HLA-DQ+ve, HLA-DR+ve epidermal cells after a six week course of UVB irradiation.

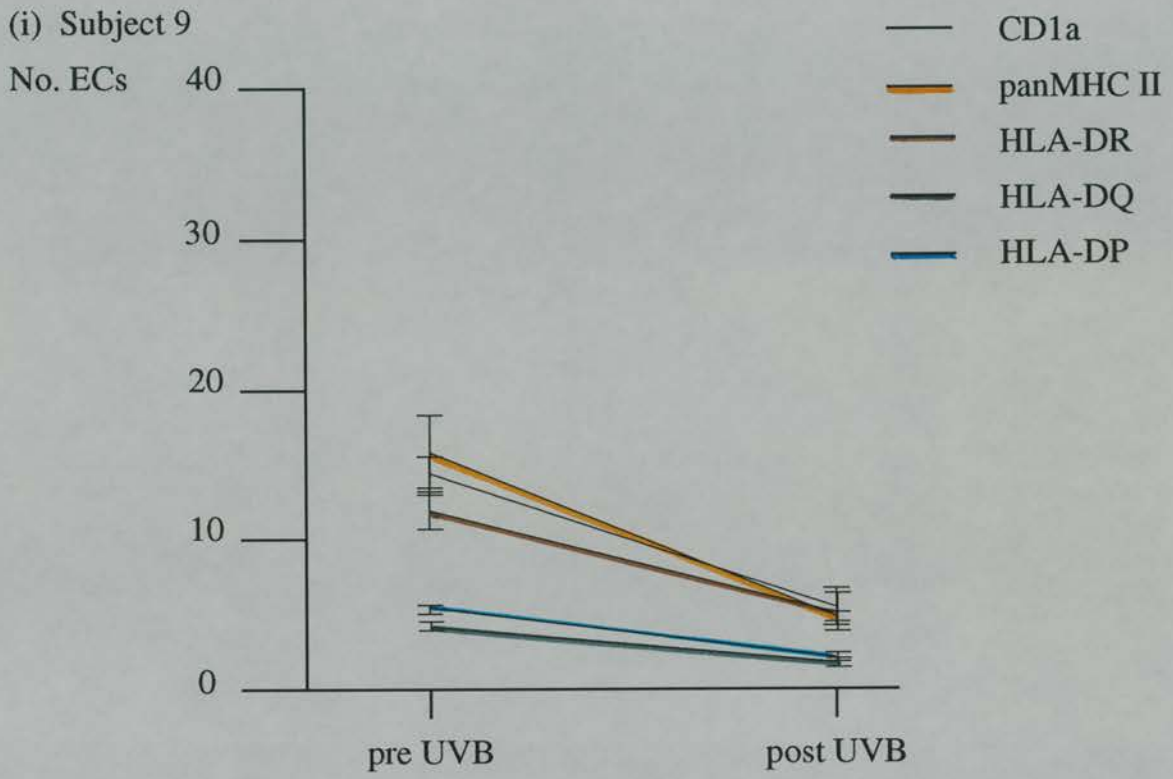

Fig 5.7 j) Graph to demonstrate the correlation between the drop in epidermal LC numbers and total dose of UVB in MEDs

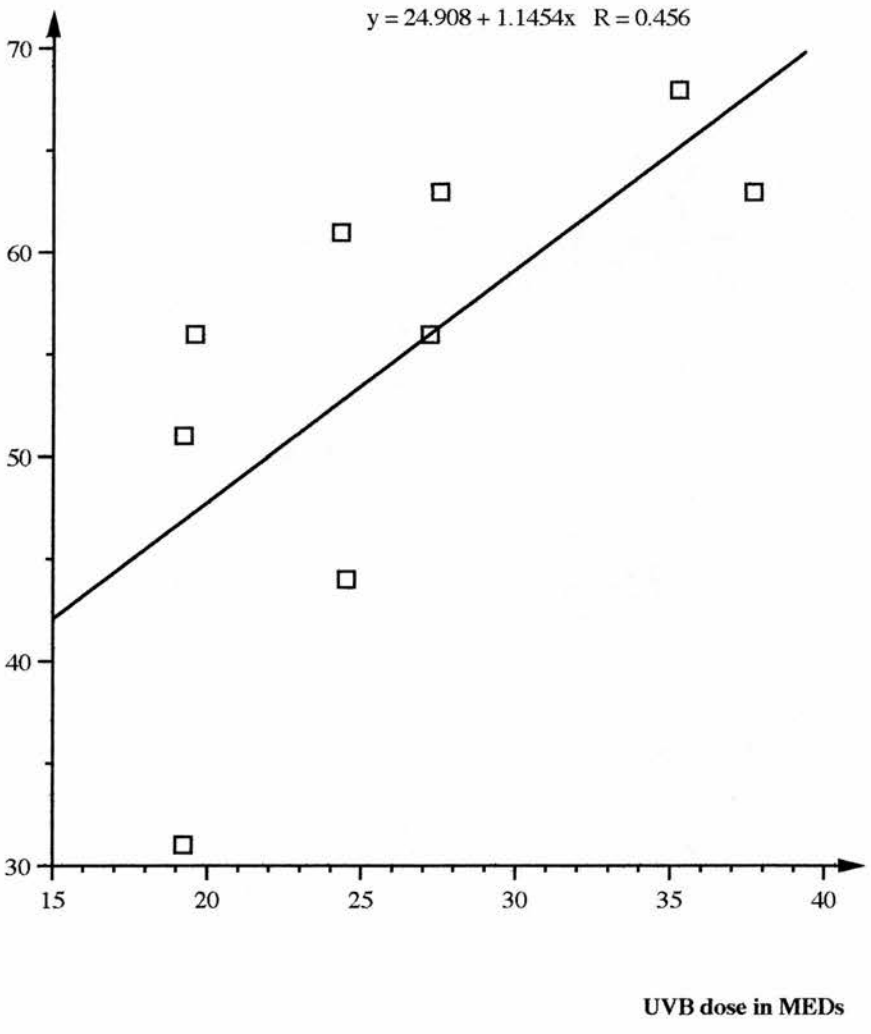

Table 5.2 The mean number of CD1a+ve, pan MHC II+ve, HLA-DP+ve, HLA-DQ+ve, and HLA-DR+ve ECs per mm basal cell membrane measured from five vertical sections through a) control epidermis and b) UVB-irradiated epidermis of nine subjects.

a)

subj	Monoclonal antibody				
	CD1a	**pan MHC II**	**HLA-DR**	**HLA-DQ**	**HLA-DP**
1	**37.38 (1.95)**	**29.26 (1.75)**	**21.09 (1.24)**	**13.18 (1.77)**	**8.73 (1.01)**
2	**23.20 (2.77)**	**19.91 (2.67)**	**15.50 (1.18)**	**13.02 (0.34)**	**10.05 (1.68)**
3	**21.07 (1.12)**	**23.25 (3.20)**	**16.31 (0.68)**	**0**	**6.83 (0.72)**
4	**24.75 (2.77)**	**22.89 (1.46)**	**16.65 (0.99)**	**5.72 (0.60)**	**6.14 (0.70)**
5	**35.76 (1.68)**	**33.09 (1.24)**	**19.10 (2.10)**	**14.03 (0.90)**	**6.99 (0.69)**
6	**20.62 (0.96)**	**18.51 (1.57)**	**17.13 (0.84)**	**11.39 (1.68)**	**6.14 (0.70)**
7	**20.28 (2.34)**	**19.11 (2.04)**	**20.21 (0.85)**	**0**	**11.87 (1.19)**
8	**21.13 (2.39)**	**21.82 (0.98)**	**20.26 (1.50)**	**16.44 (1.68)**	**12.93 (0.95)**
9	**14.10 (1.25)**	**15.91 (2.08)**	**12.57 (1.03)**	**4.43 (0.13)**	**5.90 (0.50)**

*standard error of the mean is given in parentheses.

Table 5.2 b)

subj	Monoclonal antibody				
	CD1a	**pan MHC II**	**HLA-DR**	**HLA-DQ**	**HLA-DP**
1	**12.17 (2.30)**	**10.67 (1.87)**	**6.56 (0.84)**	**3.81 (0.78)**	**2.12 (0.42)**
2	**11.49 (0.99)**	**11.09 (2.53)**	**12..29 (2.90)**	**7.74 (0.93)**	**3.76 (0.41)**
3	**13.27 (0.82)**	**16.04 (2.52)**	**8.31 (0.68)**	**8.98 (1.67)**	**6.15 (0.58)**
4	**14.72 (2.22)**	**9.95 (1.63)**	**9.79 (3.64)**	**3.56 (0.55)**	**4.71 (0.94)**
5	**20.56 (4.06)**	**12.32 (2.07)**	**10.82 (0.80)**	**0.66 (0.27)**	**2.98 (0.84)**
6	**12.24 (1.22)**	**8.20 (0.81)**	**6.51 (1.01)**	**5.22 (1.43)**	**2.70 (0.54)**
7	**9.90 (1.05)**	**7.48 (0.32)**	**9.74 (1.23)**	**0**	**6.41 (1.38)**
8	**9.29 (0.74)**	**10.63 (1.02)**	**8.93 (1.09)**	**4.49 (0.84)**	**3.78 (0.78)**
9	**5.98 (1.21)**	**5.02 (0.37)**	**5.64 (0.79)**	**2.31 (0.41)**	**2.55 (0.25)**

*standard error of the mean is given in parentheses.

5.2 The morphology of LCs and indeterminate cells in UVB-exposed epidermis.

LC and indeterminate cell morphology *in situ* was examined and analysed quantitatively with the aid of an image analyer using images obtained by confocal laser scanning microscopy. The data obtained from two-dimensional reconstructions is given in appendix 5, and examples of three-dimensional recontructions of LCs after UVB exposure are given in figs. 5.8-5.10. Note the reduction in the number of LC dendrites detected after UVB irradiation.

Figure 5.8: **The central image is a three-dimensional reconstruction of a UVB-irradiated Langerhans cell and the surrounding images represent different views of the same cell which would be seen if the cell was rotated by steps of 30° around its central axis.**

Figure 5.9: **The central image is a three-dimensional reconstruction of a UVB-irradiated Langerhans cell and the surrounding images represent different views of the same cell which would be seen if the cell was rotated by steps of 30° around its central axis.**

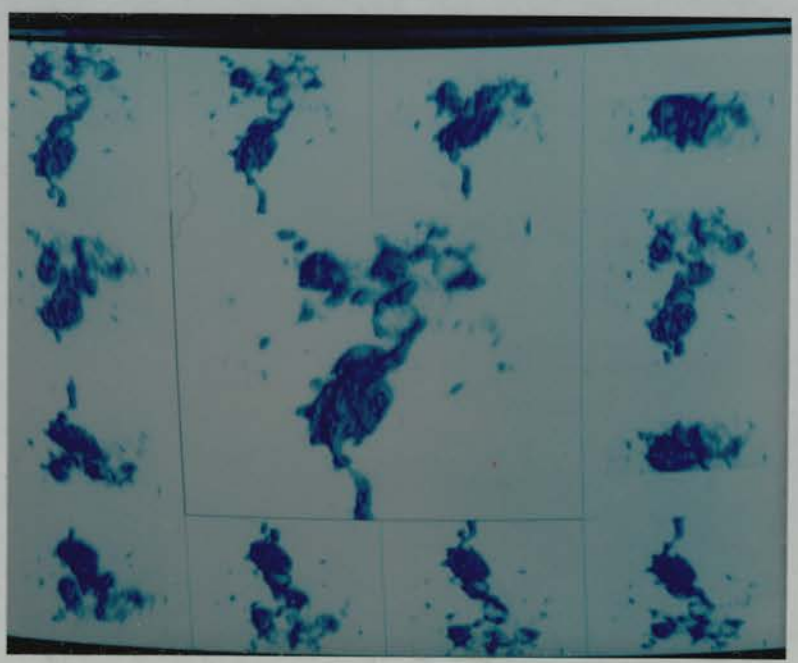

Figure 5.10: **The central image is a three-dimensional reconstruction of a UVB-irradiated Langerhans cell and the surrounding images represent different views of the same cell which would be seen if the cell was rotated by steps of 30° around its central axis.**

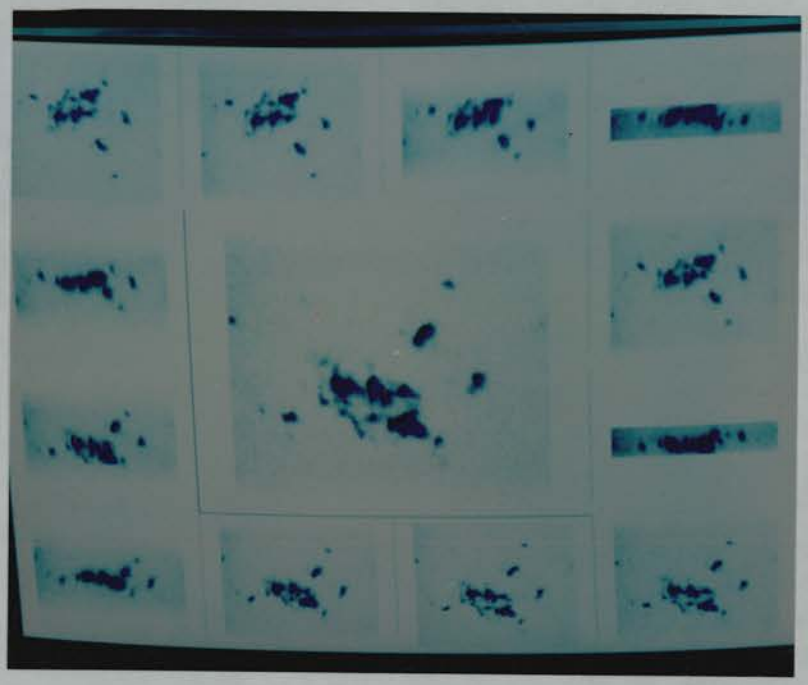

Various parameters of LC or indeterminate cell morphology *in situ* within control epidermis, and in epidermis which has been UVB-irradiated are given in table 5.3. The data in table 4.3 has been repeated here for ease of reference, for comparison with data from UVB-irradiated samples.

Table 5.3 Quantitative analysis of the morphology of a) control LCs and indeterminate cells and b) UVB-irradiated LCs and indeterminate cells reconstructed in two dimensions.

a)

cell parameter n=38	mean	sem*	range
cell area (μm^2)	285	15.5	167-501
dendrite area (μm^2)	144	14.5	38-407
dendrite length (μm)	12.7	1.7	1.2-49.1
number of dendrites/cell	5.0	1.9	2-9
dendricity (arbitrary units)	3.4	0.2	1.7-7.4

b)

cell parameter n=38	mean	sem*	range
cell area (μm^2)	220.3	19.5	71-454
dendrite area (μm^2)	93.6	17.7	0-611
dendrite length (μm)	11.5	2.2	1.0-99.9
number of dendrites/cell	3.4	0.3	0-9
dendricity (arbitrary units)	2.9	0.3	1.0-9.8

* standard error of the mean

n = number of cells

The mean cell area, mean dendrite area and mean number of dendrites per cell were all significantly decreased after UVB exposure. No statistically significant changes were noted in the mean cell body area, mean length of dendrites or mean dendricity of the cells after UVB irradiation. However, the range of dendrite lengths was greater after UVB exposure and the median value for dendrite lengths was decreased in all of the four cases after UVB irradiation. This indicates that the majority of dendrites were shorter after UVB exposure, but a minority of dendrites were greatly attenuated.

The ultrastructural morphology of UVB-irradiated LCs in suspension was examined, and was found to be similar to that of control unirradiated LCs i.e. highly variable with respect to dendricity, electron density of cytoplasm, presence or absence of long cell surface projections ('veils'), and the shape of the cell section profile (figs 5.11-5.21). However, the morphologies of these cells fell within six main categories; the five described previously in chapter 4, section 4.2, page 97, and type VI, where the cell is extremely elongated in profile.

Moreover, the proportions of UVB-exposed LCs in suspension which possessed ultrastructural morphologies I - V was unaltered when compared with the proportions of unirradiated LCs and indeterminate cells in suspension (table 5.4). However, 3/200 UVB-irradiated LCs examined had a different morphology compared with LCs prior to UVB irradiation, and appeared greatly elongated with little evidence of membrane damage (fig. 5.21).

Table 5.4 Comparison of LC and indeterminate cell ultrastructural morphology before and after a standard six week course of phototherapy.

Type of morphology	Proportion of LCs/ICs within category	
	pre UVB	post UVB
I	174/200	172/200
II	6/200	6/200
III	9/200	6/200
IV	7/200	9/200
V	4/200	4/200
VI	0/200	3/200

Figure 5.11: Langerhans cell in suspension with type I morphology.
Magnification 17,700 x

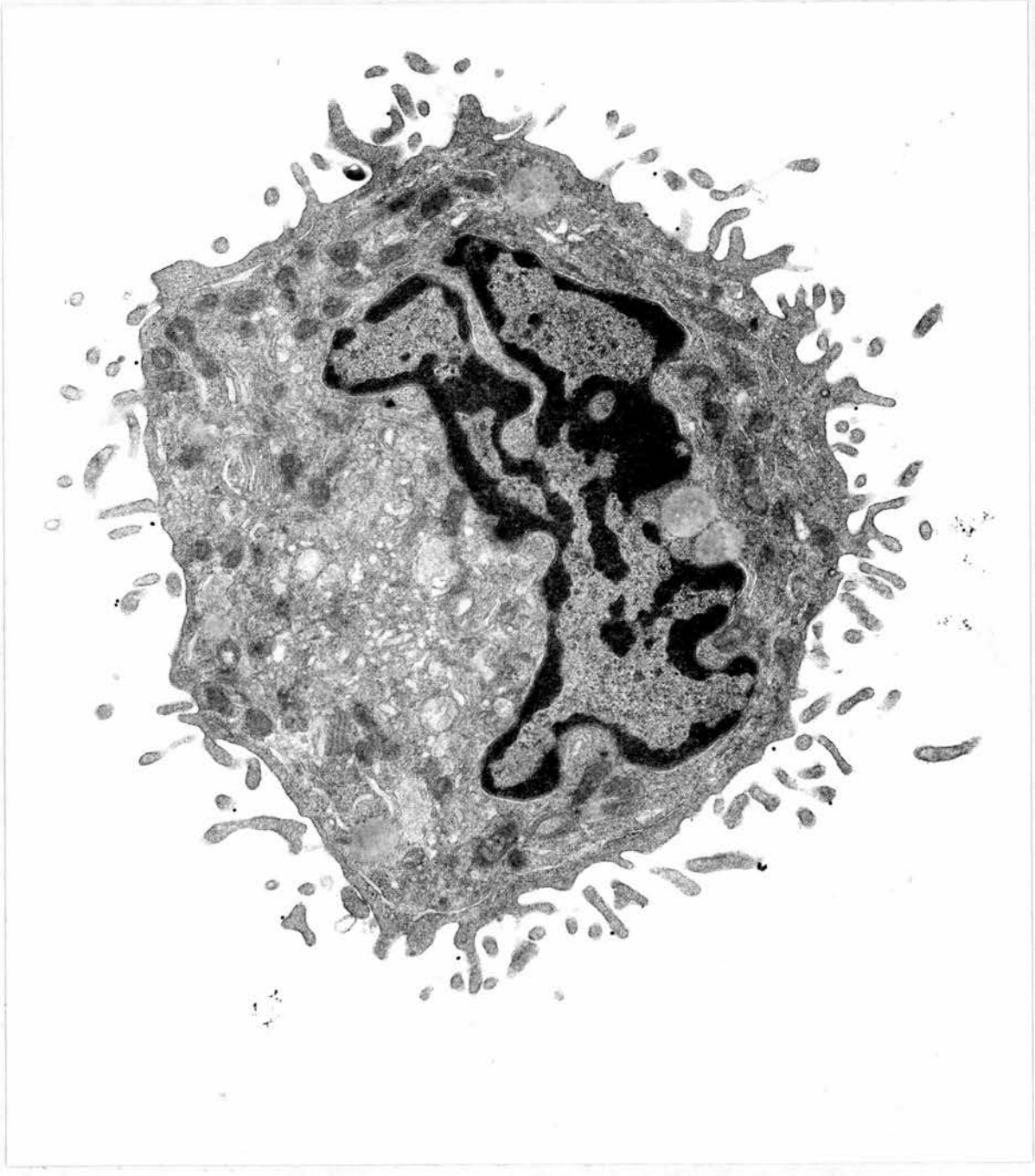

Figure 5.12: Langerhans cell in suspension with type II morphology.
Magnification 23,100 x

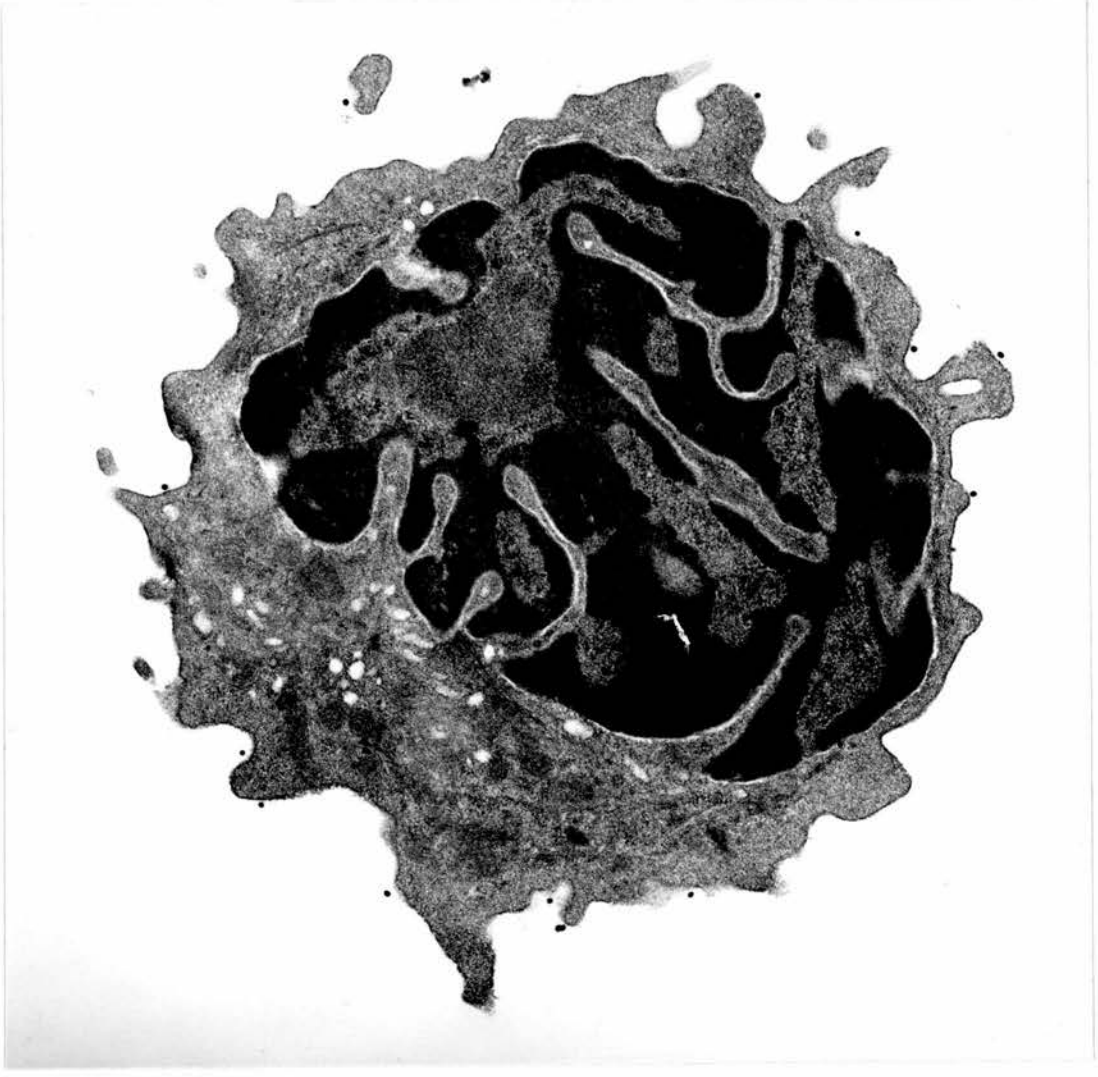

Figure 5.13: Langerhans cell in suspension with type III morphology.
Magnification 18,400 x

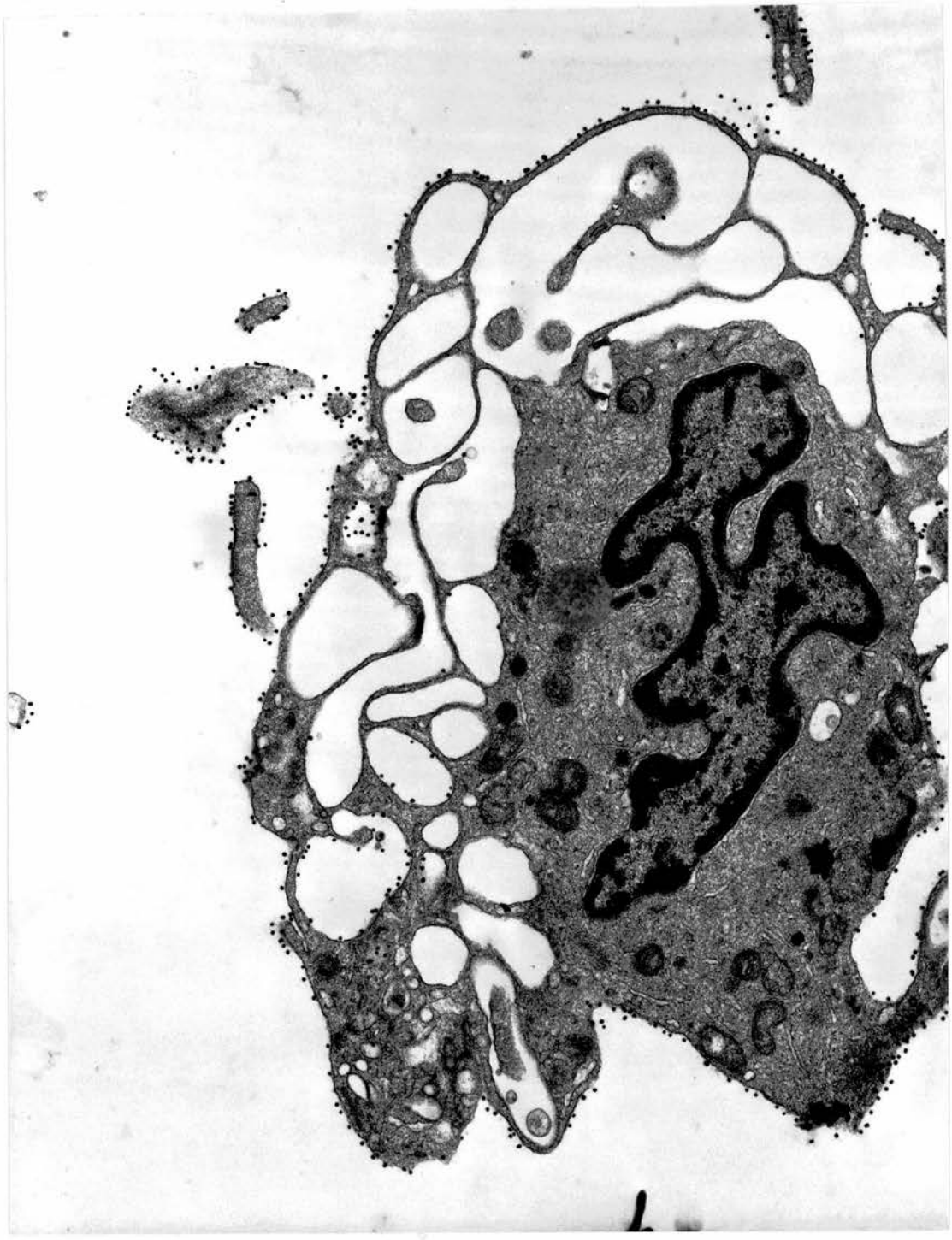

Figure 5.14: Langerhans cell in suspension with type IV morphology.
Magnification 19,800 x

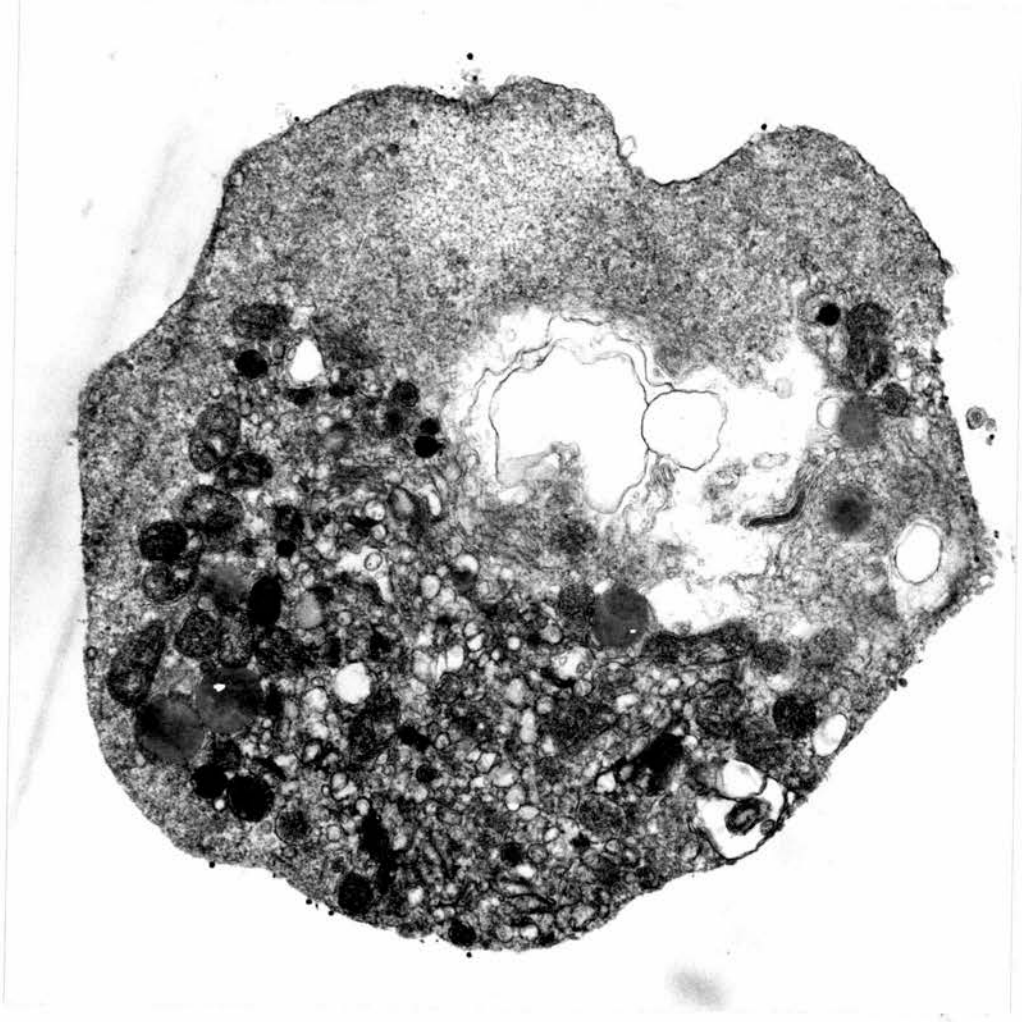

Figure 5.15: Langerhans cell in suspension with type V morphology.
Magnification 19,900 x

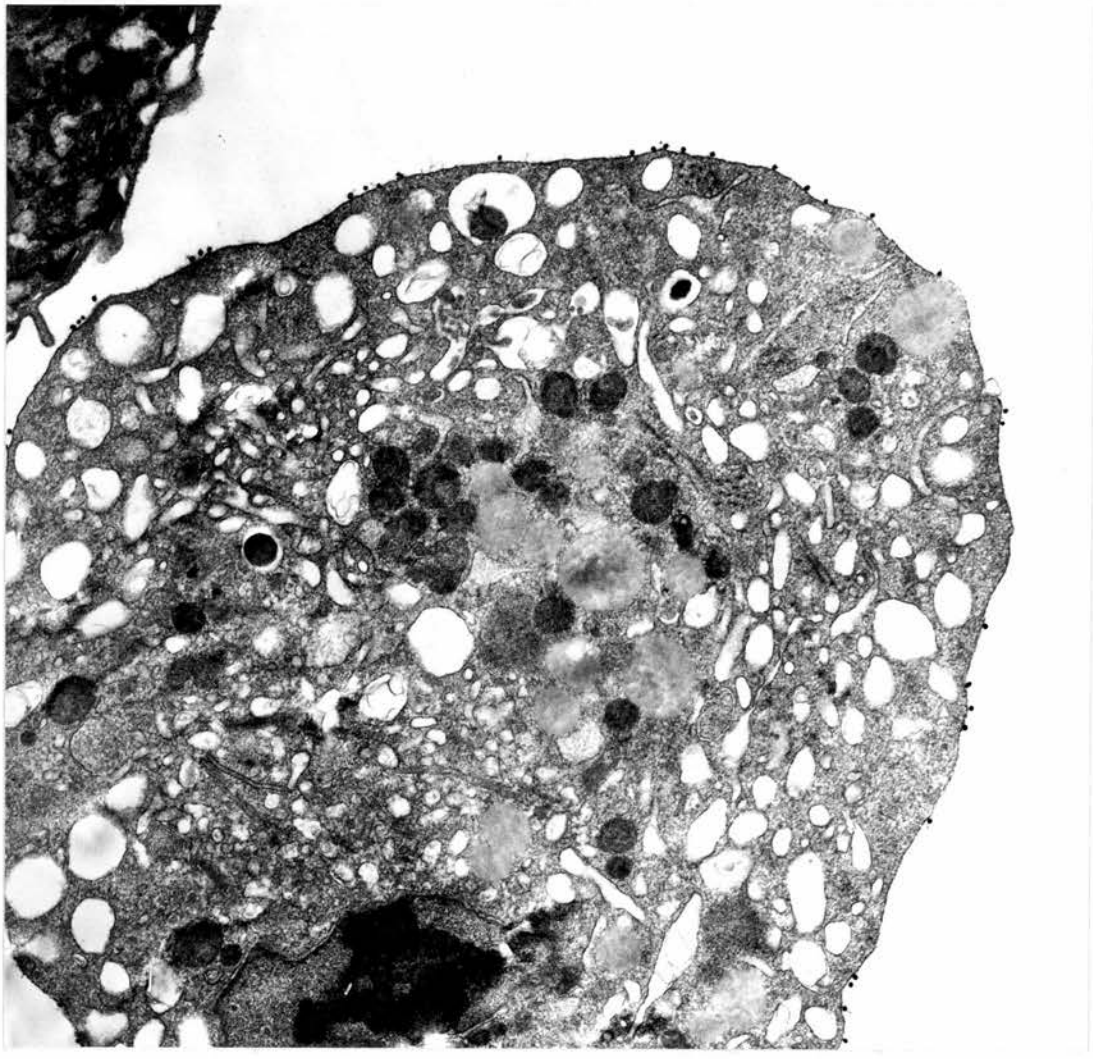

Figure 5.16: UVB-irradiated Langerhans cell in suspension with type I morphology. Magnification 12,200 x

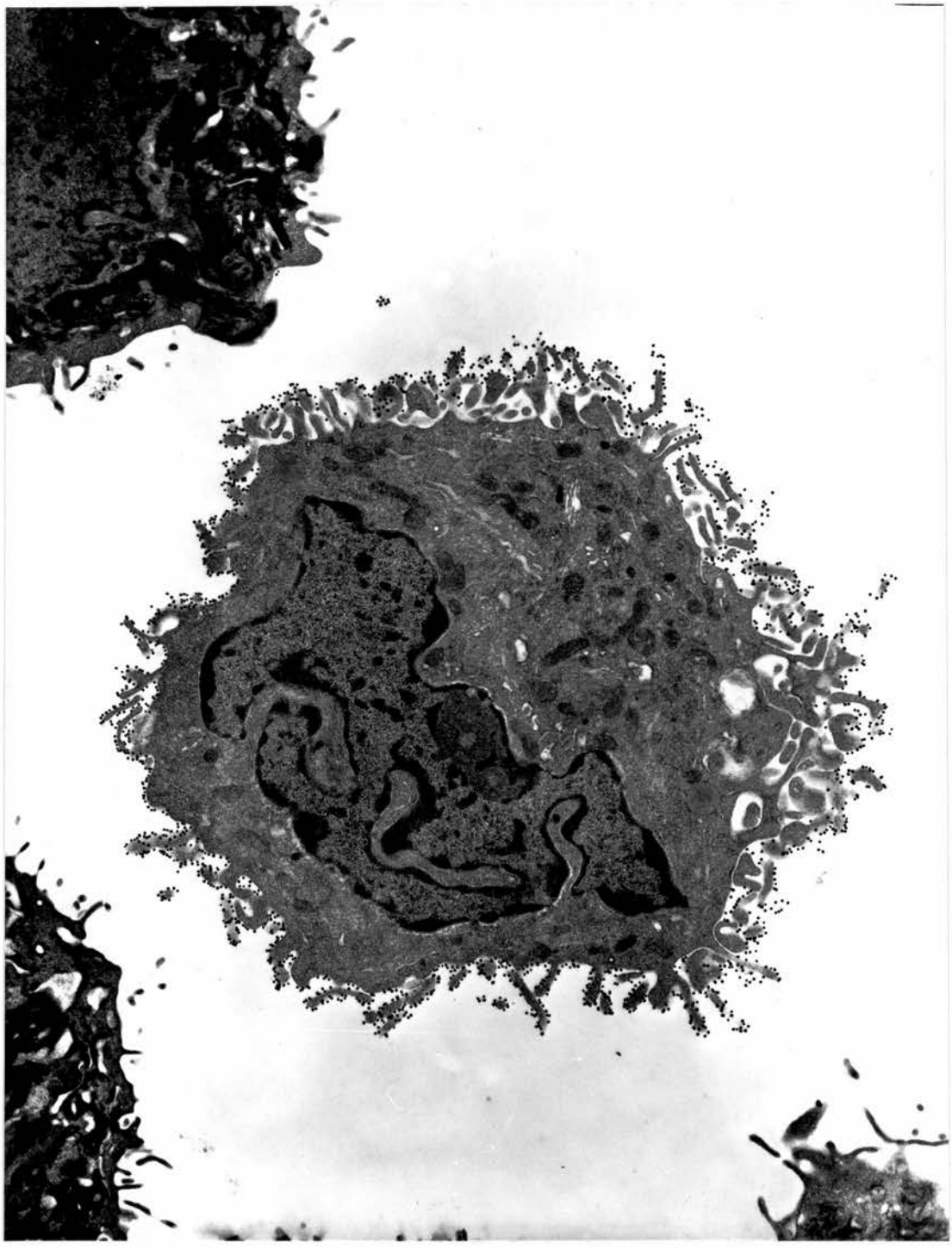

Figure 5.17: UVB-irradiated Langerhans cell in suspension with type II morphology. Magnification 14,800 x

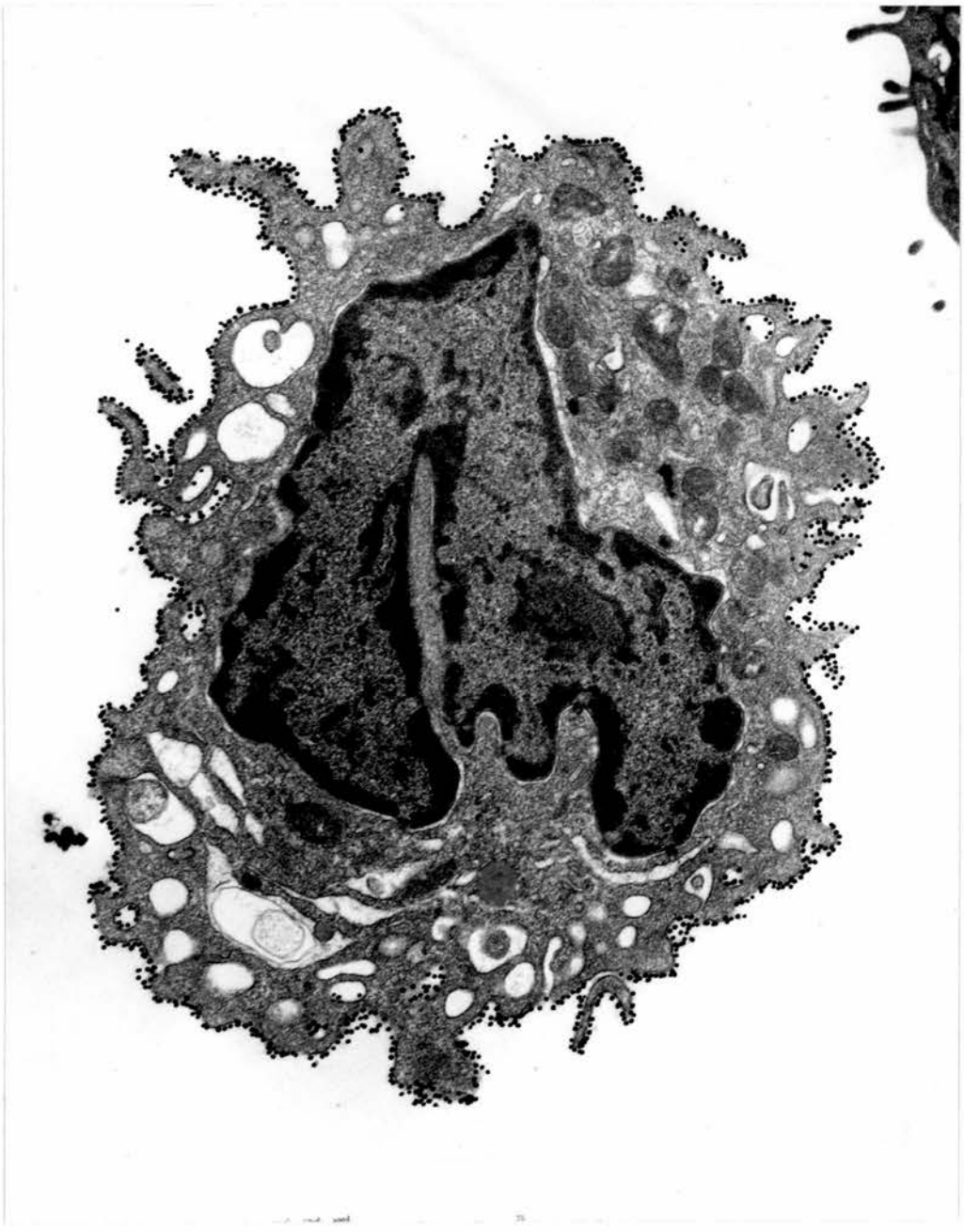

Figure 5.18: UVB-irradiated Langerhans cell in suspension with type III morphology. Magnification 20,600 x

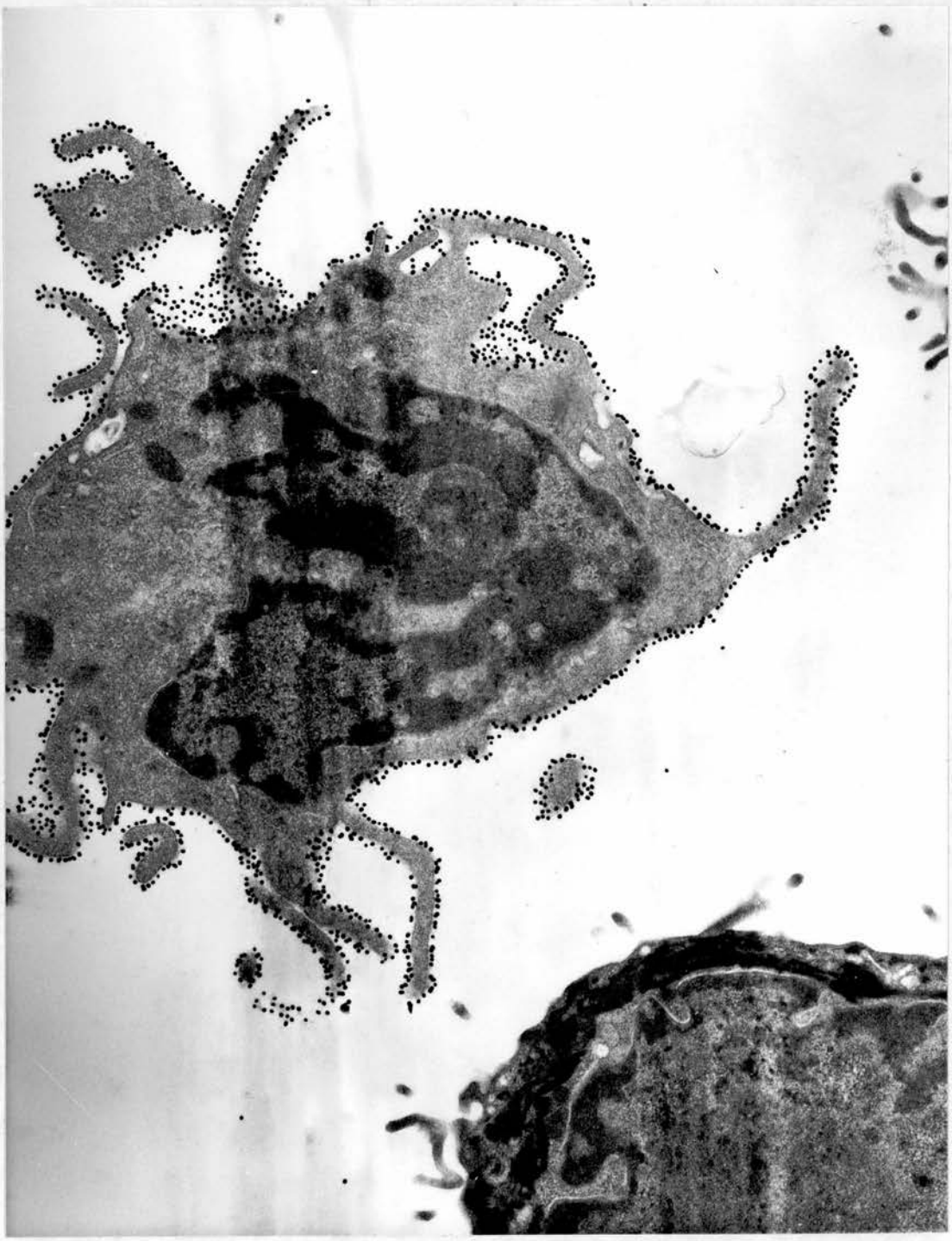

Figure 5.19: UVB-irradiated Langerhans cell in suspension with type IV morphology. Magnification 17,900 x

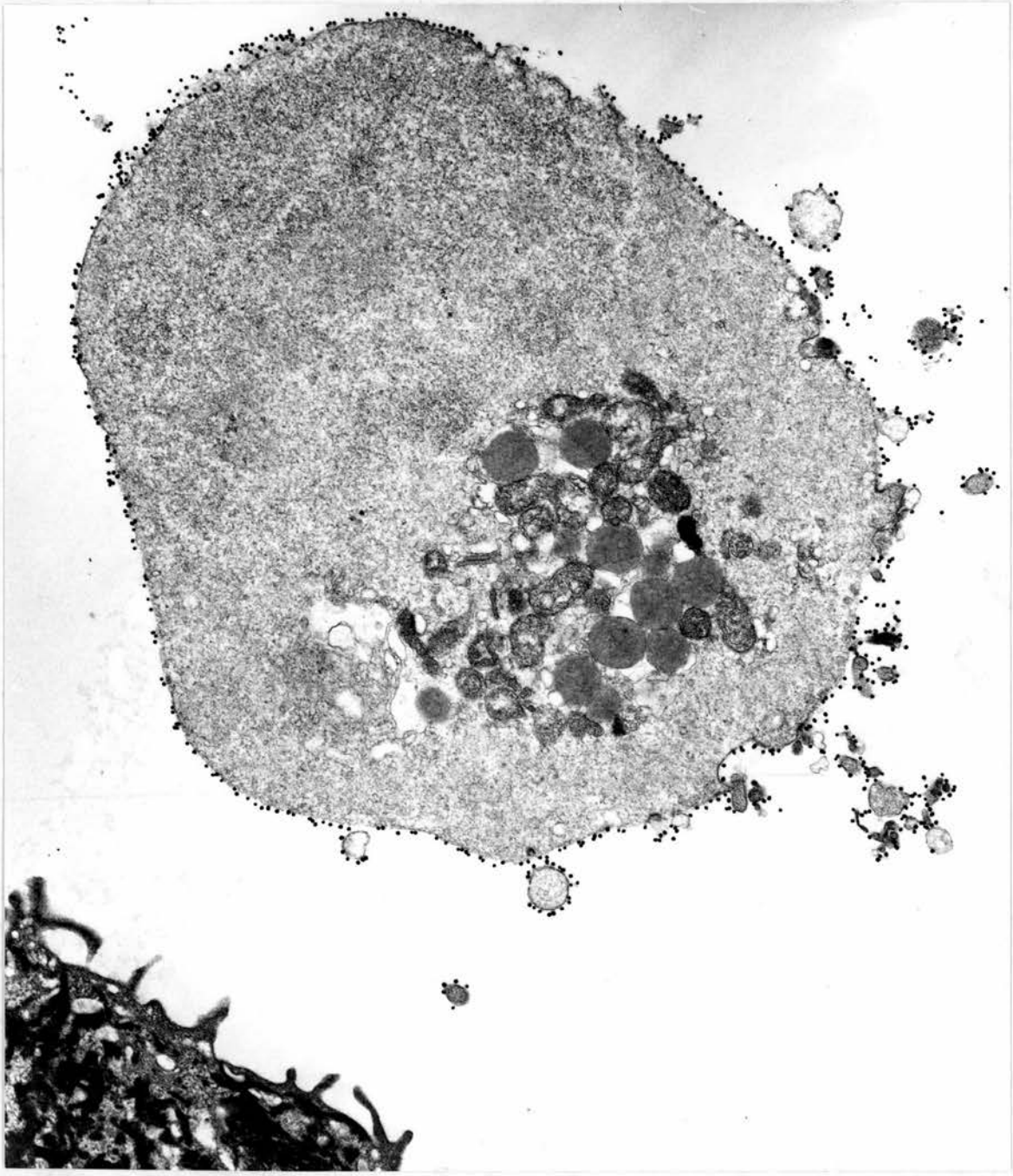

Figure 5.20: UVB-irradiated Langerhans cell in suspension with type V morphology. Magnification 15,900 x

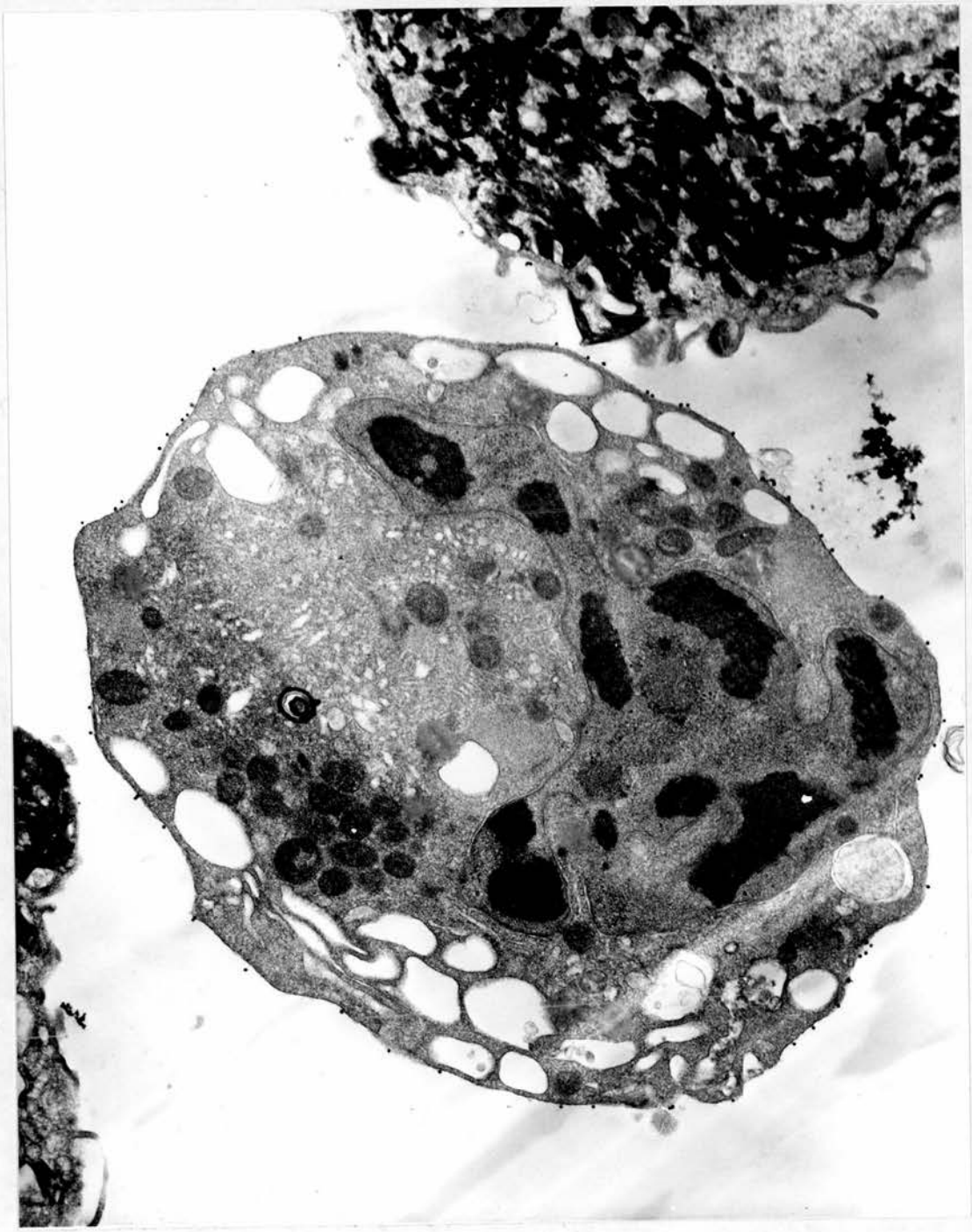

Figure 5.21: UVB-irradiated Langerhans cell in suspension with type VI morphology. Magnification 12,600 x

Whereas no CD1a-ve LCs or indeterminate cells were observed in normal unirradiated epidermis, a small number of CD1a-ve dendritic cells were detected in epidermis which had been exposed to UVB irradiation. These cells were present in small numbers, possessed no BGs or other distinguishing cytoplasmic granules, little cytoplasm and the distribution of nuclear heterochromatin was similar to that seen in lymphoid cells. However, the cells also appeared similar in ultrastructure to cells of the macrophage/dendritic cell lineage (fig 5.22).

After UVB irradiation, some keratinocytes (which did not resemble acrosyringeal keratinocytes in ultrastructure) were detected which expressed cell surface pan MHC II (as detected by DA6.231 antibody labelling) in quantities similar to those expressed by LCs (fig. 5.23). Although no pan MHC II+ve keratinocytes were observed in normal unirradiated epidermis, a small group of HLA-DQ+ve keratinocytes, with an ultrastructure compatible with acrosyringial keratinocytes, were seen in unirradiated epidermis (fig. 5.24).

Figure 5.22: A CD1a-ve dendritic cell in UVB-irradiated epidermal cell suspension. Magnification 19,700 x

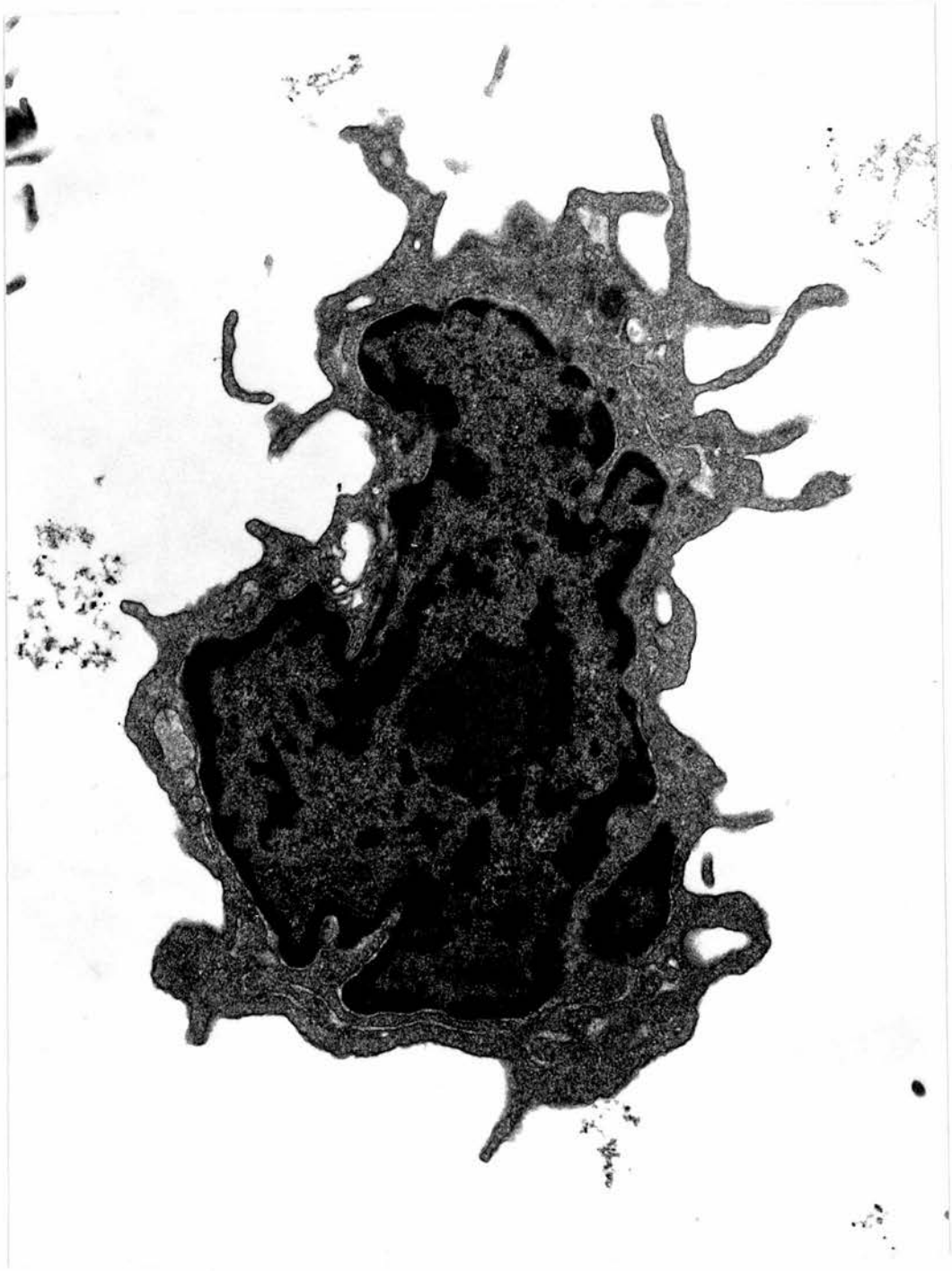

Figure 5.23: A pan-MHC II +ve keratinocyte in UVB-irradiated epidermal cell suspension. The MHC II molecules are labelled with DA6.231 primary antibody and secondary antibody conjugated to 30nm gold particles (arrowheads). Magnification 15,200 x

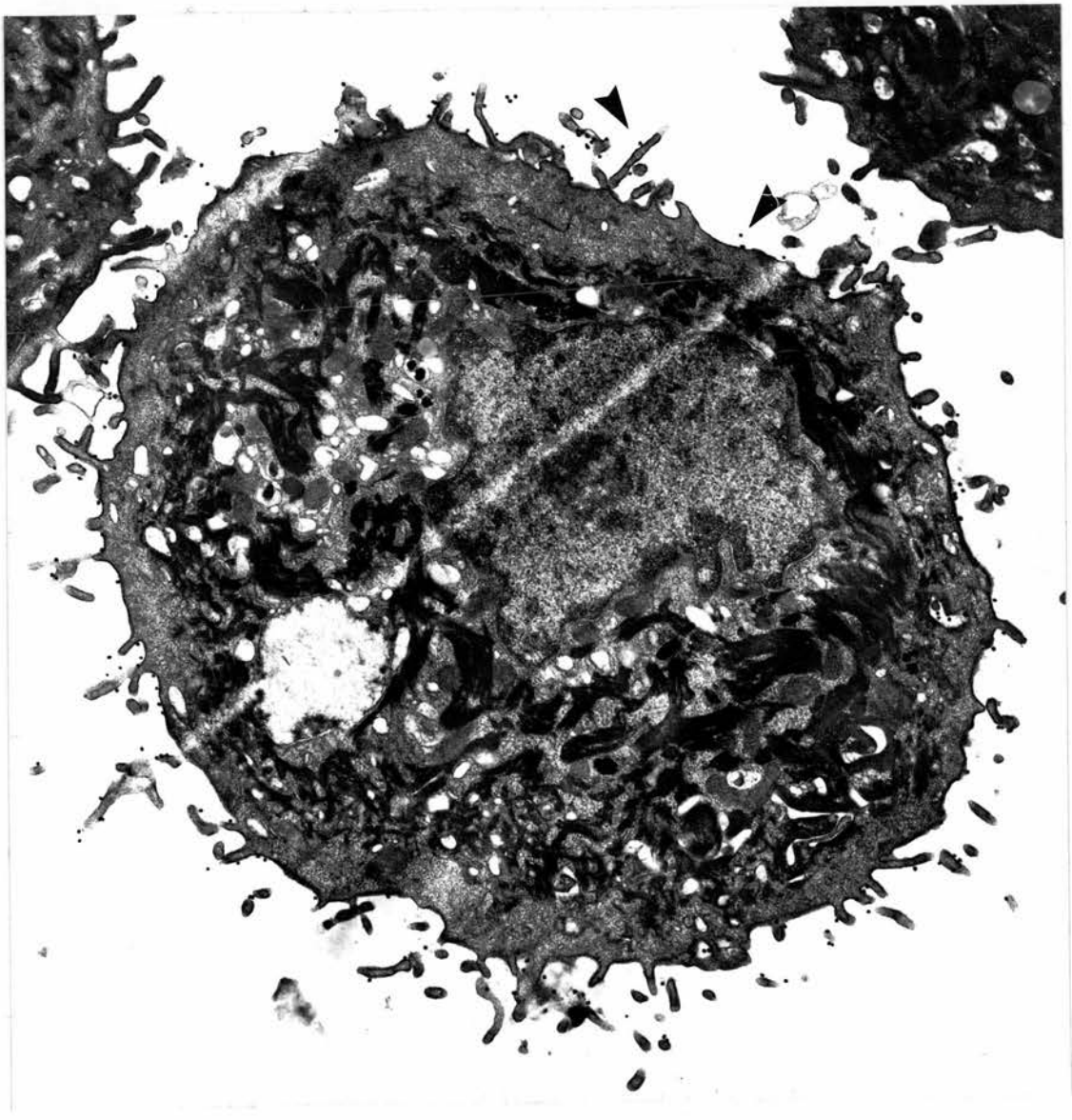

Figure 5.24: HLA-DQ +ve keratinocytes with ultrastructure compatible with that of acrosyringeal keratinocytes, present in unirradiated epidermal cell suspension. The HLA-DQ molecules are labelled with TU22 and secondary antibody conjugated to 30nm gold particles (arrowheads). Magnification 13,300 x

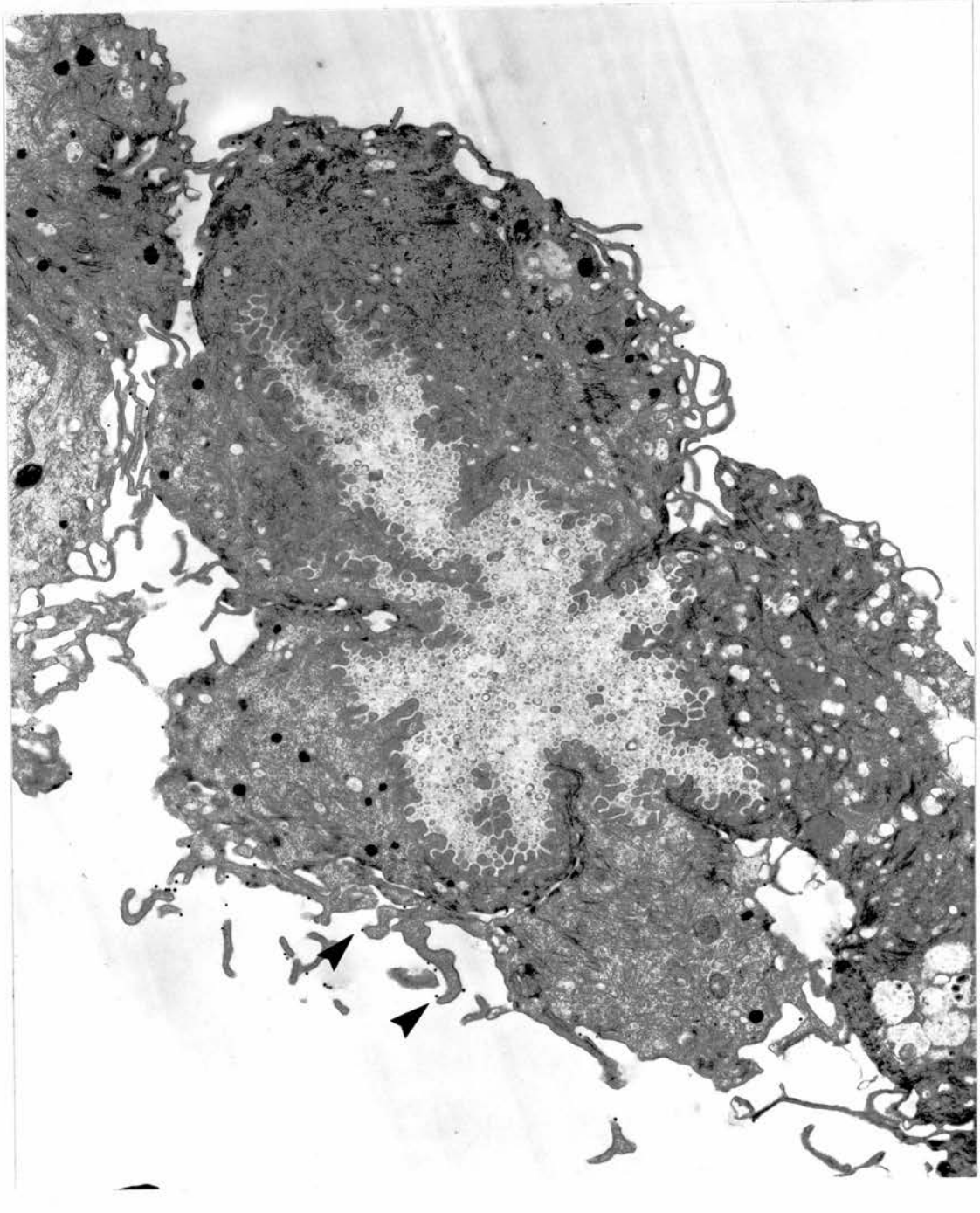

5.3 The influence of UVB irradiation on LC surface expression of CD1a and MHC II antigens.

The density of surface CD1a, Pan-MHC II, HLA-DP, HLA-DQ and HLA-DR was quantified semi-automatically on five different LC sections from each subject (for results see appendix 4 and table 5.5). The data from table 4.4 is repeated in table 5.5 a) for ease of reference.

Increases in the surface expression of all five molecules were detected. The statistical significance of these increases were tested and the p values found to be $p<0.005$ for all except for the increase in L243 antigen expression which was $p<0.05$.

Table 5.5 The mean number of gold particles per micron plasma membrane on five CD1a+ve, pan MHC II+ve, HLA-DP+ve, HLA-DQ+ve, and HLA-DR+ve LCs or indeterminate cells per subject a) before and b) after a standard six week course of phototherapy

a) (measurements made on sections of both LCs and indeterminate cells).

subj	Monoclonal antibody				
	CD1a	**pan MHC II**	**HLA-DR**	**HLA-DQ**	**HLA-DP**
1	**0.90 (0.45)***	**3.49 (0.33)**	**2.13 (1.24)**	**0.40 (0.08)**	**0.29 (0.08)**
2	**0.25 (0.05)**	**4.06 (1.13)**	**0.09 (0.05)**	**0.54 (0.20)**	**0.45 (0.13)**
3	**0.78 (0.11)**	**6.60 (1.29)**	**0.23 (0.03)**	**0.16 (0.04)**	**0.71 (0.14)**
4	**0.82 (0.22)**	**5.03 (1.24)**	**0.12 (0.03)**	**0.32 (0.10)**	**0.33 (0.13)**
5	**1.03 (0.23)**	**5.09 (0.94)**	**0.39 (0.13)**	**0.58 (0.13)**	**1.05 (0.16)**
6	**0.55 (0.09)**	**6.13 (0.47)**	**1.13 (0.74)**	**ND**	**ND**
7	**0.99 (0.06)**	**5.85 (0.74)**	**0.10 (0.06)**	**0**	**ND**
8	**0.24 (0.05)**	**5.33 (0.77)**	**0.35 (0.11)**	**ND**	**ND**
9	**1.51 (0.24)**	**4.77 (0.91)**	**ND**	**ND**	**ND**

b) (measurements made on LC sections, not indeterminate cell sections).

subj	Monoclonal antibody				
	CD1a	**pan MHC II**	**HLA-DR**	**HLA-DQ**	**HLA-DP**
1	**3.20 (0.36)***	**7.00 (1.94)**	**0.84 (0.26)**	**1.06 (0.29)**	**2.20 (1.18)**
2	**1.33 (0.28)**	**4.60 (1.79)**	**0.95 (0.84)**	**1.17 (0.38)**	**1.31 (0.71)**
3	**1.55 (0.24)**	**9.27 (1.49)**	**1.58 (0.46)**	**1.23 (0.64)**	**1.77 (0.69)**
4	**1.62 (0.53)**	**6.62 (1.13)**	**0.59 (0.31)**	**1.11 (0.49)**	**1.27 (0.53)**
5	**2.06 (0.65)**	**11.61 (1.46)**	**3.94 (1.04)**	**1.66 (0.55)**	**3.08 (0.79)**
6	**1.34 (0.12)**	**5.52 (1.33)**	**ND**	**ND**	**ND**
7	**1.00 (0.29)**	**8.50 (1.15)**	**ND**	**ND**	**ND**
8	**0.38 (0.14)**	**5.71 (1.24)**	**ND**	**ND**	**ND**
9	**1.38 (0.13)**	**6.92 (2.64)**	**ND**	**ND**	**ND**

* numbers in parentheses are standard errors of the means.

5.4 The effect of UVB irradiation on epidermal UCA and on TNF-α levels in suction blister fluid.

Only four of the nine subjects could be examined with respect to UCA and TNF-α quantification. The significance of these factors was not appreciated until the study had progressed to the stage where five subjects had already finished the course of irradiation and time constraints did not allow recruitment of further volunteers.

Samples of cellotape-stripped epidermis and samples of suction blister fluid were taken from four subjects before the start of UVB irradiation, and during the course of UVB irradiation (after four weeks of UVB exposure). The percentage of *cis*-UCA rose in both the epidermis and in the blister fluid during the course of UVB irradiation (see table 5.6).

Table 5.6 The total UCA and percentage *cis*-UCA in epidermis and suction blister fluid before and during a standard six week course of UVB phototherapy.

sample	n	before treatment		during treatment		after treatment	
		Total UCA	%cis-UCA	Total UCA	%cis-UCA	Total UCA	%cis-UCA
epidermis (nM cm^{-2})	4	2.9 (0.7)*	13.7 (7.0)	5.9 (2.3)	54.4 (13.3)	3.6 (1.1)	5.9 (3.3)
blister fluid (mM)	4	89.9 (10.9)	4.1 (1.1)	73.2 (23.9)	23.4 (8.2)	ND	ND

ND = not done
n = number of subjects
The standard errors of the means are given in parentheses.

The increase in percentage *cis*-UCA during treatment in epidermal samples was statistically significant ($p < 0.05$) as was that in suction blister fluid ($p < 0.001$). The increases in total UCA in epidermal and suction blister fluid were not statisitically significant.

Three of the four subjects in which TNF-α was measured showed increased levels of this cytokine during treatment (fig. 5.25).

Figure 5.25: TNF-α concentration in suction blister fluid before and during a six week course of UVB phototherapy.

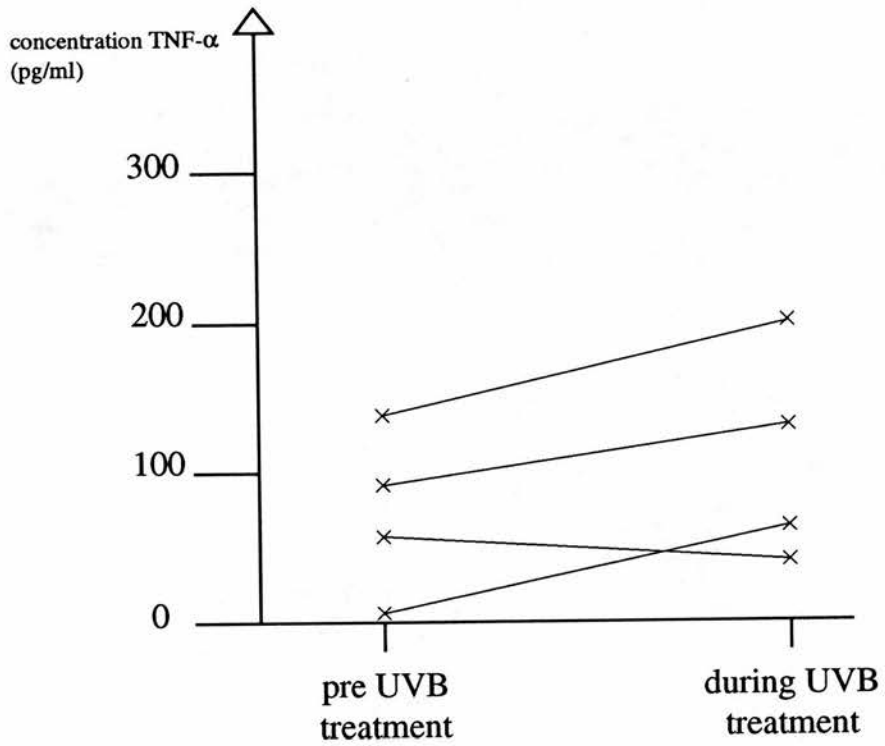

Chapter 6 Discussion

6.1 Introduction.

This study has characterized the influence of suberythemal doses of UVB radiation, similar to those used therapeutically, on human LC morphology, number and surface antigen expression.

LC morphology was studied *in situ* in both control and UVB-irradiated epidermis using confocal laser scanning microscopy. UVB-exposed LCs were found to be less dendritic than LCs in control, unirradiated skin. The majority of LC dendrites in UVB-exposed skin were shorter than those in control skin, but a few were greatly attenuated, giving the appearance of cells in the process of emigrating from the epidermis. After UVB irradiation, 48 hours after the last irradiation, a reduced number of LCs were detected using both immunohistochemical and immunofluorescence methods. Great variation in the density of surface MHC II and CD1a antigen expression on LCs was demonstrated using an ultrastructural immunogold technique. At 48 hours after the last UVB irradiation, increased surface MHC II and CD1a antigen expression was demonstrated on residual LCs. These results will be discussed in detail in the following sections.

6.2 Justification of the methodologies used in this thesis.

Immunoelectron microscopy was the method chosen to examine the cell surface expression of CD1a and MHC II antigens and its modulation by UV irradiation. The technique is very sensitive and allows the examination of the surface expression of antigens on single cells. However, the size of gold particles conjugated to the secondary antibodies is critical in determining the density of cell surface gold label, with small gold particles generally giving higher gold label densities than larger gold particles due to steric hinderance. Therefore immunogold labelling would not be expected to give data which reflects the absolute number of antigens on a cell surface, as if one gold particle were bound to one antigen; but immunoelectron microscopy can be effectively used to examine the distribution of cell surface antigen and in some cases to compare gold label densities on cells which have been experimentally manipulated. If large gold particles which might cause steric hinderance are utilized then alterations in surface antigen density may not be detectable using immunoelectron microscopy (fig. 6.1).

Figure 6.1: Diagram to illustrate the principle of Steric Hinderance.

a) Continous surface antigen labelled with antibody conjugated to small gold particles (left hand side) and large gold particles (right hand side). Due to steric hinderance the large gold particles do not allow one antigen to one antibody labelling.

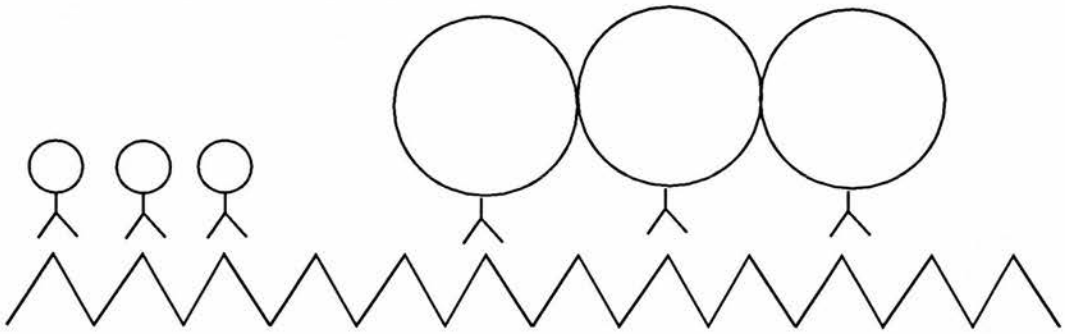

b) Discrete surface antigen labelled with antibody conjugated to small gold particles (left hand side) and large gold particles (right hand side). Here one antigen is labelled by one antibody despite the gold particle size differences.

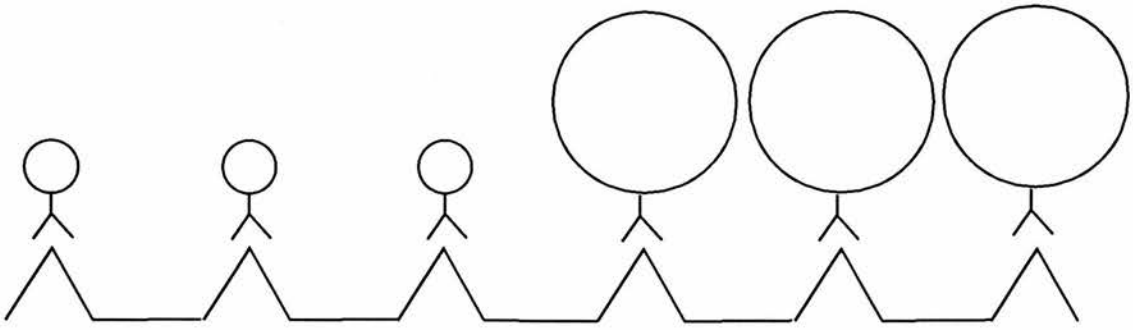

The mean density of immunogold-labelled surface antigen on entire cells can be estimated mathematically by approximating the cell to a sphere, assuming that one gold particle is bound to one antigen and that no steric hinderance is occurring. This was performed previously on B cell lines and panning-enriched LCs (Trucco *et al.*, 1980; Dezutter-Dambuyant *et al.*, 1984). Others have simply counted the number of gold particles on LC sections which were sectioned close to their mid-plane in order to get semi-quantitative data reflecting antigen density on cells labelled by immunogold electron microscopic techniques (Schmitt *et al.*, 1984; De Panfilis *et al.*, 1991).

A much quicker, but less sensitive method for examination of LC surface antigen expression would be to analyse the cells using a fluorescence-activated cell analyser. The fluorescence-activated cell analyser is less sensitive because it would be unlikely to detect the presence of LCs expressing no surface antigen and may not detect LCs expressing very low levels of surface antigen. Although it would have been interesting to compare the two techniques of immunoelectron microscopy and fluorescence-activated cell analysis, the limiting factor in this study was the amount of suction blister-derived epidermis volunteers were willing to donate.

Although the overall variation in expression of surface MHC II (HLA-DP,-DQ,-DR) antigens between different LCs was considerable due to small numbers of outlying values (see chapter 4, section 4.3), most cells expressed surface densities within a reasonably narrow range. Because of this and due to the scarcity of LCs in the irradiated EC suspensions, it was decided to examine five cells per subject in order to address the question of UV-induced alterations in surface MHC II antigens. However, the examination of such small numbers of cells may lead to sampling errors. It is therefore possible that the observed increases in LC surface antigen densities shown in chapter 5, section 5.3, were simply due to sampling error and that UVB-induced alterations in cell surface antigen expression may not be detectable using this methodology. However, the consistency with which this result was shown for all cell surface antigens examined (for a total of 45 CD1a+ve and 45 pan-MHC II+ve LCs both before and after irradiation, and for a total of 25 HLA-DP, 25 HLA-DQ, and 25 HLA-DR+ve LCs both before and after irradiation), may give us some confidence in the result.

No time-sequence studies were performed during the six week phototherapy course, but a sampling point at 48 hours after the last irradiation was chosen because it was consistent with a time point in which the nadir in reduction of human LC number occurred after a single dose of UVB (Koulu and Jansen, 1988). However, single doses

of UVB may have different influences on human skin when compared to multiple doses. In addition, it is possible that the timing of LC surface antigen modulation may precede the 48 hour time point after irradiation sampled here or may include other surface antigens than the MHC II and CD1a antigens studied here. However, at the 48 hour post irradiation time point, immunocytochemical techniques demonstrated that LC numbers were reduced to approximately 50% of pre-irradiation values. At this same time point, immunoelectron microscopic techniques were used to demonstrate increased levels of LC surface MHC and CD1a molecule expression. Therefore, the reduction in LC numbers shown at this time cannot be explained simply by a reduction or by the absence of LC surface MHC or CD1a expression.

6.3 Morphometric methods

Throughout this work there was an attempt to mimimize the sampling errors associated with the ultrastructural morphometric methods used. For example, the number of objects projected onto the observation plane is increased when the section thickness is larger. This is known as the Holmes effect (see figure 6.2). Therefore the estimation of surface density of objects, such as the gold label density determined on LCs in this project, may be biased if wide variations in section thickness exist. The thickness of an ultrathin section may be measured in several ways including the use of an interference microscope, measurement of folds in the section and direct measurement of re-sectioned sections.

Interference microscopy is reported to be the most accurate non-destructive method for precise measurement of ultrathin section thickness (Calverley *et al.*, 1988). The measurement of the width of folds in a section gives a value which should represent twice the section thickness (Small, 1968). The principle of the re-sectioned section method is to transversally resection sections embedded in resin and to measure the section profiles from electron micrographs (Phillips and Short, 1964). The demonstration (see chapter 3, section 3.3) that re-sectioned sections of pale-gold interference colour were relatively uniform in thickness confirms that errors relating to section thickness were minimal.

Figure 6.2: Holmes effect due to section thickness (after Weibel, 1979).

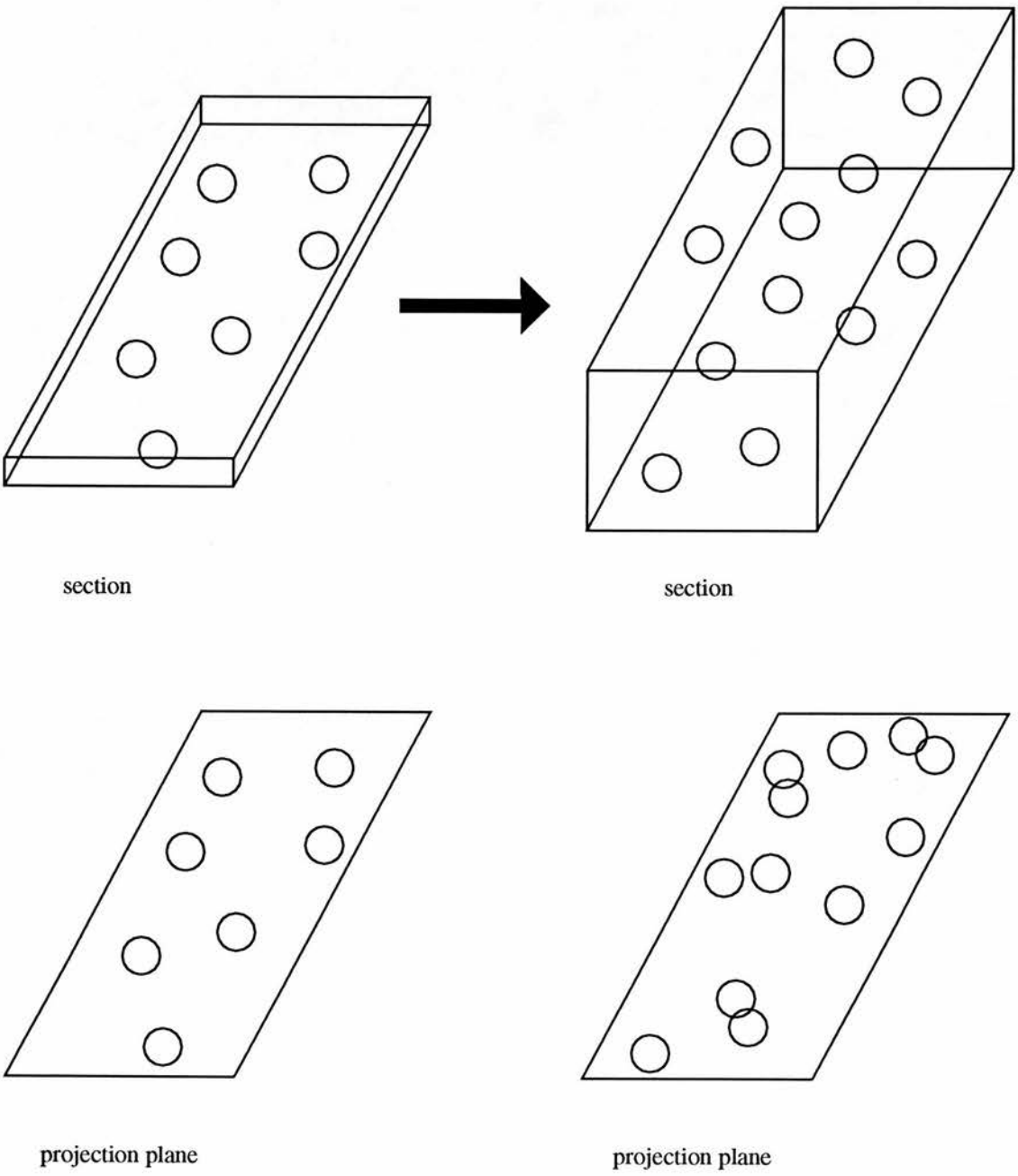

The sampling method for LCs and indeterminate cells in suspension was designed to obtain a random sample without cell size bias. Therefore, all LCs or indeterminate cells present in a section were photographed irrespective of whether they were partially obscured by bars of the grid on which the sections were collected. This prevents the size bias which may occur if measurements are taken only on cells with their entire cell perimeter visible, since cells not obscured by grid bars are likely to be smaller than those partially obscured by grid bars. However, measurements of label density were not made if the visible portion of the cell appeared to be less than a quarter of the cell perimeter.

The precise distribution of gold particles on the surface of single LCs and indeterminate cells was examined in order to determine whether the observed variations in label density reflected differences within or between cells. Firstly, the cell sections were divided into small portions (halves and quarters) and the gold label density on them was quantified. No significant differences in gold label density were detected between portions of a single section (see chapter 3, section 3.4). Secondly, a small number of individual cells (LCs and indeterminate cells in control samples, and LCs in UVB-irradiated samples) were repeatedly sectioned and the gold label density on these step-sections was measured. The gold label appeared to be evenly distributed over the cell surface (see chapter 3, section 3.5) and thus any one cell section or portion of a section (of approximately 1/4 cell perimeter or more) was considered to be representative of that cell concerning CD1a or MHC II density. It was concluded that any variation in surface label density on sections from separate LCs or indeterminate cells was due to differences in antigen expression between cells.

6.4 Image analysis

A high correlation, acceptable agreement and similar reproducibility were demonstrated between manual and image analysis methods for assessing gold particle densities on LC plasma membrane in the immunogold labelling experiments (see chapter 3, section 3.6). Because of this and because the semi-automatic image analysis method was faster than the manual one, which allowed the examination of a greater number of specimens and is therefore statistically advantageous, the image analysis system was adopted for all gold particle density measurements. The only exception was for the measurement of 15nm gold particles on DA6.231+ve unirradiated ECs, which were counted manually because the image analyser failed to count separate closely adjacent particles.

6.5 LC morphology.

LCs visualised *in situ* using light and electron microscopy have been shown to be dendritic cells which form a discontinuous network (Shelley and Juhlin, 1976; Yu *et al.*, 1992). The majority of work concerning LC morphology has been performed on chemically fixed and/or sectioned epidermal samples. Chemical fixation may cause tissue shrinkage and sectioning may cause mechanical damage.

Confocal laser scanning microscopy in conjunction with image analysis has been used to examine and quantify features relating to the morphology of both unirradiated LCs and UVB-irradiated LCs in epidermal samples which were not chemically fixed or sectioned. Although the epidermal samples used to study LC morphology by confocal laser scanning microscopy were suction blister-derived, similar results were obtained with epidermal samples taken by scalpel without anaesthetic (data not shown). This implies that the suction blister technique did not alter LC morphology.

The results described in this thesis are similar to those obtained in a previous confocal laser scanning microscopic study of the morphology of acetone-fixed LCs (Yu *et al.*, 1992). These authors described LCs as large cells with 5-7 long dendritic processes per cell which did not directly contact adjacent LCs. They measured the mean cell volume as 213 μm^3, and the mean cell density per unit volume as 1.6×10^5 cells/mm^3. The work presented in this thesis demonstrated that unirradiated LCs possess 2-9 dendrites which extended predominantly in the horizontal plane of the epidermis and only very occasionally contacted neighbouring LCs. A small proportion of the adjacent cells which did contact each other might have been dividing, since at least one interconnecting pair of LCs detected in this study were approximately spherical and were connected to each other by processes which were unusually broad and straight.

Another recent application of confocal microscopy was to quantify the total amount of CD1a label in control skin samples and in irritant contact dermatitis reactions (Scheynius *et al.*, 1992). Although a large decrease in the total epidermal CD1a reactivity was reported after exposure to 80% nonanoic acid, and small decreases after exposure to 2% or 4% sodium lauryl sulphate, no morphological comparisons were made between irritant-exposed and normal LCs.

UVB-induced morphological alterations to LCs have often been described (but not quantified) using immunohistochemical visualization of LCs and conventional light

microscopy. In one study, the majority of LCs were reported to disappear after exposure of murine skin to single doses of UVB or PUVA, due to UV-induced cell damage (Obata and Tagami, 1985). Although 20-30% of UVB-exposed LCs remained morphologically normal, others were considered to be ultrastructurally damaged and possessed swollen and ruptured mitochondria and lysosmes. More severely damaged LCs were highly vacuolar and contained pyknotic nuclei or nuclear fragments (Obata and Tagami, 1985). In direct contrast, little evidence of LC damage was observed after mice or guinea pigs received single exposures of low dose UVB (Humm and Cole, 1986; Hanau *et al.*, 1985) or after humans were exposed to summer sunlight (Zelickson and Mottaz, 1970). Furthermore, PUVA therapy or low doses of UVA or UVB caused a small proportion of human LCs to become round, vacuolar and damaged with cytoplasmic condensation but most remained morphologically unaltered (Aberer *et al.*, 1981, 1986; Friedmann *et al.*, 1983) and no ultrastructural evidence of LC death was observed *in situ* after PUVA therapy (Friedmann *et al.*, 1983). In one study, human LC dendrites were shorter after UVB or UVA irradiation (Koulu *et al.*, 1985). In another study, LCs were rounded with short dendrites at 48 hours after UVB irradiation, but thereafter LCs were enlarged with elongated dendrites (Humm and Cole, 1986). Similarly, irradiation of human skin with simulated sunlight or UVA caused a dimorphism of HLA-DR positive epidermal cells; some were extremely dendritic and large while others were small and rounded (Scheibner *et al.*, 1986; Liu *et al.*, 1987). In addition, giant LCs have been seen in the epidermis of patients undergoing bath PUVA therapy (Tjernlund and Juhlin, 1982). After UV exposure residual LCs appeared to have enlarged to a degree closely related to the extent of LC depletion, suggesting a process compensating for the LC loss (Obata and Tagami, 1985; Juhlin and Shelley, 1979 ; Koulu and Jansen, 1982). Quantification of various morphological parameters of normal and UVB-exposed LCs reconstructed in two dimensions was achieved in this study (see chapters 4 and 5, sections 4.2 and 5.2). In addition, qualitative images of LCs reconstructed in three dimensions were produced. Care must be exercised when interpreting data generated from LCs reconstructed in two dimensions, however, since dendrites or portions of them which extend exactly vertically through the epidermis or which lie immediately above or below the cell body may be indistinguishable.

The main UVB-evoked morphological alterations in LCs noted in the two-dimensional confocal laser scanning microscopy analysis performed in this study (see chapter 5, section 5.2), were reductions in the mean cell size, which was due to a reduction in the mean area occupied by dendrites per LC and a reduced mean number of dendrites per cell. However, following UVB exposure, some residual LCs retained fewer dendrites,

which were mainly shortened although some cells possessed one or two dendrites which were greatly attenuated. This was consistent with a decrease in median dendrite length and increase in range of dendrite length without significant alteration in mean dendrite length after UVB irradiation (see chapter 5, section 5.2). The biological significance of these findings is unclear, but it is possible that the cells with elongated dendrites might reflect a compensation for the UV-induced reduction in epidermal LC number. It is also possible that the LCs with attenuated dendrites are LCs which are in the process of emigrating from the epidermis, and this explanation would agree with the findings of others in which increased numbers of DCs were observed in the draining lymph nodes of UVB -irradiated mice (Moodycliffe *et al.*, 1992).

Six different types of ultrastructural morphology of LCs in suspension were evident, as described in chapter 5, section 5.2. In this study three types of morphology were of particular interest regarding UVB-induced LC alterations; Types IV, V and VI. The type IV LC morphology was exemplified by damage to the plasma membrane and/or damage within the cytoplasm. Since the question of low-dose UVB-induced damage to LCs is unresolved, it was interesting to note that there were very few LCs with this morphological type either before or after irradiation and no significant difference in the number of LCs with this morphological type after irradiation. It is possible that the experimental procedures necessary to produce EC suspensions were responsible for the cellular damage seen in LCs with type IV morphology. The LCs with type V morphology were exemplified by lack of surface microvilli, an unusual number of vacuoles and BGs, and clumped nuclear heterochromatin. These morphological features might imply that the cells are mitotic. Although mitosis has been noted previously after UVB irradiation (Miyauchi and Hashimoto, 1987; Bos, Teunissen, Kapsengerg, 1988), in this study the number of LCs with this morphological type was unaltered after UVB irradiation. However, LCs with the type VI morphology in EC suspensions, which were greatly elongated cells, were detected only after UVB irradiation. They may represent cells which were compensating for the reduction in LC numbers by extending enlarged dendrites and thus spanning greater areas of epidermis or perhaps the more likely explanation is that these LCs were emigrating from the epidermis. The ultrastructure of these cells suggests that they are identical to LCs with few but extremely long dendrites which were described using confocal laser scanning microscopy, but it is unclear whether the morphology of LCs in suspension bear any resemblance to that *in situ* . The trypsinization and lengthy processing entailed in the production of cell suspensions may cause morphological alterations.

There was little evidence of UVB-induced LC ultrastructural damage in this study. However, LC damage may be difficult to detect using the pre-embedding immunogold labelling technique on ECs in suspension, due to the epidermal disruption (trypsinization) required for production of cell suspensions. The lengthy processing of ECs involved in immunogold TEM preparation may reduce the chances of retaining damaged LCs in suspension, because they might be less dense than other ECs and therefore be erroneously discarded with changes of solution during these processing procedures. In a recent ultrastructural study of UVB-irradiated LCs *in situ*, in contrast to the findings reported here, significant LC damage was documented, although the expression of MHC II antigens on residual LCs was unaltered (Mommaas *et al.*, 1993)

6.6 LC and indeterminate cell surface expression of pan MHC II, HLA-DP,-DQ,-DR and CD1a antigens.

Using histochemical methods in conjunction with light microscopy or FACS analysis it has been observed by various authors that more ECs are labelled with anti-CD1a than anti-MHC II antibodies (Harrist *et al.*, 1983), or anti-HLA-DR antibodies (Scheibner *et al.*, 1986) or that there are three different subsets of human LCs which differ with respect to their surface expression of CD1a and HLA-DR (Czernielewski *et al.*, 1983). Others have claimed that similar numbers of LCs are detected by anti-CD1a, anti-HLA-DR, anti-HLA-DQ and anti-HLA-DP monoclonal antibodies in human skin or in oral mucosa (Sontheimer *et al.*, 1986; Crutchley *et al.*, 1989).

The numbers of LCs and indeterminate cells detected using an immunohistochemical method with anti-CD1a and anti-pan MHC II antibodies were similar (see chapter 4, section 4.1). However, fewer cells were detected by this immunohistochemical method with anti-HLA-DP, -DQ, and -DR antibodies than with anti- CD1a or anti-pan MHC II antibodies, and these differences were statistically significant. One possible explanation for this is that only certain proportions of LCs and indeterminate cells express the HLA-D subregion products, with a small proportion expressing HLA-DP and progressively larger proportions expressing HLA-DQ and HLA-DR.

Another possible explanation is that some LCs or indeterminate cells may have expressed levels of certain surface HLA-D molecules which were too low for detection using an immunoperoxidase labelling technique. This possibility was examined using the more sensitive quantitative ultrastructural immunogold labelling technique for measuring cell surface MHC II. The results given in chapter 4, section 4.3 indicate that most LCs and indeterminate cells express all three HLA-D subregion antigens,

although surface densities of the antigens may be very low. Therefore, it appears that most LCs and indeterminate cells constitutively express all three MHC II subregion products, and that differences in results obtained by different investigators may be due to variation in methodologies, antibodies or demonstration techniques.

Using the immunogold labelling technique it was shown that the majority of LCs and indeterminate cells expressed densities of MHC II antigens within a narrow range of values, but that small numbers of LCs and indeterminate cells were either especially densely labelled for HLA-DP,-DQ, or -DR antigens or were HLA-DP,-DQ, or -DR antigen negative. There were great differences between the least and the most densely-labelled cells (approaching 400 fold differences in the case of HLA-DP+ve LCs, see chapter 4, section 4.3, p101). This raises the possibility that subpopulations of MHC II positive cells exist on the basis of such phenotypic heterogeneity. Alternatively, the frequency distributions of HLA-DP, -DQ or -DR surface densities on LCs and indeterminate cells may be normal but greatly skewed. However, of two subjects in whom no epidermal labelling with anti-HLA-DQ antibody was demonstrated using an immunohistochemical technique, one was subsequently shown to possess LCs and indeterminate cells which expressed HLA-DQ antigens at extremely low surface densities by ultrastructural immunogold labelling. The other was shown to possess LCs and indeterminate cells which were completely HLA-DQ negative. The TU22 monoclonal antibody used to demonstrate HLA-DQ is haplotype specific, so one of nine subjects included in this study appears not to express the haplotype recognized by the antibody.

LCs and indeterminate cells exhibited a uniform distribution of MHC II over the whole cell surface before and after UVB irradiation. There have been few previous reports of the surface distribution of these antigens on ECs by TEM, perhaps because of the difficulty of producing semi-serial sections (step-sections) through single cells. These results agree with previous investigations using both TEM and scanning electron microscopy (Tadini *et al.*, 1988; De Panfilis *et al.*, 1988,1989).

There was no evidence in this study of either capping or clustering of low densities of MHC II antigens on ECs, as had been suggested previously using an immunofluorescence technique (Sontheimer *et al.*, 1986). There was also no evidence for aggregation of HLA-DR gold label on the cell surface of LCs or indeterminate cells, as has previously been demonstrated by TEM and an immunogold method on EDTA split skin *in situ* (Imayama *et al.*, 1992).

It has been suggested that HLA-DR+ve ECs, including LCs, may be divided into subsets expressing high or low levels of surface HLA-DR. Indeterminate cells were described as expressing uniformly high levels of this antigen (Dezutter-Dambuyant *et al.*, 1984). In this study, no differences in the densities of either pan MHC II, or HLA-DP, -DQ or -DR were noted between the LCs and indeterminate cells. This provides further evidence that indeterminate cells may be a sampling phenomenon in which LC sections which contain no BGs may be mistaken as a separate cell type (Bartosik, 1991).

The MHC II label density on unirradiated LCs and indeterminate cells reveals a greater density of pan MHC II antigens than the sum of the densities of surface HLA-DP,-DQ and -DR antigens. This may be because the anti-pan MHC II antibody (DA6.231) recognizes more than one determinant on the common core of the MHC II molecules, or that this antibody may have higher avidity than the other anti-MHC II antibodies used here.

In a study using ultracryomicrotomy and an immunogold labelling technique for the examination of pan-MHC II, HLA-DR and HLA-DQ expression by LCs in suspension, immunogold labelling of these molecules was present in cytoplasm, intracellular vesicles, and on LC surfaces (Vermeer *et al.*, 1988). The presence of intracellular HLA-DR and HLA-DQ molecules suggests that some degree of recycling of cell surface MHC II may occur in LCs. The LCs in suspension used in this study were lightly pre-fixed before antibody labelling, approximately one hour after removal from the subject and it is possible that some MHC II molecules may have been recycled from the cell membrane during the period of time before fixation. Recently, the same investigators used cryo-immunogold techniques to demonstrate surface LC MHC II labelling, albeit at low levels, which was mainly restricted to dendrites, but the majority of MHC II molecules were located within lysosomes and endosomes (Mommaas *et al.*, 1993; and personal communication, 1994). Therefore they concluded that LCs *in situ* do not constitutively express high levels of MHC II molecules. They suggested that the isolation of LCs into a suspension, a technique utilized in this study and one which is commonly used for LC immunogold labelling, might activate them even within 1 hour of isolation, thereby causing increased MHC II expression. This would explain the discrepancy between their results and those of others who have suggested that LCs do constitutively express high surface levels of MHC II. Whatever the explanation of this difference, it seems reasonable to assume that, providing the conditions of the preparation are kept constant, as in the study reported in this thesis, comparisons which have been made are valid.

6.7 LC subpopulations

The results reported in chapter 4, section 4.3 may be consistent with the suggestion that there is a subpopulation of densely-labelled HLA-DR+ve ECs (Dezutter-Dambuyant *et al.*, 1984). However, the densely-labelled HLA-DR+ve ECs detected in our study only constituted approximately 1% of HLA-DR+ve ECs, a much lower proportion than that described previously (which was reported as approximately 25% of HLA-DR+ve ECs; Dezutter-Dambuyant *et al.*, 1984). The densely-labelled HLA-DR+ve cells reported by Dezutter-Dambuyant and co-authors were detected by immunofluorescence and cells were directly counted or assessed by flow cytometry (Dezutter-Dambuyant *et al.*, 1984). Such methods are probably less sensitive for detecting cells expressing low levels of surface antigen than the ultrastructural immunogold method used here. Indeed, a spurious overestimate of densely-labelled HLA-DR+ve ECs might be expected when using immunofluorescence methods to detect HLA-DR+ve ECS, because cells expressing very low surface densities of HLA-DR antigen may be below the level of resolution of this method. There were also small numbers of densely-labelled HLA-DP and HLA-DQ+ve LCs and indeterminate cells and a small proportion of HLA-DP and HLA-DQ and HLA-DR-ve LCs and indeterminate cells. The results reported in this thesis are similar to those of a previous study in which a subpopulation of intensely MHC II+ve LCs were detected in murine epidermal sheets (Schuler *et al.*, 1985a). The question of whether the densely labelled HLA-DR+ve LCs also express high surface densities of HLA-DP and HLA-DQ has not been addressed in this study. This could be determined using a double or triple immunogold or immunofluorescence labelling technique, as has been described previously for various LC surface antigens (Dezutter-Dambuyant *et al.*, 1985; Sontheimer *et al.*, 1986; De Panfilis *et al.*, 1988).

Quantitative variation in MHC II expression may play a role in determining the functional ability of a cell during an immune response (Janeway *et al.*, 1984). DCs which constitutively express high levels of MHC II are the main APCs in spleen (Steinman and Nussenzweig, 1980), and quantitative variation in HLA-DR and HLA-DQ on plastic-adherent cells of the blood influences T cell activation (Nunez *et al.*, 1985). Moreover, macrophages which facultatively express Ia antigens become excellent APCs after they have been induced to express Ia antigens by co-culture with *Listeria* (Unanue, 1981). It is possible that the epidermal LCs with high densities of surface MHC II described in this thesis might comprise a functionally distinct subset with an increased ability to present antigen to T cells.

Certain functional and phenotypic alterations have been demonstrated after short-term culture of LCs; these include loss of the Fc gamma receptor type II and BGs, and increased expression of surface MHC I, MHC II, ICAM-1 and LFA-3 (Witmer-Pack *et al.*, 1988; Teunissen *et al.*, 1990, 1991). These changes are considered to be similar to those occurring when LCs "mature" into potent APCs after migration from the epidermis into draining lymph nodes (Romani *et al.*, 1989). In general, cultured human and murine LCs are much more efficient than freshly prepared LCs in the generation of primary allogeneic or autologous T cell proliferation, in the presentation of haptens to antigen-specific T cells, and the presentation of peptides to T cell hybridomas (Inaba *et al.*, 1986; Picut *et al.*, 1988; Demidem *et al.*, 1991). Furthermore, the enhanced presentation of the antigen TNP by cultured LCs was accompanied by increased expression of MHC II which could be abrogated by treatment with UVR or cyclohexamide (Shimada *et al.*, 1987). Therefore, increased MHC II expression by cultured LCs may be accompanied by an increased ability to present antigen to primed T cells.

Evidence suggests that resident or freshly isolated LCs represent a phenotypically heterogeneous cell population. Thus, approximately 70% of CD1a+ve ECs contained CD1a mRNA and 70% expressed the low affinity receptor for the Fc portion of IgG. Other subgroups of LCs have been distinguished by their ability to take up L-DOPA (Warfvinge *et al.*, 1991), by their lectin binding profiles (Schuler *et al.*, 1983; Nakamura *et al.*, 1990) and by their cell surface expression of CD23, the low affinity receptor for the Fc portion of IgE (Torresani *et al.*, 1991), CD45RA, an antigen associated with suppressor-inducer capabilities, (De Panfilis *et al.*, 1990b), CD32, the low affinity receptor for the Fc portion of IgG (Schmitt *et al.*, 1992), and CD36, a receptor for thrombospondin and collagen (Taylor *et al.*, 1991). Additional heterogeneity may exist with respect to LC morphology, as described in section 6.3. Recently two types of LC have been distinguished within murine epidermis. These LC types differed with respect to their ultrastructural morphology: type II was shown to possess BGs within the perinuclear space, whilst type I was devoid of BGs in this intracellular area. Type II LCs differed from type I LCs in that they included more rough and smooth endoplasmic reticulum, endosomes, ribosomes and mitochondria, and were more dendritic than type I LCs (Karas *et al.*, 1992).

It is not known whether the phenotypic heterogeneity of LCs which was noted here is due to the existence of genuine subpopulations of LCs, or whether such differences might simply correlate with particular stages of the cell cycle or state of cell activation (Aiba and Katz,1990).

6.8 UVB-induced LC depletion.

The therapeutic doses of UVB used in this study depleted immunoperoxidase-labelled CD1a, pan MHC II, HLA-DR, HLA-DP, and HLA-DQ+ve ECs. The percentage decrease in CD1a+ve and pan MHC II+ve LC number at 48 hours after the last irradiation ranged from between 31 and 68%, and was on average 49% for CD1a+ve cells and 55% for pan MHC II+ve cells. For each subject the percentage LC depletion was similar, irrespective of the antibody used to demonstrate them. An exception to this was a rise in number of immunoperoxidase-labelled HLA-DQ+ve ECs in one subject after UVB irradiation. This was due to an inability to detect any HLA-DQ+ve ECs prior to UVB irradiation using the immunoperoxidase labelling technique, because of their unusually low surface expression of HLA-DQ antigen which was below the level of resolution by the immunoperoxidase labelling method. The presence of HLA-DQ antigen (albeit at low levels) on these ECs was subsequently demonstrated using the more sensitive immunogold labelling method. After UVB irradiation, however, the levels of surface HLA-DQ expression appeared to have increased to the level at which they could be demonstrated using the immunoperoxidase labelling technique. Thus, the results gave the spurious impression of increased numbers of HLA-DQ+ve ECs.

There was considerable variation in the percentage drop in LC numbers after irradiation between different subjects. This was found to be weakly correlated to the total dose of UVB received when measured in MEDs, but was not correlated to the total number of Joules/cm^2 of UVB that a subject had received (see chapter5, section 5.3).

These results confirm the well-documented LC depletion after irradiation with high and low dose UVB, UVA, PUVA and sunlight (Zelickson and Mottaz, 1970; Toews, Bergstresser, and Streilein, 1980b; Lynch *et al.*, 1981; Hanau *et al.*, 1985; Koulu *et al.*, 1985; Hum and Cole, 1986; Liu *et al.*, 1987; Scheibner *et al.*, 1987; Koulu and Jansen, 1988). However, these results are in variance with the reported increase in MHC II+ve LCs in mice after UV irradiation (Nordlund *et al.*, 1981). The MHC II+ve ECs in Nordlund's study were presumed to be LCs, however this may have been an erroneous assumption in UV-irradiated skin since the MHC II+ve ECs may have included other MHC II+ve UVB-induced APCs.

It is plausible that the reductions of immunoperoxidase-labelled EC numbers noted in this study were due to reduced surface expression of all five antigens on LCs and indeterminate cells, and that the reductions were of a similar magnitude. However, a

more plausible explanation for the data is that a reduction in LC number had occurred and not a reduction of surface antigen on LCs which had remained in the epidermis.

Two methods were used to count LCs in this project. One method involved the quantification of immunoperoxidase labelled LCs in epidermal sections. All labelled cells with cell bodies in the section (the presence of dendrites was ignored) were counted and expressed per mm basal cell plasma membrane. The other method involved counting fluorescence labelled CD1a+ve LCs in five low power fields of epidermal sheets, visualized by confocal laser scanning microscopy. These two methods gave similar results since the percentage reduction in LC number in vertical epidermal sections paralleled the percentage reduction in CD1a+ve LC number in epidermal sheets and the percentage reduction of total CD1a +ve fluorescence label after UVB irradiation.

The cause of the decrease in epidermal LC number after the therapeutic UVB treatment reported here is not clear. The possibilities include alteration in LC surface antigen expression, LC damage or death, and LC migration from the epidermis. In this study, little evidence of UVB-induced LC damage or death was obtained (see section 6.3). In some experimental systems the doses of UVB required to cause immunosuppression have been shown to be cytotoxic, whilst in others this has not been the case. For example, doses of UVR which can suppress the mixed skin cell lymphocyte reaction of human ECs *in vitro* appear not to be cytotoxic (Czernielewski *et al.*, 1984), but fluences of UVB which suppress immune responses initiated by murine LCs and which decrease LC expression of ICAM-1 *in vivo* are cytotoxic to LCs *in vitro* (Tang and Udey, 1992). Whether such doses of UVB administered to LCs *in vitro* are similar to UVB doses reaching LCs *in vivo* has not been established.

An increase in murine DCs has been noted in draining lymph nodes at 42 and 66 hours after exposure to single doses of UVB. This provides evidence of LC migration from the epidermis to draining lymph nodes after UVB exposure. The migration appeared to occur mainly between 12 and 48 hours after irradiation. The mean intensity of Ia labelling per cell, however, was unaltered throughout the experiment (Moodycliffe *et al.*, 1992). Therefore, some evidence exists that UVB may cause LC emigration from the epidermis in the murine model of UVB-induced immunosuppression. This may be the cause of the reduction in epidermal LC number after irradiation with UVB. However, the examination of DCs in draining lymph nodes after UVB irradiation has revealed surface antigen profiles which may not be consistent with an epidermal origin

and imply that these DCs might have been macrophages rather than LCs (Kripke *et al.*, 1992).

6.9 UVB-induced alterations in LC and KC surface antigen expression.

Residual epidermal LCs after UVB phototherapy have been shown in this study to express increased surface densities of MHC II and CD1a antigens. The mean increase in LC surface expression of either HLA-DP, -DQ or -DR after UVB treatment approached ten times in some subjects. There was no consistent pattern with respect to the magnitude of these increases in expression of CD1a or HLA-D subregion products. These results are in contrast with those of other investigators who have demonstrated using fluorescence-activated cell analysis and immunoelectron microscopy that no changes in surface marker expression or ability to present antigen per LC occurred after PUVA or UVB therapy was administered to healthy human volunteers (Ashworth *et al.*, 1989b; Mommaas *et al.*, 1993).

The reasons for the observed increases in LC surface MHC II and CD1a molecule expression are unclear, but include:

1) The influence of cytokines produced in the epidermis as a result of UVB irradiation, such as T cell-derived γ-IFN as a result of minimal inflammation, or EC-derived GM-CSF and TNF-α. All of these cytokines may regulate the expression of MHC II (see section 6.10) and might have caused increased MHC II and CD1a expression on residual LCs.

2) The doses of UVB irradiation used in these studies may cause total LC depletion, and then lead to subsequent replacement by LCs which have recently migrated into the epidermis and which express higher surface densities of MHC II and CD1a antigens.

3) UVB irradiation may cause partial LC depletion, perhaps mainly depleting those cells which express low surface densities of MHC II and CD1a antigens. If this occurred, there would be a group of residual LCs expressing higher surface antigen densities.

4) Since the numbers of LCs examined per subject were low, the observed increases in MHC II and CD1a molecule expression may simply be due to sampling errors (see section 6.9).

Other investigators have noted increased intensity of fluorescence label on human CD1a+ve or murine MHC II+ve LCs after irradiation with UV which may have been due to increased expression of surface antigen (Nordlund *et al.*, 1981; Scheibner *et al.*, 1987). However, the only other previous attempts to quantify LC MHC II expression are reported in two recent studies by Mommaas' group, one of which reported no alteration in MHC II antigen expression by long-term UVB-irradiated LCs *in situ* examined using a post-embedding ultracryomicrotomy technique. They reported a decrease in the mixed epidermal cell -lymphocyte reaction by irradiated ECs, but no alteration in number of LCs or MHC II expression on LCs after irradiation. It is interesting that these investigators did not examine the intercellular variation in expression of MHC II or state the number of LCs examined by ultracryomicrotomy, and therefore the validity of the conclusions they draw may be questionable (Mommaas *et al.*, 1993; Van Praag *et al.*,1994).

The functional implications of an increase in MHC II expression by UVB-irradiated LCs are unclear. Increased expression of MHC II and CD1a antigens by residual LCs, however, may be accompanied by an increased ability to present antigen to T cells, which might be compensating to some extent for their depletion. In a previous study, presentation of HSV antigen *in vitro* by UVB-irradiated ECs was impaired when compared to normal ECs (Gilmour *et al.*, 1993). However, this probably simply reflects a UV-induced depletion in number of LCs. It would be possible to assess the antigen presentation of UVB-irradiated LCs on a per cell basis if the LCs were separated out of EC suspension either by antibody panning, centrifugation techniques, magnetic beads or by using FACS. Although this is a theoretical possibility, the total number of ECs needed in order to separate out the required number of LCs for functional analyses would be large. Although this may be feasible in animal experiments, it may be difficult to persuade human volunteers to participate in such an experiment.

It would also be interesting to assess the adhesiveness of UV-irradiated and control LCs to T cells by looking at their ability to form clusters with T cells *in vitro,* although this has not been addressed here. The expression of LC surface ICAM-1 appears to be decreased after low-dose UVB irradiation, but it is unknown whether UVB irradiation may also influence LFA-3 and B7 expression. The surface expression of these antigens may influence the way in which LCs can adhere to T cells during antigen presentation.

The reason for examining the expression of CD1a antigens in this study was to provide a control antigen for any observed changes in MHC II expression. CD1a was chosen because it shows considerable homology with MHC I and is considered to be similar to MHC I. Since there is no evidence for alteration in MHC I antigen expression by UVR, anti-CD1a was believed to be an appropriate control antibody. Any alterations in expression of both CD1a and MHC II antigens, might represent non-specific findings. However, CD1 molecules may be involved in the interaction between certain T cells and accessory cells via the TCR-CD3 complex. For example, the mixed epidermal cell lymphocyte reaction was inhibited by the use of anti-CD1a antibodies (Moulon *et al.*, 1991). Furthermore, the CD1 molecule was induced on monocytes by GM-CSF (Kasinrerk *et al.*, 1993). In view of this, the observed increase in expression of both CD1a and MHC II after UVB phototherapy (chapter 5, section 5.3) might be expected since GM-CSF is induced by UVB irradiation and might be of some functional significance. With the benefit of hindsight, therefore, a more appropriate control antibody would be one directed against MHC I molecules.

Others have described the retention of HLA-DR and CD1a antigens by human ECs after *in vitro* UVB exposure using FACs analysis of surface antigens (Czernielewski *et al.*, 1984). PUVA therapy resulted in depletion of epidermal LCs and reduction of the alloantigen-presenting capacity of the ECs derived from PUVA treated skin. The residual LCs from PUVA treated epidermis, however, retained normal fluorescence labelling with anti-CD1a and anti-HLA-DR antibodies and retained *in vitro* alloantigen-presenting function on a per-cell basis (Ashworth *et al.*, 1989b).

A decreased expression of some LC surface antigens has been reported after UV irradiation, such as ATPase activity and the expression of the S-100 protein (Schneider *et al.*, 1985; Humm and Cole, 1987; Koulu and Jansen, 1988). In the murine model, UVB irradiation may lead to decreased expression of surface adhesion molecules, ICAM-1 on LCs and accessory cells of peripheral blood (Krutmann *et al.*, 1990; Tang and Udey, 1991).

Most unirradiated keratinocytes were CD1a and MHC II negative, although occasional keratinocytes of the sweat gland acrosyringium were MHC II positive. However, after UVB irradiation some keratinocytes expressed MHC II but did not appear to be acrosyringeal cells, although this possibility could not be excluded. Murine and human MHC II+ve keratinocytes are unable to induce primary allogeneic T cell responses or to present antigens such as ovalbumin, hen egg lysozyme, pigeon cytochrome C or PPD to CD4+ve T cells (Gaspari, Jenkins and Katz, 1988; Niederweisser *et al.*, 1988; Bal *et*

al., 1990). However MHC II+ve keratinocytes may induce antigen-specific unresponsiveness or clonal anergy. It has recently been demonstrated that MHC II+ve keratinocytes may present *Mycobacterium leprae* to antigen specific CD4+ve T cells and cause antigen-driven T cell proliferation (Mutis *et al.*, 1993). Therefore, it is unclear whether the MHC II+ve keratinocytes noted here after UVB irradiation may play a functional role in immunosuppression by inducing clonal anergy, or whether they may compensate for the loss of LCs by assuming APC function to CD4+ve T cells.

A small number of CD1a-ve dendritic cells were detected in the EC suspensions after UVB irradiation (see chapter 5, section 5.3), although none were found in the unirradiated EC samples. The CD1a-ve dendritic cells in UVB-irradiated epidermal samples were detected in small numbers and appeared similar in ultrastructure to either lymphoid cells or to cells of the macrophage/dendritic cell lineage. They did not contain BGs or melanosomes, but contained lysosomes (their ultrastructure was relatively indeterminate). These CD1a-ve dendritic cells may correspond to the CD1a-ve, OKM5+ve ECs previously described in human skin after UVB and UVA irradiation (Cooper *et al.*, 1986, 1992; Scheibner *et al.*, 1986; Liu *et al.*, 1987). Such CD1a-ve cells, which appeared after UVB irradiation, were reported to be HLA-DR+ve and HLA-DQ+ve and to contain numerous melanosomes, lysosomes, lipid bodies but no keratin, premelanosomes or BGs. Furthermore, CD1a-ve cells made up approximately 4% of UVB-exposed ECs whereas LCs made up 0.6% of UVB-exposed ECs (Cooper *et al.*, 1992). The differences in number and ultrastructure of the CD1a-ve cells described in this study (chapter 5, section 5.3) and those reported by Cooper *et al.* may be due to widely differing experimental UVB regimens or due to different sampling times after cessation of irradiation: they used single 4 MED doses of UV and took epidermal samples 72 hours later, whereas subjects in this study received suberythemal doses and samples were taken 48 hours after irradiation. Since the peak in numbers of CD1a-ve, HLA-DR+ve cells was reported to occur on the 4th day after irradiation of human epidermis with UVA, the sample point used in this study may have been too early to have detected them in the same proportions (Liu *et al.*, 1987). A further study indicated that erythemogenic UVB doses may be more likely to induce epidermal OKM5+ve, CD1a-ve macrophages than suberythemogenic UVB doses (Cooper *et al.*, 1992).

6.10 The regulation of MHC II expression.

It is probable that the factors which result in altered expression of LC MHC II after UVB-irradiation include cytokines and prostaglandins released by ECs (TNF-α, TGF-α , GM-CSF, PGE), and T cells (γ-IFN). TNF-α may enhance MHC II expression on LCs and act synergistically with γ-IFN for MHC II induction on monocytes (Chang and Lee, 1986; Belsito *et al.*, 1989). In this study (see chapter 5, section 5.4), three of four subjects in which TNF-α was measured showed increased levels of this cytokine during UVB treatment (Gilmour *et al.*, 1993).

GM-CSF may increase MHC II expression on LCs and macrophages (Willman *et al.*, 1989; Belsito *et al.*, 1989). It has been demonstrated that the production of GM-CSF by cultured keratinocytes may be induced by UVB exposure (Matsue *et al.*, 1992). TGF-β, on the other hand, may prevent the induction of MHC II on LCs by γ-IFN or other cytokines although it was shown to have no effect on the constitutive expression of MHC II by LCs (Epstein *et al.*, 1991). In addition, prostaglandin E may suppress the expression of MHC II (Warren and Vogel, 1985).

Table 6.1 Factors regulating MHC II expression (Fabre, 1991).

factors	examples
cytokines	IFN α, β, γ.
	IL-4
	GM-CSF
	TNF-α,β
	Epidermal growth factor
	TGF-α,β1
hormones	thyroid stimulating hormone
	corticosteroids
viruses	neurotropic murine hepatitis virus (JHM)
non-specific cell activators	phorbol esters
prostaglandins of the E series	PGE

Human keratinocytes were induced to synthesize and express MHC II after incubation *in vitro* with γ-IFN (Basham *et al.*, 1984; Griffiths *et al.*, 1989). The differential

induction of MHC II subregion product expression on various cells by γ-IFN has been well-documented. For example, the expression of HLA-DR in greater amounts than either HLA-DP or -DQ has been shown to occur on keratinocytes in lesional skin of inflammatory dermatoses and was thought to be induced by γ-IFN (Gawkrodger *et al.*, 1987). In addition, eight of eleven patients with cutaneous T cell lymphoma and three of eleven patients with lichen planus demonstrated keratinocyte expression of HLA-DR and HLA-DQ which was presumably induced by T cell-derived γ-IFN (Volc-Platzer *et al.*, 1987). The expression of HLA-DR and HLA-DP but not HLA-DQ antigens was induced on amniotic fluid cells and on dermal fibroblasts by culturing in the presence of γ-IFN (Geppert and Lipsky, 1985; Maurer *et al.*, 1987). In contrast, the induction of HLA-DQ by γ–IFN was reported on melanocytes and on monocytes which were previously HLA-DQ-ve (Basham *et al.*, 1984; Tsujisaki *et al.*; 1987).

The expression of MHC II on LCs may also be increased after culture with cytokines such as γ-IFN (Belsito *et al.*, 1989). Enriched human LCs in suspension were induced to express higher levels of HLA-DR molecules but not HLA-DQ or CD1a molecules after incubation for 24 hours with γ-IFN (Schmitt *et al.*, 1987).

It has also been shown that *cis*-UCA may also modulate MHC II expression. Decreased numbers of HLA-DR+ve ECs and decreased expression of HLA-DR on the surface of peripheral blood monocytes were noted after incubation with *cis*-UCA *in vitro* (Rasanen *et al.*, 1989). The percentages of *cis*-UCA in both epidermis and suction blister fluid of four subjects in this study were shown to be increased during the course of UVB irradiation (see chapter 5, section 5.4; Gilmour *et al.*, 1993).

Altered LC surface expression of MHC II may also occur after exposure to contact allergens *in vivo*. DCs isolated from draining lymph nodes 18 hours after application of FITC to murine skin displayed signs of cellular activation and internalization of MHC II (Bucana *et al.* 1992). Murine LCs have also been shown to internalize MHC II after application of DNCB, DNFB, oxazolone and $K_2Cr_2O_7$ and displayed simultaneous reductions in surface MHC II (Becker *et al.*, 1992). Therefore, antigen processing or presentation may be associated with internalization of MHC II and thus decreased cell surface MHC II.

The influence of UVB-induced factors within the epidermis on LC MHC II expression may be difficult to establish, since the effects of these factors is usually dependent upon their concentration and interaction with other factors. However, a combination of

factors may be responsible for the observed increase in MHC II on LCs and the induction of MHC II on keratinocytes following UV exposure.

6.11 Mechanisms involved in UVB-induced immunosuppression.

There are various ways in which UVB is thought to exert its immunosuppressive effects (a model is given in fig. 6.3). In the outermost layers of the epidermis urocanic acid absorbs UVB and transforms from the *trans*- to the *cis*-isomer. The subsequent binding of *cis*-urocanic acid to histamine-like receptors may lead to a local release of cytokines. In addition, UVB can induce the synthesis of various keratinocyte mediators such as IL-1, IL-3, IL-6, IL-10 and TNF-α. UVB may also generate free radicals (such as the superoxide anion) which have been implicated in the generation of "sunburn cells" (damaged keratinocytes), and in the depletion and morphological alteration of epidermal LCs. The peroxidation of EC membrane lipids by free radicals can result in the release of prostaglandins and other inflammatory mediators, and lead to leucocyte infiltration.

TNF-α appears to induce LC emigration leading to suppression of the induction of the CHS response by a mechanism which is independant of *cis*-UCA induced immunosuppression (Moodycliffe *et al.*, 1994). This changes antigen presentation either by LCs which have been functionally altered, or through presentation by alternative APCs, or possibly by a combination of both events which results in the suppression of cell-mediated immune responses.

Figure 6.3: Model of The Mechanisms of UVB-induced Immunosuppression.

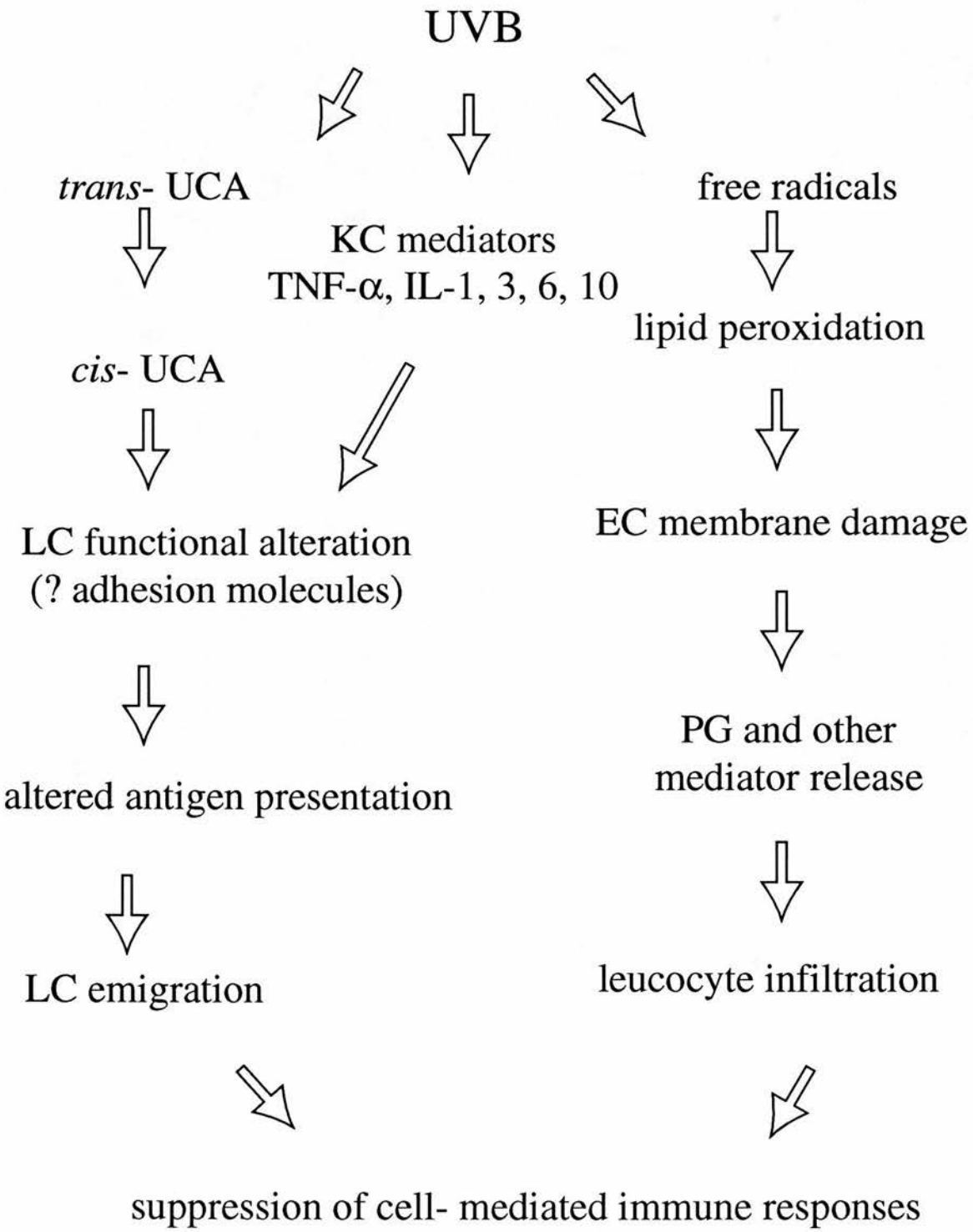

6.12 Conclusions and areas in which this work might be extended.

Conclusions:

In conclusion, the studies described in this thesis have:

1) clarified the normal expression of MHC II and CD1a on both single LCs and between many LCs from an individual: both CD1a and MHC II antigens were evenly distributed over the surface of single cells, but wide ranges of antigen densities were noted between cells from an individual.

2) defined the influence of therapeutic UVB irradiation on LC morphology: LCs were generally less dendritic after irradiation, but a small proportion of LCs possessed elongated dendrites and may have been emigrating from the epidermis.

3) defined the influence of therapeutic UVB irradiation on LC numbers: The number of LCs was decreased to approximately 50% of the number prior to irradiation, irrespective of the antibody used to demonstrate them.

4) defined the influence of therapeutic UVB irradiation on LC surface antigen expression: residual LCs at 48 hours after the final UVB irradiation diplayed increased surface densities of CD1a and MHC II antigens.

Therefore, a six week course of suberythemal, therapeutic UVB irradiation resulted in a genuine reduction in the number of epidermal LCs, which were mainly rounded and no longer dendritic. This LC depletion could not be explained merely by the loss of LC surface MHC II or CD1a antigen expression. This result implies that moderate, suberythemal doses of UVB irradiation experienced over a six week period, in similar doses to those one might expect to receive during British spring or summertime and which produce little visible evidence of epidermal alteration, cause significant reductions in number of epidermal LCs. This could have profound effects on the ability of the skin to respond to potentially harmful antigens which are encountered there for the first time,whether the antigen be endogenous or exogenous. This therapeutic UVB regimen is given to many patients suffering from skin diseases, particularly to those suffering from psoriasis and eczema. These results imply that it would be wise to limit the use of phototherapy as far as possible, and to monitor patients who are receiving phototherapy regularly for signs of cutaneous carcinogenesis.

Areas in which this work might be extended:

A number of questions regarding UVB-induced immunomodulation remain unresolved and deserve further attention, and these include:

1) The question of whether human LC damage or death occurs in response to moderate doses of UVB irradiation is unresolved. It would be interesting to compare both the general ultrastructural features and the DNA of LCs before and after exposure to suberythemal doses of UVB. For example, membrane alterations could be assessed ultrastructurally, DNA damage in the form of thymidine dimers (which are implicated in UV-induced LC damge) could be assessed by calculating the number of endonuclease-sensitive sites in LCs derived from irradiated skin (Wolf *et al.*, 1993; Schothorst *et al.*, 1991)

2) It would be interesting to examine the effect of UVB, in similar fluences to those used in this study, on the quantitative expression of other LC surface antigens, such as the accessory / adhesion molecules ICAM-1, LFA-3 and B7. Since there is evidence that reduced expression of ICAM-1 may play a role in the low-dose UVB-induced suppression of immune reponses in murine and human epidermis (Simon *et al.*, 1992), this may also be important in the human response to UVB irradiation in therapeutic doses.

3) Some evidence for UVB-induced alterations in antigen presentation by human ECs has already been demonstrated (Gilmour *et al.*, 1993). Comparisons of the ability of human LCs to process and present antigens on a per cell basis or to form T cell clusters *in vitro* (which is an indication of their adhesive properties and may reflect alterations in surface expression of ICAM-1, LFA-3 or B7) before and after moderate doses of UVB irradiation *in vivo* might yield further information regarding the underlying mechanisms of UVB-evoked immunosuppression in humans.

4) A logical continuation of these studies would be to examine the human epidermal and dermal expression of TNF-α, GM-CSF, IFN-γ, TGF-β, PGE and *cis*-UCA before, during and after UVB exposure by immunohistochemical methods and also to examine the transcription of those genes using *in situ* hybridisation techniques. In addition, the effects of these factors could be determined both singly and in combination on MHC II and CD1a expression on LCs *in vitro* using FACS analysis in order to establish the time-course and dose-response curves for the UVB-evoked increased expression of LC surface antigens.

5) The influence of therapeutic doses of UVB irradiation on LC numbers, surface antigen expression and function in patients who receive phototherapy with various skin diseases is not very clear. This information may determine whether immune dysfunctions in patients occur as a result of therapeutic UVB exposure.

REFERENCES

Aberer W., Schuler G., Stingl G., Honigsmann H., Wolff K. Ultraviolet light depletes surface markers of Langerhans cells. J. Invest. Dermatol. 1981; 76: 202-210.

Aberer W., Romani N., Elbe A., Stingl G. Effects of physicochemical agents on murine epidermal Langerhans cells and Thy-1-positive dendritic epidermal cells. J. Immunol. 1986; 136: 1210-1216.

Aiba S., Katz S.I. Phenotypic and functional characteristics of *in vivo*-activated Langerhans cells. J. Immunol. 1990; 145: 2791-2796.

Anderson R.R., Parrish J.A. The optics of human skin. J. Invest. Dermatol. 1981; 77: 13-19.

Ansel J.C., Luger T.A., Green I. The effect of *in vitro* and *in vivo* UV irradiation on the production of ETAF activity by human and murine keratinocytes. J. Invest. Dermatol. 1983; 81: 519-523.

Aprile J.A., Deeg H.J., Castner T., Miller L., Storb R. Impaired expression of class-II antigens on canine dendritic cells following ultraviolet irradiation. Exp. Haematol. 1987; 15: 452.

Ashworth J.A., Kahan M.C., Breathnach S.M. Flow cytometrically-sorted residual HLA-DR+ T6+ Langerhans cells in topical steroid-treated human skin express normal amounts of HLA-DR and CD1a/T6 antigens and exhibit normal alloantigen-presenting capacity. J. Invest. Dermatol. 1989a; 92: 258-262.

Ashworth J.A., Kahan M.C., Breathnach S.M. PUVA therapy decreases HLA-DR+CD1a+ Langerhans cells and epidermal antigen-presenting capacity in human skin, but flow cytometrically-sorted residual HLA-DR+CD1a+ Langerhans cells exhibit normal alloantigen-presenting function. Br. J. Dermatol. 1989b; 120: 329-339.

Aubock J., Romani N., Grubauer G., Fritsch P. HLA-DR expression on keratinocytes is a common feature of diseased skin. Br. J. Dermatol. 1986; 114: 465-472.

Azizi E., Bucana C., Goldberg L., Kripke M.L. Perturbation of epidermal Langerhans cells in basal cell carcinoma. Am. J. Dermatopathol. 1987; 9: 465-473.

Baadsgaard O., Wulf H.C., Wantzin G.L., Cooper K.D. UVB and UVC, but not UVA potently induce the appearance of T6-DR+ antigen-presenting cells in human epidermis. J. Invest. Dermatol. 1987a; 89:113-118.

Baadsgaard O., Cooper K.D., Lisby S., Wulf H.C., Wantzin G.L. Dose response and time course for induction of T6-DR+ human epidermal antigen-presenting cells by *in vivo* ultraviolet A,B, and C irradiation. J. Amer. Acad. Dermatol. 1987b; 17; 792-800.

Baadsgaard O., Fox D.A., Cooper K.D. Human epidermal cells from ultraviolet light-exposed skin preferentially activate autoreactive CD4+ 2H4+ suppressor-inducer lymphocytes and CD8+ suppressor/cytotoxic lymphocytes. J. Immunol. 1988; 140: 1738-1744.

Baadsgaard O., Salvo B., Mannie A., Dass B., Fox D.A., Cooper K.D. *In vivo* ultraviolet -exposed human epidermal cells activate T suppressor cell pathways that involve CD4+ CD45 RA+ suppressor-inducer T cells and Thy-1+ epidermal cells. J. Immunol. 1990; 145: 2845-2861.

Baadsgaard O. *In vivo* ultraviolet irradiation of human skin results in profound perturbation of the immune system. Arch. Dermatol. 1991; 127: 99-109.

Bachem A., Reed C.I. Penetration of ultraviolet light through human skin. Arch. Physical Therapy 1930; 11: 49-56.

Baden H.P., Pathak M.A. The metabolism and function of urocanic acid in skin. J. Invest. Dermatol. 1967; 48: 11-17.

Bal V., McIndoe A., Denton G., Hudson D., Lombardi G., Lamb J., Lechler R. Antigen presentation by keratinocytes induces tolerance in human T cells. Eur. J. Immunol. 1990; 20: 1893-1897.

Balfour B.M., Drexhage H.A., Kamperdijk E.W.A.. Hoefsmit E.Ch.M. Antigen-presenting cells, including Langerhans cells, veiled cells and interdigitating cells. Microenvironment in haemopoietic and lymphoid differentiation. London: Pitman Medical. (Ciba Foundatio n Symposium 84) 1981; pp281-311.

Balk S.P., Ebert E.C., Blumenthal R.L., McDermott F.V., Wucherpfennig K.W., Landau S.B., Blumberg R.S. Oligoclonal expansion and CD1 recognition by human intestinal intra-epithelial lymphocytes. Science 1991; 253: 1411.

Barker J.N., Ophir J., MacDonald D.M. Products of class II major histocompatibility complex gene subregions are differentially expressed on keratinocytes in cutaneous diseases. J. Amer. Acad. Dermatol. 1988; 19: 667-672.

Bartosik J. The non-keratinocytes of normal human skin. Eur. J. Dermatol. 1991; 1: 131-134.

Bartosik J. Cytomembrane-derived Birbeck granules transport horseradish peroxidase to the endosomal compartment in the human Langerhans cells. J. Invest. Dermatol. 1992; 99: 53-58.

Basham T.Y., Nickoloff B.J., Merigan T.C., Morhenn V.B. Recombinant gamma interferon induces HLA-DR expression on cultured human keratinocytes. J. Invest. Dermatol. 1984; 83: 88-90.

Becker D., Neiss U., Neis S., Reske K., Knop J. Contact allergens modulate the expression of MHC class II molecules on murine epidermal Langerhans cells by endocytotic mechanisms. J. Invest. Dermatol. 1992; 98: 700-705.

Beller D.I., Unanue E.R. Regulation of macrophage populations. II. Synthesis and expression of Ia antigens by peritoneal exudate macrophages is a transient event. J. Immunol. 1981: 126: 263-269.

Belsito D.V., Epstein S.P., Schultz J.M., Baer R.L., Thorbecke G.J. Enhancement by various cytokines or 2-beta-mercaptoethanol of Ia antigen expression on Langerhans cells in skin from normal aged and young mice. Effect of cyclosporin A. J. Immunol. 1989; 143: 1530-1536.

Bergstresser P.R., Tigelaar R.E., Dees J.H., Streilein J.W. Thy-1 antigen bearing dendritic cells populate murine epidermis. J. Invest. Dermatol. 1983; 81: 286-288.

Bevan M.J. Antigen recognition. Class discrimination in the world of immunology. Nature 1987; 325: 192-194.

Bickers D.R. Photobiology 1937-1987. J. Invest. Dermatol. 1989; 92: 25s-31s.

Bigby M., Kwan T., Sy M.-S. Ratio of Langerhans cells to Thy-1 dendritic epidermal cells in murine epidermis influences the intensity of contact hypersensitivity. J. Invest. Dermatol. 1987; 89: 495-499.

Birbeck M.S., Breathnach A.S., Everall J.D. An electron microscopic study of basal melanocytes and high-level clear cells (Langerhans cells) in vitiligo. J. Invest. Dermatol. 1961; 37: 51-63.

Bjercke S., Elgo J., Braathen L., Thorsby E. Enriched epidermal Langerhans cells are potent antigen-presenting cells for T cells. J. Invest. Dermatol. 1984; 83: 286-289.

Bjercke S. Effect of interferon gamma on expression of HLA-class II molecules on blood-derived dendritic cells. Acta Pathol. Microbiol. Immunol. Scand. 1987; 95: 137-140.

Bjorkman P.J., Saper M.A., Samraoui B., Bennett W.S., Strominger J.L., Wiley D.C. The foreign antigen binding site and T cell recognition regions of class I histocompatibility antigens. Nature 1987; 329: 512-518.

Black A.K., Fincham N., Greaves M.W. Time course changes in levels of arachidonic acid and prostaglandins D2, E2, F2 in human skin following ultraviolet B irradiation. Br. J. Clin. Pharmacol. 1980; 10: 453-457.

Black A.K., Hensby C.N., Greaves M.W. Incresed levels of 6-oxo-PGF1 in human skin following ultraviolet-B radiation. Br. J. Dermatol. 1982;13:351-354.

Bland J.M., Altman D.G. Statistical methods for assessing agreement between two methods of clinical measurement. Lancet 1986; (8476): 307-310.

Blum H.F. Carcinogenesis by ultraviolet light. Princeton N.J.:Princeton University Press, 1959.

Bos J.D., Kapsenberg M.L. The skin immune system. Its cellular constituents and their interactions. Immunol. Today 1986; 7: 235-240.

Bos J.D., Teunissen M.B.M., Kapsenberg M.L. Dendritic cells of the skin immune system (SIS). In: The Langerhans cell (Eds. J. Thi volet, D. Schmitt). Colloque INSERM/ John Libbey Eurotext Ltd. 1988; 172: p9-19.

Bouillot M., Choppin J., Cornille F., Martinon F., Papo T., Gomard E., Fournie-Zaluski M.C., Levy J.P. (Letter to the editor). Physical association between MHC class I molecules and immunogenic peptides. Nature 1989; 339: 473-475.

Bouwes-Bavinck J.N., Koote A.M.M., Claas F.H.J., Vermeer B.J. The association of major histocompatibility antigens with the occurrence of cutaneous epithelial malignancies in renal transplant recipients. (abstr.) J. Invest. Dermatol. 1989; 92: 407A.

Boyle J., Mackie R.M., Briggs J.D., Junor B.J., Aitchison T.C. Cancer, warts, and sunshine in renal transplant patients. A case-control study. Lancet 1984; 1: 702-705.

Braathen L.R., Thorsby E. Studies on human epidermal Langerhans cells. I. Allo-activating and antigen-presenting capacity. Scand. J. Immunol. 1980; 11: 401-408.

Braciale T.J., Morrison L.A., Sweetser M.T., Sambrook J., Gething M.-J., Braciale V.L. Antigen presentation pathways to class I and II MHC-restricted T lymphocytes. Immunol. Rev. 1987; 98: 95-114.

Braciale T.J. Antigen processing for presentation by MHC class I molecules. Curr. Opinion Immunol. 1992; 4: 59-62.

Brash D.E., Rudolph J.A., Simon J.A., Lin A., McKenna G.J., Baden H.P., Halperin A.J., Ponten J. A role for sunlight in skin cancer: UV-induced p53 mutations in squamous cell carcinoma. Proc. Natl. Acad. Sci. USA 1991; 88: 10124-10128.

Breathnach A.S. Aspects of epidermal ultrastructure. J. Invest. Dermatol. 1975; 65: 2-15.

Breathnach A.S. Branched cells in the epidermis: an overview. J. Invest. Dermatol. 1980; 75: 6-11.

Breathnach A.S., Katz S.I. Thy-1 dendritic cells in murine epidermis are bone marrow derived. J. Invest. Dermatol. 1984; 83: 83-87.

British Standards Institution. Precision of test methods. I. Guide for the determination and reproducibility for a standard test method. (BS5497, part 1) London: BSI, 1979.

Brooks C.F., Moore M. Differential MHC class II expression on human peripheral blood monocytes and dendritic cells. Immunol. 1988; 63: 303-311.

Brown J.H., Jardetsky T., Saper M.A., Samraoui B., Bjorkman P.J., Wiley D.C. A hypothetical model of the foreign antigen binding sites of class II histocompatibility molecules. Nature 1988; 332: 845-850.

Bucana C.D., Munn G., Song M.J., Dunner K., Kripke M.L. Internalization of Ia molecules into Birbeck granule-like structures in murine dendritic cells. J. Invest. Dermatol. 1992; 99: 365-373.

Byrne J., Butler J., Reinherz E., Cooper M. Virgin and memory T cells have different requirements for activation via the CD2 molecule. Int. Immunol. 1989; 1: 1

Calverley R.K.S., Bedi K.S., Jones D.G. Estimation of the numerical density of synapses in rat neocortex. Comparison of the disector with an unfolding method. J. Neurosci. Meth. 1988; 23: 195-205.

Carr M.M., McVittie E., Guy K., Gawkrodger D.J., Hunter J.A.A. MHC class II antigen expression in normal human epidermis. Immunol. 1986; 59: 223-227.

Cerio R., Griffiths C.E., Cooper K.D., Nickoloff B.J., Headington J.T. Characterization of factor XIIIa positive dermal dendritic cells in normal and inflamed skin. Br. J. Dermatol. 1989; 121: 421-431.

Cerutti P.A. Prooxidant states and tumor promotion. Science 1985; 227: 375-381.

Chang R.J., Lee S.H. Effects of interferon-gamma and tumor necrosis factor-alpha on the expression of Ia antigen on a murine macrophage cell line. J. Immunol. 1986; 137: 2853-2856.

Chen B.P., Parham P. Direct binding of influenza peptides to class I HLA molecules. Nature (London) 1989; 337: 743-745.

Chen Y.X., Evans R.L., Pollack M.S., Lanier L.L., Phillips J.H., Rousso C., Warner N.L., Brodsky F.M. Characterization and expression of the HLA-DC antigens defined by anti-Leu 10. Hum. Immunol. 1984; 10: 221-222.

Cook J.S. Photoreactivation in animal cells. Photophysiology 1970; 5: 191.

Cooper K.D., Fox P., Neises G., Katz S.I. Effects of ultraviolet radiation on human epidermal cell alloantigen presentation: initial depression of Langerhans cell-dependent function is followed by the appearance of T6-DR+ cells that enhance epidermal alloantigen presentation. J. Immunol. 1985; 134: 129-137.

Cooper K.D., Neises G.R., Katz S.I. Antigen-presenting OKM5+ melanophages appear in human epidermis after ultraviolet radiation. J. Invest. Dermatol. 1986; 86: 363-370.

Cooper K.D., Oberhelman L., Hamilton T.A., Baadsgaard O., Terhune M., Le Vee G., Anderson T., Koren H. UV exposure reduces immunization rates and promotes tolerance to epicutaneous antigens in humans: Relationship to dose, CD1a-DR+ epidermal macrophage induction, and Langerhans cell depletion. Proc. Natl. Acad. Sci. USA 1992; 89: 8497-4501.

Cresswell P. Chemistry and function of the invariant chain. Curr. opinion Immunol. 1992; 4: 87-92.

Cripps D. Natural and artificial photoprotection. J. Invest. Dermatol. 1981; 76: 154-157.

Cruchley A.T., Williams D.M., Farthing P.M., Lesch C.A., Squier C.A. Regional variation in Langerhans cell distribution and density in normal human oral mucosa determined using monoclonal antibodies against CD1a, HLADR, HLADQ and HLADP. J. Oral Pathol. Med. 1989; 18: 510-516.

Cruz P.D.Jr., Nixon-Fulton J., Tigelaar R.E., Bergstresser P.R. Disparate effects of *in vitro* low-dose UVB irradiation on intravenous immunization with purified epidermal cell subpopulations for the induction of contact hypersensitivity. J. Invest. Dermatol. 1989; 92: 160-165.

Cumberbatch M., Kimber I. Phenotypic characteristics of antigen-bearing cells in the draining lymph nodes of contact sensitized mice. Immunology 1990; 71: 404-410.

Cumberbatch M., Illingworth I., Kimber I. Antigen-bearing dendritic cells in the draining lymph nodes of contact sensitized mice: cluster formation with lymphocytes. Immunology 1991; 74: 139-145.

Cumberbatch M., Kimber I. Dermal tumour necrosis factor-α induces dendritic cell migration to draining lymph nodes, and possibly provides one stimulus for Langerhans' cell migration. Immunology 1992a; 75: 257-263.

Cumberbatch M., Kimber I. Ultraviolet B light-induced alterations in epidermal Langerhans cells are mediated in part by tumour necrosis factor-alpha. Photdermatol. Photimmunol. Photomed. 1992b; 32: 398-405.

Czernielewski J.M., Schmitt D., Faure M.R., Thivolet J. Functional and phenotypic analysis of isolated human Langerhans cells and indeterminate cells. Br. J. Dermatol. 1983; 108: 129-138.

Czernielewski J., Vaigot P., Asselineau D., Prunieras M. *In vitro* effect of UV radiation on immune function and membrane markers of human Langerhans cells. J. Invest. Dermatol. 1984; 83: 62-65.

Davis A.L., McKenzie J.L., Hart D.N.J. HLA-DR-positive leukocyte subpopulations in human skin include dendritic cells, macrophages, and CD7-negative T cells. Immunol. 1988; 65: 573-581.

Davis M.M., Bjorkman P.J. T-cell antigen receptor genes and T-cell recognition. Nature 1988; 334: 395-402.

De Fabo E.C., Kripke M.L. Dose-response characteristics of immunologic unresponsiveness to UV-induced tumors produced by UV irradiation of mice. Photochem. Photobiol. 1979; 30: 385-390.

De Fabo E.C., Kripke M.L. Wavelength dependence and dose-rate independence of UV radiation-induced immunologic unresponsiveness of mice to a UV-induced fibrosarcoma. Photochem. Photobiol. 1980; 32: 183-188.

De Fabo E.C., Noonan F.P. Mechanism of immune suppression by ultraviolet irradiation *in vivo*. I. Evidence for the existence of a unique photoreceptor in skin and its role in photoimmunology. J. Exp. Med. 1983a; 158: 84-98.

De Fabo E., Noonan F.P, Fisher M., Burns J., Kacser H. Further evidence that the photoreceptor mediating UV-induced systemic immunosuppression is urocanic acid. J. Invest. Dermatol. 1983b; 80: 319.

De Fraissinette A., Staquet M.-J., Dezutter-Dambuyant C., Schmitt D., Thivolet J. Langerhans cells in S-phase in normal skin detected by simultaneous analysis of cell surface antigen and BrdU incorporation. J. Invest. Dermatol. 1988; 91: 603-605.

De Gruijl F.R., Van der Leun J.C. Systemic influence of pre-irradiation of a limited skin area on UV-tumorigenesis. Photochem. Photobiol. 1982; 35: 379-383.

De Panfilis G., Manara G.C., Ferrari C., Torresani C. Simultaneous colloidal gold immunoelectronmicroscopy labeling of CD1a, HLA-DR, and CD4 surface antigens of human epidermal Langerhans cells. J. Invest. Dermatol. 1988; 91: 547-552.

De Panfilis G., Soligo D., Manara G.C., Ferrari C., Torresani C. Adhesion molecules on the plasma membrane of epidermal cells. Human resting Langerhans cells express two members of the adherence-promoting CD11/CD18 family, namely, H-Mac-1 (CD11b/CD18) and gp 150 ,95 (CD11c/CD18). J. Invest. Dermatol. 1989; 93: 60-69.

De Panfilis G., Soligo D., Manara G.C., Ferrari C., Torresani C., Zucchi A. Human normal-resting epidermal Langerhans cells do express the type 3 complement receptor. Br. J. Dermatol. 1990a; 122: 127-136.

De Panfilis G., Manara G.C., Ferari C., Torresani C., Rowden G. Subsets of keratinocytes and Langerhans cells express epitopes associated with suppressor-inducer capabilities in resting normal human epidermis. Immunology 1990b; 69: 622-625.

De Panfilis G., Manara G.C., Ferrari C., Torresani C. Adhesion molecules on the plasma membrane of epidermal cells. III. keratinocytes and Langerhans cells constitutively express the lymphocyte function-associated antigen 3. J. Invest. Dermatol. 1991; 96: 512-517.

Deeg H.J., Aprile J.A., Severns E., Rajantie J., Schmidt E., Raff R.F., Green K.E., Storb R. Phenotypic and functional alterations of recipient lymphocytes after transfusion of UV-irradiated and normal blood- implications for marrow transplantation. Transplant. Proc. 1987; 19: 2709-2714.

Deeg H.J., Sigaroudinia M. Ultraviolet B-induced loss of HLA class II antigen expression on lymphocytes is dose, time, and locus dependent. Exp. Haematol. 1990; 18: 916-919.

Demidem A., Taylor J.R., Grammer S.F., Streilein J.W., T-lymphocyte-activating properties of epidermal antigen-presenting cells from normal and psoriatic skin: evidence that psoriatic epidermal antigen-presenting cells resemble cultured normal Langerhans cells. J Invest. Dermatol. 1991; 97: 454-460.

Dezutter-Dambuyant C., Cordier G., Schmitt D., Faure M., Laquoi C., Thivolet J. Quantitative evaluation of two distinct cell populations expressing HLA-DR antigens in normal human epidermis. Br. J. Dermatol. 1984; 111: 1-11.

Dezutter-Dambuyant C., Schmitt D., Faure M., Horisberger M., Thivolet J. Immunogold technique applied to simultaneous identification of T6 and HLA-DR antigens on Langerhans cells by electron microscopy. J. Invest. Dermatol. 1985; 84: 465-468.

Doll R., Payne P., Waterhouse J. Cancer incidence in five continents. New York, N.Y.: Springer-Verlag NY Inc.; 1970.

Drexhage H.A., Mullink H., de Groot J., Clarke J., Balfour B.M. A study of cells present in peripheral lymph of pigs with special reference to a type of cell resembling the Langerhans cell. Cell Tissue Res. 1979; 202: 407-430.

Drijvestijn A., Hamann A. Mechanisms and regulation of lymphocyte migration. Immunol. Today 1989; 10: 23-28.

Emmrich F. Cross-linking of CD4 and CD8 with the T-cell receptor complex: quaternary complex formation and T-cell repertoire selection. Immunol. Today 1988; 9: 296-300.

Emtestam L., Marcusson J.A., Moller E. HLA class II restriction specificity for nickel-reactive T lymphocytes. Acta Derm. Venereol. 1988; 68: 395-401.

Epstein S.P., Baer R.L., Thorbecke G.J., Belsito D.V. Immunosuppressive effects of transforming growth factor beta: inhibition of the induction of Ia antigen on Langerhans cells by cytokines and of the contact hypersensitivity response. J. Invest. Dermatol. 1991; 96: 832-837.

Everett M.A., Yearger E., Sayre R.M. Penetration of epidermis by ultraviolet rays. Photochem. Photobiol. 1966; 5: 533-542.

Everness K.M., Gawkrodger D.J., Botham P.A., Hunter J.A.A. The presentation of nickel sulphate by epidermal cells of nickel-sensitive and non-nickel-sensitive subjects: a preliminary report. In: The Langerhans cell. (Eds. J. Thivolet, D. Schmitt). Colloque/INSERM/John Libbey Eurotext Ltd. 1988; 172: p321-327.

Fabre J.W. Regulation of MHC expression. Immunol. Lett. 1991; 29:3-8.

Farrow S.J., Mohammad T., Baird W., Morrison H. Photochemical covalent binding of urocanic acid to polynucleic acids. Chem.-Biol. Interactions, 1990;75:105-118.

Faure F., Jitsukawa S., Miossec C., Hercend T. CD1c as a target recognition structure for human T lymphocytes: analysis with peripheral blood γ/δ cells. Eur. J. Immunol. 1990; 20: 703.

Festenstein H., Ollier B. Cellular typing and functional heterogeneity of MHC-encoded products. Br. Med. Bull. 1987; 43: 122-155.

Finsen N.R. In: Phototherapy. London: Edward Arnold, 1901.

Fitzpatrick T.B., Pathak M.A. Historical aspects of psoralens and other furocoumarins. J. Invest. Dermatol. 1959; 32: 229-231.

Forbes P.D., Davies R.E., Urbach F. Experimental ultraviolet photocarcinogenesis: wavelength interactions and time-dose relationships. Natl. Cancer Inst. Monogr. 1978; 50: 31-38.

Frain-Bell W. In: Cutaneous photobiology. Oxford University Press. 1985; p5.

Frank S.J., Niklinska B.B., Orloff D.G., Mercep M., Ashwell J.D., Klausner R.D. Structural mutation of the T-cell receptor chain and its role in T-cell activation. Science 1990; 249: 174-177.

Friedmann PS., Ford G., Ross J., Diffey B.L. Reappearance of epidermal Langerhans cells after PUVA therapy. Br. J. Dermatol. 1983; 109: 301-307.

Gahring L., Baltz M., Pepys M.B., Daynes R. Effect of ultraviolet radiation on production of epidermal cell-derived thymocyte activating factor/ interleukin 1 *in vivo and in vitro.* Proc. Natl. Acad. Sci. USA 1984; 81: 1198-1202.

Gaspari A.A., Jenkins M.K., Katz S.I. Class II MHC-bearing keratinocytes induce antigen-specific unresponsiveness in hapten-specific TH1 clones. J. Immunol. 1988; 141: 2216-2220.

Gawkrodger D.J., Carr M.M., McVittie E., Guy K., Hunter J.A. Keratinocyte expression of MHC class II antigens in allergic sensitization and challenge reactions and irritant contact dermatitis. J. Invest. Dermatol. 1987; 88: 11-16.

Gawkrodger D.J., Haftek M., Botham P.A., Carr M.M., Spencer M.-J., Ross J.A., Hunter J.A.A., Thivolet J. The hapten in contact hypersensitivity to dinitrochlorobenzene: Immunoelectron microscopic and immunofluorescent studies. Dermatologica 1989; 178: 126-130.

Geppert T.D., Lipsky P.E. Antigen presentation by interferon-gamma-treated endothelial cells and fibroblasts: differential ability to function as antigen-presenting cells despite comparable Ia expression. J. Immunol. 1985; 135: 3750-3762.

Gerlier D., Rabourdin-Combe C. Antigen processing - from cell biology to molecular interactions. Immunol. Today 1989; 10: 3-5.

Germain R.N. Immunology. The ins and outs of antigen processing and presentation. Nature 1986; 322: 687-689.

Germain R.N., Hendrix L.R. MHC class II structure, occupancy and surface expression determined by post-endoplasmic reticulum antigen binding. Nature (London) 1991; 353: 134-139.

Giannini M.S.H. Suppression of pathogenesis in cutaneous leishmaniasis by UV-irradiation. Infect. Immun. 1986; 51: 838-846.

Gilchrest B.A., Soter N.A., Stoff J.S. The human sunburn reaction: Histologic and biochemical studies. J. Am. Acad. Dermatol. 1981; 5: 411-422.

Giles R.C., De Mars R., Chang C.C., Capra J.D. Allelic polymorphism and transassociation of molecules encoded by the HLA-DQ subregion. Proc. Natl. Acad. Sci. USA 1985; 82: 1776-

Gilmour J.W., Vestey J.P., Norval M. The effect of UV therapy on immune function in patients with psoriasis. Br. J. Dermatol. 1993; 129: 28-38.

Girolomoni G., Sanantonio M.L., Bergstresser P.R., Cruz P.D., Giannetti A. Membrane ecto-ATPase on epidermal Langerhans cells. J. Invest. Dermatol. 1992; 99: 18s-19s.

Glass M.J., Bergstresser P.R., Tigelaar R.E., Streilein J.W. UVB radiation and DNFB skin painting induce suppressor cells universally in mice. J. Invest. Dermatol. 1990; 94: 273-278.

Gonwa T.A., Picker L.J., Raff H.V., Goyert S.M., Silver J., Stobo J.D. Antigen-presenting capabilities of human monocytes correlates with their expression of HLA-DS, an Ia determinant distinct from HLA-DR. J. Immunol. 1983; 130: 706-711.

Gonwa T.A., Frost J.P., and Karr R.W. All human monocytes have the capability of expressing HLA-DQ and HLA-DP molecules upon stimulation with interferon-γ. J. Immunol. 1986; 137: 519-524.

Gordon J.L. Extracellular ATP: effects, sources and fate. Biochem. J. 1986; 233: 309-319.

Gothelf Y., Hanau D., Tsur H., Sharon N., Sahar E., Cazenave J.-P., Gazit E. T6 positive cells in the peripheral blood of burn patients: are they Langerhans cell precursors? J. Invest. Dermatol. 1988; 90: 142-148.

Grabbe S., Bruvers S., Gallo R.L., Knisely T.L., Nazareno R., Granstein R.D. Tumor antigen presentation by murine epidermal cells. J. Immunol. 1991; 146: 3656-3661.

Grabbe S., Bruvers S., Lindgren A.M., Hosoi J., Tan K.C., Granstein R.D. Tumor antigen presentation by epidermal antigen-presenting cells in the mouse: modulation by granulocyte-macrophage colony-stimulating factor, tumour necrosis factor alpha, and ultraviolet radiation. J. Leukocyte Biol. 1992; 52: 209-217.

Granstein R.D., Askari M., Whitaker D., Murphy G.F. Epidermal cells in activation of suppressor lymphocytes: further characterization. J. Immunol. 1987; 138: 4055-4062.

Green A.E.S., Findley G.B., Klenk K.F., Wilson W.M., Mo T. The ultraviolet dose dependence of non melanoma skin cancer incidence. Photochem. Photobiol. 1978; 24: 353-362.

Green C., Diffey B.L., Hawk J.L. Ultraviolet radiation in the treatment of skin disease. Phys. Med. Biol. 1992; 37: 1-20.

Greene M.H., Tucker M.A., Clark W.H.Jr., Kraemer K.H., Elder D.E., Fraser M.C. Hereditary melanoma and the dysplastic nevus syndrome: the risk of cancers other than melanoma. J. Am. Acad. Dermatol. 1987; 16: 792-797.

Griffiths C.E., Vorhees J.J., Nickoloff B.J. Gamma interferon induces different keratinocyte cellular patterns of expression of HLA-DR and DQ and intercellular adhesion molecule-1 (ICAM-1) antigens. Br. J. Dermatol. 1989; 120: 1-8.

Guo Z., Okamoto H., Danno K., Imamura S. The effects of non-interval PUVA treatment on Langerhans cells and contact hypersensitivity. J. Dermatol. Sci. 1992; 3: 91-96.

Guy K., Van Heyningen V., Cohen B.B., Deane D.L., Steel C.M. Differential expression and serologically distinct subpopulations of human Ia antigens detected with monoclonal antibodies to Ia alpha and beta chains. Eur. J. Immunol. 1982; 12: 942-948.

Hackett C.J., Yewdell J.W., Bennink J.R., Sysocka M. Class-II MHC restricted T cell determinants processed from either endosomes or the cytosol with similar requirements for host protein transport but different kinetics of production. J. Immunol. 1991; 146: 2944-2951.

Hanau D., Fabre M., Lepoitterin J.P., Stampf J.L., Grosshans E., Benezra C. ATPase and morphologic changes induced by UVB on Langerhans cells in guinea pigs. J. Invest. Dermatol. 1985; 85: 135-138.

Hanau D., Fabre M., Schmitt D.A., Garaud J.-C., Pauly G., Tongio M.-M., Mayer S., Cazenave J.-P. Human epidermal Langerhans cells cointernalize by receptor-mediated endocytosis "nonclassical" major histocompatibility complex class I molecules (T6 antigens) and class II (HLA-DR antigens). Proc. Natl. Acad. Sci. U.S.A. 1987; 84: 2901-2905.

Hanau D., Schmitt D.A., Fabre M., Cazanave J.-P. A method for the rapid isolation of human epidermal Langerhans cells using immuno-magnetic microsheres. J. Invest. Dermatol.1988; 91: 247-279.

Hanau D., Fabre M., Schmitt D.A., Lepoittevin J.-P., Stampf J.-L., Grosshans E., Benezra C., Cazanave J.-P. ATPase and morphologic changes in Langerhans cells induced by epicutaneous application of a sensitizing dose of DNFB. J. Invest. Dermatol. 1989; 92: 689-694 .

Haniszko J., Suskind R.R. The effect of ultraviolet radiation on experimental cutaneous sensitization in guinea pigs. J. Invest. Dermatol. 1963; 40: 183-191.

Harber L.C., Bickers D.R. Ultraviolet carcinogenesis. In: Photosensitivity Diseases. Ed. W.B. Saunders, Philadelphia 1981; 246-257.

Harrist T.J., Muhlbauer J.E., Murphy G.F., Mihm M.C.Jr., Bhan A.K. T6 is superior to Ia (HLA-DR) as a marker for Langerhans cells and indeterminate cells in normal epidermis: a monoclonal antibody study. J. Invest. Dermatol. 1983; 80: 100-103.

Hawk J.I.M., Black A.K., Jaenicke K.F. Increased concentrations of arachidonic acid, prostaglandins E2 , D2 , and 6-oxo-F1 and histamine in skin following UVA radiation. J. Invest. Dermatol. 1983; 80: 496-499.

Haynes B.F., Hensley L.L., Jegasothy B.V. Phenotypic characterization of benign cutaneous T-cell infiltrates. Blood 1882; 60: 463-467.

Heufler C., Koch F., Schuler G. Granulocyte/macrophage colony-stimulating factor and interleukin-1 mediate the maturation of murine epidermal Langerhans cells into potent immunostimulatory dendritic cells. J. Exp. Med. 1988; 167: 700-705.

Hirayama K., Matsushita S., Kikuchi I., Iuchi M., Ohta N., Sasazuki T. HLA-DQ is epistatic to HLA-DR in controlling the immune response to schistosomal antigen in humans. Nature 1987; 327: 426-430.

Hogg N. The leukocyte integrins. Immunol. Today 1989; 10: 111-114.

Honigsmann H., Wolff K., Konrad K. Epidermal lysosomes and ultraviolet light. J. Invest. Dermatol. 1974; 63: 337-342.

Howie S.E.M., Norval M., Maingay J. Exposure to low dose ultraviolet B light suppresses delayed type hypersensitivity to herpes simplex virus in mice. J. Invest. Dermatol. 1986; 86: 125-128.

Humm S.A., Cole S. Changes with time in Langerhans cell number, ATPase reactivity and morphology in murine epidermis after exposure to UVB. Photodermatol. 1986; 67: 174-178.

Hunter J.A.A. The Langerhans cell: from gold to glitter. Clin. Exp. Dermatol. 1983; 8: 569-592.

Iacobelli D., Hashimoto K., Takahashi S. Effect of ultraviolet radiation on guinea pig epidermal Langerhans cell cytomembrane: light and electron microscopic studies. Photodermatol. 1985; 2: 132-143.

Imayama S., Yashima Y., Hori Y. Differing cell surface distribution of human immunoelectronmicroscopic study. J. Histochem. Cytochem. 1992; 40: 1191-1196.

Inaba K., Schuler G., Witmer M.D., Valinsky J., Atassi B., Steinman R.M. Immunologic properties of purified epidermal Langerhans cells. Distinct requirements for stimulation of unprimed and sensitized T lymphocytes. J. Exp. Med. 1986; 164: 605-613.

Janeway C.A., Bottomly K., Babich J., Conrad P., Conzen S., Jones B., Kaye J., Katz M., McVay L., Murphy D.B., Tite J. Quantitative variation in Ia antigen expression plays a central role in immune regulation. Immunology Today 1984; 5: 99-105.

Jansen C.T., Lammintausta K., Pasanen P., Neuvonen K., Varjonen E., Kalimo K., Ayras P. A non-invasive chamber sampling technique for HPLC analysis of human epidermal urocanic acid isomers. Acta Derm. Venereol. 1991; 71: 143-145.

Jeevan A., Evans R., Brown E.L., Kripke M.L. Effect of local ultraviolet irradiation on infections of mice with Candida albicans, Mycobacterium bovis BCG, and Schistosoma mansoni. J. Invest. Dermatol. 1992; 99: 59-64.

Jenssen P.E. Regulation of antigen presentation by acidic pH. J. Exp. Med. 1990; 171: 1779-1784.

Jessup J.M., Hanna N., Palaszynski E., Kripke M.L. Mechanisms of depressed reactivity to dinitrochlorobenzene and ultraviolet -induced tumors during ultraviolet carcinogenesis in BALB/c mice. Cell. Immunol. 1978; 38: 105-115.

Jones D.A., Morris A.G., Kimber I. Assessment of the functional activity of antigen-bearing dendritic cells isolated from the lymph nodes of contact-sensitized mice. Int. Arch. Allergy appl. Immunol. 1989; 90: 230-236.

Juhlin L., Shelley W.B. New staining techniques for the Langerhans cell. Acta Derm. Venereol. (Stockh.) 1977; 57: 289-296.

Juhlin L., Shelley W.B. Giant Langerhans cells induced by psoralen and ultraviolet radiation. Arch. Dermatol Res. 1979; 266: 311-314.

Karas Z., Warchol J.B., Jaroszewski J. Three-dimensional reconstruction and stereometric analysis of Langerhans cells in mouse epidermis. J. Invest. Dermatol. 1992; 99: 774-778.

Karnovsky M.J. A formaldehyde-glutaraldehyde fixative of high osmolarity for use in electron microscopy. J. Cell Biol. 1965; 27: 137-138.

Kartasova T., Ponec M., van de Putte P. Induction of proteins and mRNAs after UV irradiation of human epidermal keratinocytes. Exp. Cell Res. 1988; 174; 421-432.

Kashihara M., Ueda M., Horiguchi Y., Furukawa F., Hanaoka M., Imamura S. A monoclonal antibody specifically reactive to human Langerhans cells. J. Invest. Dermatol. 1986; 87: 602-607.

Kasinrerk W., Baumruker T., Majdic O., Knapp W., Stockinger H. CD1 molecule expression on human monocytes induced by granulocyte-macrophage colony-stimulating factor. J. Immunol. 1993; 180: 579-584.

Katz S.I., Tamaki K., Sachs D.H. Epidermal Langerhans cells are derived from cells originating in the bone marrow. Nature 1979; 282: 324-326.

Kiistala U., Mustakallio K.K. Dermo-epidermal separation with suction. Electron microscopic and histochemical study of initial events of blistering on human skin. J. Invest. Dermatol. 1967; 48: 466-477.

Kimber I., Kinnaird A., Peters S.W., Mitchell J.A. Correlation between lymphoid proliferative responses and dendritic cell migration in regional lymph nodes following skin painting with contact sensitizing agents. Int. Arch. Allergy Appl. Immunol. 1990; 93: 47-53.

Kligman A. Comments on the stratum corneum. In: The Biologic Effects of Ultraviolet Radiation (with emphasis on the skin). (F. Urbach, Ed. Oxford: Pergamon Press 1969: p165-167.

Knight S.C., Krejci J., Malkovsky M., Colizzi V., Gautam A., Asheron G.L. The role of dendritic cells in the initiation of immune responses to contact sensitizers. I. *In vivo* exposure to antigen. Cell. Immunol. 1985; 94: 427-434.

Knight S.C., Stagg A., Hill S., Fryer P., Griffiths S. Development and function of dendritic cells in health and disease. J. Invest. Dermatol. 1992; 99: 33s-38s.

Koch F., Heufler C., Kampgen E., Schneeweiss D., Bock G., Schuler G. Tumor necrosis factor alpha maintains the viability of murine epidermal Langerhans cells in culture, but in contrast to granulocyte/macrophage colony-stimulating factor, without inducing their functional maturation. J. Exp. Med. 1990; 171: 159-171.

Kock A., Schwarz T., Kirnbauer R., Urbanski A., Perry P., Ansel J.C., Luger T.A. Human keratinocytes are a source for tumor necrosis factor α. Evidence for synthesis and release upon stimulation with endotoxin or ultraviolet light. J. Exp. Med. 1990; 172: 1609-1614.

Koulu L., Jansen C.T. Effect of oral methoxsalen photochemotherapy on human Langerhans cell number. Dose-response and time-sequence studies. Arch. Dermatol. Res. 1982; 274: 79-83.

Koulu L., Jansen C.T., Viander M. Effect of UVA and UVB irradiation on human epidermal Langerhans cell membrane markers defined by ATPase activity and monoclonal antibodies (OKT6 and anti-Ia). Photodermatol. 1985; 2: 339-346.

Koulu L., Jansen C.T. *In vivo* PUVA and UVB sensitivity of various human epidermal Langerhans cell markers (ATPase, HLA-DR and T6)- Dose-response and time-sequence studies. Clin. Exp. Dermatol. 1988; 13: 173-176.

Koyasu S., Dadamio L., Clayton L.K., Reinherz E.L. T-cell receptor isoforms and signal transduction. Curr Opin. Immunol. 1991; 3: 32-39.

Kraal G., Breel M., Janse M., Bruin G. Langerhans' cells, veiled cells, and interdigitating cells in the mouse recognized by a monoclonal antibody. J. Exp. Med. 1986; 163: 981-997.

Kraemer K.H., Lee M.M., Scotto J. DNA repair protects against cutaneous and internal neoplasia: evidence from xeroderma pigmentosum. Carcinogenesis 1984; 5: 511-514.

Kripke M.L. Antigenicity of murine skin tumors induced by ultraviolet light. J. Natl. Cancer Inst. 1974; 53: 1333-1336.

Kripke M.L., Fisher M.S. Immunologic responses of the autochthonous host against tumors induced by ultraviolet light. Adv. Exp. Med. Biol. 1976; 66: 445-449.

Kripke M.L. Latency, histology, and antigenicity of tumors induced by ultraviolet light in three inbred mouse strains. Cancer Res. 1977; 37: 1395-1400.

Kripke M.L. Immunological aspects including photoimmunology of skin cancers. J. Dermatol. Surg. Onc. 1983; 9: 608-610.

Kripke M.L., Cox P.A., Alas L.G., Yarosh D.B. Pyrimidine dimers in DNA initiate systemic immunosuppression in UV-irradiated mice. Proc. Natl. Acad. Sci. USA 1992; 89: 7516-7520.

Krueger G.G., Stingl G. Immunology/inflammation of the skin - A 50 year perspective. J. Invest. Dermatol. 1989; 92: 32s-51s.

Krutmann J., Khan I.U., Wallis R.S., Zhang F., Rich E.A., Ellner J.J., Elmets C.A. Cell membrane is a major locus for Ultraviolet B-induced alterations in accessory cells. J. Clin. Invest. 1990; 85: 1529-1536.

Kupper T.S., Chua A.O., Flood P., McGuire J., Gubler U. Interleukin 1 gene expression in cultured human keratinocytes is augmented by ultraviolet irradiation. J. Clin. Invest. 1987; 80: 430-436.

Langerhans P. Uber die Nerven der Menschlichen Haut. Virchows Arch. Pathol. Anat. Physiol. 1868; 44: 325-335.

Le Varlet B., Dezutter-Dambuyant C., Staquet M.J., Delorme P., Schmitt D. Human epidermal Langerhans cells express integrins of the β1 subfamily. J. Invest. Dermatol. 1991; 96: 518-521.

Lee J.A.H. Melanoma and exposure to sunlight. Epidemiol. Rev. 1982; 4: 110-136..

Lieberman M.W., Beach L.R., Palmiter R.D. Ultraviolet radiation-induced metallothionein-I gene activation is associated with extensive DNA demethylation. Cell 1983; 35: 207-214.

Liu H.H., Muller S.A., Schroeter A.L. Quantitative and morphologic changes of Langerhans cells after Ultraviolet A irradiation of human epidermis. Acta Derm. Venereol. (Stockh.). 1987; 67: 411-416.

Long E.O., Jakobson S. Pathways of viral antigen processing and presentation to CTL: defined by the mode of virus entry? Immunol. Today 1989; 10: 45-48.

Lotteau V., Teyton L., Peleraux A., Nilsson T., Karlsson L., Schmid S.L., Quaranta V., Peterson P.A. Intracellular transport of class II MHC molecules directed by invariant chain. Nature (London) 1991; 348: 600-605.

Lu C., Changelian P.S., Unanue E.R. Alpha-fetoprotein inhibits macrophage expression of Ia antigens. J. Immunol. 1984; 132: 1722-1727.

Luger T.A. UVL and epidermal cell cytokine production. Photodermatol. 1986; 3: 123-124.

Lynch D.H., Gurish M.F., Daynes R.A. Relationship between epidermal Langerhans cell density, ATPase activity and the induction of contact hypersensitivity. J. Immunol. 1981; 126: 1892-1897.

Macatonia S.E., Knight S.C., Edwards A.J., Griffiths S., Fryer P. Localization of antigen on lymph node dendritic cells after exposure to the contact sensitizer fluorescein isothiocyanate. Functional and morphological studies. J. Exp. Med. 1987;166:1654-1667.

McGregor J.M., Barker J.N., Allen M.H., MacDonald D.M. Antigenic profile of human acrosyringium. Br. J. Dermatol. 1991; 125: 413-418.

Mackie R.M., Freudenberger T., Aitchison T.C. Personal risk-factor chart for cutaneous melanoma. Lancet 1989; 26: 487-490.

McNicholas J.M., King D.P., Jones P.P. Biosynthesis and expression of Ia and H-2 antigens on a macrophage cell line are stimulated by products of activated spleen cells. J. Immunol. 1983; 130: 449-456.

MacPherson G.G. Lymphoid dendritic cells: their life history and roles in immune responses. Res. Immunol. 1989; 140: 877-926.

Marrack P., Kappler J. The antigen-specific major histocompatibility complex-related receptor on T cells. Adv. Immunol. 1986; 38: 1 -30.

Mathur G.P., Ghandi V.M. Prostaglandin in human and albino rat skin. J. Invest. Dermatol. 1972; 58: 291-295.

Matsue H., Cruz P.D., Bergstresser P.R., Takashima A. Cytokine expression by epidermal cell subpopulations. J. Invest. Dermatol. 1992; 99: 42s-45s.

Matsue H., Cruz P.D., Bergstresser P.R., Takashima A. Langerhans cells are the major source of mRNA for IL-1β and MIP-1α among unstimulated mouse epidermal cells. J. Invest. Dermatol. 1992; 99: 537-541.

Maurer D.H., Hanke J.H., Mickelson E., Rich R.R., Pollack M.S. Differential presentation of HLA-DR, DQ, and DP restriction elements by interferon-gamma-treated dermal fibroblasts. J. Immunol. 1987; 139: 715-723.

McKinney E.C., Streilein J.W. On the extraordinary capacity of allogeneic epidermal Langerhans cells to prime cytotoxic T cells *in vivo.* J. Immunol. 1989; 143: 1560-1564.

McLean I.W., Nakane P.K. Periodate-lysine-paraformaldehyde fixative. A new fixative for immunoelectron microscopy. J. Histochem. Cytochem. 1974; 22: 1077-1083.

Miller J.F.A.P. Immunological function of the thymus. Lancet 1966; 2: 748-749.

Miyauchi S., Hashimoto K. Epidermal Langerhans cells undergo mitosis during the early recovery phase after Ultraviolet-B irradiation. J. Invest. Dermatol. 1987; 88: 703-708.

Miyauchi S, Hashimoto K. Mitotic activities of normal epidermal Langerhans cells. J. Invest. Dermatol.1989; 92: 120-121.

Mommaas A.M., Mulder A.A., Vermeer B.J., Boom B.W., Tseng C., Taylor J.R., Streilein J.W. Ultrastructural studies bearing on the mechanism of contact hypersensitivity to DNCB in man. Clin. Exp. Immunol. 1993; 92: 487-493.

Mommaas A.M., Mulder A.A., Vermeer B.J., Koning F. Human Langerhans cells in situ do not constitutively display high cell surface expression of HLA class II molecules. J. Invest. Dermatol. 1993; 100:436.

Monaco J.J. Genes in the MHC that may affect antigen processing. Curr. Opinion Immunol. 1992; 4: 70-73.

Moodycliffe A.M., Kimber I., Norval M. The effect of ultraviolet B irradiation and urocanic acid isomers on dendritic cell migration. Immunology 1992; 77: 394-399.

Moodycliffe A.M., Kimber I., Norval M. Role of tumour necrosis factor-α in ultraviolet B light-induced dendritic cell migration and suppression of contact hypersensitivity. Immunol. 1994; 81: 79-84.

Morhenn V.B., Nickoloff B.J. Gamma interferon treated human keratinocytes can stimulate allogeneic, resting T lymphocytes in the presence of interleukin-2. J. Invest. Dermatol. 1987; 88: 508 (Abstr.).

Morimoto C., Letvin N.L., Boyd A.W. The isolation and characterization of the human helper inducer T cell subset. J. Immunol. 1985a; 134: 3762-3769.

Morimoto C., Letvin N.L., Distaso J.A., Aldrich W.R., Schlossman S.F. The isolation and characterization of the human suppressor-inducer T cell subset. J. Immunol. 1985b; 134: 1508-1515.

Morison W.L., Parrish J.A., Woehler M.E., Bloch K.J. The influence of ultraviolet radiation on allergic contact dermatitis in the guinea-pig. I. UVB radiation. Br. J. Dermatol. 1981; 104: 161-164.

Morison W.L., Bucana C., Kripke M.L. Systemic suppression of contact hypersensitivity by UVB radiation is unrelated to UVB-induced alterations in the morphology and number of Langerhans cells. Immunology 1984; 52: 299-306.

Morison W.L. Systemic suppression of contact hypersensitivity associated with suppressor lymphocytes: is a lesion in DNA an essential step in the pathway? Photodermatol. Photoimmunol. Photomed. 1990; 7: 202-206.

Morrison H., Avnir D., Zarella T. Z-E photoisomerization of urocanic acid. Photochem. Photobiol. 1980; 32: 711-714.

Morrison H., Bernasconi C., Pandy G. A wavelength effect on urocanic acid E/Z photoisomerization. Photochem. Photobiol. 1984; 40: 549-550.

Morrison H. Photochemistry and photobiology of urocanic acid. Photodermatol. 1985; 2: 158-165.

Moulon C., Peguet-Navarro J., Schmitt D. A potential role for CD1a molecules on human epidermal Langerhans cells in allogeneic T-cell activation. J. Invest. Dermatol. 1991; 97: 524-528.

Murphy G.F., Bhan A.K., Sato S., Mihm M.C.Jr., Harrist T.J. A new immunologic marker for human Langerhans cells. N. Engl. J. Med. 1981: 304: 791-792.

Murphy G.F., Bhan A.K., Harrist T.J., Mihm M.C.Jr. *In situ* identification of T6-positive cells in normal human dermis by immunoelectron microscopy. Br. J. Dermatol. 1983; 108: 423-431.

Murphy G.M., Quinn D.G., Camp R.D.R., Hawk J.L.M., Greaves M.W. *In-vivo* studies of the action spectrum and time course for release of transforming growth factor-α by ultraviolet irradiation in man. Br. J. Dermatol. 1991; 125: 566-568.

Mutis T., De Burger M., Bakker A., Ottenhof T.H. HLA class II+ human keratinocytes present mycobacterium leprae antigens to CD4+Th1-like cells. Scand. J. Immunol. 1993; 37: 43-51.

Nakamura K., Ishii A., Takami K. Subpopulation of murine epidermal Langerhans cells identified by lectin-binding sites. Arch. Dermatol. Res. 1990; 282: 253-257.

Navarette C., Jaraquemada D., Hui K., Awad J., Okoye R., Festenstein H. Different functions and associations of HLA-DR and HLA-DQ (DC) antigens shown by serological, cellular and DNA assays. Tissue antigens 1985; 25: 130-141.

Nickoloff B.J., Basham T.Y., Merigan T.C., Morhenn V.B. Keratinocyte class II histocompatibility antigen expression. Br. J. Dermatol. 1985; 112: 373-374.

Nickoloff B.J., Basham T.Y., Merigan T.C., Torseth J.W., Morhenn V.B. Human keratinocyte-lymphocyte reactions *in vitro*. J. Invest. Dermatol. 1986; 87: 11-18.

Nieda M., Juji T., Imao S., Minami M. A role of HLA-DQ molecules of stimulator-adherent cells in the regulation of human autologous mixed lymphocyte reaction. J. Immunol. 1988; 141: 2975-2979.

Niederwieser D., Aubock J., Troppmair J., Herold M., Schuler G., Boeck G., Lotz J., Fritsch P., Huber C. IFN-mediated induction of MHC antigen expression on human keratinocytes and its influence on *in vitro* alloimmune responses. J. Immunol. 1988; 140: 2556-2564.

Noelle R., Snow E.C. T helper cells. Curr. Opinion Immunol.1992; 4: 333-337.

Noonan F.P., Kripke M.L., Pederson G.M., Greene M.I.Suppression of contact hypersensitivity in mice by ultraviolet irradiation is associated with defective antigen presentation. Immunology 1981; 43: 527-533.

Noonan F.P., Bucana C., Sauder D.N., De Fabo E.C. Mechanism of systemic immune suppression by UV irradiation *in vivo*. II. The UV effects on number and morphology of epidermal Langerhans cells and the UV-induced suppression of contact hypersensitivity have different wavelength dependencies. J. Immunol. 1984; 132: 2408-2416.

Noonan F.P., De Fabo E.C., Morrison H. *Cis*-urocanic acid, a product formed by ultraviolet B irradiation of the skin, initiates an antigen presentation defect in splenic dendritic cells *in vivo*. J. Invest. Dermatol. 1988; 90: 92-99.

Noonan F.P., De Fabo E.C. Ultraviolet-B dose-response curves for local and systemic immunosuppression are identical. Photochem. Photobiol. 1990; 52: 801-810.

Nordlund J.J., Ackles A.E., Lerner A.B. The effects of ultraviolet light and certain drugs on Ia-bearing Langerhans cells in murine epidermis. Immunology 1981; 60: 50-63.

Norval M., McIntyre C.R., Simpson T.J., Howie S.E., Badshiri E. Quantification of urocanic acid isomers in murine skin duringdevelopment and after irradiation with UVB light. Photodermatol. 1988; 5: 179-186.

Norval M., Simpson T.J., Bardshiri E., Crosby J. Quantification of urocanic acid isomers in human stratum corneum. Photodermatol. Photoimmunol. Photomed. 1989a; 6: 142-145.

Norval M., Simpson T.J., Bardshiri E., Howie S.E.M. Urocanic acid analogues and the suppression of the delayed type hypersensitivity response to herpes simplex virus. Photochem. Photobiol. 1989b; 49: 633-639.

Norval M., Simpson T.J., Ross J.A. Urocanic acid and immunosuppression. Photochem. Photobiol. 1989c; 50: 267-275.

Norval M., Gilmour J.W., Simpson T.J. The effect of histamine receptor antagonists on immunosuppression induced by the *cis*-isomer of urocanic acid. Photodermatol. 1990; 7: 243-248.

Nunez G., Giles R.C., Ball E.J., Hurley C.K., Capra J.D., Stastny P. Expression of HLA-DR, MB, MT and SB antigens on human mononuclear cells. Identification of two phenotypically distinct monocyte populations. J. Immunol. 1984; 133: 1300-1313.

Nunez G., Ball E.J., Myers L.K., Stastny P. Allostimulating cells in man. Quantitative variation in the expression of HLA-DR and HLA-DQ molecules influences T-cell activation. Immunogenetics 1985; 22: 85-91.

Obata M., Tagami H. Alteration in murine epidermal Langerhans cell population by various UV irradiations: quantitative and morphologic studies on the effects of various wavelengths of monochromatic radiation on Ia-bearing cells. J. Invest. Dermatol. 1985; 84: 139-145.

Odling K.A., Halliday G.M., Muller H.K. Effects of low or high doses of short wavelength ultraviolet light (UVB) on Langerhans cells and skin allograft survival. Immunol. Cell. Biol. 1987; 65: 337-343.

Odum N., Hofmann B., Jakobsen B.K., Langhoff E., Morling N., Platz P., Ryder L.P., Svejgaard A. HLA-DP related suppression of mixed lymphocyte reaction with alloactivated lymphocytes. Tissue Antigens 1986; 27: 32-43.

Okamoto H, Kripke M.L. Effector and suppressor circuits of the immune response are activated *in vivo* by different mechanisms. Proc. Natl. Acad. Sci. USA 1987; 84: 3841-3845.

Olerup O., Moller E., Persson U. HLA-DP incompatibilities induce significant proliferation in primary mixed lymphocyte cultures in HLA-A, -B, -DR, and -DQ compatible individuals: Implications for allogeneic bone marrow transplantation. Tissue Antigens 1990; 36: 194-202.

Palazynski E.W., Noonan F.P., De Fabo E.C. *Cis*-urocanic acid down regulates the induction of adenosine 3',5'-cyclic monophosphate by either *trans*-urocanic acid or histamine in human dermal fibroblasts *in vitro*. Photochem. Photobiol. 1992; 55: 165-171.

Pamphilon D.H., Czudek R., Wallington T.B. Br. J. Haematol. 1989; 71: 533 (abstr.)

Parrish J.A., Fitzpatrick T.B., Tanenbaum L., Pathak M.A. Phototherapy of psoriasis with oral methoxsalen and longwave ultraviolet light. N. Engl. J. Med.; 1974: 1207-1211.

Parrish J.A., Anderson R.R., Urbach F., Pitts D. In: UVA: Biological effects of ultraviolet radiation with emphasis on human responses to longwave ultraviolet. New York: Plenum Press, 1978: p4.

Parrish J.A., Jaenicke K.F., Anderson R.R. Erythema and melanogenesis action spectra of normal human skin. Photochem. Photobiol. 1982; 36: 187-191.

Parrish J.A., Kripke M.L., Morrison W.L. In: Photoimmunology. J.A. Parrish, M.L. Kripke, W.L. Morrison, Eds. 1983; p84.

Pasanen P., Reunala T., Jansen C.T., Rasanen L., Neuvonen K., Ayras P. Urocanic acid isomers in epidermal samples and suction blister fluid of non-irradiated and UVB-irradiated human skin. Photodermatol. Photoimmunol. Photomed. 1990; 7: 40-42.

Pathak M.A., Stratton K. Free radicals in human skin following exposure to ultraviolet light. Arch. Biochem. Biophys. 1968; 123: 468-476.

Patrick M.H., Gray D.M. Independence of photoproduct formation on DNA conformation. Photochem. Photobiol. 1976; 24: 507-513.

Pawelec G.P., Shaw S., Ziegler A., Muller C., Wernet P. Differential inhibition of HLA-D- or SB- directed secondary lymphoproliferative responses with monoclonal antibodies detecting human Ia-like determinants. J. Immunol. 1982; 129: 1070-1075.

Pawelec G., Wernet P., Rosenlund R., Blaurock M., Schneider E.M. Strong lymphoproliferative suppressive function of PLT clones specific for SB-like antigens. Hum. Immunol. 1984; 9: 145-157.

Phillips R., Short T. The re-sectioned section technique and its application to the study of the topography and thickness of thin sections. J. R. Microscop. Soc. 1964; 82: 263.

Picut C.A., Lee C.S., Dougherty E.P., Anderson K.L., Lewis R.M. Immunostimulatory capabilities of highly enriched Langerhans cells *in vitro*. J. Invest. Dermatol. 1988; 90: 201-206.

Plastow S.R., Harrison J.A., Young A.R. Early changes in dermal collagen of mice exposed to chronic UVB irradiation and the effects of a UVB sunscreen. J. Invest. Dermatol. 1988; 91: 590-592.

Pober J.S., Collins T., Gimbrone M.A. Jr., Cotran R.S., Gitlin J.D., Fiers W., Clayberger C., Krensky A.M., Burakoff S.J., Reiss C.S. Lymphocytes recognize human vascular endothelial and dermal fibroblast Ia antigens induced by recombinant immune interferon. Nature 1983; 305: 726-729.

Polla L. Margolis R., Goulsten C., Parrish J.A., Granstein R.D. Enhancement of the elicitation phase of the murine contact hypersensitivity response by prior exposure to ultraviolet radiation. J. Invest. Dermatol. 1986; 86: 13-17.

Porcelli S., Brenner M.B., Greenstein J.L., Balk S.P., Terhorst C., Bleicher P.A. Recognition of cluster of differentiation 1 antigens by human CD4-CD8- cytolytic T lymphocytes. Nature 1989; 341: 447-450.

Ptak W., Ruzycka D.W., Askenase P.W., Gershon R.K. Role of antigen-presenting cells in the development and persistence of contact hypersensitivity. J. Exp. Med. 1980; 151: 362-375.

Punnonen B.M., Puustinen T., Jansen C.T. Ultraviolet B irradiation induces changes in the distribution and release of arachidonic acid, dihomo-γ-linolenic acid, and eicosapentanoic acid in human keratinocytes in culture. J. Invest. Dermatol. 1987; 88:611-614.

Pure E., Inaba K., Crowley M.T., Tardelli I., Witmer-Pack M.D., Ruberti G., Fathman G., Steinman R.M. Antigen processing by epidermal Langerhans cells correlates with the level of biosynthesis of Major histocompatibility complex class-II molecules and expression of invariant chain. J. Exp. Med. 1990; 172: 1459-1469.

Qvigstad E., Moen T., Thorsby E. T-cell clones with similar antigen specificity may be restricted by DR, MT (DC), or SB class II HLA molecules. Immunogenetics 1984; 19: 455-460.

Rasanen L., Lehto M., Jansen C., Reunala T., Leinikki P. Human epidermal Langerhans cells and peripheral blood monocytes. Accessory cell function, autoactivating and aloactivating capacity and ETAF/IL-1 production. Scand. J. Immunol. 1986; 24: 503-508.

Rasanen L., Jansen C.T., Hyoty H., Reunala T., Morrison H. *Cis*-urocanic acid stereospecifically modulates human monocyte IL-1 production and surface HLA-DR antigen expression, T-cell IL-2 production and CD4/CD8 ratio. Photodermatol. 1989; 6: 287-292.

Res P., Kapsenberg M.L., Bos J.D., Stiekema F. The crucial role of human dendritic antigen-presenting cell subsets in nickel-specific T cell proliferation. J. Invest. Dermatol. 1987; 88: 550-554.

Robertson I., Cook M.G. Multiple melanomas associated with diffuse melanocytic dysplasia. Histopathol. 1987; 11: 395-402.

Romani N., Lenz A., Glassel H., Stossel H., Stanzl U., Majdic O., Fritsch P., Schuler G. Cultured human Langerhans cells resemble lymphoid dendritic cells in phenotype and function. J. Invest. Dermatol. 1989; 93; 600-609.

Rosenthal A.S., Shevach E.M. Function of macrophages in antigen recognition by guinea pig T lymphocytes. I. Requirement for histocompatible macrophages and lymphocytes. J. Exp. Med. 1973; 138: 1194-1212.

Ross J.A., Howie S.E., Norval M., Maingay J., Simpson T.J. Ultraviolet-irradiated urocanic acid suppresses delayed-type hypersensitivity to herpes simplex virus. J. Invest. Dermatol. 1986; 87: 630-633.

Ross J.A., Howie S.E.M., Norval M., Maingay J.P. Two phenotypically distinct T cells are involved in UV-irradiated urocanic acid induced suppression of the efferent DTH response to HSV-1 *in vivo*. J. Invest. Dermatol. 1987; 89: 230-233.

Rotzschke O., Falk O., Deres K., Schild H., Norda M., Metzger J., Jung G., Rammensee H.G. Isolation and analysis of naturally processed viral peptides as recognized by cytotoxic T cells. Nature 1990; 348: 252-253.

Rottier P.B. The erythematous action of ultraviolet light on human skin. Some measurements of the spectral response with a continuous and intermittent light. J. Clin. Invest. 1953; 32: 681-689.

Rowden G., Lewis M.F., Sullivan L.C. Ia antigen expression on human epidermal Langerhans cells. Nature 1977; 268: 247-248.

Rowden G., Davis D., Luckett D. Identification of suppressor-inducer T cells (CD4+,2H4+) in normal human skin. In: The Langerhans cell. (Eds. J. Thivolet, D. Schmitt). Colloque/INSERM/John Libbey Eurotext Ltd. 1988; 172: p205-214.

Sasportes M., Fradelizi D., Dausset J. HLA-DR specific human suppressor lymphocytes generated by repeated *in vitro* sensitization against allogeneic cells. Nature (London) 1978; 276: 502-504.

Sauder D.N., Tamaki K., Moshell A.W., Fujiwara H., Katz S.I. Induction of tolerance to topically applied TNCB using TNP-conjugated ultraviolet light-irradiated epidermal cells. J. Immunol. 1981; 127: 261-265.

Sauder D.N., Noonan F.P., De Fabo E.C., Katz S.I. Ultraviolet radiation inhibits alloantigen presentation by epidermal cells: partial reversal by the soluble epidermal cell product, epidermal cell-derived thymocyte activating factor (ETAF). J. Invest. Dermatol. 1983; 81: 185-186.

Sauder D.N., Dinarello C.A., Morhenn V.B. Langerhans cell production of interleukin-1. J. Invest. Dermatol. 1984; 82: 605-607.

Scheibner A., Hollis D.E., McCarthy W.H., Milton G.W. Effects of sunlight exposure on Langerhans cells and melanocytes in human epidermis. Photodermatol. 1986; 3: 15-25.

Scheibner A., Hollis D.E., Murray E., McCarthy W.H., Milton G.W. Effects of exposure to ultraviolet light on epidermal Langerhans cells and melanocytes in Australians of Aboriginal, Asian and Celtic descent. Photodermatol. 1987; 4: 5-13.

Scheper R.J., Van Dinther-Janssen A.Ch.M., Polak L. Specific accumulation of hapten-reactive T cells in contact sensitivity reaction sites. J. Immunol. 1985; 134: 1333-1336.

Scheynius A., Tjernlund U., Johansson C., Hagforsen E., Nilsson H. Effects on the T cell response to PPD by Langerhans cell depleted epidermal cell suspensions containing HLA-DR expressing keratinocytes. In: The Langerhans cell. Ed. J. Thivolet, D.Schmitt. Col loque/ INSERM/John Libbey Eurotext Ltd. 1988;172: p301-312.

Scheynius A., Lundahl P. Three-dimensional visualization of human Langerhans' cells using confocal scanning laser microscopy. Arch. Dermatol. Res. 1990; 281: 521-525.

Scheynius A., Dalenberg M., Carlsson K., England R., Lindberg M. Quantitative analysis of Langerhans' cells in epidermis at irritant contact reactions using confocal laser scanning microscopy. Acta Derm. Venereol. (Stockh.) 1992; 72: 348-351.

Schmitt D., Faure M., Dezutter-Dambuyant C., Thivolet J. The semi-quantitative distribution of T4 and T6 surface antigens on human Langerhans cells. Br. J. Dermatol. 1984; 111:655-661.

Schmitt D., Gomes M., Dezutter-Dambuyant C., Haftek M., Thivolet J. Effects of gamma-interferon on HLA-DR and HLA-DQ antigen expression by human Langerhans cells. Clin. Exp. Dermatol. 1987; 12: 226 (abstr.)

Schmitt D., Bieber T., Cazenave J.P., Hanau D. Fc gamma RII / CD32-negative human Langerhans cells may be responsible for the immunostimulatory activity of freshly isolated epidermal cells. Cell. Immunol. 1992; 140: 507-512.

Schneider S.A., Fukuyama K., Maceira J., Epstein W.L. Effect of ultraviolet B radiation on S-100 protein antigen in epidermal Langerhans cells. J. Invest. Dermatol. 1985; 84: 146-148.

Schothorst A.A., Evers L.M., Noz K.C., Filon R., van Zeeland A.A. Pyrimidine dimer induction and repair in cultured human skin keratinocytes or melanocytes after irradaition with monochromatic ultraviolet light. J. Invest. Dermatol. 1991; 96: 916-920.

Schreiber S., Kilgus O., Payer E., Kutil R., Elbe A., Mueller C., Stingl G. Cytokine pattern of Langerhans cells isolated from murine epidermal cell cultures. J. Immunol. 1992; 149: 3525-3534.

Schuler G., Romani N., Linert J., Shevach E.M., Stingl G. Subsets of epidermal Langerhans cells as defined by lectin binding profiles. J. Invest. Dermatol. 1983; 81: 397-402.

Schuler G., Romani N., Steinman R.M. A comparison of murine epidermal Langerhans cells with spleen dendritic cells. J. Invest. Dermatol. 1985a; 85: 99s-106s.

Schuler G., Steinman R.M. Murine epidermal Langerhans cells mature into potent immunostimulatory dendritic cells *in vitro* . J. Exp. Med. 1985b; 161: 526-546.

Schwarz T., Gschnait F., Greiter F. Photoprotective effect of topical indomethacin - an experimental study. Dermatologica 1985; 171: 450-458.

Schwarz T., Urbanska A., Gschnait F., Luger T.A. Inhibition of the induction of contact hypersensitivity by a UV-mediated epidermal cytokine. J. Invest. Dermatol. 1986; 87: 289-291.

Schwarz T., Urbanski A., Kirnbauer R., Koch A., Gschnait F., Luger T.A. Detection of a specific inhibitor of interleikin-1 in sera of UVB-treated mice. J. Invest. Dermatol. 1988; 91: 536-540.

Schwarz T., Luger T.A. Effect of UV irradiation on epidermal cell cytokine production. J. Photochem. 1989; 4: 1-13.

Schwarz W., Langer K., Schell H., Schonberger A. Distribution of urocanic acid in human stratum corneum. Photodermatol. 1986a; 3: 239-240.

Scott I.R. Factors controlling the expressed activity of histidine ammonia-lyase in the epidermis and the resulting accumulation of urocanic acid. Biochem. J. 1981; 194: 829-838.

Scott I.R., Harding C.R., Barrett J.G. Histidine rich protein of the keratohyalin granules. Source of the free amino acids, urocanic acid and pyrrolidone carboxylic acid in the stratum corneum. Biochim. Biophys. Acta 1982; 719: 110-117.

Scotto J., Fears T.R. The association of solar ultraviolet and skin melanoma incidence among caucasians in the United States. Cancer Invest. 1987; 5: 275-283.

Setlow J.K., Setlow R.B. Nature of the photoreactivable ultraviolet lesion in DNA. Nature 1963; 197: 560.

Shelley W.B., Juhlin L. Langerhans cells form a reticuloepithelial trap for external contact allergens. Nature 1976; 261: 46-47.

Shelley W.B., Juhlin L. Selective uptake of contact allergens by the Langerhans cell. Arch. Dermatol. 1977; 113: 187-192.

Shimada S., Caughman S.W., Sharrow S.O., Stephany D., Katz S.I. Enhanced antigen-presenting capacity of cultured Langerhans' cells is associated with markedly increased expression of Ia antigen. J. Immunol. 1987; 139: 2551-2555.

Shiohara T., Moriya N., Saizawa K., Nagashima M. Role of Langerhans cells in epidermotropism of T cells. Arch. Dermatol. Res. 1988; 280: 33-38.

Silberberg I. Apposition of mononuclear cells to Langerhans cells in contact allergic reactions. An ultrastructural study. Acta Derm. Venereol. 1973; 51: 1-12.

Silberberg I., Thorbecke G.J., Baer R.L. Antigen-bearing Langerhans cells in skin, dermal lymphatics and in lymph nodes. Cell. Immunol. 1976; 25: 137-151.

Silberberg-Sinakin I., Gigli I., Baer R.L., Thorbecke G.J. Langerhans cells: role in contact hypersensitivity and relationship to lymphoid dendritic cells and to macrophages. Immunol. Rev. 1980; 53: 816-821.

Simon J.C., Cruz P.D., Bergstresser P.R., Tigelaar R.E. Low-dose UVB-irradiated Langerhans cells preferentially activate CD4 cells of the Th1 subset. J. Immunol. 1990; 145: 2087-2091.

Simon J.C., Cruz P.D., Tigelaar R.E., Sontheimer R.D., Bergstresser P.R. Adhesion molecules CD11a, CD18, and ICAM-1 on human epidermal Langerhans cells serve a functional role in the activation of alloreactive T cells. J. Invest. Dermatol. 1991a; 96: 148-151.

Simon J.C., Tigelaar R.E., Bergstresser P.R., Edelbaum D., Cruz P.D. UVB radiation converts Langerhans cells from immunogenic to tolerogenic antigen presenting cells. Induction of specific clonal anergy in CD4+ T helper 1 cells. J. Immunol. 1991b; 146: 485-491.

Simon J.C., Edelbaum D., Bergstresser P.R., Cruz P.D.Jr. Distorted antigen-presenting function of Langerhans cells induced by tumor necrosis factor α via a mechanism that appears different from that induced by ultraviolet B radiation. Photdermatol. Photimmunol. Photomed. 1991c; 8: 190-194.

Simon J.C., Krutmann J., Elmets C.A., Bergstresser P.R., Cruz P.D.Jr. Ultraviolet B-irradiated antigen-presenting cells display altered accessory signaling for T-cell activation: relevance to immune responses initiated in skin. J. Invest. Dermatol. 1992; 98: 66s-69s.

Small J.V. Measurement of section thickness. In: Proceedings 4th European Congress on Electron Microscopy; 1968; 1. (Ed. D.S. Bocciarelli) Tipografia Poliglotta Vaticana. Rome.

Snyder D.S., Eaglestein W.H. Intradermal ani-prostaglandin agents and sunburn. J. Invest. Dermatol. 1974; 62: 47-50.

Snyder D.S., Beller D.I., Unanue E.R. Prostaglandins modulate macrophage Ia expression. Nature (London) 1982; 299: 163.

Sontheimer R.D., Bergstresser P.R., Gailiunas P.Jr., Helderman J.H., Gilliam J.N. Peturbation of epidermal Langerhans cells in immunosuppressed human renal allograft recipients. Transplantation 1984; 37: 168-174.

Sontheimer R.D. The mixed epidermal cell-lymphocyte reaction. II. Epidermal Langerhans cells are responsible for the enhanced allogeneic lymphocyte-stimulating capacity of normal human epidermal cell suspensions. J. Invest. Dermatol. 1985; 85: 21s-26s.

Sontheimer R.D., Stastny P., Nunez G. HLA-D region antigen expression by human epidermal Langerhans cells. J. Invest. Dermatol. 1986; 87: 707-710.

Sontheimer R.D., Matsubara T., Seelig L.L. Jr. A macrophage phenotype for a constitutive, class II antigen-expressing, human dermal perivascular dendritic cell. J. Invest. Dermatol. 1989; 93: 154-159.

Spellman C.W., Daynes R.A. Modification of immunological potential by ultraviolet radiation. II. Generation of suppressor cells in short-term UV-irradiated mice. Transplantation 1977; 24: 120-126.

Staquet M.J., Dezutter-Dambuyant C., Schmitt D., Thivolet J. Adhesion-mediating molecules of human epidermal Langerhans cells. (abstr.) J. Invest. Dermatol.1989; 92: 522.

Steinman R.M., Nussenzweig M.C. Dendritic cells: features and functions. Immunol. Rev. 1980; 53: 125-147.

Sterenborg H.J., Van der Leun J.C. Tumorigenesis by a long wavelength UV-A source. Photochem. Photobiol. 1990; 51: 325-330.

Stingl G., Wolff-Schreiner E.C., Pichler W., Gschnait F., Knapp W.,Wolff K. Epidermal Langerhans cells bear Fc and C3 receptors. Nature 1977; 268: 245-246.

Stingl G., Katz S.I., Clement L., Green I., Shevach E.M. Immunological functions of Ia-bearing epidermal Langerhans cells. J. Immunol. 1978; 121: 2005-2013.

Stingl G., Gazze-Stingl L.A., Aberer W., Wolff K. Antigen presentation by murine epidermal Langerhans cells and its alteration by ultraviolet B light. J. Immunol. 1981; 127: 1707-1713.

Stockinger B., Pessara U., Lin R.H., Habich I.J., Grez M., Koch N. A role of Ia-associated invariant chains in antigen processing and presentation. Cell 1989; 56: 683-689.

Stolarski R., Bojkov R., Bishop L., Zerefos C., Staehelin J., Zawodny J. Measured trends in stratospheric ozone. Science 1992; 256: 342-349.

Streilein J.W. Lymphocyte traffic, T cell malignancies and the skin. J. Invest. Dermatol. 1978;71:167-171.

Streilein J.W., Bergstresser P.R. Haptens can serve as surrogate transplantation antigens in a manner that demonstrates H-2 restriction of graft rejection. J. Exp. Med. 1983; 157: 1354-1359.

Streilein J.W., Bergstresser P.R. Genetic basis of ultraviolet-B effects on contact hypersensitivity. Immunology 1988; 27: 252-258.

Streilein J.W., Grammer S.F., Yoshikawa T., Demidem A., Vermeer M. Functional dichotomy between Langerhans cells that present antigen to naive and to memory/effector T lymphocytes. Immunol. Rev. 1990; 117: 159-183.

Sullivan S., Bergstresser P.R., Tigelaar R.E., Streilein J.W. Induction and regulation of contact hypersensitivity by resident bone marrow-derived, dendritic epidermal cells: Langerhans cells and Thy-1+ epidermal cells. J. Immunol. 1986; 137: 2460-2467.

Tabachnik J. Urocanic acid, the major acid soluble, UV-absorbing compound in guinea pig epidermis. Arch. Biochem. Biophys. 1957; 70: 295-298.

Tadini G., Cerri A., Clementi E., Brusasco A., Berti E., Soligo D., Quirici N., Lambertenghi-Deliliers G. Immunogold staining of human Langerhans cells in suspension. In: The Langerhans Cell. (Eds. Thivolet J, Schmitt D.) Colloque INSERM/John Libbey Eurotext Ltd., London, Paris, 1988; 172: 99-107.

Takahashi S., Hashimoto K. Derivation of Langerhans cell granules from cytomembrane. J. Invest. Dermatol. 1985; 84: 469-471.

Takigawa M., Iwatsuki K., Yamada M., Okamoto H., Inamura S. The Langerhans cell granule is an adsorptive endocytic organelle. J. Invest. Dermatol. 1985; 85: 12-15.

Talve L., Sterback F., Jansen C.T. UVA irradiation increases the incidence of epithelial tumors in UVB-irradiated hairless mice. Photodermatol. Photoimmunol. Photomed. 1990; 7: 109-115.

Tang A., Udey M.C. Inhibition of epidermal Langerhans cell function by low dose ultraviolet B radiation. Ultraviolet B radiation selectively modulates ICAM-1 (CD54) expression by murine Langerhans cells. J. Immunol 1991; 146: 3347-3355.

Tang A., Dunner K., Kripke M.L., Bucana C. Characterisics of antigen-presenting cells involved in contact sensitizing of normal and UV-irradiated mice. J. Invest. Dermatol. 1992; 99; 20s-22s.

Tang A., Udey M.C. Effects of ultraviolet radiation on murine epidermal Langerhans cells: doses of ultravilet radiation that modulate ICAM-1 (CD54) expression and inhibit Langerhans cell function cause delayed cytotoxicity *in vitro*. J. Invest. Dermatol. 1992; 99: 83-89.

Taylor R.S., Baadsgaard O., Hammerberg C., Cooper K.D. Hyperstimulatory CD1a+CD1b+ CD36+ Langerhans cells are responsible for increased autologous T lymphocyte reactivity to lesional epidermal cells of patients with atopic dermatitis. J. Immunol. 1991; 147: 3794-3802.

Teunissen M.B., Vormmeester J., Krieg S.R., Peters P.J., Vogels I.M., Kapsenberg M.L., Bos J.D. Human epidermalLangerhans cells undergo profound morphologic and phenotypical changes during *in vitro* culture. J. Invest. Dermatol. 1990; 94: 166-173.

Teunissen M.B.M., Wormmeester J., Rongen H.A.H., Kapsenberg M.L., Bos J.D. Conversion of human epidermal Langerhans cells into interdigitating cells *in vitro* is not associated with functional maturation. Eur. J. Dermatol. 1991; 1: 45-54.

Teyton L., O'Sullivan D., Dickson P.W., Lotteau V., Sette A., Fink P., Peterson P.A. Invariant chain distinguishes between the exogenous and endogenous antigen presentation pathways. Nature (London) 1990; 348: 39-44.

Thomas D.W., Yannashita U., Shevach E.M. Nature of the antigenic complex recognized by T lymphocytes. UV inhibition of antigen-specific T cell proliferation by antibodies to stimulator macrophage Ia antigens. J. Immunol. 1977; 119: 223-232.

Thorn R.T. Specific inhibition of cytotoxic memory cells produced against UV-induced tumors in UV-irradiated mice. J. Immunol. 1978; 121: 1920-1926.

Thorn R.T., Fisher M.S., Kripke M.L. Further characterization of immunological unresponsiveness induced in mice by ultraviolet radiation. II. Studies on the origin and activity of ultraviolet-induced suppressor lymphocytes. Transplantation 1981; 31: 129-133.

Tiegs S.L., Evavold B.D., Akihito Y., Stec S., Quintans J., Rowley D. Delayed antigen presentation by epidermal Langerhans cells to cloned T h1 and T h2 cells. J. Invest. Dermatol. 1990; 95: 446-449.

Tjernlund U., Juhlin L. Effect of UV-irradiation on immunological and histochemical markers of Langerhans cells in normal appearing skin of psoriatic patients. Arch. Dermatol. Res. 1982; 272: 171-176.

Tjernlund U., Scheynius A. Amplification of T-cell response to PPD by epidermal cell suspensions containing HLA-DR-expressing keratinocytes. Scand. J. Immunol. 1987; 26: 1-6.

Toews G.B., Bergstresser P.R., Streilein J.W. Langerhans cells: sentinels of skin associated lymphoid tissue. J. Invest. Dermatol. 1980a; 75: 78-82.

Toews G.B., Bergstresser P.R., Streilein J.W. Epidermal Langerhans cell density determines whether contact hypersensitivity or unresponsiveness follows skin painting with DNFB. J. Immunol. 1980b; 124: 445-453.

Torresani C., Manara G.C., Ferrari C., De Panfilis G. Immunoelectron microscopic characterization of a subpopulation of freshly isolated Langerhans cells that reacts with anti-CD23 monoclonal antibody. Br. J. Dermatol. 1991; 124: 533-537.

Townsend A., Bodmer H. Antigen recognition by class I-restricted T lymphocytes. Annu. Rev. Immunol. 1989; 7: 601-624.

Trowsdale J., Young J.A.T., Kelly A.P. Structure, sequence and polymorphism in the HLA-D region. Immunol. Rev. 1985; 85: 5-44.

Tschachler E., Schuler G., Hutterer J., Leibl H., Wolff K., Stingl G. Expression of Thy-1 antigen by murine epidermal cells. J. Invest. Dermatol. 1983; 81: 282-285.

Tse Y., Cooper K.D. Cutaneous dermal Ia+ cells are capable of initiating delayed type hypersensitivity responses. J. Invest. Dermatol. 1990; 94: 267-272.

Tsujisaki M., Igarashi M., Sakaguchi K., Eisinger M., Herlyn M., Ferrone S. Immunochemical and functional analysis of HLA class II antigens induced by recombinant immune interferon on normal epidermal melanocytes. J. Immunol. 1987; 138: 1310-1316.

Turk J.L., Oort J.A. A histological study of the early stages of the development of the tuberculin reaction after passive transfer of cells labelled with [H^3] thymidine. Immunol. 1963; 6: 140-147.

Turk J.L. Hypersensitivity. Scott. Med. J. 1971;16: 273-279.

Unanue E.R. The regulatory role of macrophages in antigenic stimulation. Part Two: symbiotic relationship between lymphocytes and macrophages. Adv. Immunol. 1981; 31: 1-136.

Unanue E.R. Cellular studies on antigen presentation by class II MHC molecules. Curr. Opinion Immunol. 1992; 4: 63-69.

Van de Rijn M., Lerch P.G., Bronstein B.R., Knowles R.W., Bhan A.K., Terhorst C. Human cutaneous dendritic cells express two glycoproteins T6 and M241 which are biochemically identical to those found on cortical thymocytes. Hum. Immunol. 1984; 9: 201-210.

Van Praag M.C.G., Mulder A.A., Claas F.H.J., Vermeer B.-J., Mommaas A.M. Long-term ultravioletB-induced impairment of Langerhans cell function: an immunoelectron microscopic study. Clin. Exp. Immunol. 1994; 95: 73-77.

Van Voorhis W.C., Valinsky J., Hoffman E., Luban J., Hair L.S., Steinman R.M. Relative efficacy of human monocytes and dendritic cells as accessory cells for T cell replication. J. Exp. Med. 1983; 158: 174-191.

Vermeer B.J., Mommaas A.M., Wijsman M.C., Koning F., Claas F.H.J. Ultrastructural localization of HLA-DR and HLA-DQ molecules in Langerhans cells and B cells: an immunoelectronmicroscopic study. Reg. Immunol. 1988; 1: 85-91.

Vestey J.P. Antigen presentation and systemic immune responses to herpes simplex virus in patients with recrudescent facial herpetic infections. M.D. Thesis 1990a.

Vestey J.P., Norval M., Howie S.E.M., Maingay J.P., McNeill W. Antigen presentation in patients with recrudescent orofacial herpes simplex virus infections. Br. J. Dermatol. 1990b; 122: 33-42.

Vitiliano P.P, Urbach F. The relative importance of risk factors in non melanoma carcinoma. Arch. Dermatol. 1980; 116: 454-456.

Volc-Platzer B., Leibl H., Luger T., Zahn G., Stingl G. Human epidermal cells synthesize HLA-DR alloantigens *in vitro* upon stimulation with gamma-interferon. J. Invest. Dermatol. 1985; 85: 16-19.

Volc-Platzer B., Groh V., Wolff K. Differential expression of class II alloantigens by keratinocytes in disease. J. Invest. Dermatol. 1987; 89: 64-68.

Volc-Platzer B., Steiner A., Radaszkiewicz Th., Wolff K. Recombinant gamma interferon and *in vivo* induction of HLA-DR antigens. Br. J. Dermatol. 1988; 119: 155-160.

Walker E.B., Lanier L.L., Warner N.L. Concomitant induction of the cell surface expression of Ia determinants and accessory cell function by a murine macrophage cell line. J. Exp. Med. 1982; 155: 629-634.

Wan S., Anderson R.R., Parrish J.A. Analytical modelling for the optical properties of skin with *in vitro* and *in vivo* applications. Photochem. Photobiol. 1981; 34: 493-499.

Wan S., Parrish J.A., Jaenicke K.F. Quantification of ultraviolet-induced erythema. Photochem. Photobiol. 1983; 37: 643-648.

Warfvinge K., Mikulowska A., Falck B. Functionally different Langerhans' cells in human epidermis. Acta Derm. Venereol. (Stockh.) 1991; 71: 429-430.

Warren M.K., Vogel S.N. Opposing effects of glucocorticoids on interferon-gamma-induced murine macrophage Fc receptor and Ia antigen expression. J. Immunol 1985; 134: 2462-2469.

Watson A.J., DeMars R., Trowbridge I.S., Bach F.H. Detection of a novel human class II HLA antigen. Nature 1983; 304: 358-361.

Weibel E.W. In: Stereological methods. Practical methods for biological morphometry. 1979; Vol. 1. New York Academic Press.

Willman C.L., Stewart C.C., Miller V., Yi T.-L., Tomasi T.B. Regulation of MHC class II gene expression in macrophages by hematopoietic colony-stimulating factors (CSF). J. Exp. Med. 1989; 170: 1559-1567.

Witmer-Pack M.D., Valinsky J., Olivier W., Steinman R,M, Quantitation of surface antigens on cultured murine epidermal Langerhans cells: rapid and selective increase in the level of surface MHC products. J. Invest. Dermatol. 1988; 90: 387-394.

Wolf P., Yarosh D.B., Kripke M.L. Effects of sunscreens and a DNA excision repair enzyme on ultraviolet radiation-induced inflammation, immmune suppression, and cyclobutane pyrimidine dimer formation in mice. J. Invest. Dermatol. 1993; 101: 523-527.

Wolff K., Schreiner E. Uptake, intracellular transport and degradation of exogenous protein by Langerhans cells. An electron microscopic cytochemical study using peroxidase as tracer substance. J. Invest. Dermatol. 1970; 54: 37-47.

Wolff K., Stingl G. The Langerhans cell. J. Invest. Dermatol. 1983; 80: 17s-21s.

Yoshikawa T., Rae V., Bruins-Slot W., Van den Berg J., Taylor J.R., Streilein J.W. Susceptibility to effects of UVB radiation on induction of contact hypersensitivity as a risk factor for skin cancer in humans. J. Invest. Dermatol. 1990; 95: 530-536.

Yoshikawa T., Streilein J.W. Genetic basis of the effects of ultraviolet light B on cutaneous immunity: evidence that polymorphisms at the Tnfα and Lps loci govern susceptibility. Immunogen. 1990; 32: 398-405.

Yoshikawa T., Kurimoto I., Streilein J.W. Tumor necrosis factor-alpha mediates ultraviolet-B enhanced expression of contact hypersensitivity. Immunology 1992; 76: 264-271.

Young A.R. Senescence and sunscreens. Br. J. Dermatol. 1990; 122: 111-114.

Yu R.C.H., Abrams D., Alaibac M., Lemieux L., Springall D.R., Polak J., Chu A.C. The application of confocal scanning laser micrsocopy in the study of epidermal Langerhans cells. J. Invest. Dermatol. 1992; 98: 519 (abstr.)

Zanovello P.,Bronte V., Rosato A., Pizzo P., Di Virgilio F. Responses of mouse lymphocytes to ATP. II. Extracellular ATP causes cell type-dependent lysis and DNA fragmentation. J. Immunol. 1990; 145: 1545-1550.

Zelickson A., Mottaz J. The effect of sunlight on human epidermis. Arch. Dermatol. 1970;101:312-315.

Zenisek A., Kral A.J., Hais I.M. Sunscreening effect of urocanic acid. Biochim. Biophys. Acta 1955; 18: 589-591.

Zinkernagel R.M., Doherty P.C. H-2 compatibility requirement for T-cell mediated lysis of target cells infected with lymphocytic choriomeningitis virus. Different cytotoxic T-cell specificities are associated with structures coded for in H-2K or H-2D. J. Exp. M ed. 1975; 141: 1427-1436.

Appendix 1

a) Gold label density on sections of CD1a positive cells divided into halves.

cell	label density on 1st cell half	label density on 2nd cell half
1	1.07	0.99
2	0.77	1.10
3	1.67	1.43
4	1.15	1.14
5	0.45	0.47
6	0.66	0.77
7	0.81	0.65
8	1.80	1.55
9	1.62	1.08
10	0.41	0.37

$t = 0.62$ (18 degrees of freedom).

Appendix 1

b) Gold label density on sections of CD1a positive cells divided into quarters.

cell	A	B	C	D
1	0.76	1.38	1.18	0.80
2	0.76	0.78	1.03	1.18
3	2.03	1.31	1.18	1.69
4	1.36	0.94	1.04	1.24
5	0.49	0.41	0.59	0.35
6	0.50	0.82	0.71	0.84
7	0.89	0.74	0.61	0.70
8	1.75	1.86	1.59	1.52
9	1.39	1.85	1.24	0.93
10	0.33	0.50	0.32	0.43

Two sample t tests were used to compare these data.

t (comparison of A and B) = -0.12
t (comparison of A and C) = 0.36
t (comparison of A and D) = 0.26
t (comparison of B and C) = 0.52
t (comparison of B and D) = 0.43
t (comparison of C and D) = -0.10

Appendix 1

c) Gold label density on sections of L243 positive cells divided into halves.

cell	label density on 1st cell half	label density on 2nd cell half
1	1.12	0.98
2	0.51	0.32
3	0.14	0.25
4	0.71	0.62
5	0.39	0.41
6	2.63	2.72
7	0.32	0.59
8	2.61	2.29
9	1.02	0.62
10	1.58	1.53

t = 0.17 (18 degrees of freedom.)

Appendix 1

d) Gold label density on sections of L243 positive cells divided into quarters.

cell	A	B	C	D
1	1.42	0.83	0.84	1.33
2	0.55	0.47	0.32	0.33
3	0.01	0.28	0.20	0.30
4	0.60	0.83	0.56	0.69
5	0.34	0.44	0.50	0.33
6	2.77	2.50	3.02	2.43
7	0.36	0.28	0.55	0.63
8	2.77	2.46	2.22	2.36
9	0.95	1.09	0.84	0.39
10	1.55	1.61	1.85	1.21

Two sample t tests were used to compare these data.

t (comparison of A and B) = 0.12
t (comparison of A and C) = 0.09
t (comparison of A and D) = 0.32
t (comparison of B and C) = 0.02
t (comparison of B and D) = 0.22
t (comparison of C and D) = 0.20

Appendix 1

e) Gold label density on sections of TU22 positive cells divided into halves.

cell	label density on 1st cell half	label density on 2nd cell half
1	0.48	0.47
2	1.90	1.74
3	0.69	1.74
4	1.62	1.25
5	2.72	2.29
6	0.41	0.69
7	0.96	0.97
8	0.19	0.16
9	0.73	0.59
10	0.42	0.37

t = 0.24 (18 degrees of freedom).

Appendix 1

f) Gold label density on sections of TU22 positive cells divided into quarters.

cell	A	B	C	D
1	0.44	0.52	0.40	0.54
2	1.90	1.80	1.27	2.21
3	0.59	0.79	0.62	0.99
4	1.33	1.92	1.25	1.25
5	2.49	2.95	2.34	2.24
6	0.44	0.39	0.69	0.69
7	0.90	1.03	1.15	0.79
8	0.15	0.23	0.12	0.21
9	0.79	0.67	0.74	0.44
10	0.35	0.50	0.40	0.34

Two sample t tests were used to compare these data.

t (comparison of A and B) = -1.0
t (comparison of A and C) = 0.29
t (comparison of A and D) = -0.20
t (comparison of B and C) = 1.27
t (comparison of B and D) = 0.80
t (comparison of C and D) = -0.50

Appendix 1

g) Gold label density on sections of B7/21 positive cells divided into halves.

cell	label density on 1st cell half	label density on 2nd cell half
1	0.83	0.78
2	1.30	1.42
3	6.60	7.33
4	0.10	0.16
5	0.26	0.23
6	0.39	0.63
7	0.49	0.46
8	0.60	0.58
9	0.65	0.53
10	8.65	9.99

t = 0.62 (18 degrees of freedom).

Appendix 1

h) Gold label density on sections of B7/21 positive cells divided into quarters.

cell	A	B	C	D
1	0.82	0.84	0.98	0.59
2	1.24	1.36	1.55	1.36
3	5.33	7.87	8.07	6.29
4	0.03	0.07	0.09	0.07
5	0.31	0.21	0.22	0.24
6	0.39	0.39	0.84	0.42
7	0.32	0.67	0.50	0.43
8	0.45	0.75	0.59	0.57
9	0.51	0.80	0.73	0.33
10	7.18	10.13	11.33	8.85

Two sample t tests were used to compare these data.

t (comparison of A and B) = -0.52
t (comparison of A and C) = 1.19
t (comparison of A and D) = -0.20
t (comparison of B and C) = -0.11
t (comparison of B and D) = 0.29
t (comparison of C and D) = 0.37

Appendix 1

i) Gold label density on sections of DA6.231 positive cells divided into halves.

cell	label density on 1st cell half	label density on 2nd cell half
1	8.44	7.00
2	13.55	12.98
3	12.44	12.54
4	7.16	8.23
5	8.07	8.21
6	7.17	9.52
7	5.16	5.55
8	7.25	6.22
9	5.58	6.36
10	11.09	12.93

t = -0.28 (18 degrees of freedom.)

Appendix 1

j) Gold label density on sections of DA6.231 positive cells divided into quarters.

cell	A	B	C	D
1	8.63	9.70	9.59	9.19
2	12.79	9.33	11.36	11.95
3	12.85	14.02	13.22	12.34
4	4.52	5.08	5.36	5.01
5	10.52	11.68	11.42	12.17
6	9.11	9.53	8.33	8.12
7	10.07	7.08	6.54	9.44
8	8.67	7.36	7.66	8.54
9	5.06	5.76	6.19	6.49
10	5.79	4.49	6.71	6.49

Two sample t tests were used to compare these data.

t (comparison of A and B) = 0.30
t (comparison of A and C) = 0.13
t (comparison of A and D) = -0.14
t (comparison of B and C) = -0.19
t (comparison of B and D) = -0.46
t (comparison of C and D) = -0.28

Appendix 2

a) Gold label density on step sections through DA6.231+ve LCs.

	LC	1st section	2nd section	3rd section	4th section	5th section
pre UVB	1	2.56	3.88	4.11		
	2	3.63	4.60	4.82		
	3	4.66	5.08	4.34		
	4	4.09	4.83	4.96	5.39	
	5	5.10	5.41	5.91		
	6	6.96	6.22	5.45		
	7	7.29	6.25	6.95		
	8	6.70	6.04	8.10		
	9	7.82	8.30	8.35		
	10	9.66	8.32	7.31	8.25	7.25
	11	9.20	8.39	8.48		
	12	8.70	8.98	10.4		
	13	11.80	11.41	10.58		
	14	12.90	13.54	15.39		
	15	15.47	17.48	15.12	14.19	
post UVB	16	5.08	4.61	5.72		
	17	5.22	5.78	6.21		
	18	6.34	6.15	7.23	5.18	
	19	7.09	7.64	6.37		
	20	7.14	5.75	6.55		
	21	8.65	6.84	6.82		
	22	7.83	7.26	7.80		
	23	8.43	7.91	8.16		
	24	8.57	8.09	8.76		
	25	12.85	11.77	12.85		
	26	10.05	11.39	1.91		
	27	12.98	13.99	12.46		
	28	12.74	14.36	14.80		
	29	13.36	14.21	14.91		
	30	25.55	24.82	19.82		

Appendix 2

b) Gold label density on step sections through L243+ve LCs.

pre or post UVB	LC	1st section	2nd section	3rd section
pre UVB	1	1.21	1.17	1.79
	2	0.56	0.66	0.41
	3	0.15	0.21	0.34
	4	0.88	0.90	0.89
	5	0.34	0.44	0.41
post UVB	6	0.04	0.08	0.04
	7	4.97	4.15	4.13
	8	3.16	3.06	3.23
	9	0.75	1.17	1.30
	10	0.07	0.10	0.08

c) Gold label density on step sections through TU22+ve LCs.

pre or post UVB	LC	1st section	2nd section	3rd section	4th section
pre UVB	1	0.55	0.46	0.34	0.53
	2	0.65	0.85	0.57	
	3	0.44	0.42	0.53	
	4	0.96	0.81	1.00	
	5	0.22	0.17	0.35	
post UVB	6	1.11	0.95	1.48	
	7	0.57	0.74	0.43	
	8	3.49	3.18	3.24	3.20
	9	1.18	1.32	1.43	
	10	1.57	1.81	1.80	

Appendix 2

d) Gold label density on step sections through B7/21+ve LCs.

pre or post UVB	LC	1st section	2nd section	3rd section
pre UVB	1	0.83	0.85	0.99
	2	0.72	0.59	0.84
	3	2.16	2.17	3.08
	4	0.04	0.12	0.08
	5	0.20	0.23	0.20
post UVB	6	0.65	0.70	0.80
	7	4.06	3.69	4.55
	8	0.66	0.33	0.57
	9	6.13	6.28	7.02
	10	9.95	10.51	10.10

Appendix 3a

The number of OKT6+ve ECs per millimetre basal keratinocyte plasma membrane.

	Number of OKT6+ve ECs/mm in five separate sections				
subject	1	2	3	4	5
MJT	38.04	42.22	40.20	35.35	31.07
JPV	33.14	25.00	19.92	20.51	17.43
EM	20.89	20.21	23.36	23.46	17.44
MJS	29.27	37.78	15.71	20.80	19.05
JAAH	38.30	35.83	38.98	36.21	29.46
SK	18.13	13.84	27.27	18.49	23.68
GCP	23.28	18.04	21.97	18.88	20.93
MG	13.95	27.91	17.58	14.63	19.23
NH	13.23	13.18	18.52	14.60	10.95

The number of OKT6+ve ECs per millimetre basal keratinocyte plasma membrane after a standard six week course of UVB phototherapy.

	Number of OKT6+ve ECs/mm in five separate sections after UVB irradiation				
subject	1	2	3	4	5
MJT	12.12	15.38	10.53	18.18	4.65
JPV	9.86	12.28	14.81	9.17	11.35
EM	14.00	13.33	13.09	15.48	10.45
MJS	21.95	9.80	10.43	16.66	14.77
JAAH	30.20	29.76	18.56	13.95	10.31
SK	8.33	8.70	13.04	7.69	11.76
GCP	11.27	11.76	15.55	14.15	8.49
MG	8.57	9.88	7.78	11.90	8.33
NH	7.64	5.85	5.69	4.31	6.43

Appendix 3b

The number of DA6.231+ve ECs per millimetre basal keratinocyte plasma membrane.

	Number of DA6.231+ve ECs/mm in five separate sections				
subject	1	2	3	4	5
MJT	29.54	29.17	34.92	23.88	28.78
JPV	26.76	20.45	16.61	24.03	11.70
EM	15.55	31.98	26.74	16.11	25.87
MJS	26.17	21.21	24.35	24.69	18.03
JAAH	33.00	35.23	29.73	36.42	31.08
SK	20.76	26.32	16.09	15.03	17.36
GCP	15.08	17.89	15.45	23.23	20.91
MG	20.79	23.08	20.69	19.54	25.00
NH	11.96	11.68	17.74	15.24	22.92

The number of DA6.231+ve ECs per millimetre basal keratinocyte plasma membrane after a standard six week course of UVB phototherapy.

	Number of DA6.231+ve ECs/mm in five separate sections after UVB irradiation				
subject	1	2	3	4	5
MJT	5.40	8.00	14.29	14.95	10.71
JPV	14.29	18.75	8.70	3.91	9.79
EM	25.35	15.85	13.09	15.48	10.45
MJS	11.76	14.52	7.50	5.22	10.77
JAAH	6.98	13.86	19.32	11.34	10.09
SK	6.78	7.25	6.94	8.00	8.45
GCP	10.46	7.22	7.14	10.20	6.00
MG	10.53	10.14	7.41	13.79	11.27
NH	4.52	4.57	6.14	5.64	4.21

Appendix 3c

The number of L243+ve ECs per millimetre basal keratinocyte plasma membrane.

	Number of L243+ve ECs/mm in five separate sections				
subject	1	2	3	4	5
MJT	21.93	21.43	24.30	16.66	21.15
JPV	13.31	14.20	13.29	18.46	18.26
EM	16.82	18.91	15.71	15.54	14.79
MJS	16.66	16.53	13.77	20.00	16.28
JAAH	21.26	15.08	21.31	13.25	24.41
SK	18.12	21.58	21.91	18.18	21.25
GCP	15.97	20.15	17.69	15.44	16.39
MG	23.33	21.84	21.11	20.48	14.56
NH	10.69	15.87	11.56	14.03	10.71

The number of L243+ve ECs per millimetre basal keratinocyte plasma membrane after a standard six week course of phototherapy

	Number of L243+ve ECs/mm in five separate sections after UVB irradiation				
subject	1	2	3	4	5
MJT	5.49	4.86	7.00	9.64	5.80
JPV	6.19	16.35	12.82	5.52	20.59
EM	8.27	7.83	10.85	6.82	7.76
MJS	12.19	4.70	10.07	14.03	7.97
JAAH	9.76	12.05	8.65	10.53	13.11
SK	7.02	8.62	7.89	11.54	13.64
GCP	5.32	5.36	7.32	4.44	10.10
MG	5.88	12.19	9.09	7.37	10.10
NH	7.23	5.96	3.42	4.25	7.34

Appendix 3d

The number of TU22+ve ECs per millimetre basal keratinocyte plasma membrane.

	Number of TU22+ve ECs/mm in five separate sections				
subject	1	2	3	4	5
MJT	19.01	13.04	11.96	13.84	8.03
JPV	13.87	12.04	12.54	13.04	13.60
EM	0	0	0	0	0
MJS	5.09	4.92	7.83	4.49	6.25
JAAH	17.42	12.19	13.09	13.29	14.17
SK	0	0	0	0	0
GCP	17.46	8.49	8.08	11.11	11.82
MG	19.05	18.68	13.83	19.54	11.11
NH	4.58	3.91	4.54	4.67	4.43

The number of TU22+ve ECs per millimetre basal keratinocyte plasma membrane after a standard six week course of phototherapy.

	Number of TU22+ve ECs/mm in five separate sections after UVB irradiation				
subject	1	2	3	4	5
MJT	4.06	0.87	4.72	5.45	3.96
JPV	8.28	6.21	5.11	8.82	10.28
EM	7.00	4.17	8.25	12.96	12.50
MJS	2.17	4.72	2.25	4.13	4.51
JAAH	1.15	1.07	1.10	0	0
SK	0	0	0	0	0
GCP	2.10	4.54	9.88	6.82	2.74
MG	6.66	2.74	2.44	5.97	4.65
NH	0.91	3.48	2.31	2.46	2.38

Appendix 3e

The number of B721+ve ECs per millimetre basal keratinocyte plasma membrane.

	Number of B721+ve ECs/mm in five separate sections				
subject	1	2	3	4	5
MJT	8.51	6.47	10.08	6.76	11.85
JPV	6.42	11.29	16.00	8.04	8.48
EM	6.87	7.72	5.37	9.04	5.17
MJS	5.43	7.59	3.80	7.41	6.45
JAAH	6.83	4.91	6.25	8.33	8.65
SK	8.88	9.21	12.71	14.06	14.47
GCP	5.64	2.40	6.72	8.66	7.26
MG	12.19	13.33	16.45	11.25	11.43
NH	4.54	5.26	5.60	7.30	6.78

The number of B721+ve ECs per millimetre basal keratinocyte plasma membrane after a standard six week course of phototherapy.

	Number of B721+ve ECs/mm in five separate sections after UVB irradiation				
subject	1	2	3	4	5
MJT	2.73	1.80	3.30	0.86	1.92
JPV	5.33	3.55	3.53	2.88	3.51
EM	4.41	7.25	5.80	5.68	7.59
MJS	3.82	2.94	2.84	6.94	7.02
JAAH	5.04	0.94	4.60	1.22	3.09
SK	4.35	3.16	9.09	5.17	10.26
GCP	1.11	3.67	2.35	4.12	2.25
MG	5.38	2.33	5.95	2.41	2.82
NH	1.69	2.87	2.31	2.94	2.96

Appendix 4a

The number of gold particles per μm plasma membrane on five CD1a+ve LCs or ICs.

	Number of gold particles per μm on five separate cells				
subject	1	2	3	4	5
MJT	0.88	1.59	0.70	0.71	0.60
JPV	0.10	0.35	0.25	0.17	0.37
EM	1.05	0.98	0.46	0.68	0.75
MJS	0.55	1.52	0.75	1.05	0.25
JAAH	0.60	0.74	0.69	1.80	1.31
SK	0.96	0.88	1.20	0.89	1.01
GCP	0.73	0.77	0.48	0.25	0.51
MG	0.15	0.23	0.25	0.45	0.14
NH	1.28	1.46	0.92	1.52	2.38

The number of gold particles per μm plasma membrane on five CD1a+ve LCs after a standard six week course of phototherapy.

	Number of gold particles per μm on five separate cells after UVB irradiation				
subject	1	2	3	4	5
MJT	3.90	3.66	3.80	2.43	2.20
JPV	1.09	1.77	1.44	0.36	1.97
EM	1.33	0.93	2.21	2.01	1.56
MJS	1.07	0.57	0.91	2.11	3.46
JAAH	2.81	4.12	1.84	1.09	0.46
SK	0.98	1.00	0.69	0.30	2.04
GCP	0.95	1.55	1.61	1.29	1.31
MG	0.68	0.71	0.12	0.31	0.06
NH	1.01	1.19	1.67	1.39	1.66

Appendix 4b

The number of gold particles per μm plasma membrane on five DA6.231+ve LCs or ICs.

	Number of gold particles per μm on five separate cells				
subject	1	2	3	4	5
MJT	2.90	3.23	3.38	4.80	3.13
JPV	1.63	8.10	3.62	2.41	4.55
EM	6.15	4.77	11.65	5.54	4.87
MJS	5.02	4.11	2.37	3.98	9.67
JAAH	4.69	4.73	3.12	4.26	8.65
SK	5.38	4.95	8.61	4.32	5.97
GCP	5.45	6.84	4.76	6.19	7.41
MG	3.49	3.24	8.28	4.22	4.61
NH	7.97	4.15	6.25	4.03	4.27

The number of gold particles per μm plasma membrane on five DA6.231+ve LCs after a standard six week course of phototherapy.

	Number of gold particles per μm on five separate cells after UVB irradiation				
subject	1	2	3	4	5
MJT	4.12	5.19	4.58	6.53	14.60
JPV	2.10	3.54	2.38	3.29	11.70
EM	8.19	9.86	4.47	13.62	10.21
MJS	7.63	8.43	2.86	8.90	5.29
JAAH	10.18	8.85	9.64	12.46	16.92
SK	5.43	8.99	6.25	10.82	11.01
GCP	10.43	3.60	2.91	5.99	4.65
MG	5.22	4.12	17.45	3.69	4.13
NH	5.33	9.83	5.94	5.45	2.00

Appendix 4c

The number of gold particles per μm plasma membrane on five L243+ve LCs or ICs.

	Number of gold particles per μm on five separate cells				
subject	1	2	3	4	5
MJT	2.77	0.14	0.41	0.61	6.72
JPV	0.06	0.28	0.08	0.03	0.00
EM	0.25	0.25	0.23	0.29	0.14
MJS	0.15	0.18	0.11	0.03	0.12
JAAH	0.20	0.25	0.19	0.42	0.91
SK	0.03	0.10	0.33	0.01	0.04
GCP	0.84	0.14	0.59	4.04	0.05
MG	0.12	0.32	0.51	0.68	0.11
NH	ND	ND	ND	ND	ND

The number of gold particles per μm plasma membrane on five L243+ve LCs after a standard six week course of phototherapy.

	Number of gold particles per μm on five separate cells after UVB irradiation				
subject	1	2	3	4	5
MJT	0.44	0.41	0.75	1.85	0.73
JPV	0.16	4.32	0.11	0	0.18
EM	2.79	0.99	2.61	0.84	0.67
MJS	1.74	0.07	0.28	0.16	0.70
JAAH	0.90	3.16	4.97	7.19	3.47
SK	ND	ND	ND	ND	ND
GCP	ND	ND	ND	ND	ND
MG	ND	ND	ND	ND	ND
NH	ND	ND	ND	ND	ND

Appendix 4d

The number of gold particles per μm plasma membrane on five TU22+ve LCs or ICs.

	Number of gold particles per μm on five separate cells				
subject	1	2	3	4	5
MJT	0.53	0.59	0.17	0.46	0.26
JPV	0.00	0.74	0.12	1.07	0.77
EM	0.23	0.22	0.14	0.00	0.22
MJS	0.13	0.39	0.62	0.35	0.09
JAAH	0.26	0.29	0.75	0.92	0.66
SK	0	0	0	0	0

The number of gold particles per μm plasma membrane on five TU22+ve LCs after a standard six week course of phototherapy.

	Number of gold particles per μm on five separate cells after UVB irradiation				
subject	1	2	3	4	5
MJT	0.75	1.63	1.81	0.85	0.26
JPV	0.37	1.38	2.51	1.00	0.59
EM	1.60	0.67	0.09	0.22	3.56
MJS	0.14	1.26	0.96	2.89	0.29
JAAH	3.01	0	2.70	1.57	1.03

Appendix 4e

The number of gold particles per μm plasma membrane on five B721+ve LCs or ICs.

	Number of gold particles per μm on five separate cells				
subject	1	2	3	4	5
MJT	0.23	0.31	0.54	0.29	0.07
JPV	0.42	0.29	0.94	0.41	0.21
EM	0.39	1.01	0.54	1.11	0.52
MJS	0.31	0.05	0.12	0.33	0.82
JAAH	0.58	1.01	0.92	1.54	1.19

The number of gold particles per μm plasma membrane on five B721+ve LCs after a standard six week course of phototherapy.

	Number of gold particles per μm on five separate cells after UVB irradiation				
subject	1	2	3	4	5
MJT	0.71	0.40	3.23	6.43	0.32
JPV	0.47	4.09	0.20	0.74	1.03
EM	0.58	1.35	4.21	0.43	2.30
MJS	0.65	0.43	0.80	3.33	1.12
JAAH	3.06	3.20	4.06	0.21	4.89

Appendix 5a

The percentage area of fluorescence label and the number of cells labelled with FITC-CD1a in epidermal sheets viewed 'en face' before and after a standard six week course of phototherapy.

		% labelled area		number of cells	
subj.	field	pre UVB	post UVB	pre UVB	post UVB
1	1	6.01	2.56	35	20
	2	3.43	2.61	40	17
	3	6.79	2.26	47	14
	4	6.26	1.86	46	23
	5	5.42	2.87	40	18
2	1	4.73	2.10	30	8
	2	7.03	1.35	28	6
	3	1.79	2.89	20	11
	4	1.06	3.15	17	4
	5	0.33	1.68	11	9
3	1	8.02	2.74	33	21
	2	7.54	3.74	32	18
	3	5.19	6.11	36	18
	4	6.15	4.53	41	15
	5	7.49	5.38	31	18
4	1	2.70	1.15	14	6
	2	1.66	0.99	13	7
	3	1.28	0.91	11	9
	4	1.33	1.11	10	12
	5	2.84	2.09	13	8

Appendix 5b The morphology of CD1a+ve cells in epidermal sheets before and after a standard six week course of phototherapy.

		total cell area (μm^2)		cell body area (μm^2)		dendrite area (μm^2)	
subj.	cell	pre UVB	post UVB	pre UVB	post UVB	pre UVB	post UVB
1	1	272	169	118	122	154	47
	2	172	282	80	127	92	155
	3	205	221	121	159	84	62
	4	302	184	135	69	167	115
	5	224	132	159	109	65	23
	6	319	175	122	133	197	42
	7	185	328	92	118	94	210
	8	241	234	131	92	110	142
	9	189	267	94	221	95	46
	10	168	454	112	220	56	234
2	1	260	116	93	60	167	56
	2	458	198	136	75	322	123
	3	167	228	91	69	76	159
	4	336	168	204	107	132	61
	5	410	320	162	249	248	71
	6	358	347	151	341	207	6
	7	484	97	200	85	284	12
	8	414	311	179	169	235	142
	9	367	183	183	173	184	10
	10	467	315	166	254	301	61
3	1	267	120	137	120	130	0
	2	416	226	109	93	307	133
	3	310	110	232	110	78	0
	4	324	336	280	92	44	244
	5	282	186	163	74	118	112
	6	268	186	171	70	97	146
	7	222	221	151	75	70	146
	8	279	116	201	62	78	54
	9	501	740	94	129	407	611
	10	247	165	71	139	176	26

4	1	233	147	82	122	151	25
	2	174	217	132	185	41	32
	3	179	125	126	125	52	0
	4	191	71	153	71	38	0
	5	191	161	106	45	85	116
	6	211	197	164	120	47	77
	7	349	203	143	125	206	77
	8	197	117	127	105	70	12
	9	190		98		92	
	10	269		194		75	

Appendix 5c

The number of dendrites, the mean length of dendrites and the dendricity (defined as the perimeter of the whole cell divided by the perimeter of the putative cell body) of CD1a+ve epidermal cells before and after a standard six week course of phototherapy.

subj.	cell	No. dendrites		dendrite length (μm)		dendricity	
		pre UVB	post UVB	pre UVB	post UVB	pre UVB	post UVB
1	1	8	4	10.6	9.2	4.9	2.4
	2	7	6	7.3	13.4	3.5	4.3
	3	3	4	17.2	8.0	2.8	1.8
	4	7	9	11.7	7.2	3.8	4.2
	5	5	3	8.6	4.8	2.0	1.5
	6	5	4	19.6	8.9	5.1	2.0
	7	6	4	7.6	8.7	2.7	3.7
	8	5	6	14.9	3.8	4.1	3.5
	9	2	4	26.7	8.1	4.1	1.9
	10	5	3	7.1	32.1	2.0	3.8
2	1	4	7	11.4	3.6	4.0	4.6
	2	9	3	10.2	15.6	5.5	3.1
	3	4	3	20.8	25.9	4.5	5.1
	4	4	2	17.2	24.3	2.9	3.1
	5	5	3	22.2	11.5	4.3	1.8
	6	3	1	23.2	6.75	3.6	1.1
	7	5	2	22.5	3.1	4.4	1.2
	8	5	5	14.7	15.5	3.3	2.9
	9	5	2	16.8	5.6	3.4	1.3
	10	8	3	16.5	9.5	4.9	1.8
3	1	4	0	12.4	0	2.7	1.0
	2	6	4	9.44	15.1	5.0	3.2
	3	7	0	15.4	0	2.5	2.1
	4	7	3	7.6	18.9	1.8	6.3
	5	5	6	11.3	12.5	3.5	5.2
	6	2	5	28.1	8.9	2.5	3.0
	7	3	3	13.7	24.1	2.6	6.2

	8	3	4	8.5	8.02	2.0	3.2
	9	4	3	10.6	4.7	7.4	9.8
	10	2	5	21.4	40.2	4.2	1.7
4	1	8	4	9.3	5.4	5.7	1.5
	2	2	3	9.2	6.5	1.9	1.2
	3	7	0	5.6	0	2.2	1.0
	4	4	0	5.8	0	1.7	1.0
	5	6	1	9.4	53.5	2.9	4.9
	6	5	2	7.7	9.8	1.7	1.9
	7	8	4	11.0	10.5	4.0	2.5
	8	3	3	12.2	3.2	2.5	1.2
	9	2		12.5		1.9	
	10	6		8.6		2.1	

Appendix 6. Publications arising from this work:

1. Spencer M.-J., Vestey J.P., Tidman M.J., McVittie E., Hunter J.A.A. Major histocompatibility class II antigen expression on the surface of epidermal cells from normal and ultraviolet B irradiated subjects. J. Invest. Dermatol. 1993; 100: 16-22.

Abstracts:

1. Spencer M.-J., Tidman M.J., Hunter J.A.A. Class II MHC antigen distribution on normal Langerhans cells assessed by a quantitative immunogold technique. Clin. Exp. Dermatol. 1990;15:313-314.

2. Spencer M.-J., Tidman M.J., McVittie E., Vestey J.P., Hunter J.A.A. The influence of ultraviolet-B radiation on MHC class II-positive Langerhans cells in normal human skin. Clin. Exp. Dermatol. 1993; 18: 183.